

**PROFILING OF MICRORNAs AND IL-10  
EXPRESSION IN INTESTINAL CD4<sup>+</sup> T CELLS  
FOLLOWING INFECTION WITH *HELICOBACTER  
HEPATICUS***

**Shraddha Rashmi Kamdar**

Doctor of Philosophy

University of York  
Biology

October 2015

## ABSTRACT

In the *Helicobacter hepaticus* (*Hh*) colitis model, *Hh* infection of either wild-type mice treated with a blocking antibody to the IL-10 receptor (anti-IL-10R) or IL-10 KO mice results in intestinal inflammation associated with inflammatory Th1 and Th17 responses. Recent findings suggest that altered expression of the post-transcriptional gene regulators microRNAs contribute to pathogenic immune responses during intestinal inflammation. Here, examination of microRNA expression during *Hh* colitis showed that microRNAs are differentially expressed in the inflamed large intestine of *Hh*<sup>+</sup> IL-10 KO mice compared to uninfected controls, both at the tissue-level and the CD4<sup>+</sup> T-cell level. Kinetic examination of the cecal and colonic levels of miR-155, miR-326 and miR-132 (microRNAs previously shown to augment Th1 and/or Th17 responses) demonstrated that miR-155 was up-regulated and miR-326 and miR-132 were down-regulated at different time points post *Hh* infection. Furthermore, the change in expression of these microRNAs coincided with inflammation development. Microarray profiling of large intestine LP CD4<sup>+</sup> T cells revealed that two microRNAs were significantly up-regulated (miR-21a and miR-31) and seven microRNAs were significantly down-regulated (miR-125a, miR-125b, miR-139, miR-181a, miR-192, miR-30a and miR-467c) in colitic IL-10 KO mice compared to uninfected controls.

The anti-inflammatory cytokine IL-10 is necessary for protection against intestinal inflammation. Here, the phenotype of IL-10-producing LP CD4<sup>+</sup> T cells was examined in a non-inflammatory immune response (*Hh*<sup>+</sup> WT mice) and in an inflammatory immune response (*Hh*<sup>+</sup>/anti-IL-10R-treated WT mice). Compared to uninfected controls, the *Hh*<sup>+</sup> mice showed a slight expansion in IL-10<sup>+</sup> IL-17A<sup>+</sup>FoxP3<sup>+/−</sup> cells whereas the *Hh*<sup>+</sup>/anti-IL-10R-treated mice showed a significant expansion in all the IL-10<sup>+</sup> LP CD4<sup>+</sup> T cells co-expressed both inflammatory cytokines IL-17A and/or IFN- $\gamma$  and/or the Treg transcription factor FoxP3.

The experiments carried out in this thesis demonstrate that the profile of two important regulatory factors, microRNAs and IL-10, is markedly different in LP CD4<sup>+</sup> T cells from the colitic setting compared to uninfected controls.

# TABLE OF CONTENTS

<b>ABSTRACT</b> .....	<b>2</b>
<b>TABLE OF CONTENTS</b> .....	<b>3</b>
<b>LIST OF FIGURES</b> .....	<b>8</b>
<b>LIST OF TABLES</b> .....	<b>10</b>
<b>ACKNOWLEDGEMENTS</b> .....	<b>12</b>
<b>AUTHOR'S DECLARATION</b> .....	<b>13</b>
<b>CHAPTER 1. GENERAL INTRODUCTION</b> .....	<b>14</b>
1.1 Overview of the mammalian immune system.....	15
1.1.1 The innate immune system .....	15
1.1.2 The adaptive immune system.....	15
1.2 CD4 <sup>+</sup> T cells .....	17
1.2.1 Effector T cells.....	18
1.2.1.1 T-helper type 1 (Th1) cells .....	18
1.2.1.2 T-helper type 2 (Th2) cells .....	18
1.2.1.3 T-helper type 17 (Th17) cells .....	19
1.2.1.4 T-helper type 22 (Th22) cells .....	19
1.2.1.5 T-helper type 9 (Th9) cells .....	20
1.2.2 Regulatory T cells .....	21
1.2.2.1 Thymically-derived Tregs (tTREGs).....	21
1.2.2.2 Peripherally-derived Tregs (pTregs) .....	23
1.2.2.3 T-helper type 3 (Th3) cells .....	23
1.2.2.4 T Regulatory 1 (Tr1) Cells .....	24
1.2.3 Treg generation in the gut.....	25
1.2.3.1 Dendritic cell subsets that promote Treg generation in the gut.....	25
1.2.3.2 Cytokine environment .....	25
1.2.3.3 Metabolic control of Treg generation in the gut.....	26
1.2.4 Mechanisms of Treg suppression.....	27
1.2.5 Th Plasticity .....	28
1.2.5.1 Th17/Th1 plasticity.....	28
1.2.5.2 Th17/Th2 hybrid cells .....	28
1.2.5.3 Th17/Tr1 plasticity .....	29
1.2.5.4 Treg/Th17 plasticity .....	29
1.2.5.5 Treg/Th1 hybrid cells .....	29
1.2.5.6 Th1/Th2 hybrid cells .....	29
1.3 MicroRNAs .....	29
1.3.1 MicroRNA Biogenesis.....	30
1.3.2 Mechanisms of mRNA repression by microRNAs.....	31

1.3.2.1	mRNA cleavage and degradation .....	31
1.3.2.2	Inhibition of translation .....	31
1.3.3	MicroRNA target recognition .....	32
1.3.4	MicroRNA nomenclature.....	32
1.3.5	MicroRNA-mediated regulation of the immune system.....	33
1.3.5.1	MicroRNA-mediated regulation of the innate immune system.....	33
1.3.5.2	MicroRNA-mediated regulation of the adaptive immune system.....	33
1.3.5.3	Dysregulated microRNAs in cancers of immune cell origin.....	34
1.3.5.4	Dysregulated microRNAs in autoimmune diseases .....	34
1.3.6	MicroRNAs as biomarkers .....	38
1.3.6.1	MicroRNAs as diagnostic biomarkers.....	38
1.3.6.2	MicroRNAs as prognostic biomarkers .....	38
1.3.7	MicroRNAs as therapy .....	38
1.3.7.1	MicroRNA-mimics .....	38
1.3.7.2	MicroRNA-antagonists.....	39
1.4	Inflammatory bowel disease.....	40
1.4.1	Aetiology of IBD .....	40
1.4.1.1	Genetic factors.....	40
1.4.1.2	Environmental factors: Microbiota.....	41
1.4.2	IBD therapy.....	41
1.4.2.1	Non-biological agents.....	41
1.4.2.2	Biological agents .....	41
1.4.2.3	Current pipeline .....	42
1.4.3	Experimental models of colitis .....	42
1.4.4	The <i>Helicobacter hepaticus</i> model of colitis .....	44
1.5	Intestinal homeostasis.....	45
1.5.1	Tregs and intestinal homeostasis .....	45
1.5.2	IL-10 and intestinal homeostasis .....	46
1.5.3	MicroRNAs and intestinal homeostasis.....	47
1.6	Aims .....	52
<b>CHAPTER 2. MATERIALS AND METHODS .....</b>		<b>53</b>
2.1	Animals .....	53
2.2	<i>Helicobacter hepaticus</i> culture and infections .....	53
2.3	Isolation and injection of anti-IL-10R monoclonal antibody.....	54
2.3.1	Isolation of anti-IL-10R mAb .....	54
2.3.2	Purification of mAb on Protein G column.....	55
2.4	Cell isolations.....	56
2.4.1	Lamina propria cell isolation .....	56

2.4.2	Spleen and mesenteric lymph node isolation.....	57
2.5	Stimulation of cells with phorbol myristate acetate and ionomycin .....	57
2.6	Flow cytometry.....	58
2.6.1	Staining for surface markers.....	58
2.6.2	Intracellular staining for cytokines and transcription factors .....	59
2.7	Cell sorting .....	61
2.7.1	Fluorescence-activated cell sorting of CD4 <sup>+</sup> T cells from the large intestinal lamina propria .....	61
2.7.2	Fluorescence-activated cell sorting of naïve CD4 <sup>+</sup> T cells from the spleen and MLN.....	61
2.8	RNA extraction.....	62
2.8.1	Total RNA extraction from sorted cells.....	62
2.8.2	Total RNA extraction from tissues .....	62
2.9	RNA precipitation protocols .....	63
2.9.1	RNA precipitation using lithium chloride.....	63
2.9.2	RNA precipitation using ethanol .....	63
2.9.3	RNA precipitation using isopropanol .....	64
2.10	Reverse transcription (RT).....	64
2.10.1	MicroRNA RT .....	64
2.10.2	Messenger RNA RT.....	64
2.11	Quantitative real-time PCR (QRT-PCR) analysis.....	65
2.11.1	qRT-PCR for microRNA .....	65
2.11.2	qRT-PCR for messenger RNA.....	65
2.12	MicroRNA microarray .....	66
2.13	Histology .....	66
2.13.1	Embedding tissues in wax and sectioning .....	66
2.13.2	Haematoxylin and eosin staining .....	67
2.14	<i>In vitro</i> CD4 <sup>+</sup> t-cell polarisation.....	68
2.14.1	Primary stimulation of naïve CD4 <sup>+</sup> T cells.....	68
2.14.2	Secondary stimulation of polarized CD4 <sup>+</sup> T cells.....	68
2.15	Enzyme-linked immunosorbent assay (elisa).....	69
2.16	Bioinformatic tools.....	70
2.17	Statistical analysis .....	70

**CHAPTER 3. AN OPTIMISED PROTOCOL FOR RNA EXTRACTION FROM LYMPHOCYTES .....71**

3.1	Introduction .....	71
3.2	Results .....	72
3.2.1	MicroRNeasy kits from Qiagen yield RNA with the least salt contamination.....	72

3.2.2	Splitting the sample into smaller aliquots and performing separate chloroform phase extraction on each aliquot improves RNA yield .....	74
3.2.3	Cold isopropanol precipitaton of RNA removes salt contamination and concentrates RNA.....	75
3.2.4	The use of glycogen as a carrier improves RNA precipitation and RNA yield.....	76
3.3	Summary .....	77
<b>CHAPTER 4. ALTERED EXPRESSION OF MICRORNAS IN <i>HELICOBACTER-INDUCED</i> INTESTINAL INFLAMMATION .....</b>		<b>78</b>
4.1	Introduction .....	78
4.2	Results .....	83
4.2.1	Expression of miR-155, miR-326 and miR-132 is altered during <i>Hh</i> -induced colitis.....	83
4.2.2	A non-inflammatory immune response to <i>Hh</i> does not induce a change in the expression of miR-155, miR-326 or miR-132.....	84
4.2.3	The basal expression of miR-132 is different in WT and IL-10 KO mice .....	84
4.2.4	Up-regulation of Ets-1 correlates with down-regulation of miR-326 in colitic mice at different time points post <i>Hh</i> infection.....	85
4.2.5	At basal levels, miR-155 is more highly expressed in the immune compartment whereas miR-326 is more highly expressed in the non-immune compartment of the large intestine. ....	85
4.2.6	MicroRNAs are differentially expressed in large intestinal CD4 <sup>+</sup> T cells from 2-wk <i>Hh</i> -infected IL-10 KO mice compared to those from uninfected .....	86
4.2.7	MiR-31, miR-21a, miR-210 and miR-96 are up-regulated whereas miR-181a is down-regulated in CD4 <sup>+</sup> Th1 and Th17 cells compared to naïve CD4 <sup>+</sup> T cells.....	92
4.2.8	Potential mRNA targets of miR-21a, miR-31, miR-210, miR-181a and miR-96. ....	94
4.3	Discussion .....	100
4.3.1	Summary .....	106
4.4	Figures .....	108
<b>CHAPTER 5. PHENOTYPIC CHARACTERIZATION OF LARGE INTESTINAL IL-10-PRODUCING CD4<sup>+</sup> T CELLS FOLLOWING <i>HELICOBACTER HEPATICUS</i> INFECTION.....</b>		<b>125</b>
5.1	Introduction .....	125
5.2	Results .....	128
5.2.1	An optimized protocol to simultaneously detect eYFP/GFP and FoxP3.....	128
5.2.1.1	The efficacy of different fixation and permeabilisation protocols in detecting Foxp3 and eYFP. ....	128
5.2.1.2	Changing the fixation and permeabilisation times when using the combination of 2% PFA/0.1% saponin does not improve FoxP3 staining.....	129

5.2.1.3	Simultaneous detection of eYFP and FoxP3 using 2% PFA and eBioscience permeabilisation buffer.....	129
5.2.2	CD4 <sup>+</sup> T cell responses in the large intestine following infection with <i>Helicobacter hepaticus</i> .....	130
5.2.3	In the colitic setting, a significant proportion of IFN- $\gamma$ -producing CD4 <sup>+</sup> T cells are derived from ex-Th17 cells .....	131
5.2.4	In both <i>Hh</i> <sup>+</sup> and <i>Hh</i> <sup>+</sup> /anti-IL-10R-treated mice, there is an expansion of both tTregs and pTregs in the large intestine LP.....	133
5.2.5	There is an expansion of LAG-3 <sup>+</sup> FoxP3 <sup>+</sup> cells following infection with <i>Hh</i> .....	134
5.2.6	In the colitic setting, there is an expansion of LAG-3 <sup>+</sup> FoxP3-negative cells .....	135
5.2.7	Simultaneous detection of Helios and GFP is impossible with current fixation and permeabilisation protocols .....	136
5.2.8	In both <i>Hh</i> <sup>+</sup> and <i>Hh</i> <sup>+</sup> /anti-IL-10R-treated mice, the majority of IL-10-producing CD4 <sup>+</sup> T cells are of a regulatory phenotype .....	137
5.2.9	In both <i>Hh</i> <sup>+</sup> and <i>Hh</i> <sup>+</sup> /anti-IL-10R-treated mice, the majority of IL-10-producing CD4 <sup>+</sup> T cells express CD25.....	138
5.2.10	In both <i>Hh</i> <sup>+</sup> and <i>Hh</i> <sup>+</sup> /anti-IL-10R-treated mice, there is an expansion in IL-10-producing CD4 <sup>+</sup> T cells that co-express inflammatory cytokines IL-17A and IFN- $\gamma$ .....	139
5.2.11	Ex-Th17 cells contribute to a small proportion of the IL-10 <sup>+</sup> IFN- $\gamma$ <sup>+</sup> cells in the colitic setting. ....	140
5.2.12	At least half the IL-10-producing CD4 <sup>+</sup> T cells that co-express IL-17A and/or IFN- $\gamma$ also express Foxp3.....	140
5.2.13	In a non-inflammatory immune response to <i>Hh</i> , a greater proportion of IL-17A and/or IFN- $\gamma$ -expressing cells also co-express FoxP3 and IL-10, compared to the colitic setting.....	141
5.3	Discussion .....	142
5.3.1	Summary .....	150
5.4	Figures .....	152
	<b>CHAPTER 6. GENERAL DISCUSSION.....</b>	<b>175</b>
	<b>APPENDICES .....</b>	<b>187</b>
	Appendix 1 MicroRNA microarray raw data .....	187
	Appendix 2 mRNA targets predicted by mirwalk .....	192
	<b>ABBREVIATIONS .....</b>	<b>209</b>
	<b>REFERENCES.....</b>	<b>216</b>

## LIST OF FIGURES

Figure 1.1 Differentiation of effector CD4 <sup>+</sup> T-cell subsets from naive precursors. ....	21
Figure 1.2 Treg subsets. ....	24
Figure 1.3 MicroRNA biogenesis. ....	31
Figure 4.1 Expression of miR-155, miR-326 and miR-132 is altered during <i>Hh</i> -induced colitis .....	108
Figure 4.2 The large intestinal levels of miR-155, miR-326 and miR-132 remain unchanged during a non-inflammatory immune response to <i>Hh</i> . ....	110
Figure 4.3 Basal expression of miR-132 is different in uninfected WT and uninfected IL-10 KO mice. ....	111
Figure 4.4 Upregulation of Ets-1 correlates with down-regulation of miR-326 in colitic mice at different time points post <i>Hh</i> infection. ....	112
Figure 4.5 At basal levels, miR-155 is more highly expressed in the immune compartment whereas miR-326 is more highly expressed in the non-immune compartment of the large intestine. ....	113
Figure 4.6 Phenotyping and isolation of CD4 <sup>+</sup> T cells from the lamina propria. ....	114
Figure 4.7 Integrity of total RNA extracted from LP CD4 <sup>+</sup> T cells. ....	115
Figure 4.8 Analysis of array sample quality. ....	116
Figure 4.9 Heat map depicting microRNAs that showed fold change $\geq 2$ in infected compared to uninfected controls. ....	117
Figure 4.10 Heat map depicting fluorescence intensities, p values and fold change differences of specific microRNAs from the microRNA microarray. ....	118
Figure 4.11 qRT-PCR validation of microRNA microarray results. ....	119
Figure 4.13 MiR-31, miR-210, miR-21a, miR-96 and miR-181a are expressed by both Th1 and Th17 cells. ....	121
Figure 4.14 Regulation of T-cell activation by miR-21a, miR-31, miR-210 and miR-181a. ....	123
Figure 4.15 MicroRNA-mediated regulation of the expression of transcription factors and cytokines in different CD4 <sup>+</sup> T-cell subsets. ....	124
Figure 5.1 Analysis of eYFP and FoxP3 expression using different fixation and permeabilisation buffers. ....	152
Figure 5.2 Altering the fixation and permeabilisation time when using the combination of 2% PFA fix/0.1% saponin perm does not improve FoxP3 staining. ....	153
Figure 5.3 Simultaneous detection of eYFP and FoxP3 expression using 2% PFA and eBioscience permeabilisation buffer. ....	154
Figure 5.4 LP cell numbers and percentage and number of LP CD4 <sup>+</sup> T cells in the large intestine of <i>Tiger</i> mice following infection with <i>Hh</i> . ....	155
Figure 5.5 CD4 <sup>+</sup> T cell responses in the large intestine of <i>Tiger</i> mice following infection with <i>Hh</i> . ....	156

Figure 5.6 LP cell numbers and percentage and number of LP CD4 <sup>+</sup> T cells in the large intestine of <i>IL-17A<sup>cre</sup>Rosa26<sup>eYFP</sup></i> mice following infection with <i>Hh</i> .	157
Figure 5.7 CD4 <sup>+</sup> T-cell responses in the large intestine of <i>Il17a<sup>cre</sup>R26R<sup>eYFP</sup></i> mice following infection with <i>Hh</i> .	158
Figure 5.8 NRP1 expression is lost following digestion of tissues with liberase.	160
Figure 5.9 Co-expression of Helios and FoxP3 in LP CD4 <sup>+</sup> T cells.	161
Figure 5.10 Expression of LAG-3 in LP CD4 <sup>+</sup> T cells and FoxP3 <sup>+</sup> LP CD4 <sup>+</sup> T cell.	162
Figure 5.11 Expression of LAG-3 in FoxP3 <sup>+</sup> tTregs and pTregs.	163
Figure 5.12 Expression of LAG-3 in FoxP3 <sup>-</sup> LP CD4 <sup>+</sup> T cells.	164
Figure 5.13 Effect of different fixation protocols on Helios staining.	165
Figure 5.14 Phenotype of IL-10-producing CD4 <sup>+</sup> T cells based on expression of FoxP3.	166
Figure 5.15 Phenotype of IL-10-producing CD4 <sup>+</sup> T cells based on LAG-3 and/or CD49b.	167
Figure 5.16 Following infection with <i>Hh</i> , the majority of IL-10-producing CD4 <sup>+</sup> T cells express CD25.	168
Figure 5.17 In the colitic setting, there is an expansion of IL-10-producing CD4 <sup>+</sup> T cells that co-express IL-17A and/or IFN- $\gamma$ .	169
Figure 5.18 A small proportion of IL-10 <sup>+</sup> IFN- $\gamma$ <sup>+</sup> cells in the colitic setting are derived from ex-Th17 cells.	170
Figure 5.19 FoxP3 expression in IL-10-producing CD4 <sup>+</sup> T cells that co-express IL-17A and/or IFN- $\gamma$ .	171
Figure 5.20 A proportion of ex-Th17 cells express IL-10 and FoxP3.	172
Figure 5.21 Schematic depicting the main findings of chapter 5.	174
Figure 6.1 Th17-phenotype shifting during inflammation and the resolution of inflammation.	180
Figure 6.2 Cartoon depicting hypothesis that Tr17 and Th17 cells switch alongside each other during <i>Hh</i> -induced intestinal inflammation.	183

## LIST OF TABLES

Table 1.1 MicroRNAs that are dysregulated in autoimmune diseases .....	35
Table 1.2 Experimental models of colitis .....	43
Table 1.3 MicroRNA profiling in tissues and peripheral blood of healthy controls and patients with active UC and CD .....	48
Table 1.4 MicroRNAs that are overexpressed in human IBD and animal models of colitis and their mRNA targets .....	49
Table 1.5 MicroRNAs that are down-regulated in human IBD and animal models of colitis and their mRNA target.....	51
Table 2.1 Combinations of fixation and permeabilisation buffers used during different flow cytometry staining protocols.....	58
Table 2.2 Monoclonal antibodies used for detection of surface markers, cytokines and transcription factors by flow cytometry.....	60
Table 3.1 Summary of different RNA extraction methods used.....	73
Table 3.2 Total RNA yield and quality obtained using different RNA extraction methods.....	74
Table 3.3 Improved RNA yield obtained by doing two phenol chloroform phase extractions and pooling the aqueous phase on to a single column to extract RNA.....	75
Table 3.4 Efficiency of different RNA precipitation protocols at removing salt contamination and concentrating RNA.....	76
Table 3.5 The use of glycogen as a ‘carrier’ greatly improves RNA recovery .....	77
Table 4.1 Modulation of development and function of CD4 <sup>+</sup> T cells by selected microRNAs ..	80
Table 4.2 Summary of total RNA yield and purity for samples from uninfected and 2-wk <i>Hh</i> <sup>+</sup> IL-10 KO mice to be used in the miR microarray.....	88
Table 4.3 Significantly up-/down-regulated microRNAs in CD4 <sup>+</sup> T cells from 2-wk <i>Hh</i> <sup>+</sup> IL-10 KO mice (compared to uninfected controls) .....	91
Table 4.4 Function of relevant predicted and experimentally validated mRNA targets of miR-21a .....	95
Table 4.5 Function of relevant predicted and experimentally validated mRNA targets of miR-31 .....	96
Table 4.6 Function of relevant predicted and experimentally validated mRNA targets of miR-210.....	97
Table 4.7 Function of relevant predicted and experimentally validated mRNA targets of miR-96.....	98
Table 4.8 Function of relevant predicted and experimentally validated mRNA targets of miR-181a.....	99
Table 5.1 Phenotypic markers of different Treg populations .....	126

Table 5.2 The similarities and differences in CD4 <sup>+</sup> T-cell responses and the phenotype of IL-10-producing CD4 <sup>+</sup> T cells in the large intestine LP of uninfected and 2-wk <i>Hh</i> <sup>+</sup> and <i>Hh</i> <sup>+</sup> /anti-IL-10R-treated mice .....	151
Table A1.1 Raw data of microRNA microarray carried out on LP CD4 <sup>+</sup> T cells from uninfected and 2-wk <i>Hh</i> <sup>+</sup> IL-10 KO mice.....	187
Table A2.1 Predicted mRNA targets of miR-31.....	192
Table A2.2 Predicted mRNA targets of miR-21a.....	196
Table A2.3 Predicted mRNA targets of miR-210.....	198
Table A2.4 Predicted mRNA targets of miR-96.....	201
Table A2.5 Predicted mRNA targets of miR-181a.....	204

## ACKNOWLEDGEMENTS

I would like to express my sincere gratitude to my supervisor Dr. Marika Kullberg for all her support and guidance, and for being a tremendous mentor and teacher. I am sure that everything I have learnt from her will stand me in good stead both for a career in research and in life! I would also like to thank my training advisory panel members, Professor Paul Kaye and Dr. Harv Isaacs for their invaluable feedback and support during the course of my PhD. I'd like to thank Dr. Dimitris Lagos for lending his expertise in microRNAs to this project.

I would like to thank everyone in the Technology Facility, particularly Karen Hogg, Karen Hodgkinson, Graeme Park, Meg Stark and Peter O'Toole for their help with my sorts and general flow cytometry angst. I'd also like to thank Dr. Sally James for doing the microRNA microarray for me and Dr. Sandy McDonald for helping with the analysis of the microarray data.

I'd like to thank the Hull York Medical School for sponsoring the research carried out in this thesis.

I'd especially like to thank Dr. James Hewittson and Steph Dyson for proof reading this thesis and all my colleagues who have made the CII such an enjoyable place to work. They have boosted my morale when I needed it and helped me in innumerable ways. In particular, I'd like to thank Peter Morrison, Steph Dyson, Naj Brown, Jack Lim, Ana Pinto, Angela Privat-Maldonado, David-Sanin Pena, Joe Doehl, Mohammed Osman, Matthew Warner, Marianna Ventouratou-Morys and Jane Dalton.

Finally, I'd like to thank my parents, my aunt Dr. Nirmala Kamdar, my siblings and my husband Mital for their unconditional love, support and encouragement. They have been there for me throughout the challenges of this PhD. I cannot thank them enough.

## **AUTHOR'S DECLARATION**

All the work presented in this thesis is original and was carried out by myself, with the exception of Figure 4.8, which was prepared by Dr. Sandy McDonald (Bioinformatics department, Technology Facility, University of York). I extracted RNA from LP CD4<sup>+</sup> T cells sorted by myself and Dr. Sally James (Genomics department, Technology Facility, University of York) ran the RNA samples on the microRNA microarray. Dr. Sandy McDonald helped with the analysis of the microarray.

None of the work described herein has been presented previously for an award at this, or any other, university.

## CHAPTER 1. GENERAL INTRODUCTION

Inflammatory Bowel Disease (IBD) is a chronic inflammatory disorder of the gastrointestinal tract and is thought to occur because of a dysregulated immune response to microbial flora. It is a complex disease and is thought to occur as a result of a mixture of immune and environmental factors in a genetically susceptible individual (Kaser et al., 2010). IBD comprises of two forms; Ulcerative colitis (UC) and Crohn's disease (CD) (Kaser et al., 2010). The main difference between these two forms of IBD is that UC is restricted to the colon and inflammation is mucosal and sub-mucosal whereas CD can affect any region of the gastro-intestinal tract and the extent of inflammation is transmural (Kaser et al., 2010).

Our lab studies intestinal inflammation using a murine model of colitis where inflammation is similar to CD. In this model, infection of IL-10 knock-out (KO) mice or wild-type (WT) mice treated with a blocking antibody to the IL-10-receptor (anti-IL-10R) with the Gram-negative bacterium *Helicobacter hepaticus* (*Hh*) results in chronic typhlocolitis (Kullberg et al., 2006; Kullberg et al., 1998). Conversely, WT mice infected with *Hh* alone do not develop intestinal inflammation (Kullberg et al., 1998). The type of inflammation seen in the *Hh* colitis model is similar to that seen in CD in that inflammation is transmural and it is associated with pathogenic CD4<sup>+</sup> Th1 and Th17 responses (Kaser et al., 2010; Kullberg et al., 1998; Morrison et al., 2013). Furthermore, the *Hh* colitis model is a good model to study CD because it takes into account the microbial component of IBD (colitis in this model is triggered by *Hh*) and it also takes into account one of the susceptibility loci for IBD which is the *IL10* gene (Lees et al., 2011).

Intestinal inflammation is thought to occur because of a breakdown in the regulatory mechanisms that keep effector CD4<sup>+</sup> T-cell responses in check. Although previous studies in our lab have extensively characterised the pathogenic effector CD4<sup>+</sup> T-cell response in *Hh* colitis (Morrison et al., 2013), the alteration in regulatory mechanisms is less well understood. The work carried out in this thesis sought to examine whether two types of regulatory mechanisms are altered in colitic mice compared to uninfected controls. At a cell-intrinsic level, we examined whether the profile of microRNAs, which are post-transcriptional gene regulators, are altered at the tissue level and CD4<sup>+</sup> T-cell level in the large intestine of colitic IL-10 KO mice compared to uninfected controls. The anti-inflammatory cytokine IL-10 has been shown to be important for preventing intestinal inflammation in the *Hh* model (Kullberg et al., 2002), as well as other models of colitis (Asseman et al., 1999; Carthew and Sontheimer, 2009) and represents one of the cell-extrinsic mechanisms of keeping pathogenic immune responses in check. Although previous work in the lab has shown that protection against *Hh*-induced inflammation is dependent on IL-10, the phenotype of these cells has not been examined before. Here, we examined the phenotype of IL-10<sup>+</sup> CD4<sup>+</sup> T cells in a non-inflammatory and an

inflammatory immune response to *Hh* to determine whether these cells exhibit an altered phenotype in the colitic setting.

In order to facilitate the understanding of the potential role different CD4<sup>+</sup> T cells and microRNAs play in *Hh* colitis, the following sections give an overview of the immune system, with particular emphasis on the different types of CD4<sup>+</sup> T-cell subsets that have been described so far, and an in-depth background on microRNAs, their biogenesis, roles in different autoimmune diseases as well as their potential use as therapy and as biomarkers.

## **1.1 OVERVIEW OF THE MAMMALIAN IMMUNE SYSTEM**

The immune system is highly sophisticated and has evolved a number of defense mechanisms to protect against invasion by a multitude of pathogens such as bacteria, viruses, fungi and parasites, whilst remaining tolerant of the organism's own cells as well as the commensal flora that inhabit mucosal surfaces (Male et al., 2006). The immune system can be broadly divided into two arms; the innate immune system, which comprises of immune cells that mount an immediate, non-specific response to a pathogen, and the adaptive immune system, which is highly specific for a particular pathogen (Male et al., 2006; Parkin and Cohen, 2001).

### **1.1.1 The innate immune system**

The innate immune system is highly conserved in mammals and forms the first line of defense against invading pathogens. Broadly defined, it comprises all aspects of the host's immune defense that are encoded in the germline genes of the host. This includes immune cells like dendritic cells, macrophages, monocytes, neutrophils, basophils and eosinophils and non-cellular components like the complement system (Chaplin, 2010; Gomez and Balcazar, 2008). Cells of the innate immune system possess germline encoded pathogen recognition receptors (PRRs) that recognize conserved molecular structures on pathogens called pathogen-associated molecular patterns (PAMPs) (Kumar et al., 2011). Activation of innate immune cells via their PRRs triggers complex signaling pathways that result in inflammatory responses mediated by various cytokines and chemokines and facilitates eradication of the pathogen (Kumar et al., 2011). Additionally, a specialized subset of innate immune cells, called antigen-presenting cells (APCs), comprised mainly of dendritic cells and macrophages, facilitate an effective immune response against infectious agents by initiating the adaptive immune response.

### **1.1.2 The adaptive immune system**

The adaptive immune system has immunological memory and manifests with exquisite specificity for its target antigen (Chaplin, 2010). It is comprised of lymphocytes, i.e. the T cells and B cells (Chaplin, 2010). Lymphocytes develop in the primary lymphoid organs (thymus and bone marrow) (Chaplin, 2010; Male et al., 2006). In the thymus, immature T cells develop into either CD4<sup>+</sup> or CD8<sup>+</sup> T cells, while B cells develop in the bone marrow (Chaplin, 2010; Male et

al., 2006). T and B cells possess antigen-specific receptors on their surface called the T-cell receptor (TCR) and immunoglobulin/B-cell receptor (BCR), respectively. These antigen-specific receptors are formed by somatic rearrangement from a collection of a few hundred germline gene elements, allowing the formation of millions of different antigen-receptors, each with a unique antigen specificity (Chaplin, 2010; Male et al., 2006). The assimilation of the TCR is random and often results in the development of auto-reactive TCRs. In a process termed 'central tolerance', T cells possessing autoreactive TCR's are killed by apoptosis in the thymus (Male et al., 2006). Any autoreactive T cells that escape central tolerance are kept in check in the periphery by a number of mechanisms termed 'peripheral tolerance', key enforcers of which are the regulatory T cells. Following development, mature T and B cells traffic to secondary lymphoid organs like the spleen and lymph nodes from where adaptive immune responses are initiated (Chaplin, 2010; Male et al., 2006).

B cells are directly activated by their cognate antigen to become antibody-secreting plasma cells, a process that is aided by CD4<sup>+</sup> T cells (Bonilla and Oettgen, 2010; Male et al., 2006). In contrast, T cells require antigens to be presented to them in the form of a shorter peptide fragment complexed to a major histocompatibility complex (MHC) molecule. There are two classes of MHC molecules; MHC class I and MHC class II (Bonilla and Oettgen, 2010; Male et al., 2006). CD8<sup>+</sup> T cells recognize antigens derived from intracellular pathogens (Bonilla and Oettgen, 2010; Male et al., 2006). These antigens are complexed to MHC class I, which is expressed by all nucleated cells (Bonilla and Oettgen, 2010; Male et al., 2006). In contrast, CD4<sup>+</sup> T cells are activated by antigenic peptides that are processed and presented by APCs expressing MHC class II molecules (Bonilla and Oettgen, 2010; Male et al., 2006). Upon antigen priming, naïve T cells become activated and differentiate into specialized effector cells. CD8<sup>+</sup> T cells become cytotoxic T cells that can kill pathogen-infected cells. CD4<sup>+</sup> T cells differentiate into T-helper (Th) cells that support other immune processes such as antibody production by B cells, CD8<sup>+</sup> T-cell responses, bacteriocidal activity of phagocytes and recruitment of other immune cells to the site of infection through secretion of cytokines and chemokines (Bonilla and Oettgen, 2010; Male et al., 2006). Differentiated lymphocytes migrate from the peripheral lymphoid organs to the site of infection (Bonilla and Oettgen, 2010; Male et al., 2006). Following the initial encounter with the pathogen, a portion of the adaptive immune cells become long-lived memory cells, which persist in a dormant state even decades after the initial sensitization, but rapidly re-express effector functions when they re-encounter their specific antigen (Chaplin, 2010; Male et al., 2006). This persistence of immune memory is an important part of an effective host response against specific pathogens or toxins when they are encountered a second time (Chaplin, 2010; Male et al., 2006).

## **1.2 CD4<sup>+</sup> T CELLS**

There are a number of different CD4<sup>+</sup> Th subsets that have been described. From a functional point of view, CD4<sup>+</sup> T cells can be broadly divided into two groups; effector T cells that provide protection against invading pathogens and regulatory T cells (Tregs) that prevent autoimmune reactions as well as limit effector T-cell responses against invading pathogens when the effector response becomes harmful to the host (Cosmi et al., 2014). The following section describes the differentiation and functions of different CD4<sup>+</sup> T-cell subsets.

### 1.2.1 Effector T cells

Depending on the antigen and co-stimulus received, naive CD4<sup>+</sup> T cells can differentiate into different Th subsets, each with distinct functions and cytokine expression profiles. Optimal activation and differentiation of CD4<sup>+</sup> T cells requires three signals. The first signal is the engagement of the TCR with the MHC-peptide complex on the APC (Male et al., 2006; Tao et al., 1997). The second signal is the engagement of the co-stimulatory molecule CD28 on the T cell with CD80 or CD86 on the APC, and the third signal are cytokines that are either present in the local milieu or secreted by the APC (Male et al., 2006; Tao et al., 1997).

#### 1.2.1.1 T-helper type 1 (Th1) cells

Th1 cells were first described in 1986 (Mosmann et al., 1986). Th1 cells produce high amounts of IFN- $\gamma$  and other inflammatory cytokines like TNF- $\alpha$  (Mosmann et al., 1986) (**Figure 1.1**). Th1 cells protect against intracellular pathogens by a number of mechanisms. Th1 cells enhance the bacteriocidal activity of phagocytes, primarily by IFN- $\gamma$  mediated activation of the oxidative and nitrosative (iNOS) microbicidal systems and upregulation of phagocytosis-promoting Fc receptors and complement receptors (Male et al., 2006). Th1 cells also support CD8 effector functions (Bevan, 2004) and influence antibody class switching by B cells into isotypes with high affinity for activating Fc receptors on phagocytes (Snapper and Paul, 1987) (Male et al., 2006). The differentiation of Th1 cells from naïve CD4<sup>+</sup> T cells is a complex process dependent on two cytokines; the heterodimeric cytokine IL-12 (made up of IL-12p35 and IL-12p40 subunits) and IFN- $\gamma$ . IL-12 through STAT4 (Thierfelder et al., 1996) and IFN- $\gamma$  through STAT1 (Afkarian et al., 2002) induce the expression of the ‘master transcription factor’ of Th1 cells, T-bet. T-bet enhances IFN- $\gamma$  production by Th1 cells and amplifies Th1 differentiation by increasing its own expression (Szabo et al., 2000). The Runt-related transcription factors Runx1 and Runx3 also play a role in Th1 cell differentiation. Runx1, in co-ordination with T-bet inhibits Th17 cell development by interfering with ROR $\gamma$ t (Lazarevic et al., 2011). Runx3, together with T-bet binds to the IFN- $\gamma$  promoter and silences the gene encoding IL-4 (Djuretic et al., 2007). In addition to their protective function, aberrant Th1 responses have been implicated in contributing to autoimmune and chronic inflammatory disorders like experimental autoimmune encephalomyelitis (EAE), type 1 diabetes, rheumatoid arthritis (Raphael and Forsthuber, 2012; Skurkovich and Skurkovich, 2005) and inflammatory bowel disease (IBD) (Noguchi et al., 1995).

#### 1.2.1.2 T-helper type 2 (Th2) cells

Th2 cells were described at the same time as the Th1 cells in 1986 (Mosmann et al., 1986). Th2 cells produce IL-4, IL-5, IL-9, IL-10, IL-13 and IL-25 as their effector cytokines (**Figure 1.1**). Th2 cells protect against extracellular parasites, including helminths (Pulendran and Artis, 2012). IL-4 production during the primary response initiates the differentiation of Th2 cells from naïve CD4<sup>+</sup> T cells (Parronchi et al., 1992). IL-4 production can be induced from naïve T

cells during initial activation by interaction of Jagged-1 expressed by DCs triggering Notch signaling in the T cells (Amsen et al., 2007). IL-25 produced by mast cells and macrophages can also trigger IL-4 production by non-B and non-T cells and thereby induces a Th2 response (Owyang et al., 2006). In the absence of IL-4, IL-13 has also been shown to promote Th2 lineage differentiation (Barner et al., 1998). IL-4 signaling induces STAT6 expression that in turn upregulates the master transcription factor for Th2 cells, GATA-3 (Kaplan et al., 1996; Zheng and Flavell, 1997). Th2 cells play a major role in allergic inflammatory conditions such as allergic asthma (Pulendran and Artis, 2012).

### **1.2.1.3 T-helper type 17 (Th17) cells**

Th17 cells provide protection against extracellular bacteria and fungi by recruiting neutrophils. The major Th17 effector cytokines are IL-17A, IL-17F, IL-21 and IL-22 (Aggarwal et al., 2003; Korn et al., 2007; Langrish et al., 2005; Liang et al., 2006; Veldhoen et al., 2006) (**Figure 1.1**). In 2000, the discovery of the heterodimeric cytokine IL-23 (made up of IL-12p40 and IL-23p19 subunits) (Oppmann et al., 2000) that could promote IL-17A production from CD4<sup>+</sup> T cells (Aggarwal et al., 2003), led to the discovery of Th17 cells. In mice, IL-6 or IL-21, in combination with TGF- $\beta$  induces differentiation of naïve CD4<sup>+</sup> T cells into Th17 cells (Bettelli et al., 2006; Korn et al., 2007; Veldhoen et al., 2006). IL-1 $\beta$  has also been shown to be important for the early development of murine Th17 cells (Chung et al., 2009). IL-6 and IL-21 preferentially activate STAT3 (Durant et al., 2010; Mathur et al., 2007; Yang et al., 2007). One of the effects of STAT3 signaling is to up-regulate of the master Th17 transcription factor ROR $\gamma$ t (Ivanov et al., 2006). Other transcription factors that influence Th17 development are IRF4 and Batf (Brustle et al., 2007; Schraml et al., 2009). Aberrant Th17 responses contribute to autoimmune and inflammatory diseases like EAE, arthritis, contact dermatitis and IBD (Zambrano-Zaragoza et al., 2014). Following differentiation, IL-23R is up-regulated on the Th17 cells allowing IL-23 to maintain and promote survival of the cells (Stritesky et al., 2008; Veldhoen et al., 2006).

### **1.2.1.4 T-helper type 22 (Th22) cells**

A subset of cells called Th22 cells has been described in humans (Duhon et al., 2009; Trifari et al., 2009). Similar to Th17 cells, Th22 cells also produce IL-22 but unlike Th17 cells, they produce little or no IL-17A (Duhon et al., 2009; Trifari et al., 2009) (**Figure 1.1**). IL-22 promotes tissue repair by promoting epithelial cell proliferation and improving cell survival. IL-22 also protects against extracellular pathogens, particularly Gram-negative bacteria such as *Klebsiella pneumoniae* and *Citrobacter rodentium* (Aujla et al., 2008; Zheng et al., 2008b). Th22 cells can be generated from naïve CD4<sup>+</sup> T cells by plasmacytoid DCs in the presence of IL-6 and TNF- $\alpha$  (Duhon et al., 2009; Trifari et al., 2009). Th22 differentiation appears to be dependent on the aryl hydrocarbon receptor (AHR), and it is unclear if ROR $\gamma$ t plays a role (Duhon et al., 2009; Trifari et al., 2009). Th22 cells are enriched in the human cecum where

they play an important role in maintaining mucosal barrier function (Wolff et al., 2012). It is currently unclear whether Th22 cells exist in the mouse. Supporting the presence of murine Th22 cells, one study found that CD4<sup>+</sup> T cells are major sources of IL-22 and that adoptive transfer of *in vitro* differentiated Th22 cells but not Th17 cells into *Citrobacter rodentium*-infected IL-22-deficient mice resulted in a host-protective response (Basu et al., 2012). In contrast, a more recent study, which fate-mapped IL-22-producing cells found that IL-22 is produced by a number of different CD4<sup>+</sup> T-cell subsets and is not expressed by a dedicated Th22 subset (Ahlfors et al., 2014).

#### **1.2.1.5 T-helper type 9 (Th9) cells**

Th9 cells are a subset of CD4<sup>+</sup> T cells that produce high levels of IL-9 as their signature cytokine, but unlike the IL-9-producing Th2 cells, Th9 cells do not produce IL-4 (Dardalhon et al., 2008; Veldhoen et al., 2008) (**Figure 1.1**). Th9 cells closely associate with Th2 cells, as the Th2 cytokine IL-4 is required for the induction of Th9 cells (Veldhoen et al., 2008) and furthermore, both Th2 and Th9 cells require the transcription factor STAT6 (Goswami et al., 2012). STAT6-deficient mice fail to develop both Th2 and Th9 cells (Goswami et al., 2012). Thus, it is unclear whether Th9 cells develop from Th2 cells or whether they are a truly distinct helper T-cell subset. Th9 cells may develop from Th2 cells upon induction of transcription factors PU.1 and IRF4, which shut off IL-4 production and turn on IL-9 production (Chang et al., 2010; Staudt et al., 2010). Supporting the idea that Th9 cells are a distinct helper T-cell subset is a study that showed that naïve CD4<sup>+</sup> T cells can be directly cultured into Th9 cells in the presence of TGF- $\beta$ , IL-4 and engagement of OX40 co-stimulation (Xiao et al., 2012). In these conditions, the non-canonical NF- $\kappa$ B pathway was more important than PU.1/IRF4 in inducing IL-9 production (Xiao et al., 2012). Th9 cells have been shown to be protective against tumors (Lu et al., 2012) and IL-9 protective against the nematode parasite *Trichuris muris* (Faulkner et al., 1998) ; however, Th9 cells were shown to be pathogenic in allergic airway inflammation (Chang et al., 2010; Kerzerho et al., 2013) and EAE (Jager et al., 2009). The fact that IL-9 is produced by a number of cells including Th2 cells, mast cells, eosinophils and neutrophils makes it difficult to study the exact role of Th9 cells (Soroosh and Doherty, 2009).

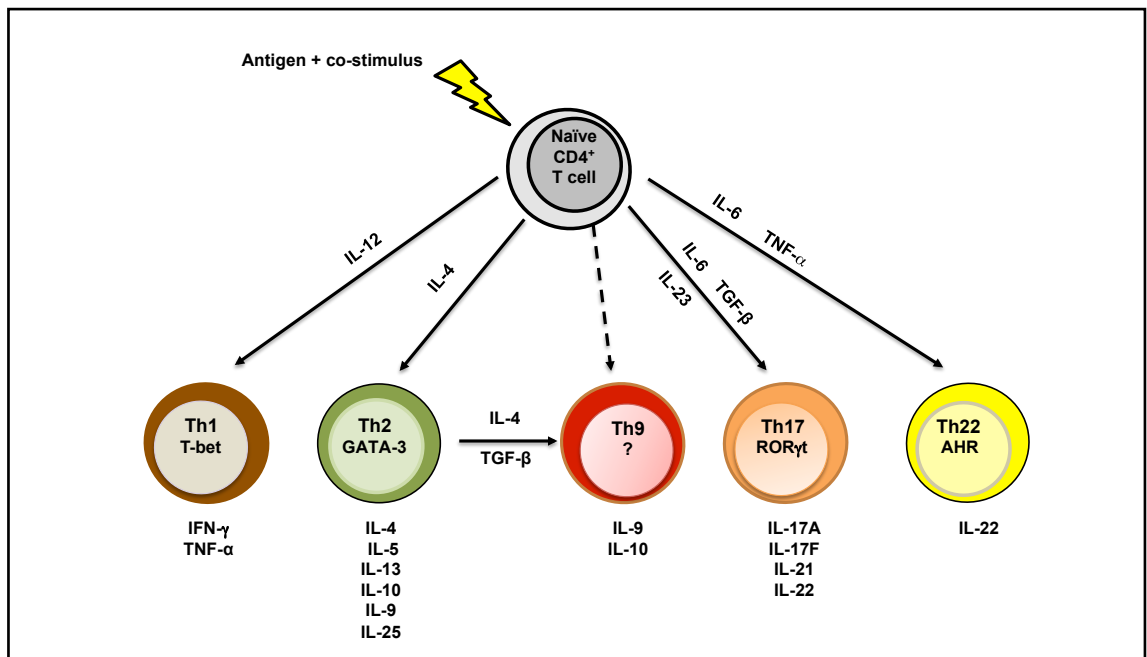


**Figure 1.1 Differentiation of effector CD4<sup>+</sup> T-cell subsets from naive precursors.**

Cartoon summarizing the different CD4<sup>+</sup> T-cell subsets that can be generated from a naïve CD4<sup>+</sup> T cell following activation with the appropriate antigen, co-stimulus and cytokine cocktail. The name of each subset and the master transcription factor for that subset is denoted in the appropriate cell. The characteristic cytokines secreted by each subset is shown below the appropriate cell.

## 1.2.2 Regulatory T cells

Regulatory T cells play an integral part in the immune response. They limit effector T cell responses to prevent excessive damage to self-tissues during the eradication of a pathogen as well as help in maintaining tolerance to self-antigens and commensals. Disruption of immune tolerance leads to autoimmune and inflammatory diseases. There are a number of intrinsic and extrinsic regulatory mechanisms that keep effector cells in check, among which regulatory T cells (Tregs) play a critical role. The following section describes the different Treg subsets and mechanisms by which they keep effector T cells in check.

### 1.2.2.1 Thymically-derived Tregs (tTREGs)

The importance of tTregs in maintaining tolerance was established in early experiments that revealed that mice that were thymectomized on day 3 of life developed multi-organ autoimmunity. This systemic autoimmunity was not observed when the thymectomy was performed on day 1 or day 7 of life or when mice thymectomized on day 3 received an infusion of thymocytes (Kojima et al., 1976; Nishizuka and Sakakura, 1969; Sakaguchi et al., 1982; Taguchi and Nishizuka, 1981). These studies showed that a suppressor population of thymocytes leave the thymus on day 3 of life and are able to keep the autoreactive thymocytes in control. Further analysis revealed that these suppressive populations expressed high levels of IL-2R $\alpha$  (CD25) (Sakaguchi et al., 1995; Sakaguchi et al., 1996) and adoptive transfer of this CD4<sup>+</sup> CD25<sup>+</sup> population into mice thymectomized on day 3 prevented multi-organ autoimmunity (Suri-Payer et al., 1998). Subsequent characterization of these cells revealed that

they failed to proliferate upon TCR stimulation and instead inhibited proliferation of responder CD4<sup>+</sup> T cells (Ermann et al., 2001; Takahashi et al., 1998; Thornton and Shevach, 1998). Furthermore, upon activation, the Tregs did not express any IL-2, but instead required IL-2 produced by other cells for their activation and survival (Sakaguchi et al., 1995). The majority of CD4<sup>+</sup> CD25<sup>+</sup> T cells were later shown to express the transcription factor FoxP3 (Fontenot et al., 2005; Wan and Flavell, 2005) (**Figure 1.2**). The finding that humans and mice deficient in CD4<sup>+</sup> CD25<sup>+</sup> T cells as a result of mutations to the *FoxP3* gene develop severe autoimmune diseases (Chatila et al., 2000; Wildin et al., 2001) suggest that FoxP3<sup>+</sup> Tregs are indispensable for the maintenance of self tolerance.

tTregs develop in the thymus from a pool of thymocytes that have high affinity for self antigens (Picca et al., 2006). Upon TCR engagement, CD25 is upregulated making these cells sensitive to IL-2 signaling and consequently activation of the STAT5 pathway (Burchill et al., 2008; Lio and Hsieh, 2008). Engagement of co-stimulatory molecule CD28 with CD80 and CD86 also aids in the promotion of FoxP3 expression (Tai et al., 2005). Together, all these signaling pathways result in transcription factors STAT5 and NFAT binding to the *Foxp3* locus and promoting FoxP3 expression, thus conferring the developing Treg cells with suppressive capacity (Yao et al., 2007; Zheng et al., 2010). tTregs were previously known as natural Tregs (nTregs), but recent changes to nomenclature of the Treg subsets have called for nTregs to now be called tTregs (Abbas et al., 2013).

### 1.2.2.2 Peripherally-derived Tregs (pTregs)

In addition to the thymically-derived Tregs, FoxP3<sup>+</sup> Tregs can also develop from naïve CD4<sup>+</sup> T cells in the periphery in response to antigenic stimulation (**Figure 1.2**). The differentiation of pTregs from naïve precursors requires the presence of TGF- $\beta$  and IL-2, and is favoured by sub-optimal DC activation and sub-immunogenic doses of antigenic peptides (Apostolou and von Boehmer, 2004; Kretschmer et al., 2005; Zheng et al., 2008a). Furthermore, optimal induction of pTregs has been observed with non-immunogenic methods of antigen delivery such as peptide pumps or oral and intravenous methods of delivery (Apostolou and von Boehmer, 2004; Kretschmer et al., 2005). Two new markers have recently been identified that are expressed on tTregs but not pTregs and that can be used to distinguish these subsets; Neuropilin-1 (NRP1) and the Ikaros family transcription factor Helios. NRP1 is a reliable marker of tTregs under non-inflammatory conditions; however during inflammation, it is up-regulated on pTregs as well (Weiss et al., 2012; Yadav et al., 2012). Helios was identified as being expressed on tTregs alone (Thornton et al., 2010). Thornton et al based their conclusion that Helios is a marker of tTregs based on three findings; i) The earliest FoxP3<sup>+</sup> Tregs to arise in the thymus of 3 day old mice, and the earliest FoxP3<sup>+</sup> Tregs to populate the spleen of 4 day old mice are all Helios<sup>+</sup>, ii) CD4<sup>+</sup> FoxP3<sup>-</sup> cells from FoxP3-GFP cells cultured *in vitro* in the presence of TGF $\beta$  to FoxP3<sup>+</sup> Tregs remain Helios-negative and iii) pTregs induced *in vivo* in a model of oral tolerance fail to express Helios (Thornton et al., 2010). Following this finding, one study reported that depending on the method of stimulation, pTregs could express Helios i.e. when cells were stimulated with their cognate antigen in the presence of APCs they expressed Helios, but not when they were stimulated with anti-CD3/CD28 (Verhagen and Wraith, 2010). A subsequent study reported that Helios is also up-regulated by effector CD4<sup>+</sup> T cells upon activation and proliferation (Akimova et al., 2011). In a communication to the editor of the Journal of Immunology, Thornton et al argue that all the studies where Helios was up-regulated on cells other than tTregs (Akimova et al., 2011; Verhagen and Wraith, 2010) were in studies where cells were stimulated *in vitro*. Further, in a review, Thornton and Shevach argued that in the study by Akimova et al, Helios expression was examined at the 3 day timepoint in suppression co-culture cells and at this timepoint, very few, if any responder T cells would have remained due to Treg-mediated depletion of IL-2 (Shevach and Thornton, 2014). Since then, a number of groups have used Helios to differentiate tTregs from pTregs *in vivo* (Daniel et al., 2015; Muller et al., 2015; Sanin et al., 2015; Smith et al., 2015)

### 1.2.2.3 T-helper type 3 (Th3) cells

Th3 cells were first described in rodents during the induction of oral tolerance (reviewed by Weiner (Weiner, 2001a)). Th3 cells differentiate from naïve precursors following antigen presentation by APCs coupled with CD86 co-stimulation and the presence of TGF- $\beta$  (Weiner,

2001b). Th3 cells produce TGF- $\beta$  as their main effector cytokine although some Th3 clones also expressed some IL-4 and/or IL-10 in addition to TGF- $\beta$  (Weiner, 2001b)(**Figure 1.2**). Th3 cells also require IL-4 rather than IL-2 for their maintenance (Inobe et al., 1998). Th3 cells do not express FoxP3 and reportedly play a role in induction of pTregs by acting on other FoxP3<sup>+</sup> cells to induce FoxP3 expression (Carrier et al., 2007).

#### 1.2.2.4 T Regulatory 1 (Tr1) Cells

Tr1 cells are Foxp3-negative regulatory T cells that differentiate from naïve CD4<sup>+</sup> T cells in a TCR/antigen-specific manner either in presence of IL-10, or during repeated stimulation with antigen or when the antigen is presented by immature DCs (Awasthi et al., 2007; Dhodapkar et al., 2001; Fitzgerald et al., 2007; Jonuleit et al., 2000). Tr1 cells produce large amounts of IL-10 in order to mediate suppression (Groux et al., 1997; Roncarolo et al., 2006; Vieira et al., 2004) (**Figure 1.2**). Transfer of Tr1 cells has been shown to protect against T cell transfer colitis (Groux et al., 1997). Recently co-expression of CD49b and LAG-3 has been identified as markers of Tr1 cells (Gagliani et al., 2013).

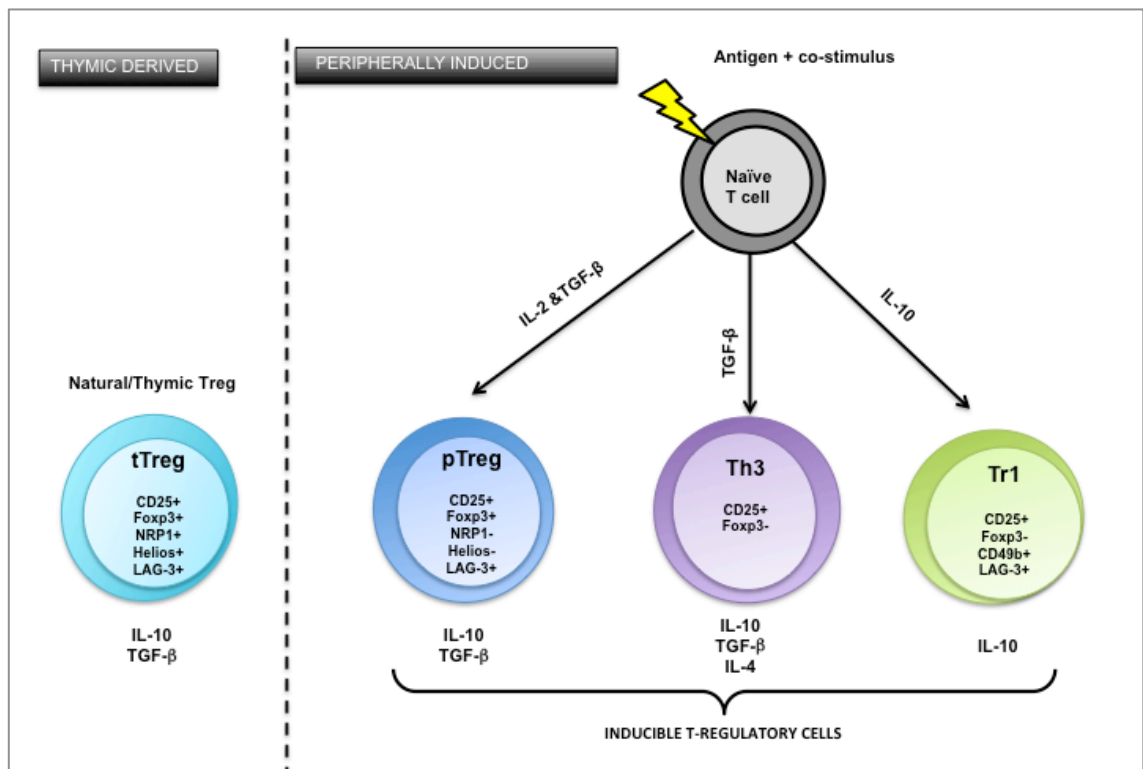


**Figure 1.2 Treg subsets.**

Cartoon depicting thymic Tregs and peripherally-induced Tregs that can be generated from naïve precursors in response to antigen, in the presence of appropriate co-stimulus and cytokines. The name of each type of Treg subset and the markers used to differentiate it are depicted within the appropriate cell. The characteristic cytokines secreted by each type of Treg is indicated below each cell.

### **1.2.3 Treg generation in the gut**

The generation of Tregs is a complex process that is influenced by the interplay of a number of factors such as the dendritic cells, cytokine environments and the presence of certain microbe and host-derived metabolites such as retinoic acid and short-chain fatty acids.

#### **1.2.3.1 Dendritic cell subsets that promote Treg generation in the gut**

The primary sites for induction of intestinal T cells are the Peyer's Patches (PPs) in the small intestine, mesenteric lymph nodes (MLNs) and isolated lymphoid follicles in the small and large intestine (Kelsall, 2008). There are multiple DC populations that have been identified at these sites that differ in surface phenotype, cytokine production and ability to drive differentiation of different effector T-cell populations (Kelsall, 2008). These DC subsets have unique functions such as promoting Treg differentiation, imprinting lymphocytes with unique homing receptors  $\alpha 4\beta 7$  (an integrin that binds to MadCAM-1 expressed on high endothelial venules of intestinal tissues) and CCR9 (a receptor for chemokine CCL25, that is constitutively expressed in the small intestine) (Campbell and Butcher, 2002; Johansson-Lindbom et al., 2003; Svensson et al., 2002). These homing receptors allow primed T cells to recirculate to the intestine.

Of the different DC subsets identified, CD103<sup>+</sup> DCs are important for imprinting naïve T and B cells with gut homing receptors and inducing the expression of FoxP3 (Coombes et al., 2007; Johansson-Lindbom et al., 2005). The ability of CD103<sup>+</sup> DCs to generate Tregs is also co-dependent on retinoic acid (RA), a metabolite of vitamin A metabolism and the cytokine TGF- $\beta$  (Bakdash et al., 2015; Coombes et al., 2007; Mucida et al., 2009).

#### **1.2.3.2 Cytokine environment**

IL-10 and TGF $\beta$  are two cytokines that are known to be important in the differentiation of peripherally induced Treg subsets. As described in the previous section, IL-10 is important for the generation of Tr1 cells (Awasthi et al., 2007; Dhodapkar et al., 2001; Fitzgerald et al., 2007; Jonuleit et al., 2000) while TGF $\beta$  is important for the generation of pTregs and Th3 cells (Apostolou and von Boehmer, 2004; Kretschmer et al., 2005; Weiner, 2001b; Zheng et al., 2008a). TGF- $\beta$  has three isoforms, TGF- $\beta$  1, 2 and 3, all of which have overlapping but non redundant functions (Annes et al., 2003). All three isoforms occur as inactive complexes, which must be activated in order to bind to their receptors and initiate signalling (Annes et al., 2003). In its inactive form, TGF $\beta$  has a propeptide called latency associated peptide (LAP) at the n-terminal region, which is covalently associated with active TGF- $\beta$  and masks the receptor binding sites (Shi et al., 2011). Two members of the  $\alpha v$  family of integrins have been found to play critical roles in converting TGF $\beta$  to its active form namely,  $\alpha v\beta 6$  and  $\alpha v\beta 8$  (Aluwihare et al., 2009). This was discovered by a study that showed that mice lacking  $\alpha v\beta 6$  and  $\alpha v\beta 8$  showed multi-organ autoimmunity similar to that seen in TGF $\beta$ 1-deficient mice (Aluwihare et al., 2009). While  $\alpha v\beta 6$  is mainly expressed by epithelial cells (Busk et al., 1992),  $\alpha v\beta 8$  was

found to be expressed by a number of cells such as CNS cells, mesangial cells in the kidney, epithelial cells and fibroblasts in the airway and in CD4<sup>+</sup> T cells and DCs (Araya et al., 2006; Khan et al., 2011; Milner et al., 1997; Travis et al., 2007). In the intestine, CD103<sup>+</sup> DCs were found to express high levels of  $\alpha\text{v}\beta\text{8}$  (Worthington et al., 2011). In fact, CD103<sup>+</sup> DCs are able to induce FoxP3<sup>+</sup> Tregs even in the absence of RA however loss of  $\alpha\text{v}\beta\text{8}$  expression on these DCs completely ablated their ability to induce pTregs (Worthington et al., 2011). Thus  $\alpha\text{v}\beta\text{8}$ -mediated activation of TGF $\beta$  plays a crucial role in Treg generation in the gut.

### **1.2.3.3 Metabolic control of Treg generation in the gut**

**Retinoic acid:** RA is a metabolite that is synthesised from Vitamin A in a series of steps that is catalysed by retinal dehydrogenases (RALDHs). RALDHs in the gut are primarily produced by the CD103<sup>+</sup> DCs (Coombes et al., 2007; Iwata et al., 2004). RA together with TGF- $\beta$ , promotes Treg generation by inducing FoxP3 expression while suppressing Th17 generation, decreasing proinflammatory cytokine production by effector T cells and by imprinting T cells primed in the MLN with gut homing receptors (Hill et al., 2008; Kang et al., 2007; Mucida et al., 2009; Sun et al., 2007).

#### **Microbe and microbial-derived metabolites that influence Treg generation in the gut:**

Germ-free or Vancomycin-treated mice exhibit a severe deficiency in colonic Tregs compared to SPF mice, suggesting that the microflora play important roles in inducing Tregs in the gut (Atarashi et al., 2011). Some microbial species such as *Clostridia* and *Bacteroides fragilis* have been shown to induce Tregs in the gut (Atarashi et al., 2013; Atarashi et al., 2011; Mazmanian et al., 2005). *Clostridia* induce Tregs by attaching to intestinal epithelial cells and stimulating TGF- $\beta$  production by these cells (Atarashi et al., 2013; Atarashi et al., 2011). *B. fragilis* produce polysaccharide A, which engages TLR2 on naïve T cells and induces them to differentiate into Tregs and also enhances Treg production of regulatory cytokines IL-10 and TGF- $\beta$  (Mazmanian et al., 2005; Round and Mazmanian, 2010).

**Short-chain fatty acids (SCFAs):** SCFAs such as butyrate, acetate and propionate are bacterial metabolites produced during bacterial fermentation of dietary fibre (Cummings et al., 1987). SCFAs have been shown to control Treg differentiation and function through several mechanisms. SCFAs signal through orphan G-protein coupled receptors (GPRs). Butyrate signals through GPR109a on macrophages and DCs to induce IL-10 and RALDHs production from these cells (Singh et al., 2014a). Butyrate is also a histone deacetylase and enhances acetylation at histone H3 lysine 27 at the Foxp3 promoter leading to Foxp3 expression (Arpaia et al., 2013; Furusawa et al., 2013). Propionate and other SCFAs signal through GPR43, which is expressed by Tregs, eosinophils and neutrophils and has been associated with dampening gut inflammation (Chang et al., 2014; Maslowski et al., 2009).

### 1.2.4 Mechanisms of Treg suppression

The following section explains the different mechanisms by which Tregs suppress effector CD4<sup>+</sup> T cells.

**Cell-cell contact dependent mechanisms of suppression:** Tregs constitutively express high levels of cytotoxic T lymphocyte antigen-4 (CTLA-4) (Wing et al., 2008). Although the mechanisms by which CTLA-4 mediates Treg suppression is currently under active investigation, one of the methods identified is that CTLA-4 ligation to CD80/86 on DCs down-regulates their expression (Wing et al., 2008). Another proposed mechanism is that CTLA-4 can capture CD80/CD86 from opposing cells by trans-endocytosis and degrade them within the CTLA-4-expressing cell (Qureshi et al., 2011). These mechanisms prevent activation of responder T cells by interfering with signal 2 of the T-cell activation process (binding of CD28 to CD80/86). Tregs also express high levels of T-cell immunoreceptor with immunoglobulin and ITIM domain (TIGIT), which can induce IL-10 production by DCs (Yu et al., 2009). This mechanism interferes with signal 3 of effector T cell activation process by DCs, (production of cytokines that modulate the differentiation or activation process) as production of IL-10 by DCs will lead to a tolerogenic immune response.

**Depletion of IL-2:** Effector CD4<sup>+</sup> T cells are dependent on IL-2 for their expansion. Tregs constitutively express high levels of IL-2R $\alpha$  (CD25) and deplete their surroundings of IL-2 leading to apoptosis of effector T cells due to IL-2 deprivation (Pandiyani et al., 2007).

**Treg-mediated cytotoxicity:** Tregs are capable of directly killing target cells in a perforin and granzyme-dependent manner (Askenasy, 2013; Cao et al., 2007; Gondek et al., 2005; Grossman et al., 2004). Granzymes enter target cells via pores made by perforins and induce apoptotic cell death by triggering the caspase pathway (Cao et al., 2007). Tregs may also induce death of target cells by employing the Fas/Fas ligand pathway (Janssens et al., 2003).

**Disruption of metabolic pathways:** CD39 and CD73 are two enzymes that are constitutively expressed by murine Tregs and these enzymes mediate the conversion of inflammatory adenosine triphosphate (ATP) to adenosine, thereby abrogating ATP-mediated inflammatory effects such as P2-receptor mediated cell toxicity and ATP-driven maturation of DCs (Borsellino et al., 2007; Dwyer et al., 2010; Fletcher et al., 2009). The importance of CD39 is highlighted by the fact that Tregs from CD39 KO mice have a 50-60% reduction in their ability to suppress effector cells (Borsellino et al., 2007). CD39 catalyses the hydrolysis of ATP to adenosine diphosphate (ADP) and adenosine monophosphate (AMP), and CD73 further hydrolyses ADP and AMP to adenosine (Borsellino et al., 2007; Dwyer et al., 2010; Fletcher et al., 2009). Adenosine signals through the A2A receptor to dampen effector T-cell activation and proliferation (Huang et al., 1997; Lappas et al., 2005) and aids in the generation of Tregs (Zarek et al., 2008).

**Secretion of anti-inflammatory cytokines:** Tregs secrete anti-inflammatory cytokines IL-10 (Asseman et al., 1999; Hara et al., 2001) and TGF- $\beta$  (Fahlen et al., 2005; Powrie et al., 1996). Blockade of TGF- $\beta$  or molecules involved in responsiveness to TGF- $\beta$  results in systemic autoimmunity, highlighting the important regulatory role of TGF- $\beta$  (Li et al., 2006a). Tregs themselves do not need to produce TGF- $\beta$  to prevent colitis, suggesting that they may induce TGF- $\beta$  from other cells to mediate suppressive effects (Fahlen et al., 2005; Kullberg et al., 2005). Selective blockade of IL-10 from Tregs, achieved by crossing *FoxP3*<sup>YFP-Cre</sup> mice with *Il10*<sup>fllox/fllox</sup> mice led to spontaneous colitis but not systemic autoimmunity observed in mice lacking Tregs altogether (Rubtsov et al., 2008) showing that IL-10 is particularly important for maintaining intestinal homeostasis.

### 1.2.5 Th Plasticity

T-cell differentiation was once considered linear; however there are now a number of studies that have demonstrated that under certain conditions like chronic inflammation, so-called committed Th cells can acquire the features of other effector CD4<sup>+</sup> T cells. Of all the T-cell subsets, the Th17 cells and Tregs exhibit the greatest degree of plasticity. The ability to combine different effector phenotypes into one cell may be an important adaptation of the immune system to deal effectively with not only the large variety of microorganisms that it is exposed to, but also the continual evolution of some of these species of microorganisms (Brucklacher-Waldert et al., 2014). The following section describes the different Th subsets that have been observed, that share phenotypes of other effector T cells. Where cells have definitively been shown to switch entirely to the transcription profile of another lineage, the term ‘plasticity’ has been used, and in instances where Th subsets display a ‘shared phenotype’ of two lineages, the term ‘hybrid’ has been used.

#### 1.2.5.1 Th17/Th1 plasticity

Th17 cells can change phenotype to become a cell that secretes both IL-17A and IFN- $\gamma$ , and then subsequently changes phenotype once again to become an ex-Th17 cell that secretes only IFN- $\gamma$ . The IL-17A<sup>+</sup> IFN- $\gamma$ <sup>+</sup> cells and ex-Th17 cells have been observed both in EAE and in the *Helicobacter hepaticus* (*Hh*) model of colitis (Hirota et al., 2011; Morrison et al., 2013). Furthermore, IL-17A<sup>+</sup>IFN- $\gamma$ <sup>+</sup> cells have also been observed in Crohn’s disease (CD) patients (Annunziato et al., 2007). Although the factors that trigger switching are not well understood, it was recently shown in mice that the transcription factors Tbet, Runx1 and Runx3 are important in driving the switching of Th17 cells to ex-Th17 cells (Wang et al., 2014d).

#### 1.2.5.2 Th17/Th2 hybrid cells

Th17/Th2 lymphocytes that secrete both IL-4 and IL-17A have been observed *in vivo* in greater proportions in patients suffering from allergic asthma compared to healthy donors (Cosmi et al., 2010). In an OVA-induced asthma model, transfer of Th17/Th2 lymphocytes induced more

severe asthma than the transfer of classical Th17 or Th2 cells, suggesting that the Th17/Th2 cells are more pathogenic (Wang et al., 2010).

#### **1.2.5.3 Th17/Tr1 plasticity**

A recent study found that during the resolution of inflammation, Th17 cells trans-differentiate into ex-Th17/Tr1-type cells that mainly produce IL-10 and help in the resolution of inflammation both in the T-cell transfer model of colitis and in EAE (Gagliani et al., 2015). The conversion of Th17 cells to ex-Th17/Tr1-type cells is mediated by TGF- $\beta$  and AhR (Gagliani et al., 2015).

#### **1.2.5.4 Treg/Th17 plasticity**

FoxP3<sup>+</sup> IL-17<sup>+</sup> cells have been identified in the inflamed mucosa of patient suffering from CD, but not in patients suffering from ulcerative colitis or healthy controls (Hovhannisyan et al., 2011). These cells express both *RORC* and *FoxP3* and were suppressive *in vitro* (Hovhannisyan et al., 2011). Examination of the TCR repertoire suggested that these cells originate from FoxP3<sup>+</sup> Tregs (Hovhannisyan et al., 2011). Similarly, analysis of T cells from human tonsils isolated after routine tonsillectomies revealed that 25% of FoxP3<sup>+</sup> Tregs produced IL-17 upon activation, and these FoxP3<sup>+</sup> IL-17<sup>+</sup> cells were suppressive (Voo et al., 2009). Conversely, in a murine model of autoimmune arthritis, FoxP3<sup>+</sup> Tregs trans-differentiated into pathogenic Th17 cells, and these ex-FoxP3 Th17 cells accumulated in the inflamed joint and were more osteoclastogenic than classical Th17 cells (Komatsu et al., 2014).

#### **1.2.5.5 Treg/Th1 hybrid cells**

FoxP3<sup>+</sup> Tregs that express T-bet, and produce IFN- $\gamma$  have been described (Koch et al., 2009). These T-bet<sup>+</sup> FoxP3<sup>+</sup> Tregs reportedly arise in response to IFN- $\gamma$  and up-regulate chemokine receptor CXCR3, enabling them to home to the site of inflammation and suppress the Th1 cells (Koch et al., 2009).

#### **1.2.5.6 Th1/Th2 hybrid cells**

Th1/Th2 hybrid cells that express both T-bet and GATA3, and produce both IL-4 and IFN- $\gamma$ , have been shown to develop directly from naïve precursors during the primary immune response to the parasites *Heligmosomoides polygyrus* (Peine et al., 2013). These cells supported Th1 and Th2 responses but caused less immunopathology (Peine et al., 2013). Furthermore, memory cells of the Th1/Th2 hybrid cells are maintained *in vivo* for months (Peine et al., 2013).

### **1.3 MICRORNAS**

MicroRNAs (sometimes called miRs) are post-transcriptional gene regulators and have been shown to regulate many biological systems including the immune system (Bartel, 2004).. MicroRNAs belong to the family of small non-coding RNAs and are short, single-stranded pieces of RNA, approximately 22 nucleotides in length (Bartel, 2004). The first microRNA, lin-4, was discovered in 1993 in the *Caenorhabditis elegans* model where it was found to down-

regulate a nuclear protein called lin-14 to initiate the second stage of larval development (Lee et al., 1993; Ruvkun and Giusto, 1989). Since then, approximately 35,800 microRNAs discovered across different species have been registered with a biological database (miRBase) that acts as an archive of microRNA sequences and annotations and provides a centralized system for assigning names to newly discovered microRNAs (Kozomara and Griffiths-Jones, 2011). More than 60% of protein-coding genes are estimated to be regulated by microRNAs (Friedman et al., 2009), and microRNAs have been found to regulate important cellular functions such as apoptosis, proliferation, differentiation and signal transduction (Ambros, 2004). The following sections give a detailed background on microRNAs including their biogenesis, nomenclature, mechanism of action, role in regulating different cells of the immune system, impact of altered microRNA expression in different immune-mediated diseases and the potential use of microRNAs as biomarkers and therapy.

### **1.3.1 MicroRNA Biogenesis**

MicroRNAs are encoded by genomic DNA. In the nucleus, microRNA genes are transcribed into primary microRNA (pri-miRNA) transcripts by RNA polymerase II (Lee et al., 2004). Maturation of these transcripts occurs in a two-step process directed by two ribonuclease III enzymes; Drosha and Dicer. Drosha forms a microprocessor complex with DGCR8 (Di George Syndrome Critical Region 8) and processes the pri-miRNA transcript to a precursor-microRNA (pre-miRNA) stem loop structure that is approximately 60 nucleotides long (Han et al., 2006) (**Figure 1.3**). This structure is exported into the cytoplasm by exportin 5 (Yi et al., 2003) and is then processed into 22-nucleotide duplexes by Dicer (Chendrimada et al., 2005) (**Figure 1.3**). These duplexes are then separated into single strands and one strand (the guide strand) is loaded into the RNA-induced silencing complex (RISC), made up of Argonaute, GW repeat-containing protein GW182 and other proteins (Eulalio et al., 2008) (**Figure 1.3**). Once loaded, the miRNA will bind to the 3' untranslated region (UTR) of its target mRNA to bring about either degradation of the target mRNA or translational repression (Chendrimada et al., 2007) (**Figure 1.3**).

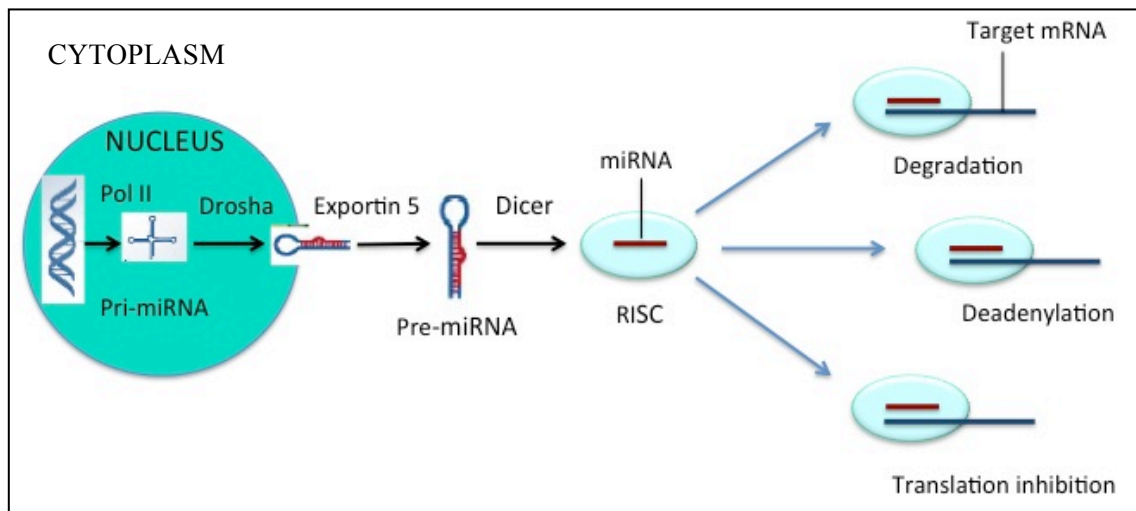


**Figure 1.3 MicroRNA biogenesis**

In the nucleus, microRNA genes are transcribed into primary microRNA (pri-miRNA) transcripts by RNA polymerase II. Maturation of these transcripts occurs in a two-step process directed by two ribonuclease III enzymes; Drosha and Dicer. Drosha forms a microprocessor complex with DGCR8 (Di George Syndrome Critical Region 8) and processes the pri-miRNA transcript to a precursor-microRNA (pre-miRNA) stem loop structure that is approximately 60 nucleotides long. This structure is exported into the cytoplasm by exportin 5 and is then processed into 22-nucleotide duplexes by Dicer. These duplexes are then separated into single strands and one strand (the guide strand) is loaded into the RNA-induced silencing complex (RISC) to form the functional microRNA. Once loaded, the miRNA will bind to the 3' untranslated region (UTR) of its target mRNA to bring about either degradation of the target mRNA or translational repression.

### 1.3.2 Mechanisms of mRNA repression by microRNAs

Although each microRNA can target hundreds of mRNAs, the overall effect on target protein expression is subtle and works more to 'fine tune' the amount of protein expressed by a given cell (Arvey et al., 2010; Fabian and Sonenberg, 2012). The following section describes the two methods by which microRNAs are known to repress mRNAs.

#### 1.3.2.1 mRNA cleavage and degradation

mRNA degradation by miRISC has been reported to occur by a number of mechanisms. With mRNAs that have high sequence complementarity to the microRNA, the mRNA is degraded via Argonaute-catalyzed slicer activity (Behm-Ansmant et al., 2006; Wu et al., 2006). In addition to this, it has also been shown that mRNAs can be decapped, deadenylated and exonucleolitically digested (Behm-Ansmant et al., 2006; Wu et al., 2006).

#### 1.3.2.2 Inhibition of translation

During translation of mRNAs, the EIF4 complex (made up of eIF4A, eIF4E and eIF4G subunits) engages with the mRNA and recruits ribosomal units that form circular structures that enhance translation (Wahid et al., 2010). MicroRNAs are thought to inhibit translation of target mRNAs by a number of mechanisms:

- MiRISC structure competes with eIF4E for binding to the mRNA 5'-cap structure thereby inhibiting translation initiation (Mathonnet et al., 2007; Thermann and Hentze, 2007).
- MiRISC inhibits mRNA circularization and thereby inhibits translation (Behm-Ansmant et al., 2006; Wakiyama et al., 2007; Wu et al., 2006).
- MiRISC causes a premature translational termination by inhibiting the assembly of the 60S ribosomal subunit with the 40S preinitiation complex (Chendrimada et al., 2007; Wang et al., 2008)
- MiRISC sequesters mRNAs in processing bodies (p-bodies). P-bodies lack translational machinery, thus mRNAs sequestered in them are unable to be translated to proteins (Valencia-Sanchez et al., 2006).

### 1.3.3 MicroRNA target recognition

The mechanism by which microRNAs recognize their target is not well understood. The general consensus is that microRNAs recognize mRNAs via conserved Watson-Crick pairing between the so-called 'seed region' between nucleotides 2-7 on the 5' end of the microRNA and the 3' untranslated region of the target mRNA (Grimson et al., 2007). Different studies have shown that a G:U wobble in the seed region significantly interrupts the interaction of a microRNA with its mRNA target (Brennecke et al., 2005). However, non-ideal pairing in the seed region can be overcome if there are additional complementary regions in the 3' end of the microRNA (Krichevsky et al., 2003). In general, the different bioinformatics target prediction tools available take into account at least two of the following parameters when predicting whether a given microRNA will bind to a certain mRNA: i) conservation of a microRNA and its targets across species (Brennecke et al., 2005), ii) free energy, which refers to how strong the binding between the mRNA and the microRNA is, and iii) accessibility energy (AE), which refers to how thermodynamically accessible the 3' UTR of the mRNA is to the microRNA (Kertesz et al., 2007). The lower the AE, the greater the likelihood of a particular microRNA targeting a given mRNA (Kertesz et al., 2007). Although microRNA target prediction programs are efficient in predicting mRNA targets, it is still necessary to experimentally validate these targets.

### 1.3.4 MicroRNA nomenclature

The parameters for microRNA nomenclature are outlined in miRBase (<http://www.mirbase.org/help/nomenclature.shtml>). Briefly, the numbering of microRNA genes is simply sequential in order of discovery. For example, in hsa-mir-121, the first three letters denote the organism (which in this case is *Homo sapiens*). Mir-121 (with the 'r' in lower case) refers to the microRNA gene and the stem-loop portion of the primary transcript. MiR-121 (with the 'R' in upper case) refers to the mature microRNA. Lettered suffixes denote closely related mature sequences e.g. miR-10a and miR-10b. Some microRNA cloning studies

revealed two mature microRNA sequences that originate from the same precursor. Where the relative abundancies of the two mature microRNA products are known, the dominant sequence is called miR-155 (for example) and the other product is called miR-155\*. Where the relative abundancies of the two mature microRNA products originating from the same precursor is unknown, they are simply referred to as miR-142-5p (from the 5' arm) and miR-142-3p (from the 3' arm).

### **1.3.5 MicroRNA-mediated regulation of the immune system**

A vast number of studies highlighted the important roles that microRNAs play in the development and function of immune cells of both the innate and adaptive immune systems. The examples cited below are a few of many.

#### **1.3.5.1 MicroRNA-mediated regulation of the innate immune system**

MicroRNA regulation of the innate immune system has been well studied, and microRNAs have the ability to influence innate immune cell differentiation, signaling pathways and cytokine production. For example, miR-17-92 targets *Runx1* to promote monocyte differentiation (Fontana et al., 2007). Toll-like receptor (TLR) signaling induces the expression of a number of microRNAs such as miR-155 (O'Connell et al., 2007) and miR-146a (Taganov et al., 2006). In murine macrophages, TLR-induced miR-155 represses *SOCS1* and *SHIP-1* that are inhibitors of TLR signaling (O'Connell et al., 2007). Conversely, TLR-induced miR-146a negatively regulates NF- $\kappa$ B via TRAF6 and IRAK1 (Taganov et al., 2006). TLR4 signaling on DCs represses PU.1 expression which in turn represses miR-142 expression and promotes the expression of miR-142 target IL-6 by DCs (Sun et al., 2013).

#### **1.3.5.2 MicroRNA-mediated regulation of the adaptive immune system**

MicroRNAs are crucial for the development of the adaptive immune system, as deletion of the microRNA biogenesis factor Dicer in CD4<sup>+</sup> T cells led to reduced numbers of these cells, poor proliferation, increased apoptosis and a tendency to produce IFN $\gamma$  (Koralov et al., 2008; Muljo et al., 2005). Deletion of Dicer in early B-cell progenitors led to increased apoptosis and a developmental block in pro- to pre-B-cell transition (Cobb et al., 2005). Highlighting the importance of microRNAs further, a number of studies have shown that individual microRNAs are critical to T- and B-cell biology. For example, loss of miR-17-92 led to increased BIM expression and apoptosis at the pro-B-cell to pre-B-cell transition, suggesting that miR-17-92 is vital for promoting early B-cell development (Thai et al., 2007; Ventura et al., 2008; Vigorito et al., 2007). MiR-155-deficient mice show defective class switching and antibody production (Thai et al., 2007; Vigorito et al., 2007). In CD4<sup>+</sup> T cells, miR-155 was shown to promote differentiation of Th1 (Rodriguez et al., 2007) and Th17 cells (O'Connell et al., 2010), and miR-326 was found to promote the differentiation of Th17 cells (Du et al., 2009).

### **1.3.5.3 Dysregulated microRNAs in cancers of immune cell origin**

Several studies have shown that microRNAs can promote oncogenesis (called oncomiRs) or act as tumour suppressors. For example, overexpression of miR-155 in mice led to a myeloproliferative disorder (Aung et al., 2015; Zhang et al., 2015b). Overexpression of miR-21 resulted in acute lymphoblastic leukemia (Zhu et al., 2014a), and miR-29a overexpression led to the development of acute myeloid leukemia (Miyazaki et al., 2014). Research in chronic lymphocytic leukemia (CLL) led to the discovery of several putative tumour suppressor microRNAs. The first microRNAs that were discovered to be tumour suppressors in CLL were miR-15a and miR-16 (Guo et al., 2014). They were down-regulated during CLL and subsequent investigations found that miR-15a and miR-16 negatively regulate cell survival by targeting the pro-survival protein BCL2 (Zhu et al., 2014b). The miR-34 family (consisting of miR34a, miR-34b and miR-34c) (Kittl et al., 2013), miR-29ab (Li et al., 2013b) and miR-181b (Li et al., 2013b) were also found to be down-regulated in CLL. Tumour suppressor p53 induces the expression of miR-34 (Zhang et al., 2014a). MiR-34 helps in tumour suppression by promoting cell cycle arrest and apoptosis (Zhang et al., 2014a). MiR-29ab and miR-181b were found to target oncogenes T-cell lymphoma 1, BCL2 and myeloid cell leukemia sequence (Li et al., 2013b).

### **1.3.5.4 Dysregulated microRNAs in autoimmune diseases**

Dysregulated microRNA expression in many autoimmune diseases has been found to augment the pathogenic immune responses in these diseases. For example, in multiple sclerosis, increased miR-326 levels in Th17 cells, suppressed negative regulator of Th17 cells, ETS-1 and promoted a Th17 response (Du et al., 2009) (**Table 1.1**). In Rheumatoid arthritis, decreased miR-146 expression in Tregs led to increased expression of miR-146 regulated target STAT1, and promoted pro-inflammatory cytokine production by Tregs (Zhou et al., 2014) (**Table 1.1**). A few more examples of the consequence of microRNA dysregulation in multiple sclerosis, rheumatoid arthritis, diabetes and systemic lupus erythematosus can be found in **Table 1.1**. These examples highlight the fact that microRNA expression levels have a profound impact on immune responses in these diseases.

**Table 1.1 MicroRNAs that are dysregulated in autoimmune diseases**

<b>Disease</b>	<b>microRNA</b>	<b>Expression</b>	<b>Location</b>	<b>Target<sup>a</sup></b>	<b>Implications of miRNA dysregulation<sup>b</sup></b>	<b>Reference</b>
Multiple Sclerosis	miR-326	Increased	Th17 cells	ETS-1	Promotes a Th17 response	(Du et al., 2009)
	miR-155	Increased	Th17 cells	ETS-1	Promotes a Th17 response	(O'Connell et al., 2010)
	miR-320a	Decreased	B cells	MMP-9	MMP-9 increases blood brain barrier permeability	(Aung et al., 2015)
	miR-26a	Decreased	Dendritic cells	IL-6	Promotes differentiation of Th17 cells over Tregs by modulating IL-6 expression	(Zhang et al., 2015b)
	miR-132	Increased	B cells	Sirtuin-1	Increased TNF $\alpha$ and lymphotoxin production by B cells	(Miyazaki et al., 2014)
	miR-20b	Decreased	Th17 cells	RoR $\gamma$ t STAT3	Promotes Th17 differentiation	(Zhu et al., 2014a)

<sup>a</sup>Target refers to the microRNA target identified by the authors.

<sup>b</sup>The implications of miRNA dysregulation stated are those suggested by the authors.

<b>Disease</b>	<b>microRNA</b>	<b>Expression</b>	<b>Location</b>	<b>Target<sup>a</sup></b>	<b>Implications of miRNA dysregulation<sup>b</sup></b>	<b>Reference</b>
<b>Rheumatoid Arthritis</b>	miR-146a	Decreased	Tregs	STAT1	Promotes inflammatory cytokines by Tregs	(Zhou et al., 2014)
	miR-155	Increased	PBMCs	SOCS1	Increased pro-inflammatory cytokine production	(Li et al., 2013b)
	miR-34a*	Decreased	Synovial fibroblasts	XIAP	Resistance to apoptosis	(Niederer et al., 2012)
	miR-124a	Decreased	Synoviocytes	MCP-1 CDK2	Promotes proliferation	(Kawano and Nakamachi, 2011)
<b>Type 1 Diabetes</b>	miR-326	Increased	PBLs		Co-related with ongoing islet autoimmunity	(Sebastiani et al., 2011)
	miR-21	-	Islet $\beta$ cells	PDCD4	Downregulates PDCD4 and protects Islet $\beta$ cells from cell death.	(Ruan et al., 2011)

<sup>a</sup> Target refers to the microRNA target identified by the authors.

<sup>b</sup> The implications of miRNA dysregulation stated are those suggested by the authors.

<b>Disease</b>	<b>microRNA</b>	<b>Expression</b>	<b>Location</b>	<b>Target<sup>a</sup></b>	<b>Implications of miRNA dysregulation<sup>b</sup></b>	<b>Reference</b>
<b>Systemic Lupus Erythematosus (SLE)</b>	miR-125b	Decreased	T cells	Ets-1 STAT3	Downreg of miR-125b negatively correlated with lupus nephritis	(Luo et al., 2013)
	miR-31	Decreased	T cells	RhoA	Decreased IL-2 production	(Fan et al., 2012)
	miR-21	Increased	T cells and B cells	PDCD4	Antiapoptotic	(Garchow et al., 2011) , (Stagakis et al., 2011)
	miR-125a	Decreased	T cells	KLF13	Increased expression of inflammatory cytokine RANTES	(Zhao et al., 2010)

<sup>a</sup>Target refers to the microRNA target identified by the authors.

<sup>b</sup>The implications of miRNA dysregulation stated are those suggested by the authors.

### **1.3.6 MicroRNAs as biomarkers**

There is a growing interest in using microRNAs as biomarkers. An ideal biomarker should be tissue and disease specific, stable and easily detected, and quantifiable by the least invasive option available. MicroRNAs fulfill all these criteria as they are present in whole blood, serum, plasma, urine and saliva (Weber et al., 2010), leading to the exciting possibility of using them as prognostic and diagnostic biomarkers. In plasma, microRNAs were found to be stable for 24 hours at room temperature and through 8 freeze-thaw cycles (Mitchell et al., 2008). MicroRNAs can be easily detected by qRT-PCR, microarrays and deep sequencing.

#### **1.3.6.1 MicroRNAs as diagnostic biomarkers**

A number of studies have identified circulating microRNAs as potential diagnostic biomarkers in a range of diseases from cancer (Shaker et al., 2015; Wang et al., 2014c) to cardiovascular disease (Kondkar and Abu-Amero, 2015), allergic inflammation (Sawant et al., 2015), diabetes mellitus (reviewed by (Guay and Regazzi, 2013) and rheumatic diseases (reviewed by (Alevizos and Illei, 2010).

#### **1.3.6.2 MicroRNAs as prognostic biomarkers**

MicroRNA expression seems to be specific for different stages of a disease. For example, in an ovarian cancer study, the serum levels of miR-200c showed an escalating trend and miR-141 showed a descending trend from early to advanced ovarian cancer, suggesting that expression of these microRNAs could be used as prognostic biomarkers for the stage of disease (Gao and Wu, 2015). A similar study in colorectal cancer patients identified high miR-21 expression with poor prognosis that associated with a significantly worse 5-year survival rate (Dong et al., 2014). These are just two examples of many studies done to identify microRNAs as potential prognostic biomarkers and although still a long way from the clinic, these studies highlight a potentially significant role for microRNAs in disease diagnostics.

### **1.3.7 MicroRNAs as therapy**

MicroRNAs are attractive as therapeutic agents because they can be easily delivered systemically using the same techniques as siRNAs (van Rooij et al., 2012). MicroRNA-based therapies generally comprise of either microRNA-mimics or microRNA-antagonists (van Rooij et al., 2012). MicroRNA-mimics are thought to be specific and well tolerated with few adverse events because they have the same sequence as endogenous microRNAs, thus will target the same genes (van Rooij et al., 2012). MicroRNA-antagonists target microRNAs already endogenously expressed in the tissue, decreasing the likelihood of inducing an adverse reaction (van Rooij et al., 2012).

#### **1.3.7.1 MicroRNA-mimics**

MicroRNA-mimics restore regulation by microRNAs that are down-regulated in a given disease condition to levels seen in normal cells, and this kind of therapy is termed 'microRNA

replacement therapy' (Bader et al., 2010). There are only two microRNA replacement therapies currently being developed by a company called miRNA Therapeutics; miR-34 (phase I) and let-7 (pre-clinical). Mimics of let-7 and miR-34 are designed to treat a number of solid tumors. Let-7 targets oncogene KRAS, which is frequently mutated in different cancer types (Johnson et al., 2005). In KRAS-G12D transgenic mice and in human non small cell lung cancer xenografts, delivery of let-7 mimics led to a significant inhibition of tumor growth (Trang et al., 2010). MiR-34 targets anti-apoptotic factors BCL2, Met and CD44. Systemic delivery of miR-34 inhibited tumour growth in mouse models of lung and prostate cancer and correlated with decreased proliferation and increased apoptosis of tumour cells (Liu et al., 2011; Wiggins et al., 2010).

### **1.3.7.2 MicroRNA-antagonists**

There are six microRNA antagonist therapies currently in development; miR-122, miR-208, miR-195, miR-21, miR-10b and miR103/105 miRagen (Janssen et al., 2013; Li and Rana, 2014).

MiR-122 is the most advanced of all the microRNA-antagonist therapies and is currently in phase II clinical trials (Guggino et al., 2015). MiR-122 is highly expressed in the liver and is an essential host factor for hepatitis C virus (HCV) replication (Girard et al., 2008). The miR-122 binding region to HCV is conserved in all the HCV genotypes, thus making miR-122 antagonistic therapy effective even in mutated strains of HCV (Jopling et al., 2005). Systemic administration of miR-122 antagonist SPC3649 in chimpanzees chronically infected with HCV led to long lasting suppression of viral RNA in serum (Lanford et al., 2010). Anti-miRs targeting miR-122 were successful at decreasing HCV RNA levels in a phase 2a study by Santaris Pharma (Janssen et al., 2013)

MiR-208, miR-195, miR-21, miR-10b and miR-103/105 antagonist therapies are currently in pre-clinical development for the treatment of cardiovascular disease (van Rooij et al., 2007). MiR-208 KO mice are resistant to cardiomyocyte hypertrophy and fibrosis in response to induction of cardiac hypertrophy and heart failure, suggesting that blocking miR-208 would ameliorate chronic heart disease (van Rooij et al., 2007). Anti-miRs against miR-208 are currently being developed by miRagen (Li and Rana, 2014).

MiR-195 belongs to the miR-15 family and overexpression in the embryonic heart led to septal defects by targeting a number of cell cycle genes and promoting cardiomyocyte proliferation (Porrello et al., 2011) Inhibition of miR-195 in mice and pigs led to protection from myocardial infarction and improved cardiac regeneration (Hullinger et al., 2012) (Porrello et al., 2013). Anti-miRs against miR-195 are currently being developed by miRagen (Li and Rana, 2014).

MiR-21 is overexpressed in many cancers and targets many tumour suppressors such as PTEN (Meng et al., 2007), TPMI (Zhu et al., 2007) and PDCD4 (Asangani et al., 2008). It is

also up-regulated during heart failure and in injured/ fibrotic kidneys (Chau et al., 2012; Thum et al., 2008) and promoted fibrosis in animal models. Anti-miR-21 is currently being investigated by Regulus Therapeutics to treat both cancer and fibrosis (Li and Rana, 2014).

Overexpression of miR-103 and miR-107 in mouse models resulted in dysregulated glucose homeostasis, however, blocking of these microRNAs resulted in increased insulin sensitivity and glucose homeostasis (Trajkovski et al., 2011). Anti-miRs against miR-103 and miR-107 are currently being developed by Regulus Therapeutics (Li and Rana, 2014).

## **1.4 INFLAMMATORY BOWEL DISEASE**

Inflammatory bowel disease (IBD) is a chronic inflammatory disorder of the gastro-intestinal (GI) tract that comprises of two major forms; ulcerative colitis (UC) and Crohn's disease (CD) (Kaser et al., 2010). The main differences between UC and CD are that UC is confined to the large intestine and the extent of inflammation is mucosal and sub-mucosal whereas CD can affect any part of the GI tract, and the type of inflammation seen is transmural (Kaser et al., 2010).

### **1.4.1 Aetiology of IBD**

IBD is caused by a breakdown in intestinal homeostasis. The current understanding is that it occurs because of dysregulated immune responses to microflora of the gut in genetically susceptible individuals (Kaser et al., 2010). Thus both genetic and environmental factors play a role in IBD.

#### **1.4.1.1 Genetic factors**

The genetic factors involved in IBD have been extensively reviewed by Lees et al (Lees et al., 2011). From genome-wide association studies (GWAS), it has become evident that there is a strong immune component in susceptibility to IBD. Of note, in both UC and CD, variants of genes involved in the IL-23 pathway, such as *IL23R*, *STAT3*, *IL12b* and those involved in IL-10 signalling such as *IL10R1* and *IL10R2* are susceptibility loci for disease. In CD, there seems to be a role for defective bacterial processing with variants of genes such as *NOD2* (Hugot et al., 2001; Ogura et al., 2001), and autophagy genes *ATG16L1* (Hampe et al., 2007) and *IRGM* (Parkes et al., 2007) conferring susceptibility. In contrast, in UC, *NOD2* and autophagy gene variants do not confer susceptibility to disease, however, a number of genes encoding epithelial barrier proteins such as *ECM1*, *CDH4* and *HNF4A* have been found to be associated with UC (Anderson et al., 2011; Consortium et al., 2009; Thompson and Lees, 2011). Other notable gene variants that confer susceptibility to UC are *HLA DRB\*0103*, *IL7R*, *IL8RA/IL8RB*, *DAP* and *IRF5* (Anderson et al., 2011).

#### **1.4.1.2 Environmental factors: Microbiota**

There are a number of human and animal studies that point to the importance of the intestinal microbiota being a major environmental factor that drives IBD. In humans, the majority of CD occur in the distal ileum and colon and all UC cases occur in the large intestine, which harbours the highest bacterial load (Bibiloni et al., 2006; Frank et al., 2007). Secondly, as mentioned in the previous section, a number of the genetic factors that predispose patients to developing IBD are involved in bacterial sensing and autophagy. Human IBD is also characterised by increased T cell and antibody responses to commensal antigens (Duchmann et al., 1995; Macpherson et al., 1996) and furthermore, treatment of patients with broad-spectrum antibiotics (Isaacs and Sartor, 2004) or probiotic bacteria (Gionchetti et al., 2003) has been shown to improve intestinal inflammation.

Some of the most compelling evidence for the involvement of microflora in driving intestinal inflammation stems from the fact that in several genetic models of colitis, the mice do not develop intestinal inflammation if they are germ-free (Rath et al., 1996; Sellon et al., 1998; Stepankova et al., 2007; Taurog et al., 1994). In some cases, the introduction of a single species of commensal bacteria is sufficient to induce colitis in susceptible mouse strains e.g. infection of germ-free IL-10 KO mice with either *Bacteroides vulgatus* or *E. faecalis* induced severe colonic inflammation (Kim et al., 2005; Sellon et al., 1998).

#### **1.4.2 IBD therapy**

There is no cure for IBD as yet. Current therapy used to treat the disease is a mixture of non-biological and biological agents.

##### **1.4.2.1 Non-biological agents**

Most of the non-biological drug therapies are broad spectrum immunosuppressants such as aminosalicylates, steroids and immunomodulators, which typically treat the symptoms of IBD, but do not cure disease or the underlying inflammatory immune processes (Burger and Travis, 2011).

##### **1.4.2.2 Biological agents**

The biological agents currently used to treat IBD fall into two groups; inflammatory cytokine blocking agents and adhesion molecule blocking agents. TNF- $\alpha$  is an inflammatory cytokine produced by a number of immune cells. Antibodies that neutralize TNF- $\alpha$  have been found to be effective in IBD patients, although a third of patients exhibit remain resistant to treatment (Altwegg and Vincent, 2014). Biological agents that target adhesion molecules  $\alpha$ 4 integrin (natalizumab) (Sandborn et al., 2005; Targan et al., 2007) and  $\alpha$ 4 $\beta$ 7 integrin (vedolizumab) (Feagan et al., 2005; Parikh et al., 2012; Sandborn et al., 2013) have also proved to be effective, because they prevent leukocytes from infiltrating the intestinal lamina propria and thereby inhibit the downstream inflammatory cascade. Natalizumab is approved for treatment of

moderate-to-severe CD after failure of anti-TNF inhibitors and Vedolizumab is approved for treatment of moderate-to-severe UC and CD when one or more of the standard therapies have not elicited an adequate response (Amiot and Peyrin-Biroulet, 2015).

#### **1.4.2.3 Current pipeline**

The biological agents currently in clinical trials are designed to either i) block inflammatory cytokines or their signalling pathways e.g. monoclonal antibodies targeting IL-6 and IL-12/IL-23 are being investigated for treatment of CD, ii) target adhesion molecules such as the  $\beta 7$  subunit of heterodimeric integrins  $\alpha 4\beta 7$  and  $\alpha E\beta 7$ , or iii) block T-cell stimulation and induce apoptosis (Amiot and Peyrin-Biroulet, 2015).

#### **1.4.3 Experimental models of colitis**

There are a number of murine models of colitis that have been developed to study different aspects of IBD pathogenesis. They can broadly be classified into spontaneous models such as the C3H-HeJBir or SAMP1Yit mouse models (Cong et al., 1998; Matsumoto et al., 1998) (**Table 1.2**) and models where intestinal inflammation is induced (**Table 1.2**). The induced models of IBD are used to study different aspects of IBD aetiology such as the roles of genes that confer susceptibility, defective barrier function, the role of immune cells known to mediate inflammation during IBD etc. In general, intestinal inflammation can be induced in three ways; i) administration of exogenous chemical agents such as Tri-nitro benzene sulphonic acid (TNBS) or dextran sodium sulphate (DSS) that disrupt the epithelial barrier (Morris et al., 1989; Okayasu et al., 1990) (**Table 1.2**), ii) knocking out of genes such as IL-2 or IL-10, which have been show to be important for preventing inflammation (Kuhn et al., 1993; Sadlack et al., 1993) (**Table 1.2**) and iii) adoptive transfer of CD4<sup>+</sup> T cells into immunodeficient mice such as RAG KO or SCID mice (Cong et al., 1998; Elson et al., 2000; Morrissey et al., 1993; Powrie et al., 1993) (**Table 1.2**).

**Table 1.2 Experimental models of colitis**

Type	Description	Reference
<b>Spontaneous models</b>		
C3H-HeJBir mouse	Restricted to ileocecal lesions. Inflammation is similar to CD in that it involves a Th1 response.	(Cong et al., 1998)
SAMP1/Yit mouse	Develop severe inflammation similar to CD in the colon and ileum.	(Matsumoto et al., 1998)
<b>Chemically induced models</b>		
TNBS	TNBS is a hapten administered rectally in ethanol as an enema. There is disruption of the mucosal barrier and intestinal inflammation is similar to both UC and CD.	(Morris et al., 1989)
Dextran sodium sulphate (DSS)	DSS is given in drinking water to disrupt the epithelial barrier and induce acute colitis resembling UC.	(Okayasu et al., 1990)
<b>Transgenic or Knock-out models</b>		
IL-2 KO	Mice develop chronic inflammation similar to UC. Display increased T- and B-cell activation and dysregulated MHC II expression.	(Sadlack et al., 1993)
IL-10 KO	Develop enterocolitis similar to CD, characterised by a Th1 response. Loss of IL-10 results in loss of regulation of normal immune responses to enteric antigens leading to overproduction of TNF- $\alpha$ and IFN- $\gamma$ .	(Kuhn et al., 1993)
STAT4 transgenic	Mice develop chronic inflammation characterised by overproduction of TNF- $\alpha$ and IFN- $\gamma$ .	(Wirtz et al., 1999)
<b>Transfer models</b>		
CD45RB <sup>high</sup> CD4 <sup>+</sup> T cells to RAG KO or SCID mice	Transfer of naive CD4 <sup>+</sup> T cells into lymphopenic mice results in chronic colitis and wasting disease characterised by elevated levels of IFN- $\gamma$ .	(Morrissey et al., 1993; Powrie et al., 1993)
C3H/HeJBir CD4 <sup>+</sup> T cells to C3H/HeSnJ SCID mice	C3H/HeJBir CD4 <sup>+</sup> T cells are inherently reactive to microflora-derived antigens and drive the development of chronic colitis when transferred into SCID mice.	(Cong et al., 1998; Elson et al., 2000)

#### 1.4.4 The *Helicobacter hepaticus* model of colitis

*Helicobacter* is a genus of Gram-negative microaerophilic bacteria that are of two types; gastric *Helicobacter* and enterohepatic *Helicobacter* (Solnick and Schauer, 2001). Gastric *Helicobacter* colonise the stomach whereas enterohepatic *Helicobacter* can infect both the intestinal tract and the liver (Solnick and Schauer, 2001).

*H. hepaticus* (*Hh*) is a type of enterohepatic bacterium that was first isolated from A/JCr mice suffering from hepatitis and hepatic tumours (Fox et al., 1996; Ward et al., 1994a; Ward et al., 1994b). *Hh* was later found to be associated with the development of intestinal inflammation in immunodeficient mice such as *nude* and SCID mice (Fox et al., 1996). Following infection, *Hh* colonises the cecum and colon of specific pathogen free IL-10 KO mice and results in the development of chronic typhlocolitis (Kullberg et al., 1998). The requirement for the absence of IL-10 or IL-10 signalling to develop *Hh*-induced typhlocolitis is evidenced by the fact that *Hh*-infected ( $Hh^+$ ) IL-10 sufficient hosts do not develop intestinal inflammation (Kullberg et al., 1998) unless treated with a blocking antibody to the IL-10R (anti-IL-10R) (Kullberg et al., 2006). The presence of intestinal flora is also vital to the development of *Hh*-induced colitis as germ-free IL-10 KO mice mono-associated with *Hh* do not develop disease (Dieleman et al., 2000).

The development of inflammation in our model of *Hh*-induced colitis is dependent on lymphocytes, as evidenced by the fact that  $Hh^+$  RAG KO mice do not develop colitis unless they are given CD4<sup>+</sup> T cells by adoptive transfer (Kullberg et al., 2002). Initial studies in the  $Hh^+$  IL-10 KO model suggested that intestinal inflammation was Th1 driven as MLN cells from these mice produced IFN- $\gamma$  and TNF- $\alpha$  upon restimulation (Kullberg et al., 1998). The IL-12p40 subunit was found to be crucial for sustaining *Hh* colitis as treatment of  $Hh^+$  IL-10 KO mice with anti-IL-12p40 antibody ameliorated colitis and mice showed decreased levels of IFN- $\gamma$  and TNF- $\alpha$  (Kullberg et al., 2001). Furthermore  $Hh^+$  IL-10/IL-12 double KO (DKO) mice were protected from colitis development (Kullberg et al., 2001). These studies suggested that IL-12 plays an important role in the development of colitis. However, soon after, it was discovered that the IL-12p40 subunit is a shared subunit between IL-12 and IL-23 (Oppmann et al., 2000). In light of this finding, the importance of IL-12 versus IL-23 in driving *Hh*-induced colitis was re-evaluated.  $Hh^+$ /anti-IL-10R-treated WT (IL-12 and IL-23 sufficient) and IL-12p35 KO mice (lacking IL-12 only) developed intestinal inflammation, however  $Hh^+$ /anti-IL-10R-treated IL-12p40 mice (lacking both IL-23 and IL-12) did not develop intestinal inflammation suggesting that IL-23 and not IL-12 is a key player driving *Hh*-induced intestinal inflammation (Kullberg et al., 2006).  $Hh^+$ /anti-IL-10R-treated WT mice also showed elevated levels of IFN- $\gamma$  and IL-17A, suggesting the involvement of both Th1 and Th17 cells in intestinal inflammation (Kullberg et al., 2006). Kinetic studies in  $Hh^+$  IL-10 KO mice revealed that at peak inflammation, there are large numbers of IL-17A<sup>+</sup>, IL-17A<sup>+</sup> IFN- $\gamma^+$  and IFN- $\gamma^+$  CD4<sup>+</sup> T

cells present in the large intestine (Morrison et al., 2013). Transfer of *ex-vivo* sorted IL-17A<sup>+</sup>, IL-17A<sup>+</sup> IFN- $\gamma$ <sup>+</sup> and IFN- $\gamma$ <sup>+</sup> into *Hh*<sup>+</sup> RAG KO mice resulted in all the mice developing colitis, suggesting that each of these cells are colitogenic (Morrison et al., 2013). Assessment of *ex-vivo* sorted IL-17A<sup>+</sup>, IL-17A<sup>+</sup> IFN- $\gamma$ <sup>+</sup> and IFN- $\gamma$ <sup>+</sup> CD4<sup>+</sup> T cells for histone modifications revealed that Th17 cells are predisposed to up-regulate the Th1 program (Morrison et al., 2013). Furthermore, fate mapping of the Th17 cells using IL-17A-eYFP fate reporter mice revealed that Th17 cells progressively change phenotype, transitioning via an IL-17A<sup>+</sup> IFN- $\gamma$ <sup>+</sup> stage to become cells that extinguish IL-17A production but continue to secrete IFN- $\gamma$  (hereafter called ex-Th17 cell) (Morrison et al., 2013).

## 1.5 INTESTINAL HOMEOSTASIS

The gut represents a unique challenge for the immune system as it has to maintain tolerance to the millions of commensal bacteria and food antigens that it is exposed to, while at the same time mount a response against pathogens. As a consequence, the gut microenvironment is inherently anti-inflammatory, with a number of different mechanisms in place that maintain intestinal homeostasis and prevent the development of intestinal inflammation. The following section describes some of the regulatory factors that are important for maintaining intestinal homeostasis.

### 1.5.1 Tregs and intestinal homeostasis

Tregs play a critical role in maintaining immune homeostasis and tolerance in the gut. This is evidenced by the fact that humans who lack Tregs or have non-functional Tregs due to genetic mutations in FoxP3 suffer from severe intestinal inflammation (Bacchetta et al., 2006; McMurchy et al., 2009). Similarly, mice lacking FoxP3<sup>+</sup> Tregs also develop severe colitis (Fontenot et al., 2003).

Among the different Treg populations defined, tTregs, pTregs and Tr1 cells (Groux et al., 1997; Mucida et al., 2007; Uhlig et al., 2006) have been shown to protect from the development of T cell transfer colitis however, it is unclear which population plays a more important role in maintaining intestinal homeostasis. Colonic Treg TCR sequencing found that both tTregs and pTregs mediate tolerance to Ag from commensal bacteria (Cebula et al., 2013; Lathrop et al., 2011) and based on expression of tTreg marker NRP1, it was shown that 50% of FoxP3<sup>+</sup> Tregs in the colon are tTregs and the other half pTregs (Weiss et al., 2012). These results suggest that both these Treg populations contribute equally to maintaining intestinal homeostasis. Interestingly, full protection from the disease observed in FoxP3-deficient mice required the presence of both pTregs and tTregs (Haribhai et al., 2011), further strengthening the notion that these cells act in concert to maintain intestinal homeostasis. Further studies to assess the contribution of Tr1 cells, pTregs and tTregs to protecting against intestinal inflammation are needed.

### 1.5.2 IL-10 and intestinal homeostasis

IL-10 is an anti-inflammatory cytokine and studies in man and mouse have shown that it is vital for maintaining intestinal homeostasis. Mutations in the IL-10-receptor (IL-10R) and defects in IL-10 expression and IL-10 signalling pathways have been associated with human IBD (Glocker et al., 2009; Lees et al., 2011; Shim and Seo, 2014). Homozygous loss of function mutations in *IL10* and the *IL10R* cause severe infantile IBD in humans (Kotlarz et al., 2012). Mice deficient in IL-10 (Kuhn et al., 1993) or the IL-10R (Spencer et al., 1998) spontaneously develop colitis. Furthermore, IL-10 was found to be protective in T-cell transfer colitis (Asseman et al., 1999; Carthew and Sontheimer, 2009) and IL-10 gene therapy improved DSS colitis (Sasaki et al., 2005) and TNBS colitis (Lindsay et al., 2002). In the *Hh* colitis model, WT mice infected with *Hh* do not develop intestinal inflammation whereas *Hh*-infection of IL-10 KO mice or WT mice concomitantly treated with a blocking antibody to the IL-10R (anti-IL-10R) leads to the development of intestinal inflammation (Kullberg et al., 2006; Kullberg et al., 1998). IL-10 therapy has been trialed in humans. Initial studies showed that IL-10 therapy was safe and well tolerated (Colombel et al., 2001; Fedorak et al., 2000; Schreiber et al., 2000). Subsequent studies showed that while IL-10 therapy did improve Crohn's disease activity index, this change was not significant (van Deventer et al., 1997). In fact, IL-10 treatment did not result in significant clinical improvement or remission rates in CD patients compared to those treated with the placebo (Buruiana et al., 2010; Herfarth and Scholmerich, 2002). There are several possible explanations for this. Firstly, it is possible that the dose of IL-10 is too low to elicit a response. Secondly, different individuals have different disease phenotypes/severity of disease. Patients with inherently low IL-10-levels benefited more from IL-10 supplementation (Colombel et al., 2001). Furthermore, patients with very severe disease benefited from IL-10-supplementation compared to patients with less severe disease (Schreiber et al., 2000). Thirdly, animal models of colitis suggest that IL-10 may only be effective at preventing disease development and not effective at ameliorating established disease (Barbara et al., 2000; Herfarth et al., 1998), therefore IL-10 therapy may be better suited to be given during remission phase rather than to treat active inflammation. Finally, IL-10 alone may fail to suppress all the pro-inflammatory mediators. As such, IL-10 therapy may still be beneficial to treat human IBD and is still under active investigation.

IL-10 is mainly produced by T cells, B cells, macrophages, NK cells and DCs (reviewed by (Paul et al., 2012)). Although few studies have been done to assess the importance of IL-10 derived from different cells in maintaining intestinal homeostasis, current findings suggest that in the gut, CD4<sup>+</sup> T-cell derived IL-10 constitutes an important source of IL-10 as CD4<sup>+</sup> T-cell specific deletion of IL-10 led to the development of spontaneous colitis (Roers et al., 2004). Macrophage-specific deletion of IL-10 however, did not induce spontaneous colitis, suggesting that macrophage-derived IL-10 is dispensable for gut homeostasis (Zigmond et al., 2014). Among the CD4<sup>+</sup> T cells, Th2, Tr1 and FoxP3<sup>+</sup> Tregs are thought to be the major sources

of IL-10. FoxP3<sup>+</sup> Treg-specific deletion of IL-10 led to the development of spontaneous colitis in the gut, but not systemic autoimmunity as seen with FoxP3-deficient mice, suggesting that Treg-derived IL-10 is specially important for maintaining homeostasis in the gut (Rubtsov et al., 2008).

IL-10 regulates immune responses in the gut through several mechanisms. IL-10R-signaling in macrophages polarizes them to an anti-inflammatory phenotype as evidenced by the fact that macrophage-specific deletion of the IL-10R resulted in severe spontaneous colitis with the production of pro-inflammatory mediators by these cells (Zigmond et al., 2014). IL-10 can directly act on Th17 cells to suppress them (Huber et al., 2011). Th17 cells express the IL-10R and are directly suppressed by Tr1 cells and FoxP3<sup>+</sup> Tregs in an IL-10-dependent manner (Huber et al., 2011). Treatment of RAG KO mice with recombinant IL-10 reduced the frequency of IL-17A<sup>+</sup> and IL-17A<sup>+</sup> IFN- $\gamma$ <sup>+</sup> cells in established T cell transfer colitis, showing that Th17 cells can be directly suppressed by IL-10 (Huber et al., 2011).

### **1.5.3 MicroRNAs and intestinal homeostasis**

The understanding of the role that microRNAs play in IBD is in its early stages. A small number of studies have profiled microRNAs and found them to be differentially expressed in tissues and peripheral blood of patients with active UC and CD when compared to healthy controls, suggesting that altered microRNA expression might contribute to driving the inflammatory response in IBD (Wu et al., 2011; Wu et al., 2010; Wu et al., 2008) (**Table 1.3**). Indeed, several studies in human IBD and animal models of colitis have shown that overexpression and down-regulation of certain microRNAs do promote the inflammatory response. For example, miR-21 is overexpressed in both human UC and in DSS colitis (Shi et al., 2013; Yang et al., 2013). In these studies, miR-21 was found to repress RhoB, a protein important for maintaining tight junction integrity and transepithelial resistance (Shi et al., 2013; Yang et al., 2013) (**Table 1.4**). Other examples of how overexpression of certain microRNAs augments the pathogenic immune response in different colitis models and human IBD can be found in **Table 1.4**. MiR-124 was found to be down-regulated in paediatric UC, DSS and IL-10 KO models of colitis (Koukos et al., 2013). Koukos et al found that down-regulation of miR-124 led to de-repression of miR-124 target STAT3, and thereby promoted the pathogenic Th17 response (Koukos et al., 2013)(**Table 1.5**). More examples of how down-regulation of certain microRNAs promotes pathogenic immune responses in different colitis models and human IBD are described in **Table 1.5**.

**Table 1.3 MicroRNA profiling in tissues and peripheral blood of healthy controls and patients with active UC and CD**

<b>IBD type</b>	<b>Tissue</b>	<b>Research findings</b>	<b>Reference</b>
Active UC	Sigmoid colon	<b>Increased expression:</b> miR-16, miR-21, miR-23a, miR-24, miR-29a, miR-126, miR-195, let-7f <b>Decreased expression:</b> miR-192, miR-375, miR-422b	<b>(Wu et al., 2008)</b>
Active CD	Sigmoid colon	<b>Increased expression:</b> miR-23b, miR-106a, miR-191 <b>Decreased expression:</b> miR-192, miR-375, miR-422b	<b>(Wu et al., 2010)</b>
Active CD	Terminal ileum	<b>Increased expression:</b> miR-16, miR-21, miR-223, miR-594	
Active CD	Peripheral blood	<b>Increased expression:</b> miR-199a-5p, miR-362-3p, miR-340*, miR-532-3p, miRplus-E1271 <b>Decreased expression:</b> miR-149*, miRplus-F1065	<b>(Wu et al., 2011)</b>
Active UC		<b>Increased expression:</b> miR-28-5p, miR-151-5p, miR-199a-5p, miR-340*, miRplus-E1271, miR-103-2*, miR-362-3p, miR-532-3p, miR-3180-3p, miRplus-E1035, miRplus-F1159 <b>Decreased expression:</b> miR-505*	

**Table 1.4 MicroRNAs that are overexpressed in human IBD and animal models of colitis and their mRNA targets**

MiR	Colitis model	Target or Pathway	Research findings	Reference
miR-21	DSS	RhoB	MiR-21 is up-regulated during inflammation. MiR-21 KO mice show improved survival in DSS colitis. RhoB is important for maintenance of integrity of epithelial tight junctions. MiR-21 targets RhoB to impair tight junction integrity and transepithelial resistance.	(Shi et al., 2013)
	Human UC			(Yang et al., 2013)
miR-21	TNBS DSS T cell transfer	Th1 pathway	MiR-21 is overexpressed in IBD. MiR-21 KO mice show exacerbated TNBS and T cell transfer colitis and reduced DSS colitis. In T cell transfer colitis, CD4 <sup>+</sup> CD45RB <sup>high</sup> cells from miR-21 KO mice were prone to Th1 polarisation.	(Wu et al., 2014)
miR-155	DSS	Th1/Th17 pathway	MiR-155 is overexpressed in DSS colitis. MiR-155 KO mice show decreased clinical scores and frequencies of Th1 and Th17 cell compared to WT mice.	(Singh et al., 2014b)
miR-155	Human UC	FOXO3a	MiR-155 is overexpressed in UC patients with active disease. MiR-155 targets FOXO3a, which suppresses IκBα resulting in an increase in TNFα and IL-8.	(Min et al., 2014)
miR-29a	DSS Human UC	MCL-1	MiR-29a is overexpressed in both UC patients and DSS colitis. It targets MCL-1 leading to apoptosis of intestinal epithelial cells.	(Lv et al., 2014)
miR-29a	DSS Human CD	IL-23	MiR-29a is induced by NOD2 signaling in DCs of CD patients and mice. MiR-29a down-regulates IL-23 by directly targeting IL-12p40 (one of the sub-units of heterodimeric cytokine IL-23). Loss of miR-29a in disease may help to promote inflammation by promoting the Th17 pathway.	(Brain et al., 2013)
miR-150	DSS Human UC	c-Myb BCL-2	MiR-150 was found to be up-regulated in the colon of humans with active UC and mice with DSS colitis. MiR-150 was found to target transcription factor c-Myb, which in turn promotes anti-apoptotic protein Bcl-2. Thus overexpression of miR-150 led to increases apoptosis via downregulation of c-Myb and Bcl-2.	(Zhang et al., 2010)

<b>MiR</b>	<b>Colitis model</b>	<b>Target or Pathway</b>	<b>Research findings</b>	<b>Reference</b>
miR-595 miR-1246	Human UC Human CD	NCAM1 FGFR2	MiR-595 and miR-1246 are overexpressed in serum of patients with active UC and CD patients compared to inactive disease. MiR-595 targets NCAM1 (a cell adhesion molecule) and FGFR2 (fibroblast growth factor receptor 2), which are necessary for differentiation, proliferation and repair of the colonic epithelium and tight junction-maintenance.	<b>(Krissansen et al., 2015)</b>
miR-106b miR-93	Human CD	ATG16L1	Increased expression of miR-106b and miR-93 was seen in colons of patients with active CD. MiR-106b and miR-93 were found to target autophagy protein ATG16LI leading to decreased autophagy-dependent clearance of bacteria.	<b>(Lu et al., 2014)</b>
miR-142-3p	Colonic epithelial cells Jurkat T cells		MiR-142-3p was found to be target autophagy gene ATG16L1. Overexpression of miR-142-3p led to reduced levels of ATG16L1 levels and thus decreased autophagy.	<b>(Zhai et al., 2014)</b>

**Table 1.5 MicroRNAs that are down-regulated in human IBD and animal models of colitis and their mRNA target**

<b>MiRNA</b>	<b>Colitis model</b>	<b>Target or Pathway</b>	<b>Research findings</b>	<b>Reference</b>
miR-124	DSS IL-10 KO Paediatric UC	STAT3	MiR-124 was down-regulated in the colon of colitic IL-10 KO mice, in the TNBS model and in paediatric UC patients (active vs inactive disease). MiR-124 was found to target STAT3. Loss of miR-124 expression, promoted STAT3 expression thus promoting the Th17 pathway.	<b>(Koukos et al., 2013)</b>
miR-146b	DSS	Siah2	MiR-146b decreases intestinal inflammation and promotes epithelial barrier repair by repressing Siah2 to activate NF-kB activity	<b>(Nata et al., 2013)</b>
miR-19a	DSS Human UC	TNF- $\alpha$	MiR-19a was found to be down-regulated in the colon of patients with UC and mice with DSS colitis. MiR-19a was found to target TNF- $\alpha$ . Thus a decrease in miR-19a levels led to an increase in TNF- $\alpha$ expression.	<b>(Chen et al., 2013a)</b>
miR-10a	IL-10 KO MyD88 KO RAG KO	IL-12/IL-23p40	MiR-10a is down-regulated by intestinal microbiota in DCs through TLR-TLR ligand interactions via the MyD88 pathway. MiR-10a targets IL-12/IL-23p40 suggesting that down-regulation of miR-10a may be a mechanism of maintaining intestinal inflammation.	<b>(Xue et al., 2011)</b>
miR-141	TNBS IL-10 KO Human CD	CXCL12 $\beta$	MiR-141 is down-regulated in TNBS and IL-10 KO colitis as well as in CD patients. MiR-141 regulates CXCL12 in epithelial cells, which promotes leukocyte infiltration. Loss of miR-141 during inflammation increases CXCL12 expression and promotes leukocyte infiltration.	<b>(Huang et al., 2014)</b>
miR-200b	Human UC Human CD	TGF- $\beta$	Mir-200b is down-regulated in the inflamed colon of UC and CD patients. MiR200b inhibits epithelial-mesenchymal transition by targeting TGF- $\beta$ and thereby promoting growth of intestinal epithelial cells.	<b>(Chen et al., 2013b)</b>

## 1.6 AIMS

IBD is a chronic inflammatory disorder of the gastrointestinal tract, that is caused in part, by a dysregulated immune response to microbial flora (Xavier and Podolsky, 2007). Our lab uses the *Hh* colitis model to study intestinal inflammation, and in this model, inflammation is associated with CD4<sup>+</sup> Th1 and Th17 cells. Previous work in the lab has extensively characterised the pathogenic effector CD4<sup>+</sup> T cell response during *Hh*-induced colitis (Morrison et al., 2013), however, the alterations in different regulatory mechanisms in the gut are less well understood. Thus the broad aim of this the work carried out in this thesis, was to examine whether cell-intrinsic and cell-extrinsic mechanisms of regulation of effector T cells are altered during *Hh*-induced colitis.

Specifically, the aims were as follows:

- **To examine whether the expression of microRNAs (a cell-intrinsic mechanism of regulation) is altered in the inflamed large intestine of *Hh*<sup>+</sup> IL-10 KO mice at the tissue level and LP CD4<sup>+</sup> T-cell level, compared to healthy controls.**

MicroRNAs represent a cell-intrinsic mechanism of regulation. Although MicroRNAs have been shown to be alternatively expressed in human IBD, and altered microRNA expression has also been shown to potentiate the pathogenic immune response in human IBD and animal models of colitis, the role of microRNAs has not been examined in *Hh* colitis. Thus, the aim of the experiments carried out in chapter four of this thesis was to examine whether microRNAs are differentially expressed in the inflamed large intestine of *Hh*<sup>+</sup> IL-10 KO mice at the tissue level and LP CD4<sup>+</sup> T-cell level, compared to healthy controls.

- **To characterise the phenotype of Tregs and IL-10-producing LP CD4<sup>+</sup> T cells in the large intestine during an inflammatory and a non-inflammatory immune response to *Hh*.**

Tregs and the anti-inflammatory cytokine IL-10 represent some of the cell-extrinsic mechanisms of regulating effector CD4<sup>+</sup> T cells. Using the modified *Hh*/RAG KO adoptive transfer model of colitis, previous studies have shown that Tregs protect against the development of *Hh* colitis in an IL-10-dependent manner (Kullberg et al., 2002). However, the phenotype of different Treg subsets and IL-10<sup>+</sup> CD4<sup>+</sup> T cells in the large intestine LP have not been examined before. Therefore, the experiments carried out in Chapter 5 of this thesis were performed in order to characterise the phenotype of Tregs and of IL-10-producing CD4<sup>+</sup> T cells in the large intestine LP during a non-inflammatory immune response to *Hh* (*Hh*<sup>+</sup> IL-10-sufficient mice) and compare it to that of an inflammatory immune response to *Hh* (*Hh*<sup>+</sup>/anti-IL-10R-treated IL-10-sufficient mice) at 2 weeks pi.

## CHAPTER 2. MATERIALS AND METHODS

### 2.1 ANIMALS

C57BL/6 (B6) IL-10 KO mice were originally developed by Ralf Kuhn and Werner Muller, University of Cologne, Cologne, Germany (Kuhn et al., 1993), and were kindly provided by Anne O'Garra at the National Institute for Medical Research (NIMR, London, UK). B6 *IL-17A<sup>cre</sup>R26R<sup>eYFP</sup>* (IL-17A-eYFP) fate-reporter mice (Hirota et al., 2011) were kindly donated by the laboratory of Brigitta Stockinger (NIMR, London, UK). B6 129S6-IL-10 mice (*tiger* mice) USA (Kamanaka et al., 2006) were originally developed by Richard Flavell, Yale University, Connecticut, and kindly provided by the laboratory of Adrian Mountford (University of York, UK). Male and female B6 IL-10 KO, B6 *IL-17A<sup>cre</sup>R26R<sup>eYFP</sup>*, B6 129S6-IL-10 and B6 CD45.2 WT mice were bred and maintained under SPF conditions at the Biological Services Facility (BSF) at the University of York. All mice were bred and maintained in individually ventilated cages (IVC) racking from Techniplast (Buggugiate, Italy) and a maximum number of five mice were housed per cage. The cages were kept in a 12 hour light cycle/ 12 hour dark cycle set to gentle rise and fall i.e. during the light cycle, lights brighten gradually to reach their maximum brightness after 30 minutes and during the dark cycle, the lights dim gradually over 30 minutes before complete darkness is attained. The mice were fed on the '2018 Teklad global 18% protein rodent diet' from Harlan Laboratories (Bicester, UK). All mice were between 6 and 24 weeks of age at the start of experimental work. As a result of limited mouse numbers, in some experiments, a mixture of male and female mice were used in some experiments. All experiments in this thesis were carried out with the approval of the UK Home Office and in accordance with the rules and regulations of the 'Animal and Scientific Procedures Act 1986' (ASPAs) and the Animal Welfare and Ethical Review Body at the University of York.

### 2.2 *HELICOBACTER HEPATICUS* CULTURE AND INFECTIONS

*Hh* (standard Frederick isolate 1A) (Fox et al., 1994) was cultured on blood agar plates containing *Campylobacter*-selective antibiotics at 37°C, kept under microaerobic conditions (88% N<sub>2</sub>, 5% CO<sub>2</sub> and 7% H<sub>2</sub>) for 48 hours. Blood agar base, laked horse blood and *Campylobacter* Selective Supplement (containing trimethoprim, vancomycin and polymixin B); based on Skirrow formulation (Skirrow, 1977), were purchased from Oxoid (Hampshire, UK). Using sterile cotton swabs, *Hh* was collected into sterile endotoxin-free PBS (Sigma-Aldrich, Dorset, UK). Optical density of this suspension was estimated by using a spectrophotometer to determine the OD<sub>600</sub> (assuming an OD<sub>600</sub> of 1 is equal to 1 x 10<sup>8</sup>/ml total bacteria) and viability was assessed using the LIVE/DEAD *BacLight* kit (Invitrogen, Paisley, UK) according to the manufacturer's instructions. *Hh* was then diluted with sterile endotoxin-free PBS to 30 x

$10^6$  *Hh*/ml for infection. Mice were inoculated by oral gavage with 0.5 ml PBS containing  $15 \times 10^6$  *Hh*.

## **2.3 ISOLATION AND INJECTION OF ANTI-IL-10R MONOCLONAL ANTIBODY**

### **2.3.1 Isolation of anti-IL-10R mAb**

The following reagents, used to isolate anti-IL-10R mAb were obtained from Sigma-Aldrich (Dorset, UK): D-glucose, meat peptone, non-essential amino acids (NEAA), Glutamine, RPMI 1640, 2-mercaptoethanol (2-ME), penicillin and streptomycin. Integra CELLline flasks were obtained from INTEGRA (Zizers, Switzerland). Hybridoma cells were obtained from ATCC via a material transfer agreement with DNAX. Ultra low IgG fetal bovine serum (FBS) was purchased from Thermo Fisher Scientific (Loughborough, UK). Two solutions were used during the course of the protocol; nutrient medium and cell compartment medium. Nutrient medium consisted of RPMI 1640 containing 100 u/ml penicillin, 100  $\mu$ g/ml streptomycin, 2 mM glutamine, 0.1 mM NEAA, 0.2% w/v meat peptone, 0.25% w/v D-glucose and 50  $\mu$ M 2-mercaptoethanol. Cell compartment medium was prepared by adding 10 ml of ultra-low IgG FBS to 90 ml of nutrient medium and sterile filtering the solution. All the steps were carried out in the hood using sterile technique.

An appropriate number of 1B1.3a anti-IL-10R hybridoma cells were diluted in cell compartment medium to a concentration of  $2 \times 10^6$  cells/ml. 15 ml of 1B1.3a anti-IL-10R hybridoma cells were carefully pipetted into the cell compartment of the CELLline flask, taking care to remove as many bubbles as possible. 1 L of pre-warmed nutrient medium was added to the medium compartment of the CELLline flask. The flask was closed and placed in an incubator at 37°C for 72 hrs. The medium was removed from the flask and cells pipetted out of the cell compartment into a 15 ml tube. Cell viability and yield were assessed by dye exclusion with trypan blue. An appropriate number of cells were kept aside for passage in a 50 ml tube, and the volume made up to 15 ml with cell compartment medium. As before, 1 L of pre-warmed RPMI 1640 containing 300  $\mu$ l 2-ME and 78 ml of nutrient medium was added to the medium compartment of the CELLline flask. The flask was closed and placed in an incubator at 37°C for a further 72 hrs.

The remaining hybridoma cells were centrifuged at 1200 RPM for ten minutes at 4°C. The supernatant was transferred to a fresh 15 ml tube and stored at -80°C until mAb could be purified on a Protein G column as described in the next section.

### **2.3.2 Purification of mAb on Protein G column**

The following reagents were used to purify mAb on the Protein G column: Protein G Sepharose 4 Fast Flow (Pharmacia, West Sussex, UK), binding buffer (20mM phosphate buffer, pH 7.0), elution buffer (0.1M glycine-HCl buffer, pH 2.7), neutralization buffer (1M Tris-HCl buffer, pH 8.0), storage buffer (20mM phosphate buffer, pH 7.0+ 20% ethanol) and PBS. 1B1.3a mAb was purified on the Protein G Column according to the manufacturer's instructions. The tube containing purified 1B1.3a was then stored at 4°C.

## 2.4 CELL ISOLATIONS

### 2.4.1 Lamina propria cell isolation

The following reagents that were used for the isolation of lamina propria cells were obtained from Sigma-Aldrich (Dorset, UK); Dubelcco's phosphate buffered saline (PBS), HEPES, EDTA, glutamine, Dithiothreitol (DTT), Non-essential amino acids (NEAA), sodium pyruvate, 2-mercaptoethanol, penicillin and streptomycin. HyClone fetal calf serum (FCS) was purchased from Thermo Fisher Scientific (Loughborough, UK) and heat inactivated by incubating in a 56°C waterbath for 30 minutes. 'RPMI Wash medium' used during the protocol was made up of RPMI-1640 containing 10mM HEPES, 100 U/ml penicillin and 100 µg/ml streptomycin. 'Complete medium' used during the protocol consisted of RPMI-1640 with 10% FCS, 100 u/ml penicillin, 100 µg/ml streptomycin, 10mM HEPES, 0.1 mM NEAA, 1 mM sodium pyruvate, 2 mM L-glutamine and 50 µM 2-mercaptoethanol.

Mice were sacrificed and the colon and cecum were removed and placed in a petri dish containing PBS/HEPES (PBS containing 10 mM HEPES, 100 U/ml penicillin and 100 µg/ml streptomycin). Tissues were cut open longitudinally using scissors and the luminal contents removed by gently scraping the surface with forceps. After cleaning, the tissues were transferred into a clean petri dish and cut into pieces 5 mm in length using a scalpel. The pieces were then transferred to a 50 ml tube containing 25 ml of PBS/HEPES. The tissue pieces were washed by vortexing the tube, the pieces were allowed to sediment and the supernatant discarded and another 20 ml of PBS/HEPES added. After washing in PBS/HEPES, the epithelial layer was removed by incubating the tissue pieces at 37°C in 15 ml of pre-warmed RPMI/EDTA (RPMI-1640 containing 2% FCS, 10 mM HEPES, 5 mM EDTA, 2 mM glutamine, 1mM DTT, 100 U/ml penicillin and 100 µg/ml streptomycin) for 20 minutes at 225 rpm in an orbital shaker. The tissue was then vortexed briefly, allowed to sediment and the supernatant discarded. 15 ml of pre-warmed RPMI/EDTA was added once again and the incubation and vortexing steps repeated. The tissue pieces were then washed twice in 15 ml of RPMI/HEPES (RPMI-1640 containing 2% FCS, 10 mM HEPES, 2 mM glutamine and 100 U/ml penicillin and 100 µg/ml streptomycin) in order to remove the EDTA and DTT. The tissue was subsequently digested with 0.3125 mg/ml Liberase TL (Roche, West Sussex, UK) and 0.125 U/ml Dnase I (Sigma, Dorset, UK) in 4 ml RPMI/HEPES per uninfected cecum and colon pool and in 8 ml RPMI/HEPES per infected cecum/colon pool. Tissues were digested for 1 hour at 37°C while shaking at 225 rpm in an orbital shaker. The suspension of digested tissue was filtered through a 100 µm cell strainer and any tissue fragments that were not filtered through were broken up with a plunger. The strainer was washed with 10ml of RPMI/EDTA and the resulting cell suspension centrifuged at 1100 rpm for 7 minutes. Depending on the experiment, one of the following 3 steps were then carried out: 1) The cell pellet was resuspended in 10 ml of RPMI

wash medium and then centrifuged at 1100 rpm for 7 minutes. The supernatant was discarded and the cell pellet resuspended in complete medium 2) The cell pellet was resuspended in 10 ml of 40% isotonic Percoll (Sigma, Dorset, UK) in RPMI 1640 and then centrifuged at 1800 rpm for 20 minutes at 10°C. The supernatant was discarded and the cell pellet washed with 10 ml RPMI wash medium by centrifuging at 1100 rpm for 7 minutes. The supernatant was discarded and the cell pellet resuspended in complete medium 3) The cell pellet was resuspended in 5 ml of 40% isotonic Percoll in RPMI 1640 and then underlayered with 3 ml of 80% isotonic Percoll in PBS and centrifuged at 1800 rpm for 20 minutes at 10°C. Following centrifugation, cells were collected from the 40/80% Percoll interface, placed in a fresh tube and washed with RPMI wash medium by centrifuging at 1100 rpm for 7 minutes. The supernatant was discarded and the resulting cell pellet was then resuspended in complete medium. In all three conditions, cell viability and yield were then assessed by dye exclusion with trypan blue and counting on an Improved Neubauer haemocytometer.

#### **2.4.2 Spleen and mesenteric lymph node isolation**

Spleens and mesenteric lymph nodes (MLNs) collected from sacrificed animals were placed in a Petri dish containing 3 ml of wash medium. The tissues were broken up into a single cell suspension with a syringe plunger, and the back of the plunger washed with a further 3 ml of wash medium. The resulting suspension was then transferred to a 15 ml tube, the Petri dish washed with a further 3ml of wash medium and the washings transferred to the 15 ml tube. Large debris was allowed to settle and the supernatant was transferred to a fresh 15 ml tube. The cells were centrifuged at 1100 rpm for 7 minutes and the supernatant discarded. The MLN cells were resuspended in 12 ml of wash medium. Spleen cells were resuspended in 1 ml/spleen of red blood cell-lysing buffer (Sigma, Dorset, UK) and incubated at room temperature for 5 minutes before adding a further 12 ml of wash medium. The spleen cells were centrifuged at 1100 rpm for 7 minutes and the supernatant discarded. The spleen cells were then resuspended in 12 ml of wash medium. Both spleen and MLN cells were centrifuged at 1100 rpm for 7 minutes and the resulting supernatant discarded. The cells were resuspended in complete medium and cell viability and yield were assessed by dye exclusion with trypan blue and counting on an Improved Neubauer haemocytometer.

### **2.5 STIMULATION OF CELLS WITH PHORBOL MYRISTATE ACETATE AND IONOMYCIN**

Following isolation of cells as described in section 2.4, LP, MLN and spleen cells were diluted to a concentration of  $5 \times 10^6$  cells/ml and 1.5 ml aliquoted into v-bottom tubes ( $7.5 \times 10^6$  cells/tube). Phorbol 12-myristate 13-acetate (PMA) and ionomycin were added to get final concentrations of 10 ng/ml of PMA and 1  $\mu$ g/ml of ionomycin. Cells were then incubated at 37 °C in 5% CO<sub>2</sub> for one hour. Brefeldin A was then added to each tube at a final concentration of

10 µg/ml, and the cells incubated for a further 3 hours at 37°C in 5% CO<sub>2</sub>. Tubes were then topped up with PBS and centrifuged at 1100 rpm for 7 minutes. The resulting supernatant was discarded and the cells resuspended in complete medium and surface stained as described in section 2.6.

## 2.6 FLOW CYTOMETRY

Depending on the experiment, cells were surface stained and fixed and then intracellularly stained with the combinations of fixatives and permeabilisation buffers summarized in **Table 2.1**.

**Table 2.1 Combinations of fixation and permeabilisation buffers used during different flow cytometry staining protocols.**

Protocol	Fixant	Permeabilisation buffer
A	2% paraformaldehyde (PFA) (Sigma-Aldrich, Dorset, UK)	Permeabilisation buffer made in-house (subsequently referred to as 0.1% saponin buffer). This buffer consists of PBS containing Mg <sup>2+</sup> and Ca <sup>2+</sup> with 0.1% saponin (Calbiochem, La Jolla, USA), 10mM HEPES, and 1% FCS.
B	2% PFA (Sigma-Aldrich, Dorset, UK)	1x eBio permeabilisation buffer (Bioscience, Hatfield, UK).
C	eBio fixation-permeabilisation buffer (eBioscience, Hatfield, UK)	1x eBio permeabilisation buffer (Bioscience, Hatfield, UK).
D	eBio fixation-permeabilisation buffer (eBioscience, Hatfield, UK)	0.1% saponin buffer

### 2.6.1 Staining for surface markers

LP, MLN and spleen-cell suspensions in complete medium were diluted to a concentration of 20 x 10<sup>6</sup> cells/ml and the desired volume was aliquoted into v-bottom tubes. Cells were then labeled with antibodies against specific surface markers (see **Table 1**), at pre-determined concentrations, a fixable live-dead dye (Aqua Dead Cell Stain, Invitrogen, Paisley, UK) and 0.125µg/100 µl FcγRIII/ FcγRII block (anti-CD16/CD32) and mixed with a pipette. The cells were left at 4°C in the dark for ten minutes and then washed by adding 2 ml of PBS and centrifuging at 1100 rpm for 7 minutes. The supernatant was removed and cells washed again with another 1ml of PBS and subsequent centrifugation at 1100 rpm for 7 minutes. The supernatant was removed and cells were fixed by adding 100ul of either 2% PFA or 1x fixation-permeabilisation buffer (eBioscience) per tube. The cells were left in fixative for 1hr in the dark at 4°C. Cells were then washed by centrifuging at 1100 rpm for 7 minutes with 2 ml of 1x PBS. The wash step was repeated with 1 ml of PBS. The supernatant was discarded and the cells then

resuspended in 500  $\mu$ l of FACS buffer (0.5% FCS in PBS). Cells were stored protected from light at 4°C until acquisition on a flow cytometer.

### **2.6.2 Intracellular staining for cytokines and transcription factors**

LP, MLN and spleen-cell suspensions in PBS were diluted to a concentration of  $10 \times 10^6$  cells/ml and 100  $\mu$ l ( $1 \times 10^6$  cells) was aliquoted into v-bottom tubes. Cells were then labeled with antibodies against specific surface markers (see **Table 1**), at pre-determined concentrations, a fixable live-dead dye (Aqua Dead Cell Stain, Invitrogen, Paisley, UK) and 0.125 $\mu$ g/100  $\mu$ l Fc $\gamma$ RIII/ Fc $\gamma$ RII block (anti-CD16/CD32) and mixed with a pipette. The cells were left at 4°C in the dark for ten minutes and then washed by adding 2ml of PBS and centrifuging at 1100 rpm for 7 minutes. The supernatant was removed and cells washed again with another 1ml of PBS and subsequent centrifugation at 1100 rpm for 7 minutes. The supernatant was removed and cells were fixed by adding 100 $\mu$ l of either 2% PFA or 1x fixation-permeabilisation buffer (eBioscience) per tube. The cells were left in fixative for 1hr in the dark at 4°C. Cells were then washed by adding 500  $\mu$ l of either 1x permeabilisation buffer (in case of protocol B and C of **Table 2.1**) or 0.1% saponin buffer (in case of protocol A and D of **Table 2.1**) and centrifuging at 1100 rpm for 7 minutes. The wash step was repeated, supernatant removed and cells resuspended in 100  $\mu$ l of either 1x permeabilisation buffer (in case of protocol B and C of **Table 2.1**) or 0.1% saponin buffer (in case of protocol A and D of **Table 2.1**) containing 0.25 $\mu$ g/100  $\mu$ l Fc $\gamma$ RIII/Fc $\gamma$ RII block (anti-CD16/CD32) and mixed with a pipette. If cells were to be stained for transcription factors (see **Table 2.2**), the required volume antibodies were added directly to the 1x permeabilisation buffer/ 0.1% saponin buffer containing FcR block and 100  $\mu$ l aliquoted per sample tube. The cells were then incubated for 30 minutes at 4°C while protected from light. After 30 minutes, anti-cytokine antibodies were added (see **Table 2.2**) at pre-determined concentrations, and the cells incubated for a further 30 minutes at 4°C while protected from light. The cells were then washed by adding 500  $\mu$ l of 1x permeabilisation buffer and centrifuging at 1100 rpm for 7 minutes. The wash step was repeated twice; once with 500  $\mu$ l of 1x permeabilisation buffer/ 0.1% saponin buffer and subsequently with 500  $\mu$ l of FACS buffer (0.5% FCS in PBS). The cells were then resuspended in 500  $\mu$ l of FACS buffer and stored protected from light at 4°C until acquisition on either a BD LSR Fortessa X-20 (BD Biosciences, Oxford, UK) or a CyAn ADP analyzer (Beckman Coulter, High Wycombe, UK).

**Table 2.2 Monoclonal antibodies used for detection of surface markers, cytokines and transcription factors by flow cytometry.**

NAME	CLONE	CONJUGATE	COMPANY
<i>SURFACE MARKERS</i>			
CD3	145-2C11	PerCP	eBioscience
		PE-Cy7	
CD4	GK 1.5	PE-Cy7	eBioscience
	RM4-5	BV605	BD Biosciences
CD8	53-6.7	FITC	BD Biosciences
CD19	eBio1D3	PE	eBioscience
CD25	PC61	PE	eBioscience
CD49b	HM $\alpha$ 2	PE	Biolegend
LAG-3	C9B7W	BV711	BD Biosciences
Pan-CD45	30-F11	PE-Cy7	eBioscience
CD45.2	A20	PE	eBioscience
CD62L	MEL-14	APC	BD Biosciences
TCR- $\beta$	H57-597	PE	eBioscience
CD16/32	2.4G2	Purified	BD Biosciences
<i>CYTOKINES</i>			
IFN- $\gamma$	XMG1.2	PE-Cy7	eBioscience
	XMG1.2	eFluor450	eBioscience
IL-17A	TC11-18H10	PE	eBioscience
	eBio17B7	FITC	eBioscience
IL-10	JES5-16E3	APC	eBioscience
<i>TRANSCRIPTION FACTORS</i>			
FoxP3	FJk-16a	eFluor450	eBioscience
Helios	22F6	APC	eBioscience

## 2.7 CELL SORTING

### 2.7.1 Fluorescence-activated cell sorting of CD4<sup>+</sup> T cells from the large intestinal lamina propria

Lamina propria cells from the large intestine of uninfected and 2-wk *Hh*-infected IL-10 KO mice were isolated as described in section 2.3.1. Cell suspensions were diluted to a concentration of  $25 \times 10^6$  cells/ml and filtered through a 40  $\mu$ m filter. Cells were then labeled with antibodies against CD45, CD4 and TCR $\beta$  (see **Table 2.2**) at pre-determined concentrations and stained in a 15 ml tube. The cells were left at 4°C in the dark for ten minutes and then washed by adding 10 ml of high FACS buffer (ice cold PBS + 5% FCS + 0.5mM EDTA) and centrifuging at 1100 rpm for 7 minutes. The supernatant was removed and cells washed again with a further 10 ml of high FACS buffer and subsequent centrifugation at 1100 rpm for 7 minutes. The samples were then resuspended in high FACS buffer and transferred to a 5ml snap-cap tube. CD4<sup>+</sup> T cells were then sorted as cells that were CD45<sup>+</sup> CD4<sup>+</sup> TCR $\beta$ <sup>+</sup> using a Mo-flo Astrios (Beckman Coulter). Cells were sorted into tubes containing complete media (RPMI-1640 with 10% FCS, 100 u/ml penicillin, 100  $\mu$ g/ml streptomycin, 10 mM HEPES, 0.1 mM NEAA, 1 mM sodium pyruvate, 2 mM L-glutamine and 50  $\mu$ M 2-mercaptoethanol). Following the sort, post-sort purities were done to ensure purity of the sorted population. Sorted cells were centrifuged at 4°C for 15 min at 1200 RPM. The supernatant was carefully removed and cell pellet resuspended in 700  $\mu$ l of Qiazol (Qiagen, Manchester, UK), vortexed for 1 minute and then snap frozen on dry ice before storing the samples at -80°C.

### 2.7.2 .Fluorescence-activated cell sorting of naïve CD4<sup>+</sup> T cells from the spleen and MLN.

Splenic and MLN cells were isolated as described in section 2.4.2. Cell suspensions were diluted to a concentration of  $25 \times 10^6$  cells/ml and filtered through a 40  $\mu$ m filter. Cells were then labeled with antibodies against CD4 and CD62L (see **Table 2.2**) at pre-determined concentrations. The cells were stained as described above in section 2.7.1. Naïve CD4<sup>+</sup> T cells were sorted as cells that were CD4<sup>+</sup> CD62L<sup>high</sup>. Cells were sorted into tubes containing complete media. Following the sort, post-sort purities were done to ensure purity of the sorted population. The cells were then centrifuged at 4°C for 15 min at 1200 RPM. The supernatant was carefully removed and cell pellet resuspended in complete medium and stored at 4 °C until ready to culture.

## 2.8 RNA EXTRACTION

### 2.8.1 Total RNA extraction from sorted cells

Sorted CD4<sup>+</sup> T-cell samples stored at -80°C in 700 µl of Qiazol were allowed to thaw and RNA extracted by carrying out a Qiazol/chloroform phase extraction. Once the samples had thawed, 200 µl of chloroform was added and the tubes shaken vigorously by hand for 2 minutes. The samples were allowed to stand at room temperature for 5 minutes and then spun at 13000 x g for 15 minutes in a microfuge at 4°C. The aqueous phase was carefully transferred with a pipette to a fresh Eppendorf tube, mixed with 1.5 volumes of 100% ethanol, and subsequent extraction carried out using the miRNeasy micro kit, according to the manufacturer's instructions (Qiagen, Manchester, UK). On-column DNase digestion was carried out to remove any contaminating genomic DNA using the RNase-free DNase set according to the manufacturer's instructions (Qiagen, Manchester, UK). The only modifications made to the manufacturer's RNA extraction protocol, in order to maximize the yield and improve RNA quality as advised by their technicians, were: i) an extra wash was carried out at each wash step and ii) instead of immediately centrifuging the columns, they were first incubated with each wash buffer for 3 minutes at room temperature before centrifuging. RNA quality and quantity was assessed by measuring the absorbance at 230, 260 and 280 nm with a NanoDrop 2000 spectrophotometer (Thermo Fisher Scientific, Loughborough, UK). All samples were then stored at -80 °C.

### 2.8.2 Total RNA extraction from tissues

Cecal and colonic tissue were collected from uninfected and 1, 2, 8 and 14-wk *Hh*-infected mice and stored overnight at 4°C in *RNAlater* (Sigma-Aldrich, Dorset, UK). Thereafter, the *RNAlater* was removed and the samples stored at -80°C until RNA extraction. RNA was extracted from tissues using TRIzol (Invitrogen, Paisley, UK) /chloroform phase extraction. In brief, tissue samples were placed in 1 ml of TRIzol and a sterile ball bearing added to each tube. Samples were then homogenized at 50 Hz for 12 minutes in a Tissue Lyser (Qiagen, Manchester, UK). The resulting suspension was transferred to a fresh tube and 0.2 ml of ice-cold chloroform added. The samples were shaken vigorously by hand for 2 minutes and then left to stand on ice for 10 minutes. The samples were then spun at 13000 x g for 15 minutes in a microfuge at 4°C. The aqueous phase was carefully transferred with a pipette to a fresh Eppendorf tube. An equal volume of ice-cold isopropanol was added and tubes inverted a few times to mix. The samples were left overnight at -20°C. The following day, samples were centrifuged at 13000 x g for 15 minutes at 4°C. The RNA precipitates at the bottom as a yellow-white pellet. The supernatant was removed and the RNA pellet washed twice by adding 1ml of ice-cold 75% ethanol and centrifuging at 13000 x g for 15 minutes at 4°C. After the second wash, the ethanol was removed and the samples allowed to air dry for ten minutes, before resuspending in 25-50 µl of RNase-free water. The samples were left on ice for 1 hour to allow

RNA to dissolve completely. Colonic and cecal RNA were quantified by measuring absorbance at 230, 260 and 280 nm with a NanoDrop 2000 spectrophotometer. RNA was diluted to between 1 and 2 µg/ml with additional RNase-free water and any contaminating genomic DNA was then removed using a DNA-free Kit (Applied Biosystems, Warrington, UK) according to the manufacturer's instructions. All samples were then stored at -80 °C.

## **2.9 RNA PRECIPITATION PROTOCOLS**

RNA was extracted from sorted cell samples as described in section 2.8.2. When analyzed on the NanoDrop 2000 spectrophotometer, some of the RNA extracted from sorted cells had poor 260:230 ratios indicating a residual phenol/guanidine contamination. In order to remove possible contaminants, we tested different RNA precipitation protocols (Rio, 2011) detailed below:

### **2.9.1 RNA precipitation using lithium chloride**

The volume of the extracted RNA was made up to 100 µl with nuclease-free water (Qiagen, UK). 0.1 volumes of 4 M lithium chloride and 3 volumes of ice cold 100% ethanol were added. The samples were mixed well and left overnight at -80 °C. Samples were allowed to thaw, and then centrifuged at 4 °C for 15 minutes at 12,000 x g. The pellet was then washed with 50 µl of ice-cold 70% ethanol and supernatant removed. The pellet was air dried for ten minutes and then resuspended in the required volume of nuclease-free water. RNA quantity and quality were assessed by measuring the absorbance at 230, 260 and 280 nm with a NanoDrop 2000 spectrophotometer.

### **2.9.2 RNA precipitation using ethanol**

The volume of the extracted RNA was made up to 100 µl with nuclease-free water (Qiagen, UK). 0.1 volumes of 3 M sodium acetate and 2.2 volumes of ice cold 100% ethanol were added. The samples were mixed well and left overnight at -80 °C. Samples were allowed to thaw, and then centrifuged at 4 °C for 15 minutes at 12,000 x g. The pellet was then washed with 50 µl of ice cold 70% ethanol and supernatant removed. The pellet was air dried for ten minutes and then resuspended in the required volume of nuclease-free water. RNA quantity and quality were assessed by measuring the absorbance at 230, 260 and 280 nm with a NanoDrop 2000 spectrophotometer.

### **2.9.3 RNA precipitation using isopropanol**

The volume of the extracted RNA was made up to 100 µl with nuclease-free water (Qiagen, UK). In some experiments, 1 µl of 10mg/ml molecular grade glycogen was added. 0.1 volumes of 3M sodium acetate and 0.7 volumes of ice cold isopropanol were then added and the samples mixed well and left overnight at -80 °C. Samples were allowed to thaw, and then centrifuged at 4°C for 15 minutes at 12,000 x g. The pellet was then washed with 50 µl of ice cold 70% ethanol and supernatant removed. The pellet was air dried for ten minutes and then resuspended in the required volume of nuclease-free water. RNA quantity and quality were assessed by measuring the absorbance at 230, 260 and 280 nm with a NanoDrop 2000 spectrophotometer.

## **2.10 REVERSE TRANSCRIPTION (RT)**

### **2.10.1 MicroRNA RT**

RNA extracted from large intestinal tissues and sorted cells were reverse transcribed using the Taqman MicroRNA Reverse Transcription kit (Applied Biosystems, Warrington, UK), according to the manufacturer's instructions. Taqman MicroRNA RT primers for mmu-miR-155, mmu-miR-326, mmu-miR-132, mmu-miR-21, mmu-miR-31, mmu-miR-96, mmu-miR-210, mmu-miR-181a and RNU6 were purchased from Applied Biosystems (Warrington, UK).

### **2.10.2 Messenger RNA RT**

RNA extracted from large intestinal tissues was reverse transcribed using the following protocol. Briefly, 1 ng-5 µg of total RNA in DEPC-treated water was transferred to a sterile nuclease-free PCR tube and the final volume made up to 14 µl with DEPC-treated water. 2 µl of 50ng/µl random hexamers (Invitrogen, Paisley, UK) and 1 µl 10mM dNTP mix (containing 2.5 mM each of the following: dATP, dGTP, dCTP and dTTP, from Promega, Southampton, UK) were added to the RNA and incubated at 65°C for 5 minutes then 4°C for 3 minutes using a DNA Engine Thermal Cycler (Bio-Rad, Hemel Hempstead, UK). All the tubes were briefly centrifuged and kept on ice. To each tube, the following were added: 5 µl 15x First strand buffer, 2 µl 0.1M DTT, 0.5 µl RNase OUT and 0.5 µl SuperScript RT II reverse transcriptase (all from Invitrogen, Paisley UK). The reaction mixture was mixed by gentle pipetting. The tubes were then incubated at 25°C for 10 minutes, then 42°C for 60 minutes, followed by 70°C for 10 minutes and finally at 4°C for 5 minutes using a DNA Engine Thermal Cycler. Samples were stored at -20°C until ready for use.

## 2.11 QUANTITATIVE REAL-TIME PCR (QRT-PCR) ANALYSIS

### 2.11.1 qRT-PCR for microRNA

Taqman-based qRT-PCR was used to quantify microRNA levels in both whole colon and cecum samples and in sorted cells. All reactions were performed in MicroAmp Optical 96-well reaction plates (Applied Biosystems, Warrington, UK). Each well contained 1.33  $\mu$ l of RT product, 10  $\mu$ l of either Taqman Universal PCR Master Mix II (2x) (without UNG) or Taqman Fast Universal PCR Master Mix II (2x) (without UNG) (Applied Biosystems, Warrington, UK), 7.67  $\mu$ l of nuclease free water (Qiagen, UK) and 1  $\mu$ l of Taqman Small RNA Assay (20x) (Applied Biosystems, Warrington, UK). Taqman Small RNA Assays for mmu-miR-155, mmu-miR-326, mmu-miR-132, mmu-miR-21, mmu-miR-31, mmu-miR-96, mmu-miR-210, mmu-miR-181a and RNU6 were purchased from Applied Biosystems (Warrington, UK). The plates were sealed, centrifuged briefly and run on either an ABI Prism 7300 Sequence Detection System or StepOnePlus Real Time PCR System (Applied Biosystems, Warrington, UK). On the ABI Prism 7300 Sequence Detection System, the following cycling conditions were used: 50°C for 2 minutes, 95°C for 10 minutes followed by 40 cycles of 95°C for 15 seconds and 60°C for 1 minute for all primer sets. On the StepOnePlus Real Time PCR System, the following cycling conditions were used: 95°C for 20 seconds followed by 40 cycles of 95°C for 1 second and 60°C for 20 seconds for all primer sets. Data were analysed using either ABI 7300 SDS or StepOne Software (Applied Biosystems, Warrington, UK). MicroRNA expression levels were normalised to RNU6 using  $\Delta$ Ct calculations. Mean relative microRNA expression levels between control and experimental groups were determined using the  $2^{-\Delta\Delta C_t}$  calculations.

### 2.11.2 qRT-PCR for messenger RNA

SYBR green-based qRT-PCR was used to quantify mRNA levels of IL-17A, IFN- $\gamma$  and ETS-1 in cecum and colon tissue. All reactions were performed in MicroAmp Optical 96-well reaction plates (Applied Biosystems, Warrington, UK). Each well contained 12.5  $\mu$ l 2x Power SYBR Green Mix (Applied Biosystems, Warrington, UK), 1  $\mu$ l each of the forward and reverse primer, 5.5  $\mu$ l of nuclease free water (Qiagen, UK) and 5  $\mu$ l cDNA (5-50ng). The final volume in each well was 25  $\mu$ l. Primers for HPRT, IL-17A, IFN- $\gamma$  and ETS-1 were purchased from Sigma-Aldrich (Dorset, UK) and their sequences are shown in **Table 2.3**. The 96-well plates were sealed and run on ABI Prism 7300 Sequence Detection System (Applied Biosystems, Warrington, UK). The following cycling conditions were used: 50°C for 2 minutes, 95°C for 10 minutes followed by 40 cycles of 95°C for 15 seconds and 60°C for 1 minute for all primer sets. Target gene expression levels were normalised to HPRT (hypoxanthine-guanine phosphoribosyl

transferase) using  $\Delta\text{Ct}$  calculations. Mean relative mRNA expression levels between control and experimental groups were determined using the  $2^{-\Delta\Delta\text{Ct}}$  calculations.

**Table 2.3. Primer sequences**

TARGET	SEQUENCE
HPRT	Forward: 5' –GCGTCGTGATTAGCGATGATGAAC-3'
	Reverse: 5' –ATCTCCTTCATGACATCTCGAGCAAGTC-3'
IL-17A	Forward: 5' –GCTCCAGAAGGCCCTCAG-3'
	Reverse: 5' –CTTCCCTCCGCATTGACA-3'
IFN- $\gamma$	Forward: 5' –GGATGCATTCATGAGTATTGC-3'
	Reverse: 5' –GCTTCCTGAGGCTGGATTC-3'
ETS-1	Forward: 5' –TCCTATCAGCTCGGAAGAACTC-3'
	Reverse: 5' –TCTTGCTTGATGGCAAAGTAGTC-3'

## 2.12 MICRORNA MICROARRAY

A mouse microRNA microarray slide (Release 19.0), containing 8 arrays and representing 1247 mouse microRNAs/array was purchased from Agilent Technologies (Stockport, UK). The microarray was kindly done by Sally James (Genomics, Technology facility, Department of Biology, University of York, York UK) according to the manufacturer's instructions and the data kindly analyzed by Sandy McDonald (Genomics, Technology facility, Department of Biology, University of York, York UK) using GeneSpring GX Software (Agilent Technologies, Stockport, UK).

## 2.13 HISTOLOGY

### 2.13.1 Embedding tissues in wax and sectioning

Colon pieces or three quarters of the cecum were removed from uninfected and 1, 2, 8 and 14-wk *Hh*-infected mice and fixed overnight in 2ml of 10% buffered formalin. Before embedding the tissue in wax, the fixative and water was removed from the tissues by dehydrating them by incubation with increasingly concentrated ethanol. Briefly, after fixation, the formalin was removed and replaced with 70% ethanol for 1 hour (or long term storage until ready to embed the tissues). Tissues were transferred to embedding cassettes and submerged in fresh 90% ethanol for 2 hours on a shaker at room temperature. The cassettes were then transferred into fresh 100% ethanol for 2 hours on a shaker at room temperature, and then transferred twice more into fresh 100% ethanol for a period of 1 hour each (on a shaker at room temperature). The ethanol was then removed from the dehydrated tissue using xylene (Thermo Fisher

Scientific, Loughborough, UK). In brief, in a fume hood, the cassettes containing tissues were transferred into a glass jar containing fresh xylene and left for 2 hours at room temperature. The cassettes were then transferred into fresh xylene 3 more times, incubating them for 2 hours followed by 1 hour and finally 30 minutes, before blotting the cassettes free of xylene, and then transferring them into a pot containing melted paraffin wax at 65 °C and left overnight. In order to get rid of any residual xylene, the cassettes were transferred thrice more into fresh wax pots, leaving them for an hour in each pot at 65 °C. Finally, tissues were removed from their cassettes, placed in a mould containing a thin layer of melted wax. The tissues were then oriented in the correct position, the mould topped up with melted wax, and the back of the cassette placed over the mould. The mould containing the tissue was subsequently left to solidify at room temperature. Once the wax had solidified and cooled, it was removed from the mould and stored at room temperature, until the samples were ready to cut. The wax-embedded tissue samples were cut into 5 µm thick sections using a manual rotary microtome RM2235 from Leica Microsystems (Milton Keynes, UK). The sections were placed in warm water (40 °C) and then picked up gently onto poly-lysine coated slides (Thermo Fisher Scientific, Loughborough, UK) and left to dry overnight before staining with haematoxylin and eosin.

### **2.13.2 Haematoxylin and eosin staining**

Paraffin sections were dewaxed by immersing the slides in xylene for 5 minutes. The slides were then transferred into fresh xylene pots twice more, immersing for 5 minutes in each pot. Tissue sections were then dehydrated by immersing them in tubs of decreasing concentrations of ethanol, starting with 3 minutes in 100% ethanol, followed by 1 minute each in 95%, 90% and 70% ethanol. The sections were washed briefly in distilled water and then stained with filtered Mayer's Haematoxylin (Leica Microsystems, Milton Keynes, UK) for 8 minutes. The sections were then rinsed in running tap water for 5 minutes and then dipped in eosin (1.5 g eosin dissolved in 95% ethanol) (Sigma-Aldrich, Dorset, UK) 12 times (1-2 seconds/immersion) and then washed in distilled water until the eosin stopped streaking. Tissue sections were then rehydrated by dipping the slides in 50% ethanol 10 times, 70% ethanol 10 times and then leaving them in 95% ethanol for 30 seconds followed by a 100% ethanol for 1 minute. Following rehydration, residual alcohol was removed from the tissue sections by immersing them in xylene for 1 minute. The sections were then transferred into another pot of xylene until ready to mount (within 2 hrs). Slides were removed from xylene and mounted with DePex Gurr (VWR, Lutterworth, UK), a xylene-based mounting medium. A drop of DePex was added onto the tissue, a cover slip placed over the tissue, and the slide left to dry for two days. The tissue sections were then blindly scored from 0-3 for each parameter of inflammation i.e. extent of hyperplasia/goblet cell depletion in the epithelium, inflammation in the lamina propria, area affected and finally, markers of severe inflammation such as submucosal inflammation,

crypt abscesses, ulceration or extensive fibrosis. A total score out of a maximum possible score of 12 calculated by adding up the individual scores.

## **2.14 *IN VITRO* CD4<sup>+</sup> T-CELL POLARISATION**

Tissue culture plasticware was purchased from Nunc (Roskilde, Denmark), Sarstedt (Numbrecht, Germany) and Sigma-Aldrich (Dorset, UK). Recombinant human TGF- $\beta$  and recombinant human IL-6 were purchased from Peprotech (London, UK). Recombinant mouse IL-23 and recombinant mouse IL-12 was purchased from eBioscience (Hatfield, UK). Recombinant human IL-2 was from Roche (West Sussex, UK).

### **2.14.1 Primary stimulation of naïve CD4<sup>+</sup> T cells**

Splenic cells were isolated from a C57BL/6 WT mouse as described in section 2.4.2 and irradiated at 3000 rad for 5 minutes in an RS2000 X-Ray Generator. Following irradiation, cells were centrifuged at 1200 rpm for 10 minutes at room temperature. The resulting cell pellet was washed twice by resuspending in RPMI wash medium and centrifuging at 1200 rpm for 10 minutes at room temperature. The cell pellet was resuspended in complete medium. Cell viability and was assessed by dye exclusion with trypan blue. Irradiated splenocytes were used as antigen presenting cells.

Naïve CD4<sup>+</sup> CD62L<sup>+</sup> cells were sorted from a pool of MLN and spleen cells from uninfected IL-10 KO mice as described in section 2.7.2. Two polarizing conditions were set up in 96-well flat-bottom plates: 'Th1' and 'Th17' conditions. Naïve CD4<sup>+</sup> T cells and irradiated splenocytes were diluted appropriately in complete medium.  $2 \times 10^5$  CD4<sup>+</sup> T cells were cultured with  $7.5 \times 10^5$  irradiated splenocytes in each well. Soluble anti-CD3 from BD biosciences (Oxford, UK) was added to each well at a final concentration of 1  $\mu$ g/ml. To the Th1 condition, IL-12 was added to each well at a final concentration of 10 ng/ml. To the Th17 condition, TGF- $\beta$ , IL-6 and IL-23 were added to each well at a final concentration of 1 ng/ml, 50 ng/ml and 10 ng/ml, respectively. The plate was incubated at 37 °C for 2 days. Cells were then split and to all Th1 wells, recombinant human IL-2 was added at a final concentration of 5 U/ml. To the Th17 wells, recombinant mouse IL-23 was added at a final concentration of 10 ng/ml. The plate was incubated at 37°C. Over the next four days, plates were monitored and depending on growth, split and fresh IL-2 or IL-23 added to the respective conditions.

### **2.14.2 Secondary stimulation of polarized CD4<sup>+</sup> T cells**

48-well plates were coated overnight at 4°C with 100  $\mu$ l/well of anti-CD3 at a concentration of 10  $\mu$ g/ml in PBS. On day 7 post primary stimulation, cells from each condition (No addition, Th1 and Th17) were pooled and cell viability and yield was assessed by dye exclusion with trypan blue.

Anti-CD3 was removed from the 48-well plates coated overnight at 4°C by washing with RPMI wash medium. Secondary cultures were set up by culturing  $3 \times 10^5$  cells/ml from each condition (Th1 and Th17) in medium alone or with plate-bound anti-CD3. Subsequently, cells were collected for RNA extraction at 0, 6, 12, 24, 48 and 72 hours post anti-CD3 stimulation. At 72 hours, supernatants were also collected, transferred into 96-well round-bottom plates and stored at -20 °C until cytokine amounts were assessed by ELISA.

## **2.15 ENZYME-LINKED IMMUNOSORBENT ASSAY (ELISA)**

The murine IL-17A ELISA was purchased from Mabtech (Nacka strand, Sweden). Rat-anti-mouse IFN- $\gamma$  (clone R4-6A2) and biotin-rat-anti-mouse IFN- $\gamma$  (clone XMG1.2) were purchased from BD Biosciences (Oxford, UK). Streptavidin-conjugated horseradish peroxidase (SA-HRP) was obtained from KPL (Maryland, USA). Bovine serum albumin (BSA) and ABTS substrate were both purchased from Sigma-Aldrich (Dorset, UK). All ELISA experiments were performed in Nune Maxisorb 96-well plates (Roskilde, Denmark).

The general protocol used to measure IL-17A and IFN- $\gamma$  amounts in supernatants of stimulated *in vitro* polarized CD4<sup>+</sup> T cells was as follows: 96-well plates were coated overnight with 100  $\mu$ l/well of appropriate capture antibody diluted in PBS (2  $\mu$ g/ml for IFN- $\gamma$  and 1  $\mu$ g/ml for IL-17A). After coating, unbound capture antibody was removed and the plates were blocked with 200  $\mu$ l/well of blocking buffer (5% milk in wash buffer [0.05% Tween20 in PBS]). After blocking, plates were washed four times with wash buffer using a Skan washer 400 plate washer (Molecular Devices, Wokingham, UK). Samples and standards were diluted appropriately with diluent (wash buffer containing 1% BSA) and added in duplicate at a final volume of 100  $\mu$ l/well. The IL-17A top standard was added at 8 ng/well and the IFN- $\gamma$  standard was added at 4 ng/well. Both standards were diluted 2-fold over eight wells. Non-specific binding was controlled for by including at least 8 'blank' wells/plate containing 100  $\mu$ l/well of diluent. Plates were incubated overnight at 4°C and then were washed four times and 100  $\mu$ l of biotinylated detection antibody (appropriately diluted in diluent to get a final concentration of 2  $\mu$ g/ml for IFN- $\gamma$  and 0.5  $\mu$ g/ml for IL-17A) added to each well. The plates were incubated at 37 °C for 2 hours and then washed four times. 100  $\mu$ l SA-HRP (1:1000) was then added to each well and the plates incubated for 1 hour at 37 °C. Plates were washed four times and 100  $\mu$ l of freshly prepared ABTS substrate at concentration of 1 mg/ml in citrate buffer added to each well. Citrate buffer contained 0.02 M citric acid, 0.04 M anhydrous Na<sub>2</sub>HPO<sub>4</sub> and 0.003% H<sub>2</sub>O<sub>2</sub>. The colour was allowed to develop, and stopped by the addition of 15  $\mu$ l/well of 10% sodium dodecyl sulphate (SDS). Optical density at 405nm was determined using a Versamax microplate reader (Molecular Devices, Wokingham, UK), and data analysed on Softmax Pro v5 software.

## **2.16 BIOINFORMATIC TOOLS**

The bioinformatics tool miRWalk was used to identify predicted mRNA targets of specific microRNAs.

## **2.17 STATISTICAL ANALYSIS**

Statistical analysis was done using GraphPad Prism (v5) software, with one-way ANOVA or Mann Whitney U-tests employed when appropriate. To control for false discovery rate, post tests were also carried out. In case where one-way Anova was used, a bonferroni correction was applied, and in cases where a Mann Whitney-U test was done, a Tukey's post test was done. Values of  $P < 0.05$  were considered significant.

For the MicroRNA microarray, samples were normalized using 90<sup>th</sup> percentile normalization, and a students t-test followed by a Benjamni-Hochberg test (False discovery rate test) applied. Following these tests, values of  $P < 0.05$  were considered significant.

# CHAPTER 3. AN OPTIMISED PROTOCOL FOR RNA EXTRACTION FROM LYMPHOCYTES

## 3.1 INTRODUCTION

Quantitative real-time polymerase chain reaction (qRT-PCR) and microarrays are techniques commonly used to measure the expression levels of microRNAs and messenger RNAs (mRNAs). The reliability of both techniques is strongly dependent on the quality of RNA used as the input material (Rio, 2011). In this study, we optimized a method to extract and concentrate total RNA from lymphocytes to yield good quality RNA that can be used for downstream applications such as a microarray.

The first step in any RNA extraction method involves lysing cells with a lysis buffer in order to release the RNA. Commonly used lysis buffers are TRIzol (Invitrogen) and Qiazol (Qiagen). TRIzol and Qiazol contain a mixture of phenol and guanidine isothiocyanate that disrupt cells, dissolve cellular components and denature protein (Rio, 2011). Once cells are lysed, chloroform is then added and the mixture centrifuged to yield 3 phases; a lower organic phase (red), an interphase that contains DNA and some denatured protein, and an upper aqueous phase (clear) that contains nucleic acids (DNA and RNA). RNA can then be extracted from the aqueous phase by using either RNA precipitation protocols in Eppendorf tubes, or commercially available kits that work on spin column technology. These spin columns contain a silica gel/glass fibre membrane (Rio, 2011). In the presence of ethanol and chaotropic salts such as guanidine isothiocyanate, RNA and DNA bind tightly to the silica membrane while less-charged cellular components flow through (Rio, 2011). DNA can then be removed by on column treatment with DNase 1 under high salt conditions to preserve the binding of RNA. The digested DNA is then washed off the membrane and the RNA can be eluted. RNA yield and purity is determined using a spectrophotometer. The bases in RNA absorb UV light at 250-265 nm, thus measuring the absorbance at 260 nm ( $A_{260}$ ) is used to quantify the amount of RNA in a sample (Rio, 2011). However, DNA, protein and phenol also absorb UV light at 260 nm. Thus, it is necessary to check that the RNA yield indicated by  $A_{260}$  is pure RNA and not contaminated with proteins/salts. Proteins absorb UV light at 280 nm while phenol and chaotropic salts absorb at 230 nm (Rio, 2011). For purified RNA, the ratio of  $A_{260}:A_{280}$  and  $A_{260}:A_{230}$  should be 1.8-2.0. Anything less than 1.8 in either of these ratios suggests a possible protein or phenol contamination, respectively. Our broad experimental aims involved extracting RNA from *ex vivo* sorted and *in vitro* cultured CD4<sup>+</sup> T cells for analysis of microRNA expression by microRNA microarray as well as by qRT-PCR. Lymphocytes generally have a low RNA content (Rio, 2011), and we found that this resulted in salt contamination not observed when RNA was extracted from high content RNA samples such as whole tissue.

In this study, we examined the quality of RNA obtained from different commercially available kits, as well as the efficiency of different RNA precipitation protocols at removing salt

contaminations and concentrating the RNA. We optimized the RNA extraction protocol of the microRNeasy micro kit from Qiagen, and identified cold isopropanol precipitation as the best RNA precipitation method to i) improve the quality of, and ii) concentrate the RNA extracted from lymphocytes.

## **3.2 RESULTS**

### **3.2.1 MicroRNeasy kits from Qiagen yield RNA with the least salt contamination**

Before extracting total RNA from our experimental samples, we wanted to test different commercially available RNA extraction kits to identify which one would be the best for our purpose. We used mesenteric lymph node (MLN) cells from uninfected IL-10 KO mice for all the optimisation experiments. We did so because using sorted CD4<sup>+</sup> T cells for our tests was prohibitive in terms of the time and cost required to procure the samples. Using MLN cells enabled us to assess total RNA yields as accurately as possible, as these cells mostly consist of lymphocytes (40% of which are CD4<sup>+</sup> T cells) and therefore were as close as possible to pure CD4<sup>+</sup> T cells in terms of RNA content. There are a number of commercially available kits to extract total RNA. Some kits only extract RNA >200 nucleotides in length and thus exclude the small RNAs such as microRNAs which are 22-25 nucleotides in length. Other kits also extract the small RNAs. We extracted total RNA from MLN cells from naïve IL-10 KO mice by 4 methods; 3 widely used commercially available kits that extract total RNA including microRNAs; 1) microRNeasy mini kits (Qiagen), 2) microRNeasy micro kits (Qiagen) and Direct-zol columns (Zymo research) and the protocol we usually use in our lab to extract RNA from tissues (using TRIzol as lysis buffer). The RNA yield and quality was measured on a NanoDrop 2000 spectrophotometer. The different RNA extraction methods vary in terms of the maximum amount of RNA that can bind to the column, the chemistry of the extraction, lysis buffer used and the final elution volume (**summarised in Table 3.1**).

**Table 3.1 Summary of different RNA extraction methods used**

RNA extraction method	Type of RNA extracted	Maximum binding capacity of the column	Chemistry	Lysis buffer used	Final Elution volume
Kullberg Lab method	Total RNA including microRNAs	Not Applicable	Phenol: Chloroform phase extraction	TRIzol	≥ 5-100 µl
miRNeasy mini kit	Total RNA including microRNAs	100 µg of RNA	Phenol: Chloroform phase extraction	Qiazol	≥ 30 µl
miRNeasy micro kit	Total RNA including microRNAs	45 µg of RNA	Phenol: Chloroform phase extraction	Qiazol	≥ 12 µl
Direct-zol Mini-prep Kit	Total RNA including microRNAs	50 µg of RNA	No phase extraction. Sample + lysis buffer loaded directly onto column	TRIzol	≥ 25 µl

The results showed that in three for the four methods where RNA was extracted from 600,000 MLN cells, the total yield of RNA obtained was 170-200 ng whereas when RNA was extracted from 1.2 million cells, the yield of RNA obtained tripled (**Table 3.2**). The results also demonstrated that in all of the four extraction methods, a low 260:230 ratio was observed, suggesting that the RNA extracted was contaminated with phenol/guanidine from the lysis buffers (**Table 3.2**).

**Table 3.2 Total RNA yield and quality obtained using different RNA extraction methods.**

Method <sup>a</sup>	MLN cell number <sup>b</sup>	Lysing Buffer	RNA Conc. ng/μl	Elution volume	Total RNA yield	260:280	260:230
Kullberg Lab method	600,000	TRIzol	12.79 ng/μl	15 μl	191.8 ng	1.81	0.71
miRNeasy mini kit	600,000	Qiazol	5.84 ng/μl	30 μl	175.2 ng	2.06	1.20
miRNeasy micro kit	600,000	Qiazol	14.70 ng/μl	12 μl	176.4 ng	1.81	1.43
Directzol kit	1.2 million	TRIzol	23.37 ng/μl	25 μl	688.8 ng	1.85	0.99

<sup>a</sup> All the data shown are representative of at least 3 replicates except for the ‘Kullberg lab method’ which was only done once.

<sup>b</sup> In all the RNA extractions except the Direct-zol Kit, the same starting pool of MLN cells were used

Poor 260:230 ratios are a common problem in samples with low RNA yield, so in order to get good quality RNA, we needed to optimize the method further. We decided to use the microRNeasy micro kits because the 260:230 ratio was the highest of all four RNA extraction methods, indicating the least salt contamination.

### **3.2.2 Splitting the sample into smaller aliquots and performing separate chloroform phase extraction on each aliquot improves RNA yield**

To try and improve the RNA yield, we decided to split samples of 600,000 MLN cells stored in Qiazol into two aliquots, perform a separate chloroform phase extraction on each of these aliquots and then pool the aqueous phases from both these aliquots and load it onto a single microRNeasy micro column to extract the RNA. The results showed that this method resulted in slightly higher RNA yields of 290-340 ng of total RNA (**Table 3.3**), compared to 170-190 ng obtained previously (**Table 3.2**). The 260:230 ratios were still poor therefore further optimization of this method was required (**Table 3.3**).

**Table 3.3 Improved RNA yield obtained by doing two phenol chloroform phase extractions and pooling the aqueous phase on to a single column to extract RNA.**

Method <sup>a</sup>	MLN cell number <sup>b</sup>	RNA Conc. ng/ml	Elution volume	Total RNA yield	260:280	260:230
miRNeasy micro kit	2 X 300,000	28.03 ng/ $\mu$ l	12 $\mu$ l	336 ng	1.81	0.71
miRNeasy micro kit	2 X 300,000	24.70 ng/ $\mu$ l	12 $\mu$ l	288 ng	2.06	1.20

<sup>a</sup> All the data shown are representative of 4 replicates.

<sup>b</sup> The same starting pool of MLN cells were used

### 3.2.3 Cold isopropanol precipitaton of RNA removes salt contamination and concentrates RNA

In spite of improving RNA yield, we were still unable to improve the 260:230 ratio nor had we managed to attain the concentration of RNA required by Agilent's microRNA microarray i.e. 100 ng/ $\mu$ l. There are different RNA precipitation methods that can be used to remove salt contamination and concentrate the RNA. RNA is inherently hydrophilic and readily dissolves in water (Rio, 2011). The principle of different RNA precipitation methods are based on reducing the hydrophilicity of RNA by the addition of salts such as lithium chloride and sodium acetate that decrease the pH (Rio, 2011). The pH is made further acidic by the addition of alcohols such as ethanol or isopropanol (Rio, 2011). Following centrifugation, the RNA is precipitated out and re-dissolved in nuclease free water. We extracted RNA from aliquots of 1.2 million MLN cells using the microRNA micro kit (Qiagen) and then tried three different RNA precipitation protocols; 1) lithium chloride and 100% ice cold ethanol, 2) sodium acetate and 100% ice cold ethanol and 3) sodium acetate and ice cold isopropanol. The results showed that all three RNA precipitation methods improved the 260:230 ratio, but precipitation with cold isopropanol was the most efficient at removing the salt contamination as the 260:230 ratio in this sample improved the most, changing from 0.3 to 1.64 (**Table 3.4**). Despite this, RNA precipitation also had notable disadvantages of the loss of approximately 50% of the total RNA and a decrease in the 260:280 ratio (**Table 3.4**). We decided to use cold isopropanol to precipitate and concentrate the RNA and try and optimize the protocol further in order to improve RNA recovery.

**Table 3.4 Efficiency of different RNA precipitation protocols at removing salt contamination and concentrating RNA.**

Sample	MLN cell number <sup>a</sup>	Method to concentrate <sup>b</sup>	RNA Conc ng/ $\mu$ l	Total RNA	% RNA recovered	260:280	260:230
Before conc	1.2 million cells	-	32	384 ng in 12 $\mu$ l	-	2.06	0.52
After conc		<b>Lithium chloride</b>	30	150 ng in 5 $\mu$ l	42%	1.64	1.22
Before conc	1.2 million cells	-	31	372 ng in 12 $\mu$ l	-	1.99	1.45
After conc		<b>Cold ethanol ppt</b>	37	185 ng in 5 $\mu$ l	54%	1.79	1.52
Before conc	1.2 million cells	-	18	216 ng in 12 $\mu$ l	-	1.9	0.3
After conc		<b>Cold isopropanol ppt</b>	21	105 ng in 5 $\mu$ l	53%	1.68	1.64

<sup>a</sup> The same starting pool of MLN cells were used.

<sup>b</sup> All the data shown are representative of at least 3 replicates.

### 3.2.4 The use of glycogen as a carrier improves RNA precipitation and RNA yield

In order to improve RNA recovery, we added glycogen as a ‘carrier’. Glycogen is a polysaccharide with limited solubility in isopropanol and forms a precipitate that traps RNA (Rio, 2011). When centrifuged, a visible pellet forms, greatly enhancing handling of RNA (Rio, 2011). We extracted total RNA from a sorted CD4<sup>+</sup> T-cell sample using the microRNA micro kit, and then added 1  $\mu$ l of a 10 mg/ml solution of glycogen to the total RNA. We then carried out cold isopropanol precipitation as before and measured RNA yield and quality using the Nanodrop 2000 spectrophotometer. The results showed that the addition of glycogen greatly improved the RNA recovered (**Table 3.5**). It is important to note that of the 924 ng of RNA originally extracted, 1  $\mu$ l was used to measure RNA yield on the nanodrop, leaving 847 ng of RNA that was subsequently precipitated. Bearing this in mind, the results suggest that the addition of glycogen as a carrier does help to precipitate most of the RNA from the sample (**Table 3.5**).

**Table 3.5 The use of glycogen as a ‘carrier’ greatly improves RNA recovery**

Sample	Cell No. <sup>a</sup>	Method to concentrate	RNA Conc ng/ $\mu$ l	Total RNA	% RNA Recovered	260:280	260:230
Before conc	3 million LP CD4 <sup>+</sup> T cells	-	77 $\mu$ l	924 ng in 12 $\mu$ l	-	2.00	1.46
After conc		<b>Isopropanol ppt (+ glycogen)</b>	139 ng/ $\mu$ l	695 ng in 5 $\mu$ l	82%	1.80	1.73

<sup>a</sup> The data shown in the table is representative of at least 3 replicates.

### 3.3 SUMMARY

In this study we have shown that:

- Of the methods examined, the MicroRNeasy micro kit from Qiagen yielded the RNA with the least salt contamination when RNA was extracted from a starting sample of relatively low cell numbers.
- The RNA yield from a given sample can be improved by splitting the sample into two aliquots and carrying out a separate chloroform phase extraction on each aliquot. The aqueous phase from each aliquot can be pooled onto a single column for subsequent RNA extraction.
- Of the different RNA precipitation methods we tested, in our hands, cold isopropanol precipitation was the most efficient at removing salt contamination and concentrating the RNA.
- The addition of glycogen as a ‘carrier’ helped to fully precipitate the RNA out of aqueous solution.

# CHAPTER 4. ALTERED EXPRESSION OF MICRORNAS IN *HELICOBACTER*-INDUCED INTESTINAL INFLAMMATION

## 4.1 INTRODUCTION

MicroRNAs are post-transcriptional gene regulators that play important roles in regulating cells of the immune system (Bartel, 2004). Altered expression of microRNAs in immune cells has been observed in several autoimmune disorders such as rheumatoid arthritis (Nakasa et al., 2008; Stanczyk et al., 2008), systemic lupus erythematosus (Dai et al., 2007) and multiple sclerosis (Du et al., 2009; Hu et al., 2013) as well as cancers of immune cell origin (Calin and Croce, 2006). Recent studies have shown that microRNAs are also dysregulated in IBD. MicroRNA microarray analysis of peripheral blood samples from patients with active UC and CD (Wu et al., 2011), sigmoid colon biopsies from chronically active UC and CD patients (Wu et al., 2008) and terminal ileal biopsies from chronically active CD patients (Wu et al., 2010) revealed a differential microRNA profile compared to healthy controls. While several studies have identified roles for altered microRNA expression contributing to intestinal pathology, in general, the full extent to which dysregulated microRNAs may potentiate the molecular mechanisms that give rise to intestinal inflammation are not very well characterized.

CD4<sup>+</sup> Th1 and Th17 cells are thought to contribute to the pathogenesis of both CD and *Hh*-induced colitis (Morrison et al., 2013; Xavier and Podolsky, 2007). There are a number of microRNAs that have been shown to have profound effects on CD4<sup>+</sup> T-cell development and function, suggesting that altered expression of microRNAs could play significant roles in promoting pathogenic T cell responses in T-cell mediated autoimmune and inflammatory diseases. For example, several studies have shown that miR-155 is overexpressed in EAE, and was found to promote Th1 and Th17 responses by repressing ETS-1, an inhibitor of the Th17 pathway and SOCS1, an inhibitor of JAK/STAT signalling (Singh et al., 2014b; Zhang et al., 2014b) (Hu et al., 2013; O'Connell et al., 2010; Yao et al., 2012). MiR-20b was found to be down-regulated in EAE. Consequently, the miR-20b targets ROR $\gamma$ t and STAT3 were overexpressed, promoting the Th17 pathway (Zhu et al., 2014a). These and other examples of how the altered expression of microRNAs plays significant roles in promoting pathogenic T cell responses in T-cell mediated autoimmune and inflammatory diseases is highlighted in **Table 4.1**.

Although expression of microRNAs has been shown to modulate the inflammatory immune responses in both IBD and animal models of colitis (as described in **Table 1.4 and 1.5** of the general introduction), the role of microRNAs in *Hh*-induced colitis has not been studied before. Utilising the *Hh*<sup>+</sup> IL-10 KO model of colitis (Kullberg et al., 1998), the broad aim of this study was to determine whether microRNAs are dysregulated at the site of *Hh* colonisation in the large intestine during *Hh*-induced intestinal inflammation compared to uninfected controls

both at the tissue level and the CD4<sup>+</sup> T-cell level. At the tissue level, we chose to examine miR-155, miR-326 and miR-132 because these microRNAs have been previously shown to potentiate the Th17 and/or Th1 response (Du et al., 2009; Fan et al., 2012; Lin et al., 2014; Nakahama et al., 2013; O'Connell et al., 2010). At the CD4<sup>+</sup> T-cell level, we profiled the expression of microRNAs from CD4<sup>+</sup> T cells isolated from the large intestine LP at the peak of intestinal inflammation (2 wks pi) and compared it to that of uninfected controls.

**Table 4.1 Modulation of development and function of CD4<sup>+</sup> T cells by selected microRNAs**

MicroRNA	Expression	Location	Target	Implications of altered microRNA expression	Reference
MiR-155	Increased	Th1 cells and Th17 cells  Th17 cells  Th17 and Tregs	Unknown target  ETS-1  SOCS1	Lack of miR-155 leads to reduction in Th1 and Th17 cell numbers and in the severity of EAE and colitis.  Th17 cells deficient in miR-155 were defective in their ability to induce EAE. Increased miR-155 confers Th17 cells with encephalitogenic potential through repression of negative regulator ETS-1, resulting in an upregulation of IL-23R expression by these cells.  MiR-155 inhibits SOCS1 to promote JAK/STAT signaling. This promotes differentiation of both Tregs and Th17 cells	(Singh et al., 2014b; Zhang et al., 2014b) (O'Connell et al., 2010)  (Hu et al., 2013)  (Yao et al., 2012)
MiR-326	Increased	Th17 cells	ETS-1	Increased miR-326 expression promotes Th17 differentiation in EAE by silencing ETS-1, a negative regulator of Th17 differentiation.	(Du et al., 2009)
MiR-132/212 cluster	Increased	Th17 cells	BCL6	Stimulation of the aryl-hydrocarbon receptor leads to induction of miR-132/212, which induces Th17 differentiation partially through miR-212-mediated inhibition of a suppressor of Th17 differentiation called BCL6.	(Nakahama et al., 2013)
MiR-210	Increased	Th17 cells	HIF-1 $\alpha$	Increased miR-210 expression inhibited Th17 differentiation by suppressing HIF1 $\alpha$ , a transcription factor important for Th17 differentiation in hypoxic environments.	Wang et al., 2014a)
MiR-310a	Increased	Th17 cells	PIAS3	Increased miR-310a in CD4 <sup>+</sup> T cells promotes Th17 differentiation by repressing an inhibitor of STAT3 called PIAS3 in EAE.	(Mycko et al., 2012)
MiR-133b MiR-206	Increased	Th17 cells	IL-17A/F Locus	MiR-133b and miR-206b are induced by IL-123 in naïve CD4 <sup>+</sup> T cells. They cluster upstream at the IL-17A/F locus and promote the production of IL-17A	(Haas et al., 2011)
MiR-20b	Decreased	Th17 cells	ROR $\gamma$ t STAT3	Down-regulation of miR-20b in Th17 cells during EAE was found to promote Th17 differentiation as miR-20b is a potent inhibitor of ROR $\gamma$ t and STAT3.	(Zhu et al., 2014a)

MicroRNA	Expression	Location	Target	Implications of altered microRNA expression	Reference
MiR181a	Decreased	Th1 cells	CXCR3 STAT1	In a rodent model of EAE, decreased miR-181a expression was shown to potentiate the Th1 response via loss of miR-181a mediated repression of CXCR3 and STAT1.	(Bergman et al., 2013)
MiR-29	Decreased	Th1 cells	T-bet IFN- $\gamma$	MiR-29 directly binds to T-bet and IFN- $\gamma$ . Loss of miR-29 leads to unrestrained T-bet expression and Th1 differentiation.	(Smith et al., 2012)
MiR-146a	Decreased	CD4 <sup>+</sup> T cells	Protein Kinase C epsilon (PRKCE)	Down-regulation of miR-146a promotes Th1 differentiation, because it allows expression of its target PRKCE, which phosphorylates STAT4 to allow Th1 differentiation.	(Mohnle et al., 2015)
MiR-155	Decreased	Th2 cells	PU.1	MiR-155 is over-expressed in a murine model of allergic inflammation. MiR-155 was found to target transcription factor PU.1, a negative regulator of Gata 3 and thus Th2 differentiation. Over-expression of miR-155 resulted in diminished PU.1 levels, allowing Th2 differentiation.	(Malmhall et al., 2014)
MiR-126a	Increased	Airway wall	POU domain class 2 activating factor 1	MiR-126a was found to target POU domain class 2 activating factor 1, an activator of PU.1. Thus overexpression of miR-126a in the airway wall of a murine model of house dust mite-induced allergic inflammation promoted Th2 responses by repressing expression of POU domain class 2 activating factor 1 and thus PU.1 (an inhibitor of Gata3 and thus Th2 differentiation).	(Mattes et al., 2009)
MiR-31	Decreased	FoxP3 <sup>+</sup> Tregs	FoxP3	MiR-31 directly binds to FoxP3 to inhibit its expression. Decreased miR-31 enhanced Treg responses by allowing greater FoxP3 expression.	(Rouas et al., 2009)
MiR-210	Increased	FoxP3 <sup>+</sup> Tregs	FoxP3	MiR-210 directly binds to FoxP3 to inhibit its expression. Increased miR-210 expression in patients suffering from psoriasis vulgaris exacerbated disease by suppressing FoxP3.	(Zhao et al., 2014)

Here, we have shown that microRNAs expression is altered in the large intestine of colitic *Hh*<sup>+</sup> IL-10 KO mice, at both the tissue level and CD4<sup>+</sup> T cell-level when compared to uninfected controls. At the tissue level, kinetic examination revealed that the change in expression of the microRNAs examined correlated with the development of intestinal inflammation. Microarray profiling of large intestinal LP CD4<sup>+</sup> T cells from uninfected and 2-wk *Hh*<sup>+</sup> IL-10 KOs revealed that two microRNAs were significantly up-regulated (miR-21a and miR-31) and seven microRNAs were significantly down-regulated (miR-125a, miR-125b, miR-139, miR-181a, miR-192, miR-30a and miR-467c) in CD4<sup>+</sup> T cells from colitic IL-10 KO mice compared to uninfected mice. These results suggest a possible role for microRNAs in modulating the inflammatory response during *Hh*-induced colitis.

## 4.2 RESULTS

### 4.2.1 Expression of miR-155, miR-326 and miR-132 is altered during *Hh*-induced colitis.

The expression of microRNAs has not been previously examined in the *Hh* model of colitis. We know from previous work in the lab that there is an accumulation of IL-17A and IFN- $\gamma$ -producing CD4<sup>+</sup> T cells that correlates with the development of *Hh*-induced intestinal inflammation (Morrison et al., 2013). Accordingly, we chose to examine the expression of three microRNAs that have previously been shown to potentiate the Th1 and/or Th17 response; miR-155, miR-326 and miR-132 (Du et al., 2009; O'Connell et al., 2010; Yao et al., 2012; Zhang et al., 2014b). We examined the expression of these microRNAs in the large intestine of uninfected and *Hh*<sup>+</sup> IL-10 KO mice at different time points pi (post infection) with *Hh* by qRT-PCR.

To confirm that the mice were inflamed, we examined colonic histology sections of uninfected and *Hh*<sup>+</sup> IL-10 KO mice at different time points pi for epithelial hyperplasia, goblet cell depletion, leukocyte infiltration and the presence of crypt abscesses. The results showed that the mice were inflamed at 1, 2, 8 and 14 wks pi compared to uninfected controls (**Figure 4.1A**). Scoring of the histological sections revealed that inflammation was established at 1 wk pi and by 8 wks pi, it had started to decrease slightly (**Figure 4.1B**). Analysis of colonic levels of IFN- $\gamma$  and IL-17A by qRT-PCR revealed that the levels of these cytokines were higher at 1, 2 and 8 wks pi compared to uninfected controls (**Figure 4.1C**). Although these results were significant for IFN- $\gamma$ , they were not significant for IL-17A because of one mouse in the uninfected group that expressed high levels of IL-17A and skewed the statistics (**Figure 4.1C**). (The same mouse also expressed higher levels of IFN- $\gamma$  (**Figure 4.1C**)). Furthermore, the colonic levels of IFN- $\gamma$  and IL-17A correlated with the development of intestinal inflammation, with the levels of these cytokines peaking at 2 wks pi after which they started to decrease (**Figure 4.1C**).

We next examined the levels of miR-155, miR-326 and miR-132 in the colon of uninfected and *Hh*<sup>+</sup> IL-10 KO mice at different time points pi with *Hh* and assessed whether their expression levels correlated with the degree of intestinal inflammation. The results showed that miR-155 was significantly up-regulated in the colon at 2, 8 and 14 wks pi and in the cecum at 2 and 8 wks pi and (**Figure 4.1D, upper panel**). In contrast, miR-326 was significantly down-regulated in the colon at 1 and 2 wks pi, whereas in the cecum it just showed a trend toward down-regulation (**Figure 4.1D, middle panel**). MiR-132 showed little change in expression in the colon, but in the cecum it was significantly down-regulated at 1 and 2 wks pi (**Figure 4.1D, lower panel**). Together, these results demonstrated that the expression of miR-155, miR-326 and miR-132 was altered in the large intestine of inflamed *Hh*<sup>+</sup> IL-10 KO mice

compared to uninfected controls, and that the change in expression of these microRNAs coincided with the development of intestinal inflammation.

#### **4.2.2 A non-inflammatory immune response to *Hh* does not induce a change in the expression of miR-155, miR-326 or miR-132**

We have previously shown that WT mice infected with *Hh* alone do not develop intestinal inflammation, whereas WT mice infected with *Hh* and concomitantly treated with a blocking antibody to the IL-10R develop typhlocolitis similar to *Hh*<sup>+</sup> IL-10 KO mice (Kullberg et al., 2006). To examine whether a non-inflammatory immune response to *Hh* could elicit a change in the large intestinal expression of miR-155, miR-326 and miR-132, or whether the expression levels of these microRNAs only changes during an inflammatory immune response to *Hh*, we examined the expression levels of these microRNAs by qRT-PCR in the cecum and colon of uninfected and 2-wk *Hh*<sup>+</sup> and *Hh*<sup>+</sup>/anti-IL-10R-treated WT mice. The results showed that miR-155 was expressed at similar levels in uninfected and *Hh*<sup>+</sup> WT mice, but showed a significant increase in the *Hh*<sup>+</sup>/anti-IL-10R-treated WT mice when compared to uninfected controls in both the colon and the cecum (**Figure 4.2A**). MiR-326 was expressed at similar levels in uninfected and *Hh*<sup>+</sup> WT mice, but showed a trend toward down-regulation in the *Hh*<sup>+</sup>/anti-IL-10R-treated WT mice in both the colon and the cecum when compared to uninfected controls (**Figure 4.2B**). MiR-132 showed similar expression in the colon of uninfected and 2-wk *Hh*<sup>+</sup> and *Hh*<sup>+</sup>/anti-IL-10R-treated WT mice. (**Figure 4.2C, left panel**). In the cecum, MiR-132 was expressed at similar levels in uninfected and *Hh*<sup>+</sup> WT mice, but although not significant, was expressed at slightly higher levels in *Hh*<sup>+</sup>/anti-IL-10R-treated WT mice compared to the uninfected controls, mainly because of 3 out of 8 mice in the group that showed high miR-132 expression (**Figure 4.2C, right panel**). Taken together, these results demonstrated that the expression levels of miR-155, miR-326 and miR-132 remained unaltered in a non-inflammatory immune response to *Hh*. In contrast, during the inflammatory immune response, miR-132 levels increased slightly in the cecum alone whereas miR-155 was significantly up-regulated and miR-326 was down-regulated (although not significantly) in both the cecum and the colon when compared to uninfected controls.

#### **4.2.3 The basal expression of miR-132 is different in WT and IL-10 KO mice**

To examine whether the basal levels of miR-155, miR-326 and miR-132 were comparable in uninfected IL-10 KO and uninfected WT mice, we examined the expression of these microRNAs by qRT-PCR in the cecum and colon of uninfected IL-10 KO mice and uninfected WT mice. The results showed no significant difference in the expression level of miR-155 (**Figure 4.3, left panel**) or miR-326 (**Figure 4.3, middle panel**) in the cecum or colon of uninfected IL-10 KO mice compared to uninfected WT mice. In contrast, the levels of miR-132 were significantly up-regulated in the cecum and the colon of uninfected IL-10 KO mice

compared to uninfected WT mice (**Figure 4.3, right panel**). As a result of this finding, we decided to exclude miR-132 from any further experiments.

#### **4.2.4 Up-regulation of Ets-1 correlates with down-regulation of miR-326 in colitic mice at different time points post *Hh* infection.**

Two recent publications validated Ets-1 as a target of miR-155 and miR-326 in CD4<sup>+</sup> T cells (Du et al., 2009; Hu et al., 2013). To determine whether Ets-1 levels correlated with levels of miR-155 and/or miR-326 during *Hh*-induced intestinal inflammation, we measured the expression levels of Ets-1, miR-155 and miR-326 by qRT-PCR in the cecum and colon of uninfected and *Hh*<sup>+</sup> IL-10 KO mice at 1, 2 and 8 weeks pi. As microRNAs are inhibitory, an increase in the expression of a microRNA should result in a decrease in the levels of its mRNA target and vice versa. The levels of Ets-1 significantly increased in the cecum at 1, 2 and 8 weeks pi and in the colon at 2 and 8 weeks pi (**Figure 4.4A**). As previously shown (**Figure 4.1D**), miR-155 was significantly up-regulated (**Figure 4.4B**) and miR-326 was significantly down-regulated (**Figure 4.4C**) in the cecum and colon of colitic mice compared to uninfected controls. These results showed that the up-regulation of Ets-1 was coincident with the down-regulation of miR-326 in the cecum and colon.

#### **4.2.5 At basal levels, miR-155 is more highly expressed in the immune compartment whereas miR-326 is more highly expressed in the non-immune compartment of the large intestine.**

As the gut contains a number of different cells, we sought to examine whether at basal levels, miR-155 and miR-326 were more highly expressed in the immune or non-immune compartment of the gut. To do this, we sorted different cell populations from the large intestine of uninfected IL-10 KO mice and determined the levels of miR-155 and miR-326 in these cells by qRT-PCR. The experiment was designed such that a piece of colon and the epithelial cell fraction were retained from each mouse. Following digestion of the tissue and subsequent isolation of the LP cells over a percoll gradient, we sorted the LP cells into hematopoietic cells, which contain all the immune cells (Sort 1A: CD45-positive) and non-hematopoietic cells (non-immune cells) (Sort 1B: CD45-negative) (**Figure 4.5A**). We further sorted an aliquot of hematopoietic cells, into CD4<sup>+</sup> T cells (Sort 2A: CD4<sup>+</sup> TCRβ<sup>+</sup>) and CD45<sup>+</sup> cells depleted of CD4<sup>+</sup> T cells (Sort 2B) (**Figure 4.5A**). Examination of post-sort purities showed that all the sorted populations were greater than 85% pure (**Figure 4.5B**). Total RNA was then extracted from the sorted populations and the levels of miR-155 and miR-326 measured by qRT-PCR. The results showed that miR-155 was more highly expressed in the hematopoietic cells compared to the non-hematopoietic cells (**Figure 4.5C**). In female mice, MiR-155 was expressed at similar levels in the LP CD4<sup>+</sup> T cells compared to the rest of the hematopoietic cells whereas in male mice, miR-155 was expressed at much higher levels in LP CD4<sup>+</sup> T cells compared to the rest of the hematopoietic cells (**Figure 4.5C**). These results suggest that the up-regulation of miR-155 seen in the large intestine during *Hh*-induced colitis could simply be because of an increase in the

number of immune cells during intestinal inflammation rather than a bona fide increase of miR-155 in a particular cell type.

In contrast to miR-155, miR-326 was more highly expressed at the total tissue level and in non-hematopoietic cells compared to the hematopoietic cells and in fact, showed its lowest expression levels in the LP CD4<sup>+</sup> T cells and the rest of the hematopoietic cells (**Figure 4.5D**). These results suggest that while it is plausible that the down-regulation of miR-326 observed in the large intestine of *Hh*<sup>+</sup> IL-10 KO mice compared to uninfected controls could be due to a down-regulation of miR-326 in non-immune cells, it might also be simply due to a decrease in the ratio of non-immune to immune cells in the inflamed tissue compared to that of uninfected controls.

#### **4.2.6 MicroRNAs are differentially expressed in large intestinal CD4<sup>+</sup> T cells from 2-wk *Hh*-infected IL-10 KO mice compared to those from uninfected**

Having determined that microRNA expression is altered in inflamed tissue from *Hh*<sup>+</sup> IL-10 KO mice compared to uninfected controls, we wanted to examine in greater detail whether microRNAs are differentially expressed in large intestinal CD4<sup>+</sup> T cells from 2-wk *Hh*<sup>+</sup> IL-10 KO mice compared to uninfected controls. We chose the 2 wk pi timepoint, because we know from previous work in the lab that intestinal inflammation peaks at 2 wks pi (Morrison et al., 2013). We began by isolating LP cells from uninfected and 2-wk *Hh*<sup>+</sup> IL-10 KO mice. To ensure the mice were inflamed and exhibited a similar profile of IL-17A and IFN- $\gamma$ -expressing LP CD4<sup>+</sup> T cells to what we have previously observed, we stimulated an aliquot of cells with PMA and ionomycin. The cells were then surface and intracellularly stained and then analyzed by flow cytometry. The gating strategy used for analysis of IL-17A and IFN- $\gamma$  in LP CD4<sup>+</sup> T cells is depicted in **Figure 4.6A**. Representative staining of IL-17A and IFN- $\gamma$  in LP CD4<sup>+</sup> T cells from each of the eight 2-wk *Hh*<sup>+</sup> infected samples and one uninfected sample is shown in **Figure 4.6B**. The results showed that similar to what has been observed previously at 2 wks pi (Morrison et al., 2013), there were high frequencies of IL-17A<sup>+</sup>, IL-17A<sup>+</sup>IFN- $\gamma$ <sup>+</sup> and IFN- $\gamma$ <sup>+</sup> LP CD4<sup>+</sup> T cells in 2-wk *Hh*<sup>+</sup> IL-10 KO mice compared to the uninfected controls (**Figure 4.6B**).

The remaining LP cells from uninfected and 2-wk *Hh*<sup>+</sup> IL-10 KO mice were stained with antibodies specific for CD4 and TCR $\beta$ , and CD4<sup>+</sup> T cells sorted by flow cytometry. The sort strategy used is shown in **Figure 4.6C**. Following the sort, post-sort purities were examined and found to be greater than 92% (**Figure 4.6D**). Total RNA was then extracted from the sorted samples for use on Agilent's mouse microRNA microarray platform. According to Agilent's protocol for their microarray, a total of 1  $\mu$ l containing at least 100 ng of total RNA is recommended and this RNA is subsequently diluted to a concentration of 50 ng/ $\mu$ l for use on the array. From our optimization studies, we found that the minimum number of cells required to get a required yield of 100 ng/ $\mu$ l of RNA was three million cells (**Chapter 3, Table 3.5**). Thus, for some of the samples, particularly those obtained from uninfected controls, LP CD4<sup>+</sup> T

cells obtained from several sorts had to be pooled to obtain enough cells to isolate RNA (**Table 4.2**). CD4<sup>+</sup> T-cell samples from uninfected IL-10 KO mice are denoted by the prefix 'A' and those from 2-wk *Hh*<sup>+</sup> IL-10 KO mice are denoted by the prefix 'B' (**Table 4.2**). Total RNA yield and purity was measured using the Nanodrop 2000 spectrophotometer (**Table 4.2**). Samples A1, A2, B3 and B5 had a poor 260:230 ratio, therefore, a cold isopropanol precipitation of RNA was carried out to remove any residual salt contaminants (**Table 4.2**). All the samples to be used on the array conformed to either the recommended RNA concentration of 100 ng/  $\mu$ l or the minimum RNA requirement of 50 ng/  $\mu$ l (**Table 4.2**).

Following RNA extraction from CD4<sup>+</sup> T cells derived from uninfected and *Hh*<sup>+</sup> IL-10 KO mice, their RNA integrity number (RIN) was measured on a bioanalyser. The RIN denotes how intact the RNA is and the scale ranges from 1-10 where 10 is intact RNA and 1 is degraded RNA. For a microarray a RIN greater than 7 is deemed acceptable (Madabusi et al., 2006). All our RNA samples had an RNA integrity number  $\geq 9.3$  (**Table 4.2** and **Figure 4.7**).

**Table 4.2 Summary of total RNA yield and purity for samples from uninfected and 2-wk *Hh*<sup>+</sup> IL-10 KO mice to be used in the miR microarray**

Microarray sample name <sup>a</sup>	No. of mice/sort that were pooled <sup>b</sup>	Tot No. of sorted CD4 <sup>+</sup> T cells	Total RNA in 14 $\mu$ l ( $\mu$ g)	RNA conc ng/ $\mu$ l	260:280	260:230	Amount of total RNA used for Isopropanol ppt. of RNA	Total RNA in 5 $\mu$ l ( $\mu$ g)	RNA conc ng/ $\mu$ l	260:280	260:230	RIN
<b>Uninfected samples<sup>c</sup>:</b>												
A1	6F	355,000	1.1	76.7	2.0	1.5	0.7 $\mu$ g	0.7	138.8	1.8	1.7	9.7
	8F	1,600,000										
	8F	486,000										
	8F	590,000										
A2	6F	180,000	0.8	53.8	2.1	1.6	0.6 $\mu$ g	0.6	132.2	1.8	1.7	9.5
	6F	578,000										
	8F	541,000										
	8F	855,000										
	7F	419,546										
	7F	430,000										
A3	10M	828,586	2.0	141.7	2.1	1.9	Not done					9.6
	13M	1,740,000										
	11M	644,000										

Microarray sample name <sup>a</sup>	No. of mice/sort that were pooled <sup>b</sup>	Tot No. of sorted CD4 <sup>+</sup> T cells	Total RNA in 14 $\mu$ l ( $\mu$ g)	RNA conc ng/ $\mu$ l)	260:280	260:230	Amount of total RNA used for Isopropanol ppt. of RNA	Total RNA in 5 $\mu$ l ( $\mu$ g)	RNA conc ng/ $\mu$ l	260:280	260:230	RIN
<b>Infected samples (2-wk <i>Hh</i><sup>+</sup>)</b>												
B1	1F	3,250,000	2.6	184.7	2.1	2.0	Not done				9.8	
B2 <sup>c</sup>	1F	1,620,000	3.1	223.4	2.1	2.0	Not done				9.7	
	1F	2,250,000										
B3	1F	2,200,000	1.6	113.3	2.0	1.7	0.8 $\mu$ g	0.8	161.2	1.9	1.9	9.7
B4 <sup>c</sup>	1M	1,120,000	1.6	115.4	2.1	2.1	Not done				9.5	
	1M	2,200,000										
B5 <sup>d</sup>	1M	1,390,000	0.2	14.0	1.9	1.3	Tot RNA from both samples pooled (0.3 $\mu$ g in total)	0.2	66.9	1.8	1.3	9.3
	1M	1,300,000	0.1	9.0	1.6	1.1						

<sup>a</sup>'A' denotes samples from uninfected IL-10 KO mice and 'B' denotes samples from 2-wk *Hh*<sup>+</sup> IL-10 KO mice.

<sup>b</sup>F denotes samples from female mice and M denotes samples from male mice.

<sup>c</sup>For samples A1, A2, A3, B2 and B4, A separate chloroform phase extraction was done on each sorted sample, before pooling the aqueous phase and extracting the RNA on a single column.

<sup>d</sup>For sample B5, the total RNA was pooled after RNA extraction from each sorted sample individually.

Once the RNA extracted from LP CD4<sup>+</sup> T cells had passed all the quality control checks, i.e. had a 260:280 and a 260:230 ratio of 1.7-2.0 and a RIN greater than 7, microRNA expression was measured on an Agilent's Sureprint mouse microRNA microarray platform (Release 19.0, which profiles the expression of 1247 microRNAs). The microarray data were analyzed using Genespring software. The array data was normalised by using the 90<sup>th</sup> percentile normalisation method. The quality of the data from the array was assessed by two methods; i) box plots that depict normalised intensity values of each sample and enable one to visualise the degree of dispersion and skewness of the data and any outliers ii) principal component analysis (PCA). PCA is an example of exploratory data analysis and is useful for identifying outliers or major differences in the data. The box plots in **Figure 4.8A** depict normalized intensity values for each sample used on the array and show that all the samples exhibited a similar spread of the data and signal intensities. PCA clusters samples based on how similar their microRNA expression profiles across probes are, and helps to highlight similarities and differences between the samples. Thus, one would expect all the samples from uninfected mice to cluster together and those from infected mice to cluster together. PCA of the samples we ran on the microarray revealed that while samples A1-A3 clustered together and B1-B4 clustered together, sample B5 did not cluster with the rest of the samples from infected mice (**Figure 4.8B**), suggesting that sample B5 is different from the other samples derived from *Hh*<sup>+</sup> IL-10 KO mice. In order not to skew the results, we left sample B5 out of any further analysis.

A student's t-test was used to test for statistically significant differences in microRNA expression levels in CD4<sup>+</sup> T cells from uninfected and *Hh*<sup>+</sup> IL-10 KO mice. To control for a 'false discovery rate', P values were corrected using the Benjamini Hochberg test (Benjamini et al., 2001). A P value <0.05 was considered statistically significant. Analysis of array results revealed that there were seven microRNAs that were significantly down-regulated (miR-125a, miR-125b, miR-139, miR-181a, miR-192, miR-30a, and miR467c) and two microRNAs that were significantly up-regulated (miR-21a and miR-31) in CD4<sup>+</sup> T cells from 2 wk *Hh*<sup>+</sup> IL-10 KO mice compared to uninfected controls (**Table 4.3**). In addition to the 9 microRNAs that were significantly different, there were 105 microRNAs that showed a fold change  $\geq 2$  between the infected and uninfected samples, but were not statistically significant. The raw data, and subsequent calculation of the fold change for the microRNAs that showed a fold change  $\geq 2$  as well as miR-155, miR-326 and miR-132 are included in the appendix (**Section 7.1**). A heat map of the normalized fluorescence intensity values of the 9 microRNAs that were significantly different and the 105 microRNAs that showed a fold change greater than 2 is depicted in **Figure 4.9**. From the heat map, it is evident that a number of microRNAs were more highly expressed in sample A3 (sample from uninfected male IL-10 KO mice) compared to samples A1 and A2 (samples from uninfected female IL-10 KO mice) (**Figure 4.9**) For some of these microRNAs, a higher expression was also observed in sample B4 that was obtained from a 2-wk *Hh*<sup>+</sup> male

IL-10 KO mouse when compared to samples B1-B3 that were from 2-wk *Hh*<sup>+</sup> female IL-10 KO mice, indicating a gender bias in their expression.

**Table 4.3 Significantly up-/down-regulated microRNAs in CD4<sup>+</sup> T cells from 2-wk *Hh*<sup>+</sup> IL-10 KO mice (compared to uninfected controls)**

SYSTEMATIC NAME <sup>a</sup>	P (Corr) <sup>b</sup>	P <sup>c</sup>	REGULATION	FOLD CHANGE
<b>mmu-miR-21a-5p</b>	<b>0.0408</b>	2.9 x 10 <sup>-4</sup>	<b>Up</b>	<b>4</b>
<b>mmu-miR-31-5p</b>	<b>0.0260</b>	1.6 x 10 <sup>-4</sup>	<b>Up</b>	<b>4</b>
<b>mmu-miR-467c-5p</b>	<b>0.0072</b>	2.8 x 10 <sup>-5</sup>	<b>Down</b>	<b>23</b>
<b>mmu-miR-125a-5p</b>	<b>0.0043</b>	6.7 x 10 <sup>-6</sup>	<b>Down</b>	<b>29</b>
<b>mmu-miR-139-5p</b>	<b>0.0043</b>	1.0 x 10 <sup>-5</sup>	<b>Down</b>	<b>29</b>
<b>mmu-miR-30a-5p</b>	<b>0.0120</b>	5.7 x 10 <sup>-5</sup>	<b>Down</b>	<b>31</b>
<b>mmu-miR-192-5p</b>	<b>0.0059</b>	1.9 x 10 <sup>-5</sup>	<b>Down</b>	<b>72</b>
<b>mmu-miR-125b-5p</b>	<b>0.0260</b>	1.6 x 10 <sup>-4</sup>	<b>Down</b>	<b>73</b>
<b>mmu-miR-181a-5p</b>	<b>0.0005</b>	3.8 x 10 <sup>-7</sup>	<b>Down</b>	<b>92</b>

<sup>a</sup> Samples in red denote microRNAs that were significantly up-regulated. Samples in blue denote microRNAs that were significantly down-regulated.

<sup>b</sup> P (corr) refers to P values corrected for ‘false discovery rate’ using the Benjamini Hochberg test.

<sup>c</sup> ‘P’ refers to P value after a student’s t-test was applied to the corrected P value.

From the microRNAs that were significantly different, we chose to examine miR-21a, miR-31 and miR-181a further, based on the fact that miR-21a and miR-31 were the microRNAs that were significantly up-regulated and miR-181a was the microRNA that was most significantly down-regulated (**Table 4.3**). From the microRNAs that showed a fold change >2, we decided to investigate miR-210 and miR-96 further, because of the microRNAs that were up-regulated, they showed the greatest fold increase (26-fold and 22-fold respectively) (**Appendix, Section 7.1**). A second heat map, highlighting the normalized fluorescence intensities of all the microRNAs in **Table 4.3**, miR-210 and miR-96, and the microRNAs examined earlier in the chapter (miR-155, miR-326 and miR-132) are shown in **Figure 4.10**. Of note, the microRNAs that we examined at tissue level (miR-155, miR-326 and miR-132) did not show any significant difference in fluorescence intensity between CD4<sup>+</sup> T cells from 2-wk *Hh*<sup>+</sup> IL-10 KO mice and uninfected controls (**Appendix, Section 7.1**). MiR-21a, miR-31 and miR-181a did not show any gender bias in terms of their expression in CD4<sup>+</sup> T cells from male and female samples of the same group, however, miR-96 and miR-210 were expressed at slightly higher levels in CD4<sup>+</sup> T cells from the uninfected male compared to uninfected females (**Figure 4.10**).

The microarray results for miR-21a, miR-31, miR-210, miR-96 and miR-181a were validated by measuring their expression levels by qRT-PCR using total RNA from the samples used on the array as well as RNA extracted from LP CD4<sup>+</sup> T cells from additional uninfected IL-10 KO mice. The results showed that, similar to the array, miR-31, miR-210 and miR-21a

were up-regulated, although only the former two were statistically significant (**Figure 4.11A**). Although miR-96 showed a 26-fold increase on the array (**Figure 4.10**), by qRT-PCR, miR-96 was only slightly up-regulated in LP CD4<sup>+</sup> T cells from 2-wk *Hh*<sup>+</sup> IL-10 KO mice compared to uninfected controls (**Figure 4.11A**). Similar to the array, miR-181a was significantly down-regulated in CD4<sup>+</sup> T cells from 2-wk *Hh*<sup>+</sup> IL-10 KO mice compared to uninfected controls (**Figure 4.11A**). When examining fold changes, only miR-31 and miR-210 showed a significant fold-increase and miR-181a showed a significant fold-decrease in expression compared to uninfected controls (**Figure 4.11B**). Together, these findings validate the array results in that all the microRNAs tested by qRT-PCR followed the same trend in expression as suggested by the array.

#### **4.2.7 MiR-31, miR-21a, miR-210 and miR-96 are up-regulated whereas miR-181a is down-regulated in CD4<sup>+</sup> Th1 and Th17 cells compared to naïve CD4<sup>+</sup> T cells.**

Given that intestinal inflammation in the *Hh* colitis model is characterized by an increase in IL-17A and IFN- $\gamma$ -producing CD4<sup>+</sup> T cells (Morrison et al., 2013), we were interested in determining whether Th1 and/or Th17 cells expressed the microRNAs that were identified by the microarray to be differentially expressed in CD4<sup>+</sup> T cells from 2-wk *Hh*<sup>+</sup> IL-10 KO mice compared to uninfected controls. To do so, we polarized naïve CD4<sup>+</sup> T cells *in vitro* to a Th1 or Th17 phenotype and then measured the expression levels of miR-21a, miR-31, miR-181a, miR-210 and miR-96 by qRT-PCR. The sort strategy used to sort naïve CD4<sup>+</sup> CD62L<sup>+</sup> T cells from spleens and MLNs of uninfected IL-10 KO mice is shown in **Figure 4.12A**. Examination of post-sort purities of the sorted naïve CD4<sup>+</sup> T cells revealed that the population was 95% pure (**Figure 4.12B**). Following the sort, naïve CD4<sup>+</sup> T cells were cultured with irradiated splenocytes, soluble anti-CD3 and polarising cytokines as follows: IL-12 for Th1-cell polarization; TGF $\beta$ , IL-6 and IL-23 for Th17-cell polarisation. After 7 days in culture, we activated the polarized CD4<sup>+</sup> T cells with plate bound anti-CD3 and collected cells at different time points post activation for RNA extraction. In addition to the Th1- and Th17-polarised cells, we also measured microRNA levels in anti-CD3-treated Clone B2 cells. Clone B2 is a *Hh*-specific CD4<sup>+</sup> Th1 clone established in our lab (Kullberg et al., 2003). To confirm that the cells had been activated, at 72 hrs, we took supernatants from anti-CD3 treated wells and measured the levels of IFN- $\gamma$  and IL-17A by ELISA. Reassuringly, supernatants from the Th17-polarised cells primarily expressed IL-17A, while those from Clone B2 and to a lesser extent, Th1-polarised cells primarily expressed IFN- $\gamma$  (**Figure 4.12C**).

For microRNA expression analysis, we extracted total RNA from sorted naïve CD4<sup>+</sup> CD62L<sup>+</sup> cells and from Clone B2, Th1- and Th17-polarized cells at 0, 6, 12, 24, 48 and 72 hrs post anti-CD3 stimulation and following reverse transcription, measured the levels of miR-31, miR-210, miR-181a, miR-21a and miR-96 by qRT-PCR.

The results showed that miR-31 was lowly expressed in naïve CD4<sup>+</sup> T cells and resting Th17, Th1 and Clone B2 cells (**Figure 4.13A**). Upon activation with anti-CD3, miR-31 levels progressively increased in Th17, Th1 and Clone B2 cells suggesting that activation of these cell types induces miR-31 expression (**Figure 4.13A**).

MiR-210 was undetectable in naïve CD4<sup>+</sup> T cells (**Figure 4.13B**). Compared to naïve CD4<sup>+</sup> T cells, there was an increase in miR-210 expression in resting Th17, Th1 and Clone B2 cells that remained more or less constant at different timepoints post anti-CD3 stimulation (**Figure 4.13B**).

MiR-21a was expressed at low levels in naïve CD4<sup>+</sup> T cells compared to resting Th17, Th1 and Clone B2 cells (**Figure 4.13C**). Subsequent stimulation of Th17 and Clone B2 cells with anti-CD3 did not result in a huge change in the expression levels of miR-21a. However in Th1 cells, miR-21a was progressively down-regulated at different timepoints post anti-CD3 stimulation (**Figure 4.13C**).

MiR-96 was expressed at very low levels in naïve CD4<sup>+</sup> T cells (**Figure 4.13D**). Compared to naïve CD4<sup>+</sup> T cells, there was an increase in miR-96 expression in resting Th17 and Th1 cells but not Clone B2 cells (**Figure 4.13D**). Following activation with anti-CD3, the expression levels of miR-96 remained at similar levels in Th17 and Clone B2 cells compared to their resting counterparts (**Figure 4.13D**). In Th1 cells, the expression of miR-96 was progressively down-regulated until 24 hrs post anti-CD3 stimulation after which the levels of miR-96 remained relatively constant (**Figure 4.13D**).

MiR-181a was expressed at higher levels in naïve CD4<sup>+</sup> T cells compared to resting Th17, Th1 and Clone B2 cells (**Figure 4.13E**). Subsequent stimulation with anti-CD3 resulted in a progressive down-regulation of miR-181a expression in Th17 cells (**Figure 4.13E**). In Th1 and Clone-B2 cells anti-CD3 stimulation had no effect on the expression of miR-181a (**Figure 4.13E**).

Together, the results in **Figure 4.13** demonstrated that miR-31, miR-21a, miR-210 and miR-96 were up-regulated and miR-181a was down-regulated in *in vitro* polarized Th1 and Th17 cells compared to the naïve CD4<sup>+</sup> T cells, suggesting that the change in expression of these microRNAs seen in LP CD4<sup>+</sup> T cells from 2-wk *Hh*<sup>+</sup> IL-10 KO mice could be attributed to the increased numbers of Th1 and Th17 cells observed in the colitic setting compared to the naive setting. Furthermore these results showed that none of these microRNAs were exclusively Th1 or Th17 microRNAs. These results also suggest that miR-31 seems to be an activation-induced microRNA, while miR-96 seemed to be down-regulated following Th1-cell activation.

#### 4.2.8 Potential mRNA targets of miR-21a, miR-31, miR-210, miR-181a and miR-96.

To identify potential mRNA targets of miR-21a, miR-31, miR-210, miR-96 and miR-181a that could influence the development of the CD4<sup>+</sup> Th1 and Th17 response during colitis, we used two methods: i) we reviewed the literature on these microRNAs to identify experimentally-validated mRNA targets, ii) we used the bioinformatic target prediction program miRwalk to identify mRNA targets that a given microRNA is predicted to bind to. In addition to its own algorithm, miRwalk has the option of collating the results of ten other target prediction programs, giving a final prediction score depending on the number of programs that predict that a given miRNA will bind to a certain mRNA. The target prediction programs support different host organisms, and most of them have algorithms that take into account at least 2 out of the following 3 features; seed match, free energy and conservation (Yue et al., 2009). We opted to collate the results of 8 target prediction programs that support mammals; miRwalk, miRanda, miRDB, RNAhybrid, PICTAR5, PITA, RNA22 and TargetScan. It is important to note that an mRNA target predicted by just a single program may also be a true target of a particular microRNA. This is evidenced by the fact that FoxP3, which is an experimentally validated target of both miR-31 (Rouas et al., 2009) and miR-210 (Fayyad-Kazan et al., 2012; Zhao et al., 2014), is only predicted to be a target of these microRNAs by one of the eight target prediction programs we opted for. In an effort to find the most likely mRNA targets of a given microRNA, we used 6 out of 8 programs as a cut off for predicting that a certain miRNA would bind to a given mRNA. In case of miR-210, we relaxed the search criteria used to 5/8 programs (yielding 50 hits) because using the more stringent cut off of 6/8 programs only resulted in 9 hits for miR-210 compared to 25-100 hits for the other microRNAs.

We collated a list of predicted and validated mRNA targets of miR-21a, miR-31, miR-210, miR-96 and miR-181a that could be involved in driving an inflammatory CD4<sup>+</sup> Th1 or Th17 response during *Hh*-induced colitis (**Tables 4.4-4.8, respectively**). A complete list of the predicted microRNA targets for each microRNA, using a cut off specified above is included in the appendix (**Section 7.2**).

**Table 4.4 Function of relevant predicted and experimentally validated mRNA targets of miR-21a**

mRNA TARGET	STATUS	FUNCTION OF mRNA TARGET
<b>Smad7</b>	Validated (Li et al., 2013a)	<p>Smad7 inhibits TGFβ by binding to and degrading TGFβ-receptor 1. In CD4<sup>+</sup> T cells, it was found to strongly correlate with T-bet, and promote Th1 responses in humans with MS and mice with EAE. Mice with T-cell specific deletion of Smad7 showed reduced CNS inflammation and reduced Th1 responses and proliferation whilst the Th17 response remained intact (Kleiter et al., 2010).</p> <p>Defective TGFβ1 activity is associated with high Smad7 levels in patients with CD and UC. Inhibition of Smad7 resulted in dampened gut inflammation in different mouse models of colitis. Inhibition of Smad7 is currently being investigated as a possible drug target for IBD (Zorzi et al., 2013) .</p>
<b>PDCD4</b>	Validated (Iliopoulos et al., 2011) (Asseman and von Herrath, 2003)	<p>Programmed cell death 4 (PDCD4) is thought to play a role in apoptosis. Increased miR-21 in T cells inhibited PDCD4 and led to hyperproliferation and increased IFNγ and IL-17A secretion as well as more severe Ag-induced arthritis (Iliopoulos et al., 2011). In T1D, miR-21 down-regulates PDCD4 and protects islet β cells from cell death (Asseman and von Herrath, 2003).</p>
<b>Peli1</b>	Validated (Marquez et al., 2010).	<p>Peli-1 inhibits NF-kB signalling and is necessary for maintaining T-cell tolerance in the periphery (Marquez et al., 2010).</p>
<b>Runx1</b>	Predicted by 4 programs	<p>Runx1 is a transcription factor that has been shown to be necessary for the development of IFNγ-producing Th17 cells (Wang et al., 2014d).</p> <p>If miR-21a is down-regulated in Th17 cells following activation <i>in vivo</i> as suggested by our <i>in vitro</i> data, this might enable Runx1 expression and promote Th17 phenotype shifting to an IFNγ-producing ex-Th17 phenotype.</p>

**Table 4.5 Function of relevant predicted and experimentally validated mRNA targets of miR-31.**

<b>mRNA TARGET</b>	<b>STATUS</b>	<b>FUNCTION OF mRNA TARGET</b>
<b>Foxp3</b>	Validated (Rouas et al., 2009)	FoxP3 is a transcription factor of thymic and a subset of peripherally-induced Tregs and thought to be necessary for their suppressive capacity. MiR-31 was found to inhibit FoxP3 expression in human Tregs (Rouas et al., 2009)
<b>KSR2 and Rhoa</b>	Validated (Fan et al., 2012; Xue et al., 2013)	KSR2 and Rhoa are inhibitors of IL-2 production. MiR-31 mediated inhibition of KSR2 and Rhoa promotes IL-2 production by CD4 <sup>+</sup> T cells
<b>Retinoic acid-inducible protein 3</b>	Validated (Zhang et al., 2015a)	MiR-31 negatively regulates pTreg generation by directly targeting Retinoic acid-inducible protein3, a factor found to be important for pTreg development (Zhang et al., 2015a).
<b>Twist1</b>	Predicted	<p>The transcriptional repressor Twist 1 is an antagonist of NF-Kb-induced cytokine expression. Expression of Twist1 in Th1 cells limited production of IFN-<math>\gamma</math>, TNF<math>\alpha</math> and IL-2 (Niesner et al., 2008).</p> <p>Twist1 prevents T-bet and Runx3 from binding to the <i>Ifng</i> locus and inhibits IFN-<math>\gamma</math> production. It leads to decreased expression of T-bet, IL-12R<math>\beta</math>2 and Runx3 (Pham et al., 2012).</p> <p>Twist1 limits the development of Th17 cells by directly repressing <i>Il6ra</i>. T-cell specific deletion of Twist1 led to early onset of EAE and Ag-induced arthritis (Pham et al., 2013).</p> <p>Thus, if Twist1 proves to be a target of miR-31, miR-31-mediated repression of Twist1 expression could promote the Th1 and Th17 response in <i>Hh</i> colitis.</p>
<b>IRF4</b>	Predicted	<p>T-bet directly represses IRF4 (Interferon regulatory factor 4) to control Th17 lineage differentiation (Gokmen et al., 2013).</p> <p>Thus, If IRF4 proves to be a target of miR-31, miR-31-mediated repression of IRF4 could promote Th1 differentiation or Th17 phenotype shifting to IFN<math>\gamma</math>-producing ex-Th17 cells.</p>

**Table 4.6 Function of relevant predicted and experimentally validated mRNA targets of miR-210.**

mRNA TARGET	STATUS	FUNCTION OF mRNA TARGET
<b>FoxP3</b>	Validated (Zhao et al., 2014) (Fayyad-Kazan et al., 2012)	Polycystic vulagris (PV) is a T-cell mediated autoimmune disease. CD4 <sup>+</sup> T cells from PV patients showed increased miR-210 expression. MiR-210 augmented immune dysfunction in PV by repressing FoxP3 (Zhao et al., 2014).
<b>Hif-1<math>\alpha</math></b>	Validated	MiR-210 inhibits Th17 differentiation in hypoxic environments by inhibiting the transcriptional regulator of Th17 differentiation, Hif1 $\alpha$ (Wang et al., 2014a).
<b>SIN3A</b>	Validated (Shang et al., 2014)	T-bet dependent removal of SIN3A-histone deacetylase complex from the <i>Ifng</i> locus has been shown to promote Th1 differentiation (Chang et al., 2008) (Tong et al., 2005).  Up-regulation of miR-210 in glioma cells compared to normal brain tissue resulted in hyperproliferation and inhibition of apoptosis via miR-210 mediated silencing of SIN3A (Shang et al., 2014)
<b>NF-<math>\kappa</math>B1</b>	Validated (Qi et al., 2012)	NF- $\kappa$ B1 is an inhibitor of transcription factor NF- $\kappa$ B. Loss of NF- $\kappa$ B1 resulted in hyperproduction of Th17 cells (Chang et al., 2009).
<b>ZMIZ1</b>	Predicted	ZMIZ1 is a susceptibility loci for IBD (Lees et al., 2011). It enhances transcriptional activity of Smad3, thereby promoting TGF-beta signaling (Li et al., 2006b).
<b>Lair1</b>	Predicted	The collagen receptor is widely expressed by immune cells. Lair1 is an immune inhibitory receptor, and is down-regulated on T cells in Rheumatoid arthritis compared to those from healthy controls. Lair1 has been shown to inhibit proliferation and induce apoptosis of T cells (Meyaard, 2008; Zhang et al., 2014c).  Thus, If Lair1 proves to be a target of miR-210, miR-210-mediated repression of Lair1 could promote proliferation and survival of CD4 <sup>+</sup> T cells in <i>Hh</i> colitis.
<b>Dapk1</b>	Predicted	It inhibits NF-Kb activation in T cells and thereby limits T-cell proliferation and IL-2 production (Chakilam et al., 2013; Chuang et al., 2008).  Thus, If Dapk1 proves to be a target of miR-210, miR-210-mediated repression of Dapk1 could promote proliferation of CD4 <sup>+</sup> T cells in <i>Hh</i> colitis.
<b>Ppp2r5c</b>	Predicted	Inhibits NF-kB activation in T cells and thereby inhibits T cell proliferation (Breuer et al., 2014).  Thus, If Ppp2r5c proves to be a target of miR-210, miR-210-mediated repression of Ppp2r5c could promote proliferation of CD4 <sup>+</sup> T cells in <i>Hh</i> colitis.

**Table 4.7 Function of relevant predicted and experimentally validated mRNA targets of miR-96.**

<b>mRNA TARGET</b>	<b>STATUS</b>	<b>FUNCTION OF mRNA TARGET</b>
<b>IRF4</b>	Predicted	<p>T-bet directly represses IRF4 (Interferon regulatory factor 4) to control Th17 lineage differentiation (Gokmen et al., 2013).</p> <p>Thus, If IRF4 proves to be a target of miR-96, miR-96-mediated repression of IRF4 could promote Th1 differentiation or Th17 phenotype shifting to IFN<math>\gamma</math>-producing ex-Th17 cells.</p>
<b>ATG16L1</b>	Predicted	<p>ATG16L1 is a susceptibility loci for IBD (Lees et al., 2011) and is necessary for autophagy.</p> <p>Thus, If ATG16L1 proves to be a target of miR-96, miR-96-mediated repression of ATG16L1 could promote CD4<sup>+</sup> T-cell survival in <i>Hh</i> colitis.</p>

**Table 4.8 Function of relevant predicted and experimentally validated mRNA targets of miR-181a.**

<b>mRNA TARGET</b>	<b>STATUS</b>	<b>FUNCTION OF mRNA TARGET</b>
<b>CXCR3</b>	Validated (Bergman et al., 2013)	Chemokine receptor CXCR3 is important for the differentiation of naïve T cells into Th1 cells in the lymph node (Groom et al., 2012). CXCR3 is also important for the migration of Th1 cells from the lymph node to the site of inflammation (Xie et al., 2003).
<b>STAT1</b>	Validated (Bergman et al., 2013)	STAT1 is one of the transcription factors that drives the production of IFN- $\gamma$ (Levy and Darnell, 2002).
<b>PTPN22</b> <b>SHP-2</b> <b>DUSP5/6</b>	Validated (Li et al., 2007).	MiR-181a targets multiple phosphatases to regulate threshold of TCR signalling. MiR-181a is highly expressed in immature thymocytes and plays a role in thymic selection (Li et al., 2007).
<b>Smad7</b>	Predicted	Smad7 inhibits TGF $\beta$ by binding to and degrading TGF $\beta$ -receptor 1. In CD4 <sup>+</sup> T cells, it was found to strongly correlate with T-bet, and promote Th1 responses in humans with MS and mice with EAE. Mice with T-cell specific deletion of Smad7 showed reduced CNS inflammation and impaired Th1 responses and proliferation but intact Th17 responses (Kleiter et al., 2010).  Defective TGF $\beta$ 1 activity is associated with high Smad7 levels in patients with CD and UC. Inhibition of Smad7 resulted in dampened gut inflammation in different mouse models of colitis. Inhibition of Smad7 is currently being investigated as a possible drug target for IBD (Zorzi et al., 2013).  If Smad7 proves to be a target of miR-181a, down-regulation of miR-181a in LP CD4 <sup>+</sup> T cells from colitic mice compared to uninfected controls could promote Smad7 expression and thus inflammation by augmenting Th1 responses.
<b>Fos</b>	Predicted	Together with JUN, C-fos forms the transcription factor AP-1. Blocking of AP-1 results in diminished Th1/Th17 differentiation and increased FoxP3 expression in GVHD (Park et al., 2014)  If C-fos proves to be a target of miR-181a, down-regulation of miR-181a in LP CD4 <sup>+</sup> T cells from colitic mice compared to uninfected controls could promote C-fos and thus AP-1 expression and thus promote inflammation by augmenting Th1/Th17 responses.

### 4.3 DISCUSSION

Altered expression of microRNAs has been shown to contribute to the pathogenesis of many autoimmune and inflammatory diseases (Hu et al., 2013). The aim of this study was to examine whether microRNA expression is dysregulated during *Hh*-induced colitis at the site of *Hh* colonization in the large intestine. In this chapter, we show that IL-10 KO mice suffering from *Hh*-induced colitis show altered expression of microRNAs both at the tissue level and CD4<sup>+</sup> T-cell level compared to uninfected controls.

In the current study, kinetic examination of miR-155, miR-326 and miR-132 expression in the colon and cecum of uninfected and *Hh*<sup>+</sup> IL-10 KO mice revealed that compared to uninfected controls, miR-155 was significantly up-regulated and miR-326 and miR-132 were significantly down-regulated at different time points pi with *Hh*. Furthermore, the change in expression of these microRNAs was coincident with the development of intestinal inflammation. Similar to CD (Globig et al., 2014; Xavier and Podolsky, 2007), inflammation in the *Hh*<sup>+</sup> colitis model is characterized by an increase of CD4<sup>+</sup> T cells that produce IFN- $\gamma$  and/or IL-17A (Morrison et al., 2013). We chose to examine the expression of miR-155, miR-326 and miR-132 because they have been implicated in modulating the Th1 and/or Th17 response (Hu et al., 2013; O'Connell et al., 2010; Singh et al., 2014b; Zhang et al., 2014b) (Du et al., 2009) (Nakahama et al., 2013). Similar to the current study, previous profiling of microRNAs in the spontaneous IL-10 KO model of colitis showed that miR-155 was up-regulated in the colon of severely inflamed IL-10 KO mice (Schaefer et al., 2011). In the DSS colitis model, miR-155 KO mice showed less severe colitis and lower Th1/Th17 numbers (Singh et al., 2014b). Although there are no studies of miR-326 and miR-132 in the context of colitis, these microRNAs, along with miR-155 have been implicated in modulating the pathogenic immune response in autoimmune diseases like EAE, where Th1 and Th17 cells have been shown to contribute to the pathogenic immune response (Du et al., 2009; Nakahama et al., 2013; O'Connell et al., 2010; Yao et al., 2012; Zhang et al., 2014b). Studies in the EAE model of disease show that miR-132/212 KO mice (Nakahama et al., 2013) and miR-155 KO mice (O'Connell et al., 2010) are resistant to the development of EAE and exhibit lower numbers of Th1 and Th17 cells compared to their WT counterparts. In vivo silencing of miR-326 led to fewer Th17 cells and mild EAE (Du et al., 2009).

Examination of the mRNA levels of *Ets-1*, a validated target of both miR-155 (Hu et al., 2013) and miR-326 (Du et al., 2009), in the large intestine of uninfected and *Hh*<sup>+</sup> IL-10 KO mice at 1, 2 and 8 wks pi revealed that compared to uninfected controls, *Ets-1* levels progressively increased at increasing time points pi, correlating with the development of intestinal inflammation. Furthermore, the change in *Ets-1* levels seemed to correlate more with the down-regulation of miR-326 rather than up-regulation of miR-155. In the current study, examination of the basal levels of miR-326 in epithelial cells, immune cells and non-immune

cells of the large intestine revealed that at steady state, miR-326 was expressed at higher levels in the epithelial cells and non-immune compartment compared to the immune compartment. These results make it tempting to speculate that perhaps down-regulation of miR-326 seen at the tissue level in colitic mice may be attributed to a down-regulation of miR-326 in epithelial cells and/or non-immune cells. The finding that miR-326 is expressed at higher basal levels in non-immune cells is corroborated by the fact that all the studies in which miR-326 is shown to be down-regulated were observed in non-immune cells. For example, decreased miR-326 was observed in adipocytes during their differentiation (Tang et al., 2009), in glioma tissues compared to normal brain tissue (Wang et al., 2013) and in colorectal cancer cells compared to controls (Wu et al., 2015). Conversely, the studies that reported an up-regulation in miR-326 levels were seen in immune cells, for example, increased miR-326 levels were seen in CD4<sup>+</sup> T cells derived from mice suffering from EAE compared to uninfected controls (Du et al., 2009), and peripheral blood lymphocytes (PBLs) from patients suffering from type 1 diabetes compared to PBLs of healthy individuals (Sebastiani et al., 2011). Ets-1 is expressed by a number of different immune and non-immune cells (reviewed by (Matsumoto et al., 1998). Interestingly, a recent study showed increased Ets-1 levels in intestinal epithelial cells (IECs) in the DSS model of colitis and in IECs of humans suffering from ulcerative colitis (Li et al., 2015). Increase in Ets-1 levels promoted apoptosis of IECs via acceleration of NF- $\kappa$ B signalling (Li et al., 2015). The study by Li et al. highlights a potential mechanism by which a decrease in miR-326 levels could promote Ets-1-induced apoptosis of IECs and thereby promote defective barrier function in *Hh*-induced colitis. Further analysis of miR-326 and Ets-1 expression in large intestine epithelial cells and non-immune cells at different time points post *Hh* infection will help to identify whether change in expression of miR-326 in these cell types correlates with the change in Ets-1 levels (if any) in these cell types. Further studies involving *in vivo* silencing/over expression of miR-326 during *Hh*-induced colitis will help elucidate whether miR-326 has any functional effect on Ets-1 levels and disease severity.

Both the studies where Ets-1 was found to be a target of miR-155 and miR-326 were in the EAE model, where increased expression of miR-155 and miR-326 in Th17 cells suppressed Ets-1 and potentiated the inflammatory response (Du et al., 2009; Hu et al., 2013). Ets-1 acts as a positive regulator of Th1 cells as Ets-1 KO CD4<sup>+</sup> CD45RB<sup>high</sup> cells failed to produce IFN- $\gamma$  or induce colitis when transferred to SCID mice (Grenningloh et al., 2005). Conversely, Ets-1 is a negative regulator of Th17 cells, although the exact mechanism by which it does so is unclear (Du et al., 2009). In the current study, microarray examination of miR-155 and miR-326 did not reveal any difference in expression in the LP CD4<sup>+</sup> T cells isolated from 2-wk *Hh*<sup>+</sup> IL-10 KO mice compared to those of uninfected controls. Unless changes in miR-155 and miR-326 levels in individual CD4<sup>+</sup> T-cell subsets is masked at the total CD4<sup>+</sup> T-cell level, it seems unlikely that Ets-1 levels are excessively promoted/inhibited by miR-155 or miR-326 in LP CD4<sup>+</sup> T cells during *Hh*-induced colitis. As we did not measure Ets-1 levels in LP CD4<sup>+</sup> T cells

from uninfected and 2-wk *Hh*<sup>+</sup> IL-10 KO mice due to insufficient amounts of RNA, we cannot say whether Ets-1 levels changed however, given the evidence in the literature (Grenningloh et al., 2005), Ets-1 may potentiate the inflammatory CD4<sup>+</sup> Th1 and perhaps ex-Th17 responses and therefore might be worth examining in the future.

In this study, we profiled microRNA expression in LP CD4<sup>+</sup> T cells from uninfected and 2-wk *Hh*<sup>+</sup> IL-10 KO mice. To our knowledge, this is the first time that microRNAs have been profiled in *ex-vivo* sorted CD4<sup>+</sup> T cells from the large intestinal lamina propria. We validated the array results by examining the expression by qRT-PCR, of five microRNAs that were significantly different and/or showed a fold change greater than two in the samples from the colitic setting when compared to controls. The qRT-PCR results confirmed the directional results of the array i.e up- or down-regulation of a given microRNA; however, the fold change observed in the microarray was much greater than that observed by qRT-PCR. For example, miR-96 showed a 29-fold increase in expression by in LP CD4<sup>+</sup> T cells from 2-wk *Hh*<sup>+</sup> IL-10 KO mice compared to controls when examined by microarray, but only showed a 1.8-fold increase when examined by qRT-PCR. Generally, the change in expression of a given microRNA observed by microarray is considered to be true if the same directional change in expression of the given microRNA is also observed by qRT-PCR (Git et al., 2010). This is because the fold change can be influenced by a number of factors. Firstly, Taqman qRT-PCRs are highly specific and measure the expression of a single microRNA sequence whereas microarrays may not be able to distinguish between isoforms of a give microRNA (Git et al., 2010). Secondly, Taqman qRT-PCRs and Agilent's microRNA microarray assay have different chemistries (Pritchard et al., 2012). Taqman qRT-PCR uses reverse transcription and microarrays use ligation, thus the two methods may not have the same microRNA yields (Pritchard et al., 2012).

MicroRNA profiling of 2-wk LP CD4<sup>+</sup> T cells revealed that miR-21a was up-regulated in LP CD4<sup>+</sup> T cells from 2-wk *Hh*<sup>+</sup> IL-10 KO mice compared to uninfected controls. Another study has shown that up-regulation of miR-21 in peripheral blood leukocytes (PBLs) of IL-10 KO mice suffering from mild inflammation precedes the up-regulation of these microRNAs in the colon of IL-10 KO mice suffering from severe intestinal inflammation (Schaefer et al., 2011). Increased miR-21 expression has been observed in dermal T cells from patients suffering from psoriasis compared to healthy controls (Meisgen et al., 2012). Increased miR-21 has also been shown to promote CD4<sup>+</sup> T cell proliferation by suppressing the pro-apoptotic factor PDCD4 (**Figure 4.14**) (Stagakis et al., 2011). A number of studies have also identified miR-21 to be up-regulated upon CD4<sup>+</sup> T-cell activation where miR-21 promoted TCR signaling by repressing Sprouty1, an inhibitor of ERK and JNK signaling (**Figure 4.14**) (Wang et al., 2014b). That study also showed that overexpression of miR-21 on Jurkat cells promoted transcription factor AP-1 activity and IL-2 expression (Wang et al., 2014b). MiR-21 also potentiates TCR signaling by repressing an inhibitor of NF-kB signaling called Peli1 (**Figure**

**4.14**) (Marquez et al., 2010). Two studies showed that miR-21 was up-regulated following activation of CD4<sup>+</sup> T cells *in vitro* (Smigielska-Czepiel et al., 2013; Stagakis et al., 2011). In the current study, although we observed an up-regulation in miR-21a expression in *in vitro* polarized Th1 and Th17 cells compared to naïve CD4<sup>+</sup> T cells, we did not observe any subsequent up-regulation of miR-21a expression upon stimulating these Th1 and Th17 cells with anti-CD3. The difference in our results compared to those by Stagakis et al and Smigielska-Czepiel et al could be explained by the fact that we used plate-bound anti-CD3 alone whereas they used anti-CD3/anti-CD28 to stimulate the cells (Smigielska-Czepiel et al., 2013; Stagakis et al., 2011). These findings suggest that perhaps CD28 signaling plays an important role in inducing miR-21 expression. One study also showed that miR-21 was selectively up-regulated in *in vitro* polarized Th17 cells and not Th1 cells and miR-21 augmented the Th17 response by inhibiting Smad7 (**Figure 4.14**) (Murugaiyan et al., 2015). The study by Murugaiyan et al also showed that miR-21 KO mice developed less severe EAE because of impaired Th17 responses (Murugaiyan et al., 2015). In the current study, although we saw an increase in miR-21a in Th17 cells compared to naïve CD4<sup>+</sup> T cells, unlike Murugaiyan et al, we also observed a similar increase of miR-21a in Th1 cells. Once again, the discrepancy between our results and those of Murugaiyan et al could once again be explained by the fact that we used plate-bound anti-CD3 alone to stimulate the cells whereas they used anti-CD3/anti-CD28 stimulation. The role of miR-21 in IBD is unclear. Increased expression of miR-21 has been observed in Crohn's ileitis compared to healthy controls (Wu et al., 2010). In animal models of colitis, miR-21 deficiency exacerbated CD4<sup>+</sup> T-cell transfer colitis but proved to be protective in TNBS and DSS colitis (Wu et al., 2014). Thus further work to determine the role of miR-21a in *Hh*-induced colitis remains to be done.

In the current study, we observed increased miR-31 expression in LP CD4<sup>+</sup> T cells from 2-wk *Hh*<sup>+</sup> IL-10 KO mice compared to uninfected controls. Increased miR-31 expression has been previously observed in peripheral blood leukocytes (PBLs) of IL-10 KO mice suffering from mild inflammation, and precedes the up-regulation of the miR-31 in the colon of IL-10 KO mice suffering from severe intestinal inflammation (Schaefer et al., 2011). Increased miR-31 expression has also been observed in splenocytes and CD4<sup>+</sup> T cells from EAE mice compared to those of healthy controls (Zhang et al., 2015a). In the current study, we also found that miR-31 was progressively up-regulated in *in vitro* polarized Th1 and Th17 cells following activation with plate-bound anti-CD3. Similar to our findings, one study showed that miR-31 was up-regulated in *in vitro* polarized Th1 and Th17 cells activated with anti-CD3/anti-CD28 (Zhang et al., 2015a). Another study showed that miR-31 is up-regulated on primary CD4<sup>+</sup> T cells upon TCR stimulation and in these cells, miR-31 promoted IL-2 expression by repressing an inhibitor of IL-2 expression called kinase repressor of Ras2 (KSR2) (**Figure 4.14**) (Xue et al., 2013). In CD4<sup>+</sup> T cells isolated from patients suffering from SLE, which show decreased miR-31 expression compared to healthy controls, loss of miR-31 mediated repression of RhoA

impaired IL-2 production by these CD4<sup>+</sup> T cells (**Figure 4.14**) (Fan et al., 2012). Importantly, miR-31 has been identified as a novel biomarker for IBD, as it was found to be up-regulated in colonic tissue (both fresh-frozen and formalin-fixed paraffin-embedded tissue) of patients suffering from UC and CD compared to healthy controls (Lin et al., 2014). Findings from the literature suggest that there are a multitude of mechanisms by which increased miR-31 expression could augment the pathogenic CD4<sup>+</sup> T-cell response in *Hh* colitis. Aside from promoting IL-2 expression by CD4<sup>+</sup> T cells, (Fan et al., 2012; Xue et al., 2013) miR-31 was found to antagonize Treg function by repressing FoxP3 (Rouas et al., 2009) and negatively regulating pTreg generation by repressing retinoic acid inducible-protein 3, a factor required for pTreg development (**Figure 4.15**) (Zhang et al., 2015a). Furthermore, in the current study, we identified transcription factor Twist1 as a potential mRNA target of miR-31. Twist1 is a repressor of both IFN- $\gamma$  production and Th17 generation (Niesner et al., 2008; Pham et al., 2012; Pham et al., 2013). Twist1 inhibits NF- $\kappa$ b-induced production of IFN- $\gamma$ , TNF $\alpha$  and IL-2 (Niesner et al., 2008). Twist1 decreases the levels of T-bet, Runx3 and IL-12R $\beta$ 2 and inhibits IFN- $\gamma$  production by preventing T-bet and Runx3 from binding to the IFN $\gamma$  promoter (**Figure 4.15**) (Pham et al., 2012). Twist1 also limits the development of Th17 cells, as Twist1 has been found to directly suppress IL-6R $\alpha$  expression (**Figure 4.15**) (Pham et al., 2013). Therefore, if Twist1 proves to be a target of miR-31, miR-31-mediated loss of Twist1 could augment the Th1 and Th17 response in *Hh* colitis.

In the current study, microRNA microarray analysis of LP CD4<sup>+</sup> T cells from uninfected and 2-wk *Hh*<sup>+</sup> IL-10 KO mice revealed that 105 microRNAs showed a 2-fold difference in expression in LP CD4<sup>+</sup> T cells from colitic animals compared to uninfected controls. Of the microRNAs that were up-regulated, miR-210 and miR-96 showed the greatest fold increase compared to samples from uninfected controls. The array was carried out using total RNA derived from LP CD4<sup>+</sup> T cells from male and female mice. In case of miR-210 and miR-96, the samples from the uninfected male showed a higher expression of these microRNAs, thus skewing the results to being less significant than they would have been with female samples alone. Similar to our finding, a recent study showed that sexual dimorphism in miR-210 expression has recently been observed in the placenta of humans, where it was found that miR-210 is expressed at higher levels in females carrying male fetuses compared to female fetuses (Muralimanoharan et al., 2015). Similar to our findings that miR-210 was up-regulated in LP CD4<sup>+</sup> T cells from colitic *Hh*<sup>+</sup> IL-10 KO mice compared to uninfected controls, a recent study showed that miR-210 was up-regulated in CD4<sup>+</sup> T cells from patients suffering from psoriasis vulgaris compared to healthy controls (Zhao et al., 2014). In the current study, when we examined miR-210 expression in naïve and *in vitro* polarised Th1 and Th17 cells, miR-210 was expressed at slightly higher levels in Th17 cells compared to Th1 cells and naïve CD4<sup>+</sup> T cells although not as highly as a similar study examining miR-210 expression in *in vitro* polarised Th subsets (Wang et al., 2014a). The fact that we did not observe as marked an

increase in miR-210 expression in Th17 vs Th1 cells as Wang et al did is likely due to the fact that we used anti-CD3 alone to stimulate the cells whereas Wang et al used anti-CD3/anti-CD28. Giving credence to this theory is the fact that Wang et al further demonstrated that co-stimulation with anti-CD28 is necessary to induce robust miR-210 expression (Wang et al., 2014a). It is unclear whether the increased expression of miR-210 in LP CD4<sup>+</sup> T cells from 2-wk *Hh*<sup>+</sup> IL-10 KO mice compared to those from uninfected controls may augment inflammation or not, as miR-210 has been shown to play both anti-inflammatory and pro-inflammatory roles. Supporting an anti-inflammatory role for miR-210, one study showed that in the T-cell transfer colitis model, miR-210 was found to limit Th17 differentiation by targeting HIF-1 $\alpha$  (**Figure 4.15**) (Wang et al., 2014a). In this study by Wang et al, CD4<sup>+</sup> T cells from miR-210 KO mice induced more severe colitis than CD4<sup>+</sup> T cells from WT counterparts as a result of an augmented Th17 response (Wang et al., 2014a). There are a few studies that suggest that miR-210 may play a pro-inflammatory role. Zhao et al found that overexpression of miR-210 potentiated psoriasis vulgaris by repressing FoxP3 expression, leading to loss of Treg mediated suppression of effector T cells and increased production of IFN- $\gamma$  and IL-17A (**Figure 4.15**) (Zhao et al., 2014). MiR-210 has also been shown to bind to SIN3A mRNA (Shang et al., 2014). SIN3A is a transcriptional regulatory protein that inhibits IFN- $\gamma$  expression and Th1 differentiation (**Figure 4.15**) (Tong et al., 2005). Furthermore, in the current study, we identified that miR-210 is predicted to repress two inhibitors of NF- $\kappa$ B signaling called Dapk1 and Ppp2r5c and a pro-apoptotic factor called Lair1 (**Figure 4.14**). Further work to determine whether miR-210 plays a pro-inflammatory or anti-inflammatory role in *Hh* colitis remains to be done.

In the current study, we found that of the microRNAs that were down-regulated in LP CD4<sup>+</sup> T cells from 2-wk *Hh*<sup>+</sup> IL-10 KO mice compared to uninfected controls, miR-181a was the most significantly down-regulated and showed the greatest fold decrease compared to uninfected controls (92 fold decrease). Furthermore, we found that miR-181a was expressed at higher levels in naïve *ex vivo* sorted CD4<sup>+</sup> T cells compared to differentiated Th1 and Th17 cells. These findings agree with those of Li et al, who also found that miR-181a was expressed at higher levels in naïve CD4<sup>+</sup> T cells compared to differentiated Th1 and Th2 cells (Li et al., 2007). Although most of the literature related to miR-181a suggests that miR-181a is most highly expressed in the thymus and plays an important role in thymic selection and modulating TCR signalling sensitivities (**Figure 4.14**) (Ebert et al., 2009; Li et al., 2007), recent research suggests a role for down-regulation of miR-181a in augmenting the inflammatory Th1 response in the periphery. Thus, in humans, miR-181a was found to repress IFN- $\gamma$  (Fayyad-Kazan et al., 2014) and in rats suffering from EAE, miR-181a was found to suppress CXCR3 and STAT1 and promote the Th1 response (**Figure 4.15**) (Bergman et al., 2013). Therefore it is possible that the down-regulation of miR-181a observed in the current study in LP CD4<sup>+</sup> T cells from 2-wk *Hh*<sup>+</sup> IL-10 KO compared to uninfected controls could play an important role in

potentiating the pathogenic Th1 response in the colitic setting. An important predicted target for miR-181a that might potentiate *Hh*-induced colitis is Smad7 (**Figure 4.14**). Smad7 is an inhibitor of TGF- $\beta$ 1, which plays a role in preventing mucosal inflammation (Heldin et al., 1997) and anti-sense oligonucleotides targeting Smad7 are currently in clinical trials for treatment of CD (Monteleone et al., 2012).

Some of the potential mRNA targets identified in the current study are common to different microRNAs. For example, FoxP3 is a validated target of both miR-210 and miR-31 (**Figure 4.15**), Runx1 is a predicted target of both miR-21a and miR-96 and IRF4 is a predicted target of both miR-31 and miR-96 (**Figure 4.15**). Thus, it is tempting to speculate that these microRNAs might work synergistically to bring about changes in mRNA expression that would augment the inflammatory response. Similarly, Smad7 is a validated target of miR-21, but a predicted target of miR-181a. In the current study, miR-21a was upregulated whereas miR-181a was down-regulated in LP CD4<sup>+</sup> T cells from colitic mice compared to those from uninfected controls. Thus it is plausible that if Smad7 is also a target of miR-181a, then loss of miR-181a-mediated suppression of Smad7 maybe partially or completely compensated for by miR-21a-mediated suppression of Smad7.

Future studies should focus on determining whether the predicted mRNA targets identified are actually targets of miR-21a, miR-31, miR-181a, miR-210 or miR-96 by carrying out luciferase assays. Once a given mRNA has been identified as a target of a particular microRNA, *in vivo* studies involving over-expression or silencing of the microRNA could be carried out to determine whether repression or de-repression of the mRNA target has any functional effect on disease severity in *Hh* colitis.

### 4.3.1 Summary

MiR-155 was significantly up-regulated and miR-326 was significantly down-regulated in the inflamed large intestine of *Hh*<sup>+</sup> IL-10 KO mice at different time points pi with *Hh*. Furthermore, the change in expression of these microRNAs coincided with the development of inflammation.

Microarray profiling of microRNAs in LP CD4<sup>+</sup> T cells from uninfected and 2-wk *Hh*<sup>+</sup> IL-10 KO mice demonstrated that several microRNAs were differentially expressed in LP CD4<sup>+</sup> T cells from the inflamed large intestine compared to those of uninfected controls. Two microRNAs were significantly up-regulated (miR-21a and miR-31), seven microRNAs were significantly down-regulated, (miR-125a, miR-125b, miR-139, miR-181a, miR-192, miR-30a, and miR467c) and a further 105 microRNAs showed a fold change of more than two in LP CD4<sup>+</sup> T cells from 2-wk *Hh*<sup>+</sup> IL-10 KO mice compared to those of uninfected controls.

Further examination of the expression of miR-21a, miR-31, miR-210, miR-96 and miR-181a in naïve CD4<sup>+</sup> T cells and *in vitro* polarized Th1 and Th17 cells revealed that with the exception of miR-181a, which was expressed at higher levels in naïve CD4<sup>+</sup> T cells compared to Th1 and

Th17 cells, miR-21a, miR-31, miR-210 and miR-96 were expressed at much higher levels in Th1 and Th17 cells compared to naïve CD4<sup>+</sup> T cells.

A number of potential mRNA targets (both predicted and experimentally validated) of miR-21a, miR-31, miR-210, miR-96 and miR-181a that might potentiate the pathogenic CD4<sup>+</sup> T-cell response in *Hh* colitis were identified.

## 4.4 FIGURES

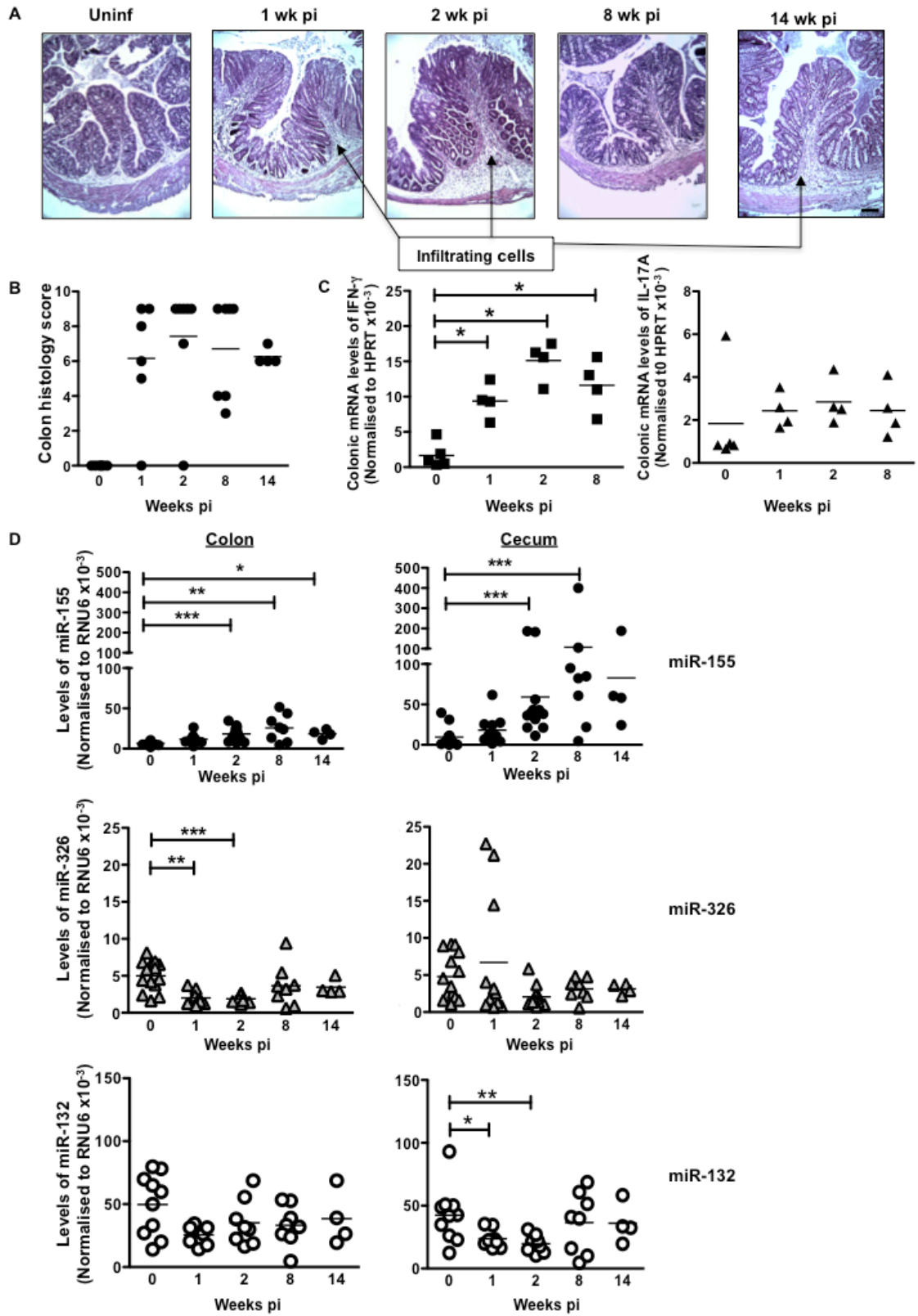
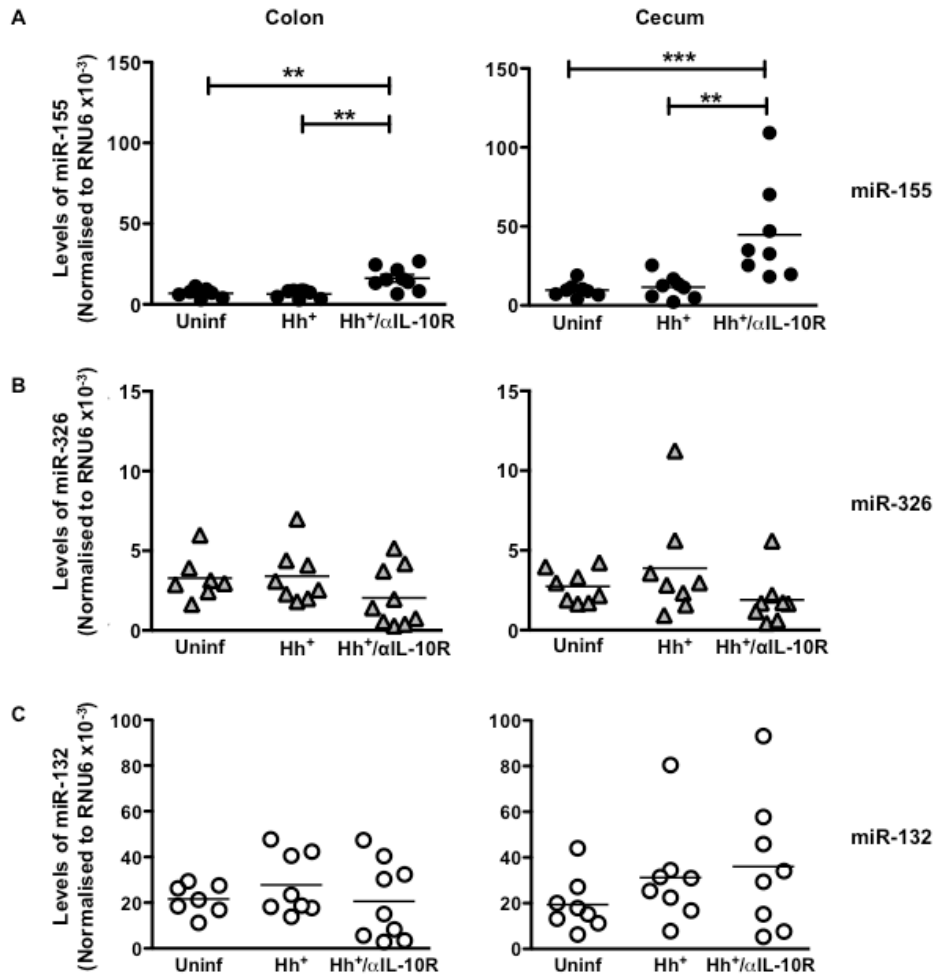


Figure 4.1 Expression of miR-155, miR-326 and miR-132 is altered during *Hh*-induced colitis

**Figure 4.1. Expression of miR-155, miR-326 and miR-132 is altered during *Hh*-induced colitis.**

Colonic and cecal tissues were collected from uninfected and *Hh*<sup>+</sup> IL-10 KO mice at 1, 2, 8 and 14 wks pi. Colon sections were fixed in formalin and a section stained with haematoxylin and eosin (H and E) for histological examination. Bar, 100  $\mu$ m. Total RNA was isolated from cecal and colonic tissue and RNA transcript levels of IFN- $\gamma$  and IL-17A and miR-155, miR-326 and miR-132 were determined by qRT-PCR. (A) Representative H and E stained sections of the colon from uninfected and *Hh*<sup>+</sup> IL-10 KO mice. (B) Scatter plots showing histology scores of ascending colon showing at least 4 mice per time point. The histology sections were scored as follows: a score of 0-3 was assigned for each of the following four parameters respectively, i) epithelium and/or goblet cell hyperplasia, ii) inflammation in the lamina propria, iii) percentage area affected and iv) any markers of severe inflammation such as crypt abscesses and fibrosis, giving a final maximum score of 12. Data shown are pooled from two independent experiments where  $n \geq 3$  mice per group per experiment. (C) Scatter plots showing colonic mRNA levels of IFN- $\gamma$  (left panel) and IL-17A (right panel). Data shown are from a single experiment. (D) Scatter plots showing colonic (left panel) and cecal (right panel) levels of miR-155 (upper panel), miR-326 (middle panel) and miR-132 (lower panel) in uninfected and *Hh*<sup>+</sup> IL-10 KO mice. Data shown are pooled from three independent experiments in case of miR-155 and miR-326 and two independent experiments in case of miR-132 where  $n \geq 3$  mice per group per experiment. In B-D, each symbol represents an individual mouse and horizontal bars depict the mean. \*\* $p < 0.01$  and \*\*\* $p < 0.001$  as determined by a two-tailed Mann-Whitney test.



**Figure 4.2 The large intestinal levels of miR-155, miR-326 and miR-132 remain unchanged during a non-inflammatory immune response to *Hh*.**

Colonic and cecal tissues were isolated from uninfected WT and 2-wk *Hh*<sup>+</sup> and *Hh*<sup>+</sup>/anti-IL-10R-treated WT female mice. Total RNA was extracted and following reverse transcription, levels of miR-155, miR-326 and miR-132 were determined by qRT-PCR. Cecal and colonic levels of (A) miR-155 (B) miR-326 and (C) miR-132 in uninfected and 2-wk *Hh*<sup>+</sup> and *Hh*<sup>+</sup>/anti-IL-10R-treated WT mice. Each symbol represents an individual mouse and horizontal bars show the mean of each/group. Data in figures are combined from two independent experiments. \*\**p*<0.01 and \*\*\**p*<0.001 as determined by a two-tailed Mann-Whitney test.

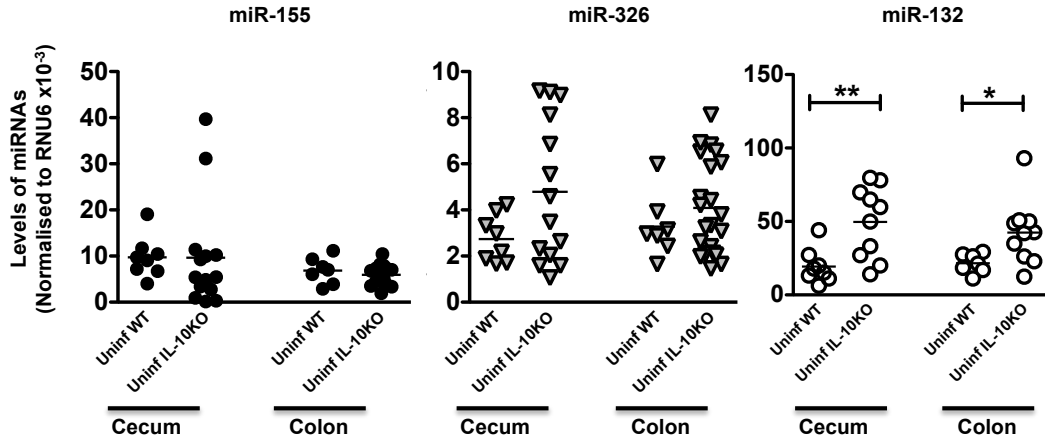


**Figure 4.3 Basal expression of miR-132 is different in uninfected WT and uninfected IL-10 KO mice.**

Colonic and cecal tissues were isolated from uninfected IL-10 KO and uninfected WT female mice. Total RNA was extracted and following reverse transcription, levels of miR-155, miR-326 and miR-132 were determined by qRT-PCR. The figure depicts cecal and colonic levels of miR-155 (left panel), miR-326 (middle panel) and miR-132 (right panel) in uninfected WT (data shown are pooled from two independent experiments) and IL-10 KO mice (data shown are pooled from three independent experiments). Each symbol represents an individual mouse and horizontal bars show the mean of each group. \* $p < 0.05$  and \*\* $p < 0.01$  as determined by a two-tailed Mann-Whitney test.

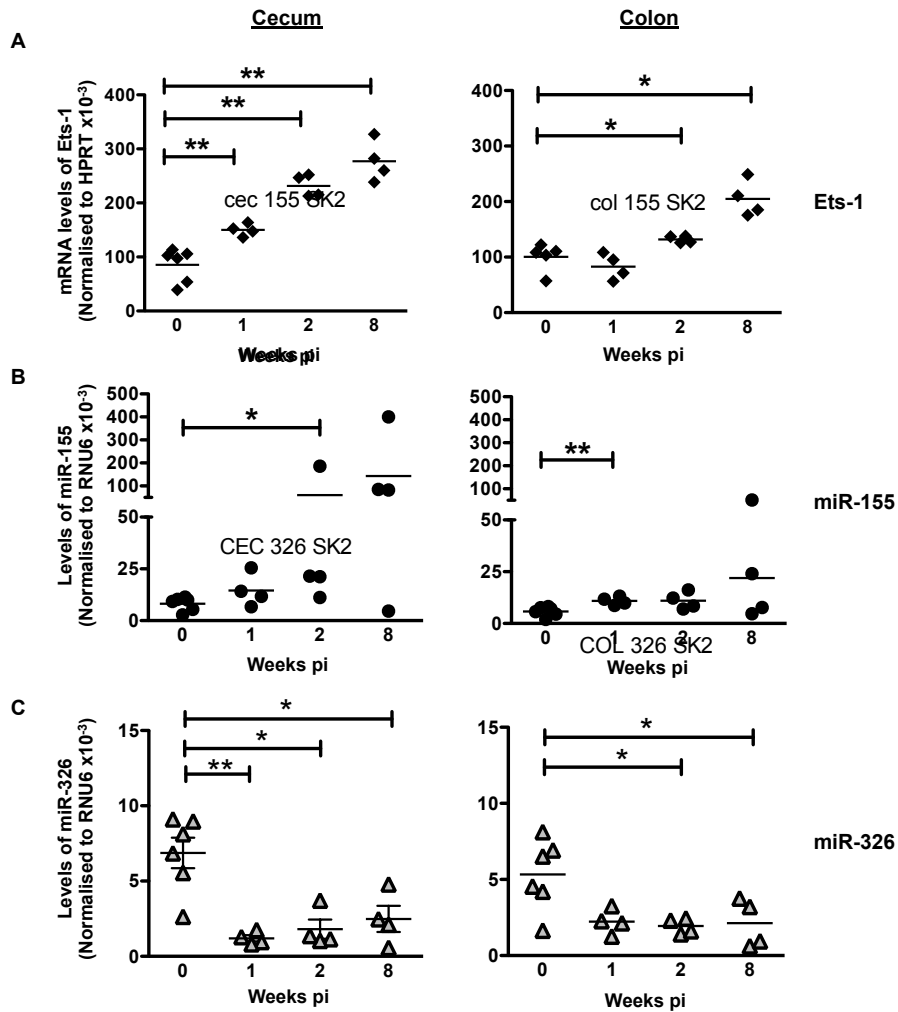


**Figure 4.4 Upregulation of Ets-1 correlates with down-regulation of miR-326 in colitic mice at different time points post *Hh* infection.**

Total RNA was extracted from colonic and cecal tissues isolated from uninfected and *Hh*<sup>+</sup> IL-10 KO male mice at 1, 2 and 8 weeks pi. Following reverse transcription, the levels of miR-155, miR-326 and Ets-1 were determined by qRT-PCR. Levels of (A) Ets-1 (B) miR-155 and (C) miR-326 in the cecum (left panel) and colon (right panel). Each symbol represents an individual mouse. Horizontal bars show the mean of  $n \geq 4$ /group. Data in figures (A-C) are from a single experiment. \* $p < 0.05$  and \*\* $p < 0.01$  as determined by a two-tailed Mann-Whitney test.

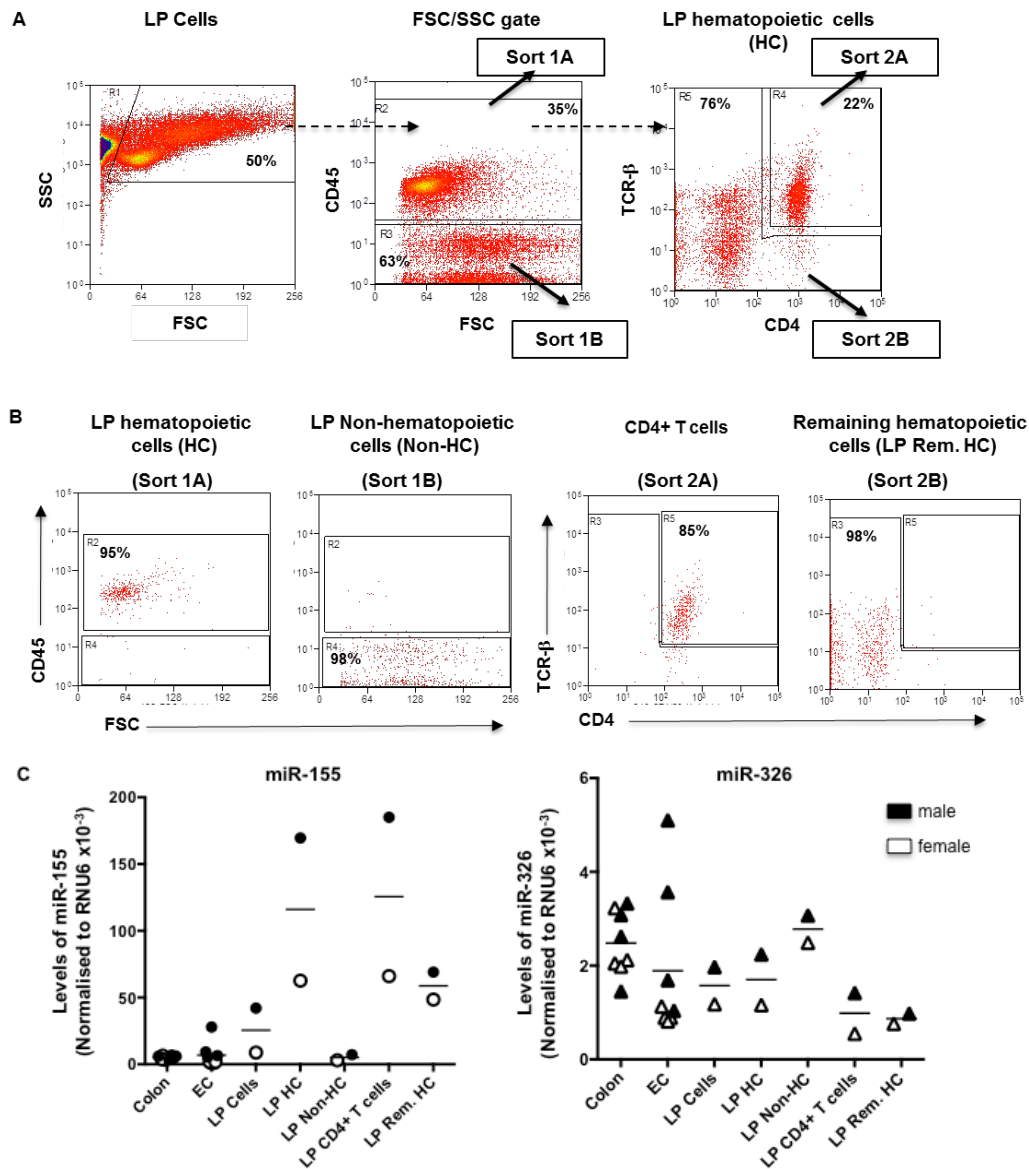


**Figure 4.5** At basal levels, miR-155 is more highly expressed in the immune compartment whereas miR-326 is more highly expressed in the non-immune compartment of the large intestine.

Colonic tissue, epithelial cells and LP cells were collected from the large intestine of uninfected IL-10 KO mice. The LP cells were surface stained with antibodies specific for CD45, CD4 and TCR $\beta$  and different cell populations sorted by flow cytometry. Total RNA was extracted from all the isolated tissues and cells and following reverse transcription, levels of miR-155 and miR-326 were determined by qRT-PCR. (A) Sort strategy used for the isolation of different cell types from the LP. From the LP cells, immune cells, contained within the hematopoietic cells (HC) were sorted as cells that were CD45<sup>+</sup> (sort 1A). Non-immune cells, which fall within the non-hematopoietic cells, were sorted as cells that were CD45<sup>-</sup> (sort 1B). From an aliquot of the CD45<sup>+</sup> HCs, CD4<sup>+</sup> T cells (CD45<sup>+</sup> CD4<sup>+</sup>TCR $\beta$ <sup>+</sup>) and all the rest of the immune cells, with the exception of the CD4<sup>+</sup> T cells (LP rem. HC) were sorted as sort 2A and sort 2B respectively. (B) Representative post-sort purities of cells sorted from the LP. (C) Levels of miR-155 (left panel) and miR-326 (right panel) in the colon, epithelial cells (EC) and different cell types isolated from the LP. Data are pooled from two independent experiments. One of the experiments consisted of male mice (solid symbols) and the other experiment consisted of female mice (open symbols). X-axis labels refer to the following: 'Col' refers to colon, 'EC' refers to epithelial cells, 'LP HC' refers to hematopoietic cells (CD45<sup>+</sup>), 'LP non-HC' refers to non-hematopoietic cells (CD45<sup>-</sup>) and 'LP Rem. HC' refers to all the hematopoietic cells excluding the CD4<sup>+</sup> T cells. Each symbol in 'col' represents tissue from an individual mouse, Each symbol in 'EC' represents a pool of epithelial cells from two mice and Each symbol in 'LP cells', 'LP HC', 'LP non-HC', 'LP CD4<sup>+</sup> T cells' and 'LP Rem. HC' represents cells pooled from  $n \geq 8$  mice.

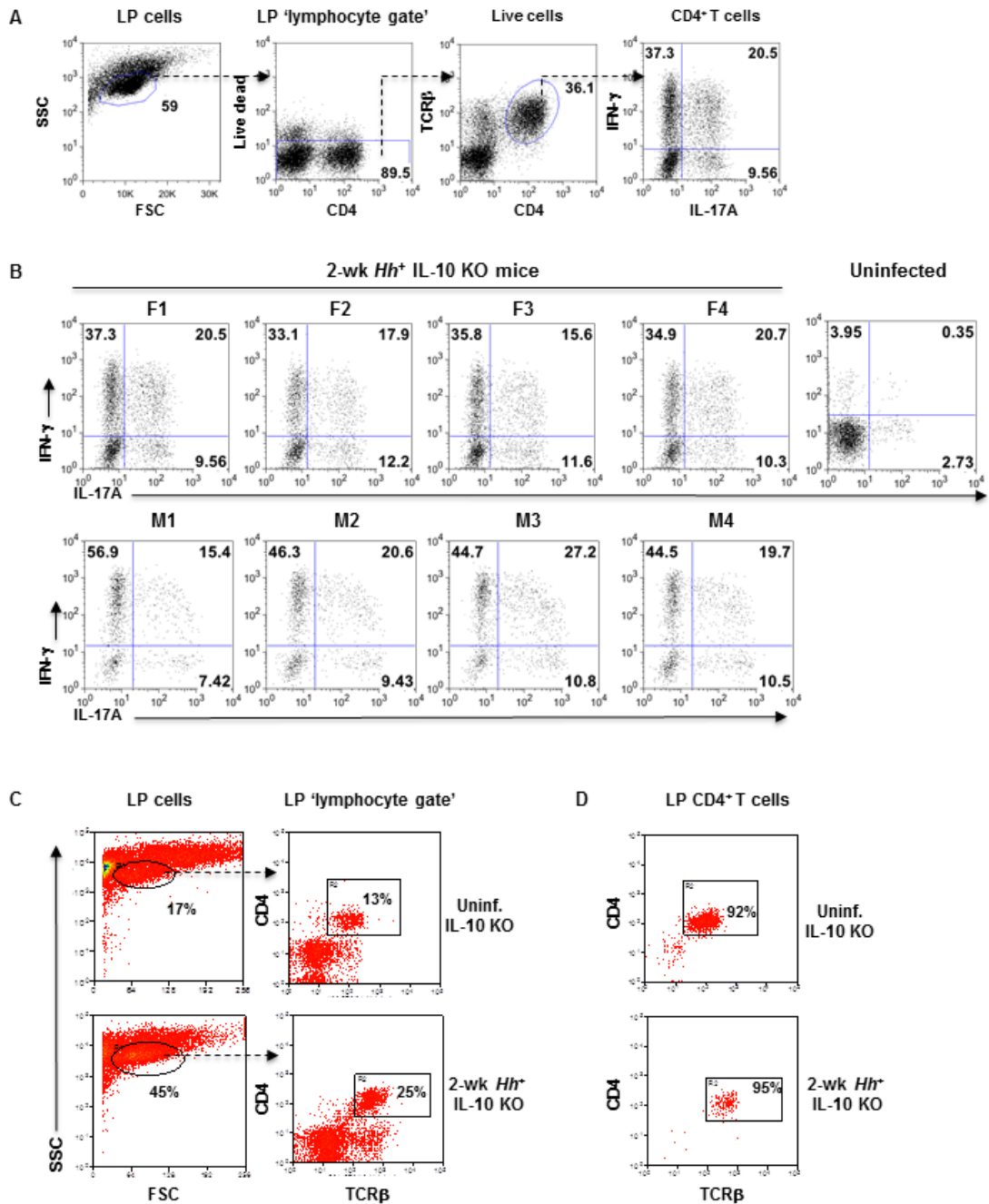


**Figure 4.6 Phenotyping and isolation of CD4<sup>+</sup> T cells from the lamina propria.**

Lamina propria cells were isolated from uninfected and 2-wk *Hh*<sup>+</sup> IL-10 KO mice. An aliquot of LP cells from the infected samples were stimulated with PMA and Ionomycin and then surface and intracellularly stained with antibodies specific to TCRβ, CD4, IFN-γ and IL-17A and a live dead exclusion dye and examined flow cytometrically. The remaining LP cells were surface stained with antibodies specific for TCRβ and CD4, and CD4<sup>+</sup> T cells sorted as cells that were TCRβ<sup>+</sup> CD4<sup>+</sup>. (A) Gating strategy used for the analysis of the IFN-γ and IL-17A profile of LP CD4<sup>+</sup> T cells. (B) Dot plots depicting the IFN-γ and IL-17A profile of LP CD4<sup>+</sup> T cells from 2-wk *Hh*<sup>+</sup> IL-10 KO mice and a representative profile of an uninfected mouse. F1-F4 denotes female IL-10 KO mice and M1-M4 denote male IL-10 KO mice. (C) Sort strategy used for the isolation of CD4<sup>+</sup> T cells from the lamina propria of uninfected (upper panel) and 2-wk *Hh*<sup>+</sup> IL-10 KO mice (lower panel). (D) Representative post sort purity of CD4<sup>+</sup> T cells sorted from the lamina propria of uninfected (upper panel) and 2-wk *Hh*<sup>+</sup> IL-10 KO mice (lower panel).

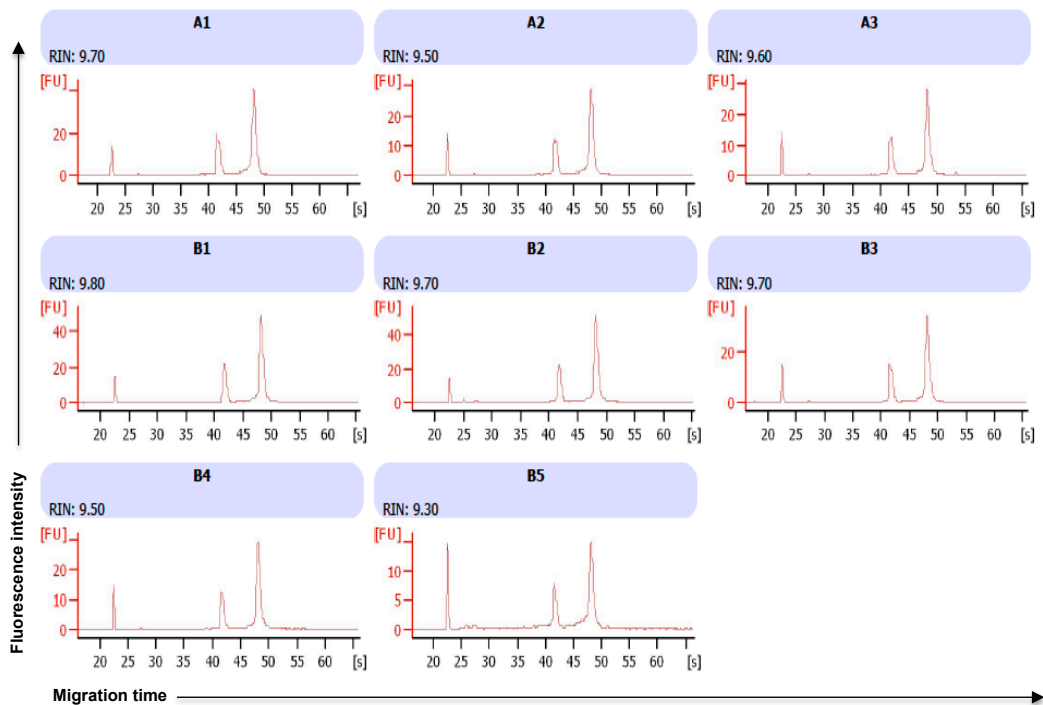


**Figure 4.7 Integrity of total RNA extracted from LP CD4<sup>+</sup> T cells.**

Total RNA was extracted from large intestinal LP CD4<sup>+</sup> T cells from uninfected and 2-wk *Hh*<sup>+</sup> IL-10 KO mice. The RNA integrity was measured by running 1  $\mu$ l of every sample on Agilent's bioanalyzer. The electropherograms depict fluorescence intensity vs. migration time for each RNA sample. A1-A3 refers to RNA samples from uninfected IL-10 KO mice and B1-B5 refers to RNA samples from 2-wk *Hh*<sup>+</sup> IL-10 KO mice. The smallest peak located at 24s represents the marker region, the peak just after 40 seconds represents the 18S ribosomal RNA fragment and the largest peak located between 45-50 seconds represents the 28S ribosomal RNA fragment. RIN indicates the RNA integrity number for each sample.



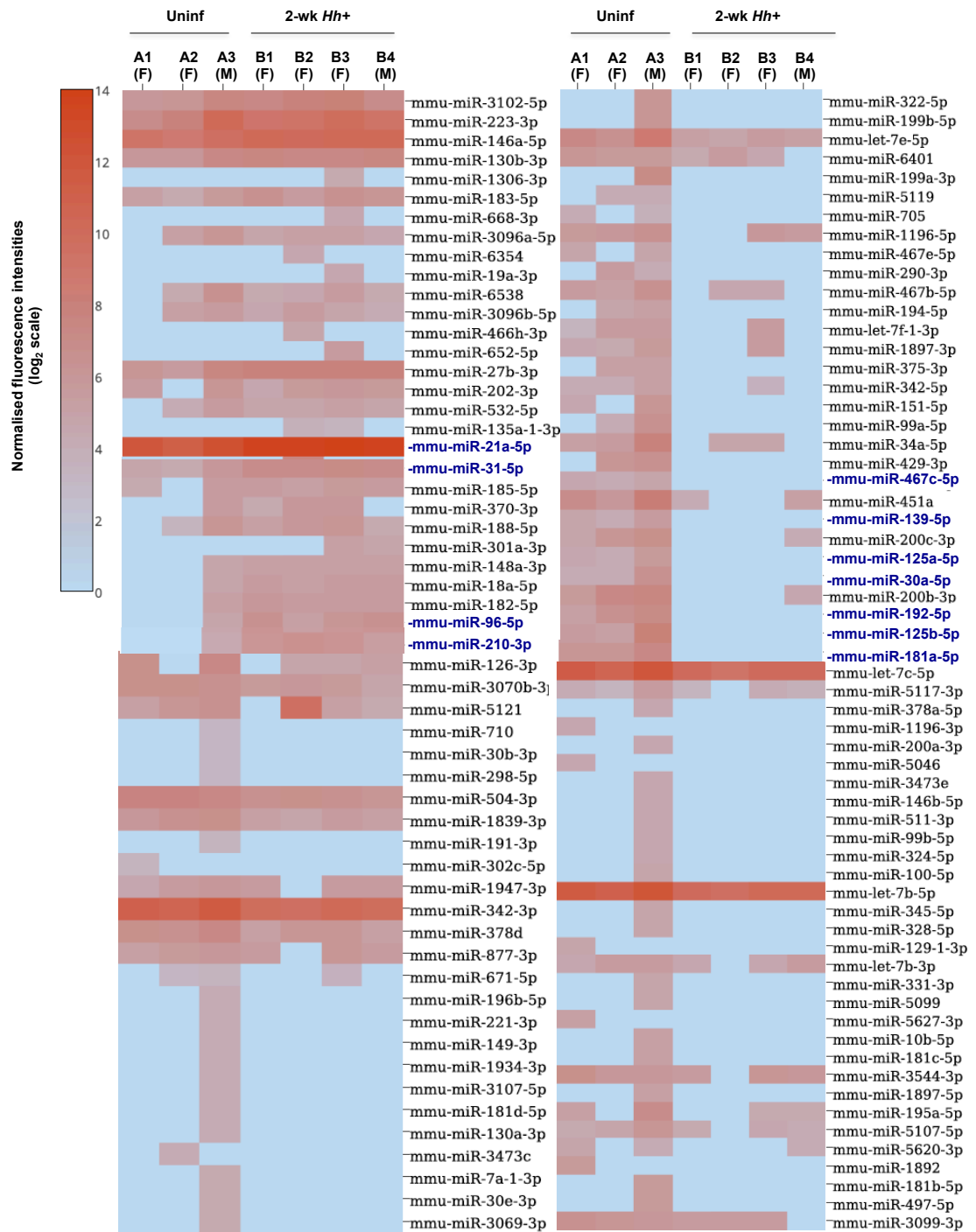


**Figure 4.9 Heat map depicting microRNAs that showed fold change  $\geq 2$  in infected compared to uninfected controls.**

Total RNA was extracted from large-intestinal CD4<sup>+</sup> T cells from uninfected and 2-wk *Hh*<sup>+</sup> IL-10 KO mice and microRNA expression profile determined by a microRNA microarray. The heat map depicts microRNAs that showed a  $\geq 2$ -fold change when compared to uninfected controls. The heat map was generated using fluorescence intensities for each microRNA that were normalised by 90th percentile normalisation method followed by subtraction of the negative control from each normalised value. The normalised fluorescence intensities are represented on a log scale. On the colour scale, blue represents the lowest fluorescence intensity and red represents the highest fluorescence intensity. On the x-axis, 'F' denotes sample derived from female IL-10 KO mice and 'M' denotes sample derived from male IL-10 KO mice. A1-A3 are from uninfected IL-10 KO mice and B1-B5 are from 2-wk *Hh*<sup>+</sup> IL-10 KO mice. With the exception of miR-210 and miR-96, all the microRNAs depicted in blue are microRNAs that were significantly different between 2-wk *Hh*<sup>+</sup> IL-10 KO mice and uninfected controls.

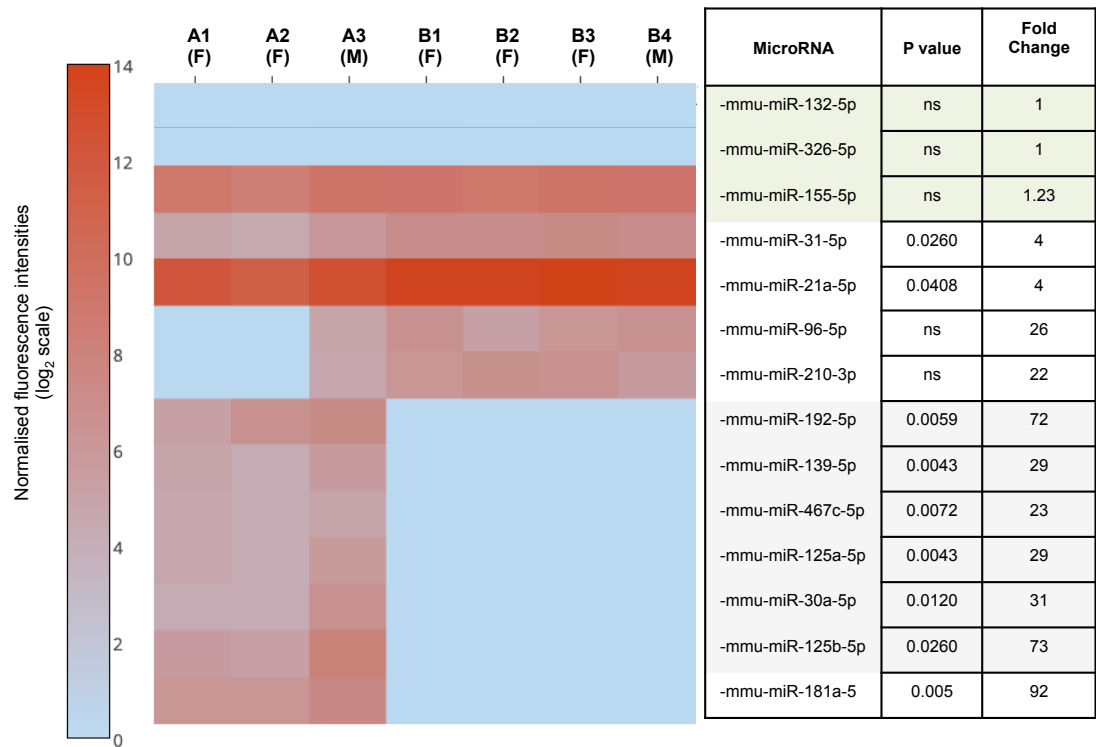


**Figure 4.10 Heat map depicting fluorescence intensities, p values and fold change differences of specific microRNAs from the microRNA microarray.**

Total RNA was extracted from large intestinal CD4<sup>+</sup> T cells from uninfected and 2-wk *Hh*<sup>+</sup> IL-10 KO mice and microRNA expression profile determined by a microRNA microarray. The heat map depicts fluorescence intensities, P values and fold change differences of specific microRNAs as indicated in the figure. The heat map was generated using fluorescence intensities for each microRNA that were normalised by 90th percentile normalisation method followed by subtraction of the negative control from each normalised value. The normalised fluorescence intensities are represented on a log<sub>2</sub> scale. On the colour scale, blue represents the lowest fluorescence intensity and deep orange, the highest fluorescence intensity. On the x-axis, 'F' denotes sample is derived from female IL-10 KO mice and 'M' denotes sample is derived from male IL-10 KO mice. A1-A3 are from uninfected IL-10 KO mice and B1-B5 are from 2-wk *Hh*<sup>+</sup> IL-10 KO mice. MicroRNAs highlighted in green did not show any change in expression between uninfected and infected samples. MicroRNAs shown in clear boxes represent the microRNAs we chose to examine further. NS denotes 'not significant'.

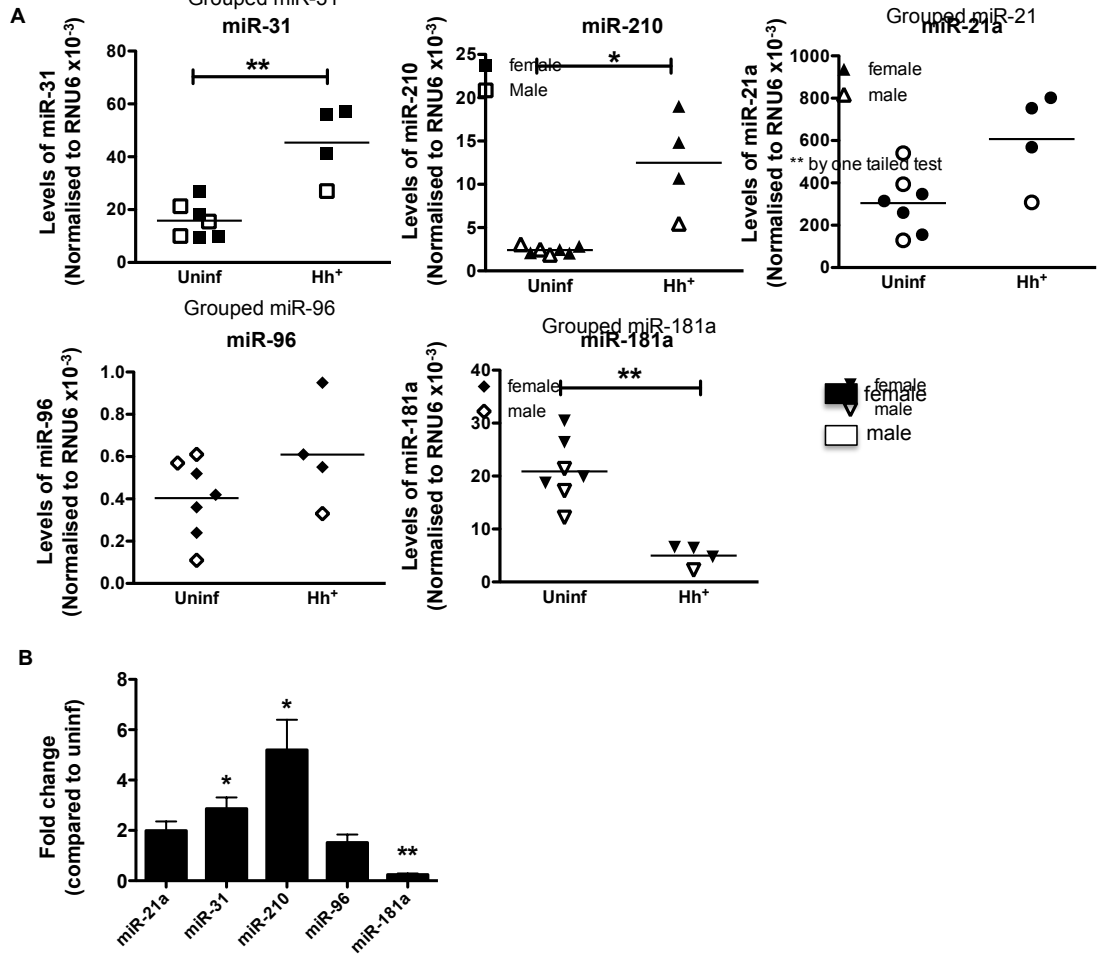


**Figure 4.11 qRT-PCR validation of microRNA microarray results.**

CD4<sup>+</sup> T cells were sorted from the large intestinal LP of uninfected and *Hh*<sup>+</sup> IL-10 KO mice. Total RNA was extracted and the expression levels of miR-31, miR-210, miR-21a, miR-96 and miR-181a determined by qRT-PCR. (A) Levels of miR-31, miR-210, miR-21a, miR-96 and miR-181a normalised to RNU6. Each symbol in the uninfected group represents miRNA levels in a pool of LP CD4<sup>+</sup> T cells derived from n≥6 mice. For the *Hh*<sup>+</sup> group, each symbol represents miRNA levels in a pool of LP CD4<sup>+</sup> T cells derived from either one mouse or a pool of two mice. Clear symbols denote male samples and filled symbols denote female samples. Horizontal bars denote the mean. (B) Expression of miR-21a, miR-31, miR-210 and miR-181a relative to that of uninfected controls. Bars show means + s.e.m. of same samples as (A). \* P<0.05 and \*\*P<0.01 as determined by a two-tailed Mann-Whitney test.

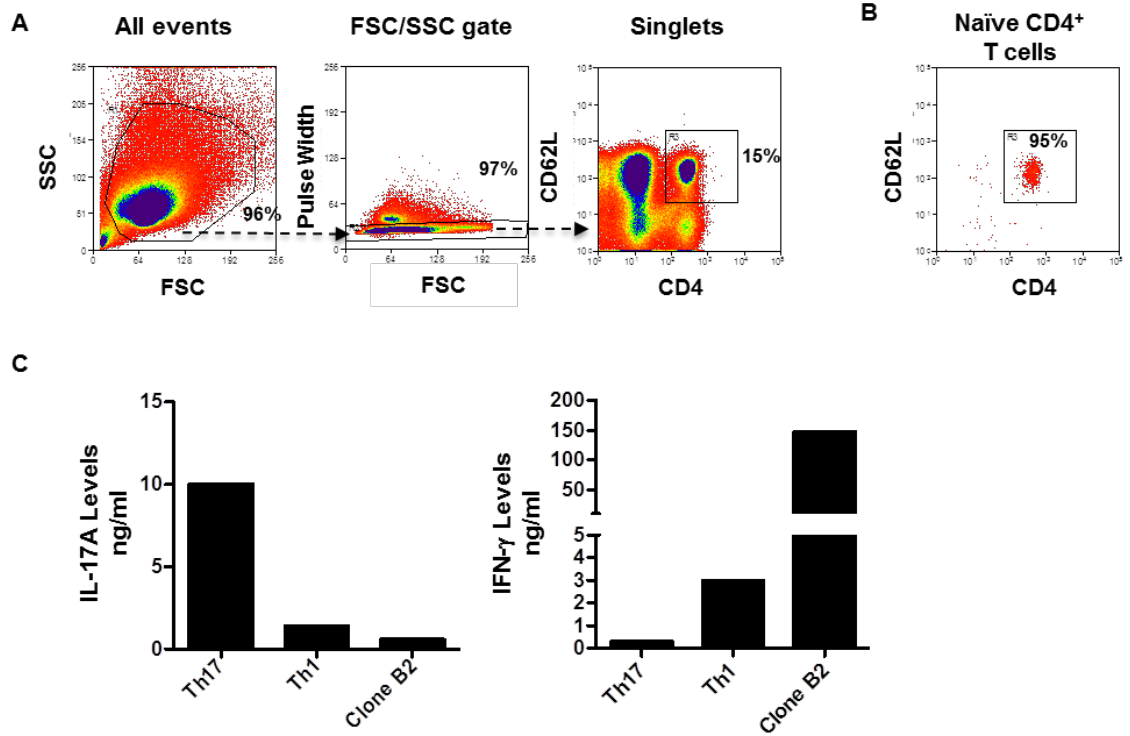


**Figure 4.12** *In vitro* polarisation of naïve CD4<sup>+</sup> T cells.

MLN cells and splenocytes were pooled from two uninfected IL-10 KO mice and surface stained with antibodies specific for CD4 and CD62L. Naïve CD4<sup>+</sup> T cells (CD4<sup>+</sup>CD62L<sup>+</sup>) were sorted by flow cytometry. In each well,  $2 \times 10^5$  naïve CD4<sup>+</sup> T cells were cultured with  $7.5 \times 10^5$  irradiated splenocytes from a WT mouse and stimulated with soluble anti-CD3. Naïve CD4<sup>+</sup> T cells being polarised to a Th1 phenotype were treated with IL-12. Naïve CD4<sup>+</sup> T cells being polarised to a Th17 phenotype were treated with a cytokine cocktail consisting of TGF $\beta$ , IL-6 and IL-23. After 48 hours, the cells were split and Th1 cells maintained with IL-2, while Th17 cells were maintained with IL-23. Clone B2 cells (a *Hh*-specific Th1 clone) were maintained in IL-2. After five days, the Th1, Th17 and clone B2 cells were collected, counted and  $3 \times 10^5$  cells/well stimulated with plate-bound anti-CD3. One well per condition containing medium only was used as a control. At 72 hrs post anti-CD3 stimulation, supernatants were isolated and the levels of IFN- $\gamma$  and IL-17A determined by ELISA. (A) Sort strategy used for the sorting of naïve CD4<sup>+</sup> T cells from the MLN and spleen of uninfected IL-10 KO mice. (B) Representative post-sort purity of sorted naïve CD4<sup>+</sup> T cells. (C) Levels of IL-17A (left panel) and IFN- $\gamma$  (right panel) in 72 hr supernatants from Clone B2 cells and *in vitro*-polarised Th17 and Th1 cells. Data shown are from one of two experiments.

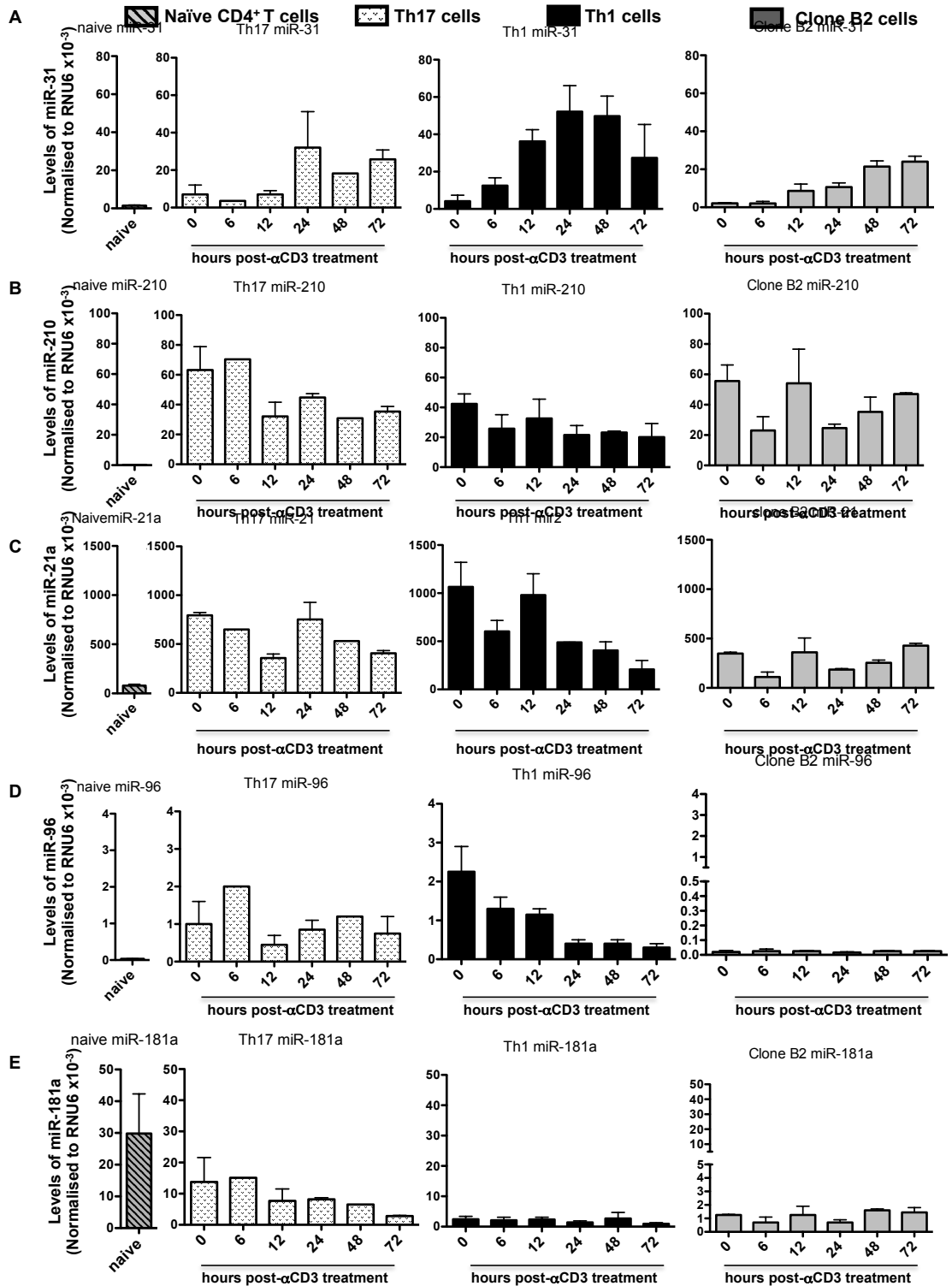


**Figure 4.13** MiR-31, miR-210, miR-21a, miR-96 and miR-181a are expressed by both Th1 and Th17 cells.

**Figure 4.13. MiR-31, miR-210, miR-21a, miR-96 and miR-181a are expressed by both Th1 and Th17 cells.** MLN cells and splenocytes were pooled from two uninfected IL-10 KO mice and surface stained with antibodies specific for CD4 and CD62L. Naive CD4<sup>+</sup> T cells (CD4<sup>+</sup>CD62L<sup>+</sup>) were sorted by flow cytometry, and cultured with irradiated splenocytes from an uninfected WT mouse at a ratio of 1:3.75 i.e.  $2 \times 10^5$  CD4<sup>+</sup> T cells were cultured with  $7.5 \times 10^5$  irradiated splenocytes/well and stimulated with soluble anti-CD3. Naïve CD4<sup>+</sup> T cells being polarised to a Th1 phenotype were treated with IL-12. Naïve CD4<sup>+</sup> T cells being polarised to a Th17 phenotype were treated with a cytokine cocktail consisting of TGFβ, IL-6 and IL-23. After 48 hours, the cells were split and Th1 cells maintained with IL-2, while Th17 cells were maintained with IL-23. Clone B2 cells (a *Hh*-specific Th1 clone) were maintained in IL-2. After five days, the Th1, Th17 and clone B2 cells were collected, counted and  $3 \times 10^5$  cells/well stimulated with plate-bound anti-CD3. One well per condition containing medium only was used as a control. At 0, 6, 12, 24, 48 and 72 hrs post anti-CD3 stimulation, cells were collected and total RNA extracted. Total RNA was also extracted from an aliquot of the *ex vivo* sorted naïve CD4<sup>+</sup> CD62L<sup>+</sup> T cells used for the Th1/Th17 polarisation. Following reverse transcription, the levels of miR-31, miR-210, miR-181a, miR-21a and miR-96 were measured by qRT-PCR. Bar charts depict levels of (A) miR-31 (B) miR-210 (C) miR-21a (D) miR-96 (E) miR-181a in naïve CD4<sup>+</sup> T cells (grey bars with diagonal black stripes), Th17 cells (white bars with dots), Th1 cells (Black bars) and Clone B2 cells (grey bars). Data are pooled from two experiments. Error bars represent standard error of the mean of two biological replicates.

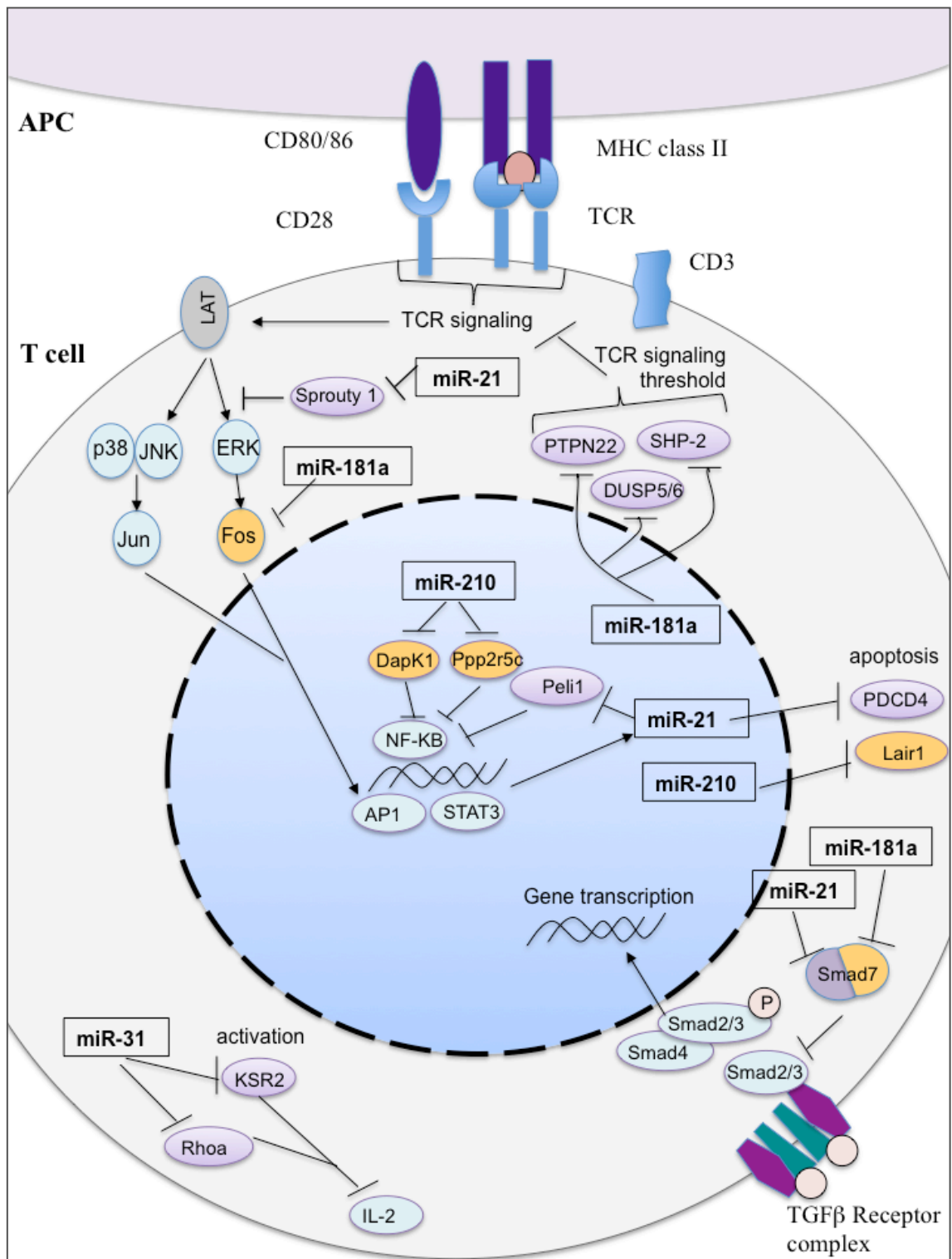


**Figure 4.14 Regulation of T-cell activation by miR-21a, miR-31, miR-210 and miR-181a.** The schematic depicts the possible roles of miR-21a, miR-31, miR-210 and miR-181a on different factors involved in T-cell activation. Targets in purple depict experimentally validated targets and targets in orange depict predicted targets. Targets in blue depict indirect downstream targets.

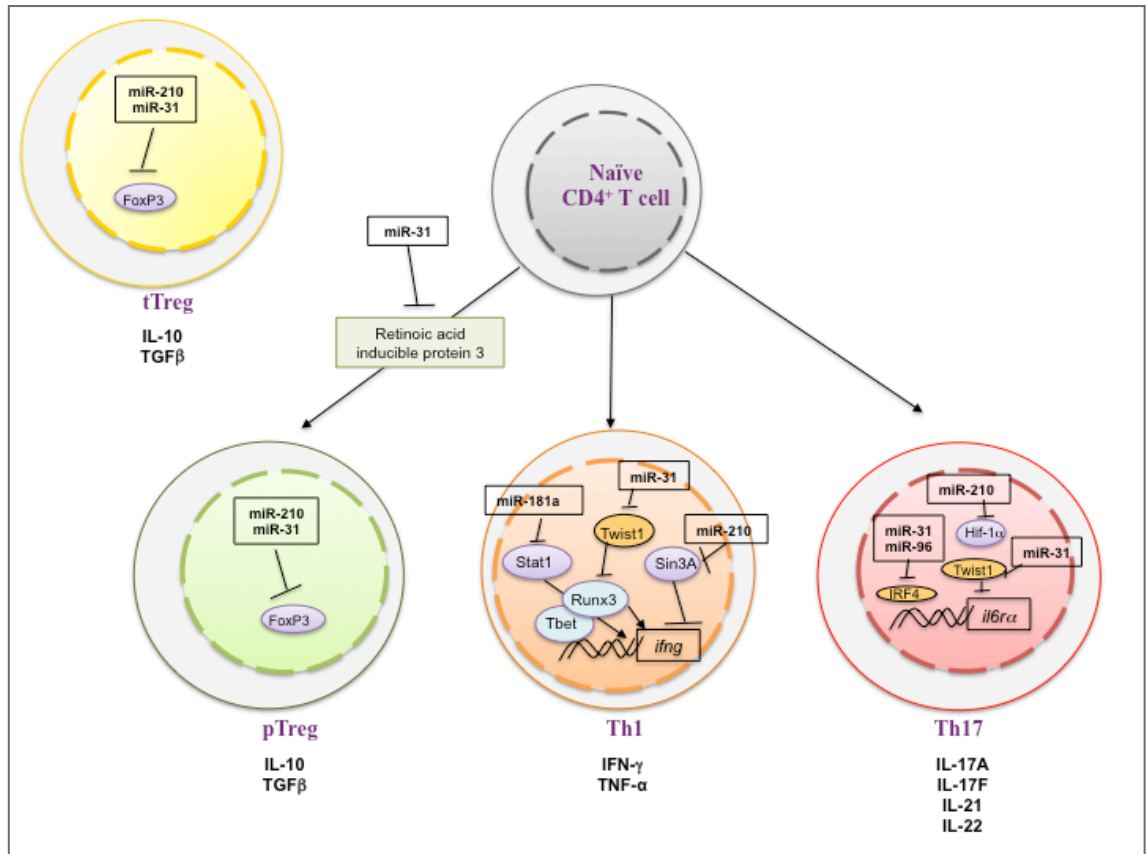


**Figure 4.15 MicroRNA-mediated regulation of the expression of transcription factors and cytokines in different CD4<sup>+</sup> T-cell subsets.**

The schematic depicts the potential roles of miR-21a, miR-31, miR-210, miR-96 and miR-181a on different factors involved in CD4<sup>+</sup> T-cell differentiation and cytokine expression. Targets in purple depict experimentally validated targets and targets in orange depict predicted targets. Targets in blue depict indirect downstream targets.

# CHAPTER 5. PHENOTYPIC CHARACTERIZATION OF LARGE INTESTINAL IL-10-PRODUCING CD4<sup>+</sup> T CELLS FOLLOWING *HELICOBACTER HEPATICUS* INFECTION

## 5.1 INTRODUCTION

The intestinal immune system has a very challenging role, as it has to maintain tolerance towards commensal bacteria and food antigens, but at the same time, mount an adequate immune response towards pathogens (Xavier and Podolsky, 2007). One of the key factors found to limit intestinal inflammation in man and mouse is the anti-inflammatory cytokine IL-10. Mutations in the IL-10 receptor (*IL10R*) and defects in IL-10 expression and IL-10 signalling pathways have been associated with human IBD (Glocker et al., 2009; Lees et al., 2011; Shim and Seo, 2014). Mice deficient in IL-10 or the IL-10R can spontaneously develop colitis (Kuhn et al., 1993; Spencer et al., 1998).

The CD4<sup>+</sup> T cells constitute an important source of IL-10 as evidenced by the fact that mice with a CD4<sup>+</sup> T-cell specific deletion of IL-10 spontaneously develop colitis (Roers et al., 2004) and in the T-cell transfer colitis model, CD4<sup>+</sup> T-cell derived IL-10 was sufficient to prevent colitis (Asseman et al., 1999). One of the major CD4<sup>+</sup> T-cell subsets that produce IL-10 are the Tregs, which, in addition to utilising other mechanisms, suppress effector T-cell responses in an IL-10 dependent manner (Asseman et al., 1999; Hara et al., 2001). In the last five years, different markers have been identified to distinguish different Treg subsets (summarized in **Table 5.1**). Helios and NRP1 have recently been identified as markers that are expressed on FoxP3<sup>+</sup> tTregs but not FoxP3<sup>+</sup> pTregs (Thornton et al., 2010; Weiss et al., 2012) (**Table 5.1**) and co-expression of CD49b and lymphocyte activation gene 3 (LAG-3) have been identified as markers of Tr1 cells (Gagliani et al., 2013) (**Table 5.1**). In addition to Tr1 cells, LAG-3 is also expressed by other Treg and CD4<sup>+</sup> T-cell subsets. LAG-3 is a type-1 membrane glycoprotein that has been shown to be required for maximal suppressive capacity of CD4<sup>+</sup> CD25<sup>+</sup> FoxP3<sup>+</sup> Tregs (Do et al., 2015; Huang et al., 2004). In the CD4<sup>+</sup> T-cell transfer model of colitis, co-transfer of CD25<sup>-</sup> LAG-3<sup>+</sup> cells (which were FoxP3<sup>-</sup>) along with naïve CD4<sup>+</sup> T cells completely prevented colitis development (Okamura et al., 2009).

**Table 5.1 Phenotypic markers of different Treg populations**

Treg Subset	Markers				
	FoxP3	Helios	NRP1	CD49b	LAG-3
Natural/Thymic-derived Tregs (tTregs)	+	+	+	-	+/-
Tregs induced in the periphery (pTregs)	+	-	-	-	+/-
Tr1 cells	-	-	-	+	+

The importance of IL-10 in maintaining intestinal homeostasis in the *Hh* colitis model is evidenced by the fact that IL-10-sufficient mice infected with *Hh* do not develop intestinal inflammation unless they are concomitantly treated with a blocking antibody to the IL-10R (anti-IL-10R) (Kullberg et al., 2006; Kullberg et al., 1998). Colitis induced in *Hh*<sup>+</sup> RAG KO mice by the transfer of CD4<sup>+</sup> T cells from IL-10 KO mice is prevented by co-transfer of CD4<sup>+</sup> T cells from *Hh*<sup>+</sup> but not uninfected WT mice, suggesting that *Hh* priming is necessary for the generation of disease-protective IL-10-producing cells (Kullberg et al., 2002). Furthermore, colitis induced in *Hh*<sup>+</sup> IL-10/RAG double knock out mice (DKO) by transfer of CD4<sup>+</sup> T cells from *Hh*<sup>+</sup> IL-10 KO mice was prevented by co-transfer of CD4<sup>+</sup> T cells from *Hh*<sup>+</sup> IL-10-sufficient mice (Kullberg et al., 2002). This protection was abrogated by anti-IL-10R mAb treatment showing that IL-10 derived from CD4<sup>+</sup> T cells alone is sufficient to confer protection against *Hh*-induced colitis (in this model) (Kullberg et al., 2002). Although we know protection against *Hh*-induced colitis is dependent on IL-10, and that in the *Hh*<sup>+</sup> IL-10/RAG DKO model, IL-10 derived from antigen-experienced CD4<sup>+</sup> T cells alone is sufficient to confer protection, the phenotype of the IL-10-producing CD4<sup>+</sup> T cells in the lamina propria (LP) during a non-inflammatory immune response (seen in *Hh*<sup>+</sup> WT mice) and an inflammatory immune response (seen in *Hh*<sup>+</sup>/anti-IL-10R-treated WT mice) has not been examined before.

In this study we have characterized the proportions of tTregs, pTregs and Tr1 cells and the phenotype of IL-10-producing CD4<sup>+</sup> T cells at the site of *Hh* colonization in the large intestine of uninfected and 2-wk *Hh*<sup>+</sup> and *Hh*<sup>+</sup>/anti-IL-10R-treated *Tiger* and IL-17A-eYFP mice. *Tiger* mice are knock-in reporter mice, wherein green fluorescent protein (GFP) is inserted in an internal ribosomal entry site (IRES) immediately before the polyadenylation site for IL-10 (Kamanaka et al., 2006). Thus in the *Tiger* mice, GFP expression correlates with the production of IL-10 protein (Kamanaka et al., 2006), enabling us to study the phenotype of IL-10-producing cells directly *ex vivo* without stimulating the cells. In IL-17A-eYFP fate-reporter mice (generated by Hirota et al), a sequence encoding cre-recombinase is inserted into the *Il17a*

locus (called  $Il17a^{cre}$ ) and crossing these  $Il17a^{Cre}$  knock-in animals with reporter mice expressing eYFP from the *Rosa26* promoter (called  $Rosa26^{eYFP}$ ) results in the fluorescent protein permanently labeling  $Il17a^+$  cells and thus allows the identification of cells that have switched on IL-17A (Hirota et al., 2011). Using IL-17A-eYFP fate reporter mice, we and others have shown that Th17 cells change phenotype during inflammation to form a transient double positive population that secretes both IFN- $\gamma$  and IL-17A and then changes phenotype to become a cell termed ‘ex-Th17 cell’ that stops secreting IL-17A, but continues to secrete IFN- $\gamma$  (Hirota et al., 2011; Morrison et al., 2013). In the current study, we used IL-17A-eYFP mice to examine whether ex-Th17 cells produce IL-10. The IL-10-producing  $CD4^+$  T cells were characterized based on markers of Tregs and co-expression of inflammatory cytokines IL-17A and/or IFN- $\gamma$ . The 2 wks pi time point was chosen because we know from previous work in the lab that intestinal inflammation peaks in  $Hh^+$  IL-10 KO mice at this time point (Morrison et al., 2013).

The experiments carried out in this chapter showed that although the phenotype of the Tregs was not markedly different in the three experimental groups, there was a striking difference in the phenotype of the IL-10-producing  $CD4^+$  T cells. The major difference in the phenotype of the IL-10 $^+$   $CD4^+$  T cells when compared to uninfected controls was that in the non-inflammatory response, there was a slight expansion in the IL-10 $^+$  IL-17A $^+$  cells and most of these cells also co-expressed FoxP3 whereas in the colitic setting, almost half the IL-10 $^+$  LP  $CD4^+$  T cells co-expressed IL-17A and/or IFN- $\gamma$  and half or slightly less than half of these cells also co-expressed FoxP3. Furthermore, in the colitic setting alone, a small proportion of ex-Th17 cells produced IL-10. These results demonstrate that in the colitic setting in particular, a large proportion of IL-10 $^+$  LP  $CD4^+$  T cells share phenotypic characteristics of both regulatory and inflammatory cells.

## 5.2 RESULTS

The aim of the experiments carried out in this chapter was to examine the phenotype of IL-10-producing LP CD4<sup>+</sup> T cells in uninfected, *Hh*<sup>+</sup> and *Hh*<sup>+</sup>/anti-IL-10R-treated mice (by flow cytometry). The IL-10<sup>+</sup> cells were to be phenotyped based on Treg markers such as FoxP3, CD49b and LAG-3 and co-expression of inflammatory cytokines IL-17A and/or IFN- $\gamma$ . Accordingly, we used two strains of mice; *Tiger* mice and IL-17A-eYFP mice. Using *Tiger* mice, we planned to characterize the phenotype of IL-10-producing CD4<sup>+</sup> T cells *ex vivo* based on GFP signal and using IL-17A-eYFP mice, we wanted to track the ex-Th17 cells and determine whether they produced IL-10 and/or expressed FoxP3. This necessitated being able to simultaneously detect FoxP3 and eYFP/GFP signal. Unfortunately we found that commonly used fixation and permeabilisation protocols were unsuccessful at doing so. Detailed below are some experiments that were carried out to optimize existing fixation and permeabilisation protocols and simultaneously detect eYFP/GFP and FoxP3.

### 5.2.1 An optimized protocol to simultaneously detect eYFP/GFP and FoxP3

#### 5.2.1.1 The efficacy of different fixation and permeabilisation protocols in detecting Foxp3 and eYFP.

The method we have traditionally used in our lab to detect intracellular cytokines and transcription factors T-bet and ROR $\gamma$ t involves fixing cells with 2% paraformaldehyde (PFA) for 15 min at room temperature, followed by permeabilisation with a buffer containing 0.1% saponin (hereafter called 0.1% saponin) (Morrison et al., 2013). However, in preliminary experiments, we found that the combination of 2%PFA/0.1% saponin yielded weak FoxP3 staining. eBioscience (eBio) has a combination of fixation/permeabilisation buffers specially designed to detect FoxP3 called ‘the FoxP3 staining buffer set’. Using the eBio kit involves fixing the cells for 1 hour with eBio fix-perm buffer (which is a mixture of fixative and permeabilisation buffer) followed by permeabilisation for 1 hour with eBio perm buffer. To compare the efficacy of these two methods (2% PFA/0.1% saponin and eBio fix-perm/eBio perm) at detecting eYFP and FoxP3, we isolated LP cells from 2-wk *Hh*<sup>+</sup>/anti-IL-10R-treated IL-17A-eYFP mice, and examined FoxP3 and eYFP expression in the CD4<sup>+</sup> T cells by flow cytometry using the combination of either 2% PFA/0.1% saponin or eBio fix-perm/eBio perm buffers to fix and permeabilise the cells. The gating strategy used for the analysis is shown in **Figure 5.1A**. The results showed that using the combination of 2% PFA/0.1% saponin was effective at retaining eYFP expression, but yielded weak FoxP3 staining (**Figure 5.1B**). In contrast, the eBio buffers gave good FoxP3 staining, but quenched the eYFP signal (**Figure 5.1B**), thus making it difficult to simultaneously detect eYFP and FoxP3 using either of these methods.

### **5.2.1.2 Changing the fixation and permeabilisation times when using the combination of 2% PFA/0.1% saponin does not improve FoxP3 staining.**

We next wanted to investigate whether altering the fixation, permeabilisation or mAb incubation times would improve FoxP3 staining when using 2% PFA/0.1% saponin. Thus, we isolated spleen cells from WT mice and examined FoxP3 expression in CD4<sup>+</sup> cells that had either been fixed with 2% PFA for 15 min at room temperature or 1 hour at 4°C and then permeabilised with either 0.1% saponin buffer plus anti-FoxP3 mAb for 1 hour or with 0.1% saponin buffer alone for either 30 minutes or 1 hour followed by the addition of anti-FoxP3 for a further 1 or 1.5 hours. As a positive control for FoxP3 staining, we also stained an aliquot of cells that had been fixed and permeabilised with the eBio fix-perm/eBio perm buffers with FoxP3 mAb. The gating strategy used for the analysis is shown in **Figure 5.2A**. The results showed that neither the change in fixation time, permeabilisation time or a longer incubation with anti-FoxP3 mAb improved FoxP3 staining when using the combination of 2% PFA/0.1% saponin (**Figure 5.2B**).

### **5.2.1.3 Simultaneous detection of eYFP and FoxP3 using 2% PFA and eBioscience permeabilisation buffer.**

Next, we sought to examine whether the loss of FoxP3 staining observed when using the combination of 2% PFA/0.1% saponin buffers and the loss of eYFP signal when using eBio fix-perm/eBio perm buffers was due to the fixative used (2% PFA or eBio fix-perm) or the permeabilising reagent (0.1% saponin or eBio perm). To do so, we isolated lamina propria cells from 2-wk *Hh*<sup>+</sup>/anti-IL-10R-treated IL-17A-eYFP mice and examined the CD4<sup>+</sup> T-cell expression of FoxP3 and eYFP using the following combination of fixation and permeabilising reagents: 1) eBio fix-perm/eBio perm 2) 2% PFA/0.1% saponin 3) eBio fix-perm/0.1% saponin, and 4) 2% PFA/eBio perm. The gating strategy used for analysis is as shown in **Figure 5.1A**. The protocol used for surface and intracellular staining in all four fix/perm conditions is depicted in **Figure 5.3A**. The results showed that the use of eBio fix-perm/0.1% saponin retained FoxP3 staining but quenched the eYFP signal (**Figure 5.3B**). In contrast, using 2% PFA/eBio perm both retained eYFP and yielded good FoxP3 staining (**Figure 5.3B**). These results suggest that the fixation afforded by 2% PFA allows retention of eYFP whereas the simultaneous fixation and permeabilisation that is employed by the eBioscience fix-perm causes the eYFP to leak out of the cell. These conclusions are supported by a study by Heinen et al who found that when using eBio fix-perm, eYFP could be detected in the supernatant that the cells were fixed in and not in the cells themselves (Heinen et al., 2014).

### 5.2.2 CD4<sup>+</sup> T cell responses in the large intestine following infection with *Helicobacter hepaticus*.

We began our experiments by examining CD4<sup>+</sup> T cell responses in the large intestine of uninfected and 2-wk *Hh*<sup>+</sup> and *Hh*<sup>+</sup>/anti-IL-10R-treated *Tiger* mice. We know from previous work in the lab, that at 2 wks pi, colitic *Hh*<sup>+</sup> IL-10 KO mice show elevated LP cell numbers and an increase in the percentage and number of LP CD4<sup>+</sup> T cells compared to uninfected controls (Morrison et al., 2013). Here, examination of LP cell numbers and the percentage and number of LP CD4<sup>+</sup> T cells revealed that *Hh*<sup>+</sup> *Tiger* mice showed similar numbers of LP cells, and percentage and number of LP CD4<sup>+</sup> T cells as uninfected controls (**Figure 5.4**). In contrast, *Hh*<sup>+</sup>/anti-IL-10R-treated *Tiger* mice had a significantly higher number of LP cells, and percentage and number of CD4<sup>+</sup> T cells compared to uninfected and *Hh*<sup>+</sup> mice (**Figure 5.4**).

We next examined the inflammatory and regulatory CD4<sup>+</sup> T-cell responses in the large intestine. Accordingly, we isolated LP cells from the large intestine of uninfected and 2-wk *Hh*<sup>+</sup> and *Hh*<sup>+</sup>/anti-IL-10R-treated *Tiger* mice and stimulated half of them with PMA and ionomycin in the presence of Brefeldin A for the detection of IL-10-GFP and IL-17A, IFN- $\gamma$  and IL-10 by ICS. The other half were left unstimulated for the *ex vivo* analysis of IL-10-GFP and FoxP3 expression. Both groups of cells (stimulated and unstimulated) were surface and intracellularly stained and the cells analysed by flow cytometry. The gating strategy used to examine the expression of IL-10-GFP and FoxP3, IL-17A, IFN- $\gamma$  and IL-10 by ICS is shown in **Figure 5.5A**. From representative stainings of IL-10 GFP and IL-10 detected by ICS in the three experimental groups, it was evident that all of the IL-10 protein detected by ICS correlated with GFP expression (**Figure 5.5B**). The presence of GFP<sup>+</sup> cells that were not positive for IL-10 protein is most likely because GFP has a longer half-life than IL-10 (Kamanaka et al., 2006).

As a measure of the inflammatory response, the LP CD4<sup>+</sup> T-cell expression of inflammatory cytokines IL-17A and IFN- $\gamma$  were examined in uninfected, *Hh*<sup>+</sup> and *Hh*<sup>+</sup>/anti-IL-10R-treated *Tiger* mice. The results demonstrated that the *Hh*<sup>+</sup> mice showed a slightly elevated, but not significant increase in the percentage and number of LP CD4<sup>+</sup> T cells expressing IL-17A and/or IFN- $\gamma$  compared to uninfected mice (**Figure 5.5C**). In contrast and similar to previous work in the lab (Morrison et al., 2013), the colitic mice showed a significant increase in the percentage and number of IL-17A<sup>+</sup>, IL-17A<sup>+</sup> IFN- $\gamma$ <sup>+</sup> and IFN- $\gamma$ <sup>+</sup> LP CD4<sup>+</sup> T cells compared to uninfected and *Hh*<sup>+</sup> mice (**Figure 5.5C**).

As a measure of the regulatory response, the expression of the Treg transcription factor FoxP3 and anti-inflammatory cytokine IL-10 (detected by both GFP signal and by ICS) were examined in uninfected, *Hh*<sup>+</sup> and *Hh*<sup>+</sup>/anti-IL-10R-treated *Tiger* mice. The results showed that the *Hh*<sup>+</sup> mice showed similar frequencies and slightly elevated numbers of FoxP3, IL-10-GFP and IL-10-producing CD4<sup>+</sup> T cells compared to uninfected controls (**Figure 5.5D**). The

*Hh*<sup>+</sup>/anti-IL-10R-treated *Tiger* mice showed decreased frequencies of FoxP3<sup>+</sup> cells and similar frequencies of IL-10-GFP and IL-10 protein to uninfected controls (**Figure 5.5D, left panel**). In terms of total numbers however, owing to the greater number of LP CD4<sup>+</sup> T cells in colitic mice, the number of FoxP3<sup>+</sup> cells, IL-10 GFP<sup>+</sup> cells and IL-10<sup>+</sup> cells by ICS were significantly higher compared to the uninfected and *Hh*<sup>+</sup> mice (**Figure 5.5D, right panel**).

Taken together, the results in **Figures 5.5C-D** demonstrated that in *Hh*<sup>+</sup> mice, the primary CD4<sup>+</sup> T cell response was a regulatory response, with both the percentage and number of IL-10<sup>+</sup> and FoxP3<sup>+</sup> cells being far greater than that of CD4<sup>+</sup> T cells expressing inflammatory cytokines IL-17A and/or IFN- $\gamma$ . Conversely, in *Hh*<sup>+</sup>/anti-IL-10R-treated mice, the primary CD4<sup>+</sup> T cell response was an inflammatory response, with a greater percentage and number of cells expressing inflammatory cytokines IL-17A and/or IFN- $\gamma$ , compared to those expressing FoxP3 or IL-10 (**Figures 5.5C-D**).

### **5.2.3 In the colitic setting, a significant proportion of IFN- $\gamma$ -producing CD4<sup>+</sup> T cells are derived from ex-Th17 cells**

Part of the experimental aims for this chapter was to determine whether ex-Th17 cells produce IL-10. This necessitated using IL-17A-eYFP mice to track the ex-Th17 population. We began by examining the CD4<sup>+</sup> T-cell responses in the large intestine of uninfected and 2-wk *Hh*<sup>+</sup> and *Hh*<sup>+</sup>/anti-IL-10R-treated IL-17A-eYFP mice to ensure that they were comparable to those observed in the *Tiger* mice, and to responses we have previously observed in IL-17A-eYFP mice (Morrison et al., 2013). Examination of the LP cell numbers and percentage and number of LP CD4<sup>+</sup> T cells revealed that similar to the *Tiger* mice, the *Hh*<sup>+</sup> IL-17A-eYFP mice showed similar numbers of LP cells, whereas the *Hh*<sup>+</sup>/anti-IL-10R-treated IL-17A-eYFP mice showed significantly higher numbers of LP cells compared to uninfected controls (**Figures 5.6, left panel**). The *Hh*<sup>+</sup> mice also showed similar percentage and number of LP CD4<sup>+</sup> T cells, whereas the *Hh*<sup>+</sup>/anti-IL-10R-treated IL-17A-eYFP mice showed significantly higher percentage and number of LP CD4<sup>+</sup> T cells compared to uninfected controls (**Figures 5.6, middle and right panel**).

We next wanted to examine the inflammatory and regulatory CD4<sup>+</sup> T-cell responses in the large intestine LP of uninfected and 2-wk *Hh*<sup>+</sup> and *Hh*<sup>+</sup>/anti-IL-10R-infected IL-17A-eYFP mice. To do so, we isolated LP cells from the large intestine and stimulated them with PMA and ionomycin in the presence of Brefeldin A. The stimulated cells were then surface and intracellularly stained with mAbs specific for surface markers, cytokines and FoxP3 and analysed by flow cytometry. To examine the expression of eYFP and inflammatory cytokines IFN- $\gamma$  and IL-17A, we used the gating strategy shown in **Figure 5.7A**. The results revealed that *Hh*<sup>+</sup> IL-17A-eYFP mice showed a significant increase in the frequency and a slight increase in the numbers of IL-17A<sup>+</sup> cells (**Figure 5.7B, upper panel**) and similar frequencies and numbers of IL-17A<sup>+</sup>IFN- $\gamma$ <sup>+</sup> and IFN- $\gamma$ <sup>+</sup> cells compared to uninfected mice (**Figure 5.7B, middle and**

**lower panel respectively**). In contrast, *Hh*<sup>+</sup>/anti-IL-10R-treated mice showed a significant increase in the frequency of cells expressing IL-17A<sup>+</sup>, IL-17A<sup>+</sup>IFN- $\gamma$ <sup>+</sup> and IFN- $\gamma$ <sup>+</sup> cells compared to uninfected and *Hh*<sup>+</sup> mice (**Figure 5.7B**). To examine the proportion of ex-Th17 cells present, we examined eYFP expression in the IFN- $\gamma$ -single positive cells and found that in uninfected and *Hh*<sup>+</sup> mice, the ex-Th17 cells (eYFP<sup>+</sup>IFN- $\gamma$ <sup>+</sup>IL-17A<sup>-</sup>) were virtually absent (**Figure 5.7C, upper panel**) and all the IFN- $\gamma$ <sup>+</sup> cells were Th1 cells (eYFP<sup>+</sup>IFN- $\gamma$ <sup>+</sup>IL-17A<sup>-</sup>) (**Figure 5.7C lower panel**). In the *Hh*<sup>+</sup>/anti-IL-10R-treated mice, the ex-Th17 cells constituted approximately 10% of the LP CD4<sup>+</sup> T cells while the Th1 cells constituted approximately 15% of the LP CD4<sup>+</sup> T cells, (**Figure 5.7C, upper and lower panels, respectively**). In terms of numbers, both the Th1 and ex-Th17 cells were significantly increased in the colitic setting compared to uninfected controls and *Hh*<sup>+</sup> IL-17A-eYFP mice (**Figure 5.7C, upper and lower panels, respectively**). Following infection with *Hh*, there was also an increase in the frequency and number of a population of cells that were eYFP<sup>+</sup> but negative for IL-17A and IFN- $\gamma$  (termed eYFP<sup>+</sup>IL-17A<sup>-</sup>IFN- $\gamma$ <sup>-</sup>) compared to uninfected controls although this increase was only significant in the colitic setting (**Figure 5.7D**).

As a measure of the regulatory response, we next examined the expression of anti-inflammatory cytokine IL-10, Treg transcription factor FoxP3 and CD25 by the LP CD4<sup>+</sup> T cells in the three experimental groups. The results showed that *Hh*<sup>+</sup> IL-17A-eYFP mice showed a significant increase in the frequency of IL-10<sup>+</sup> cells, but did not show any significant change in the frequency of FoxP3 or CD25 expression compared to uninfected mice (**Figure 5.7E, left panel**). In terms of total numbers, the *Hh*<sup>+</sup> IL-17A-eYFP mice showed a slight but not significant increase in the number of IL-10<sup>+</sup>, FoxP3<sup>+</sup> and CD25<sup>+</sup> cells compared to uninfected controls (**Figure 5.7E, right panel**). The *Hh*<sup>+</sup>/anti-IL-10R-treated IL-17A-eYFP mice showed similar frequencies of IL-10<sup>+</sup> cells, a significant decrease in FoxP3<sup>+</sup> cells and a significant increase in CD25<sup>+</sup> cells compared to uninfected mice (**Figure 5.7E, right panel**). In terms of total numbers however, the *Hh*<sup>+</sup>/anti-IL-10R-treated IL-17A-eYFP mice showed a significant increase in the numbers of IL-10<sup>+</sup>, FoxP3<sup>+</sup> and CD25<sup>+</sup> cells compared to uninfected controls (**Figure 5.7E, right panel**).

Taken together, these results showed that the CD4<sup>+</sup> T-cell responses in IL-17A-eYFP mice were comparable to the *Tiger* in that in *Hh*<sup>+</sup> IL-17A-eYFP mice, the main response was a regulatory response whereas in the *Hh*<sup>+</sup>/anti-IL-10R-treated IL-17A-eYFP mice, the main response was an inflammatory response. Secondly, these results also demonstrated that in both *Hh*<sup>+</sup> and *Hh*<sup>+</sup>/anti-IL-10R-infected IL-17A-eYFP mice, there was an increase in the frequency of eYFP<sup>+</sup>IL-17A<sup>-</sup>IFN- $\gamma$ <sup>-</sup> cells whereas in the colitic setting alone, there was an expansion of ex-Th17 cells that constitute a significant source of IFN- $\gamma$  in the large intestine LP.

#### 5.2.4 In both $Hh^+$ and $Hh^+$ /anti-IL-10R-treated mice, there is an expansion of both tTregs and pTregs in the large intestine LP.

Although functional regulatory  $CD4^+$  T cell responses in the large intestine following  $Hh$  infection have been characterised before (Kullberg et al., 2002), the proportions of different Tregs i.e. tTreg, pTreg and Tr1 cells have not been examined. Therefore, we next wanted to examine proportions of different Treg subsets *ex vivo* in the three experimental groups. To do so, we isolated LP cells from the large intestine of uninfected and 2-wk  $Hh^+$  and  $Hh^+$ /anti-IL-10R-treated *Tiger* mice. The cells were then surface and intracellularly stained directly *ex vivo* with mAbs specific for surface markers and transcription factors and analysed by flow cytometry.

We began by examining the proportions of the FoxP3-expressing Tregs i.e. the tTregs and pTregs. Recently, the cell surface receptor Neuropilin-1 (NRP1) and transcription factor Helios were identified as markers that are expressed on tTregs but not pTregs (Thornton et al., 2010; Weiss et al., 2012). Initially, we planned to examine the proportions of tTregs based on expression of both NRP1 and Helios. However, our trial stainings for NRP1 using LP cells from an uninfected WT mouse showed very few  $NRP1^+$  LP  $CD4^+$  T cells (**Figure 5.8A, upper panel**) which was in stark contrast to the findings of Weiss et al., 2012, who showed high NRP1 expression in LP  $CD4^+$  T cells from the colon of an uninfected WT mouse. Examination of NRP1 in  $CD4^+$  T cells from the spleen and MLN of the uninfected WT mouse revealed that NRP1 was detectable in these cells (**Figure 5.8A, middle and lower panel**). The major difference in the protocols we used to obtain single cell suspensions from the spleen, MLN and large intestine was that the spleen and MLN cells were mashed up to directly obtain a single cell suspension whereas the large intestine was digested with liberase. Weiss et al used collagenase instead of liberase treatment to obtain their LP cells and were able to detect NRP1 (Weiss et al., 2012). Given that in our spleen and MLN prep, we did not use liberase, and that Weiss et al used collagenase and not liberase to digest their LP cells and were able to detect NRP1, we hypothesised that perhaps liberase treatment was resulting in loss of NRP1 expression. To examine whether this was the case, we isolated spleens from uninfected WT mice and treated them with liberase for either 30 minutes or 1 hour before isolating the splenocytes. As a control, one spleen was left untreated. The results indicated that compared to the untreated spleen, the 30 minutes liberase-treated spleen showed similar NRP1 expression however, the 1 hour liberase-treated spleen only expressed half as much NRP1 (**Figure 5.8B**) showing that NRP1 expression is lost following liberase treatment.

Therefore, using Helios alone as the distinguishing marker, we further characterised the  $FoxP3^+$  LP  $CD4^+$  T cells in uninfected and 2-wk  $Hh^+$  and  $Hh^+$ /anti-IL-10R-infected *Tiger* mice into tTregs and pTregs *ex vivo*. The gating strategy used is depicted in **Figure 5.9A**. The  $Hh^+$  mice showed a similar frequency of both Helios-positive and Helios-negative  $FoxP3^+$  cells compared to uninfected controls (**Figure 5.9B, upper panels**). However, in the colitic group

there was a significant decrease in the frequencies of both Helios-positive and Helios-negative FoxP3<sup>+</sup> cells compared to uninfected controls (**Figure 5.9B, upper panels**). When examining the number of Helios-positive and Helios-negative FoxP3<sup>+</sup> cells, we found that following infection with *Hh*, there was an increase in the numbers of both Helios-positive and Helios-negative FoxP3<sup>+</sup> cells, although this increase was only significant in the colitic group (**Figure 5.9B, lower panels**). These results demonstrated that both the tTregs and pTregs expand following infection with *Hh*. Furthermore, in both the uninfected and *Hh*<sup>+</sup> group, the tTregs and pTregs made up approximately 50% each of the total FoxP3<sup>+</sup> Treg population in these mice however in *Hh*<sup>+</sup>/anti-IL-10R-treated mice, there were slightly more pTregs than tTregs in the large intestine.

### **5.2.5 There is an expansion of LAG-3<sup>+</sup> FoxP3<sup>+</sup> cells following infection with *Hh***

We next wanted to examine LAG-3 expression in different CD4<sup>+</sup> T cell subsets following infection with *Hh*. We began by examining the *ex vivo* expression of LAG-3 in CD4<sup>+</sup> T cells from the large intestine of uninfected and 2-wk *Hh*<sup>+</sup> and *Hh*<sup>+</sup>/anti-IL-10R-treated *Tiger* mice. The gating strategy used is shown in **Figure 5.10A**. The results showed that compared to uninfected mice, there was a significant increase in the frequency of LAG-3-expressing cells in *Hh*<sup>+</sup> and *Hh*<sup>+</sup>/anti-IL-10R-treated mice (**Figure 5.10B, left panel**). In terms of total numbers however, although there was an increase in LAG-3-expressing cells in both *Hh*<sup>+</sup> and *Hh*<sup>+</sup>/anti-IL-10R-treated mice, this increase was only significant in the colitic setting (**Figure 5.10B, right panel**).

LAG-3 has been shown to be required for maximal suppressive capacity of CD4<sup>+</sup> CD25<sup>+</sup> FoxP3<sup>+</sup> Tregs (Do et al., 2015; Huang et al., 2004). Thus we next examined LAG-3 expression in FoxP3<sup>+</sup> Tregs in the three experimental groups. The results showed that a significant increase in the frequency but not in the numbers of LAG-3<sup>+</sup> FoxP3<sup>+</sup> cells in *Hh*<sup>+</sup> mice compared to uninfected mice (**Figure 5.10C**). In *Hh*<sup>+</sup>/anti-IL-10R-treated mice however, there was a significant increase in both the frequency and number of LAG-3<sup>+</sup> FoxP3<sup>+</sup> cells compared to uninfected mice (**Figure 5.10C**). These results demonstrated that while the LAG-3<sup>+</sup>FoxP3<sup>+</sup> cells expand slightly in *Hh*<sup>+</sup> mice, they showed a significant expansion in the colitic setting.

The results in **Figure 5.10** showed that in *Hh*<sup>+</sup> mice, of the 25,000 LAG-3<sup>+</sup> LP CD4<sup>+</sup> T cells (**Figure 5.10B, right panel**), 13,000 co-expressed FoxP3 demonstrating that about half of LAG-3<sup>+</sup> cells were FoxP3<sup>+</sup> Tregs. In contrast, in the *Hh*<sup>+</sup>/anti-IL-10R-treated mice, of the 280,000 LAG-3<sup>+</sup> LP CD4<sup>+</sup> T cells (**Figure 5.10B, right panel**) only 28,000 co-expressed FoxP3 demonstrating that the LAG-3<sup>+</sup> FoxP3<sup>+</sup> Tregs constituted a very small proportion of the LAG-3<sup>+</sup> LP CD4<sup>+</sup> T cells in the colitic setting.

To determine whether LAG-3 expression was preferentially expressed in FoxP3<sup>+</sup> tTregs compared to pTregs or vice versa, we examined LAG-3 expression in FoxP3<sup>+</sup> Helios<sup>+</sup> (tTregs)

and FoxP3<sup>+</sup> Helios<sup>-</sup> (pTregs) LP CD4<sup>+</sup> T cells in the three experimental groups. The gating strategy is shown in **Figure 5.11A**. Our results showed that in the uninfected mice (where pTregs and tTregs were present in equal numbers as shown in **Figure 5.9B**), only 4% of tTregs expressed LAG-3 compared to 10% of pTregs suggesting that a greater proportion of pTregs express LAG-3 compared to tTregs at steady state (**Figure 5.11B, upper panels**). In the *Hh*<sup>+</sup> and *Hh*<sup>+</sup>/anti-IL-10R-treated mice, there was a significant increase in the frequency of tTregs and pTregs expressing LAG-3, compared to uninfected controls, although in both groups, the proportion of pTregs expressing LAG-3 was greater than the tTregs expressing LAG-3 (**Figure 5.11B, upper panels**). In terms of numbers, both the *Hh*<sup>+</sup> and *Hh*<sup>+</sup>/anti-IL-10R-treated mice showed an increase in tTregs and pTregs expressing LAG-3 compared to uninfected controls, however the increase was only significant in the colitic group (**Figure 5.11B, lower panels**). Given that LAG-3 has been shown to potentiate the suppressive capacity of FoxP3<sup>+</sup> Tregs (Do et al., 2015; Huang et al., 2004), it is tempting to speculate that the LAG3<sup>+</sup> FoxP3<sup>+</sup> Tregs may be more suppressive than the LAG3<sup>+</sup> FoxP3<sup>-</sup> Tregs in *Hh*-induced colitis.

### **5.2.6 In the colitic setting, there is an expansion of LAG-3<sup>+</sup> FoxP3-negative cells**

Given that in the colitic setting, only a small number of LAG-3<sup>+</sup> LP CD4<sup>+</sup> T cells co-expressed FoxP3 (**Figure 5.10**), we next examined LAG-3 expression *ex vivo* in the FoxP3-negative LP CD4<sup>+</sup> T cells in uninfected, *Hh*<sup>+</sup> and *Hh*<sup>+</sup>/anti-IL-10R-treated *Tiger* mice. The gating strategy is shown in **Figure 5.12A**. Our results showed that although there was an increase in the frequency of LAG-3<sup>+</sup> FoxP3<sup>-</sup> LP CD4<sup>+</sup> T cells in both *Hh*<sup>+</sup> and *Hh*<sup>+</sup>/anti-IL-10R-treated mice compared to uninfected mice, this increase was only significant in the colitic setting (**Figure 5.12B**). Of the FoxP3-negative populations, LAG-3 is expressed by Tr1 cells (Gagliani et al., 2013), exhausted CD4<sup>+</sup> T cells (Freeman and Sharpe, 2012) and effector CD4<sup>+</sup> T cells (Workman et al., 2002). LAG-3 is up-regulated in effector CD4<sup>+</sup> T cells following antigen activation, and binds to MHC II to send inhibitory signals, preventing T cell proliferation and cytokine secretion (Workman et al., 2002). Therefore, to determine the proportions of Tr1 cells and LAG-3<sup>+</sup> effector T cells in uninfected, *Hh*<sup>+</sup> and *Hh*<sup>+</sup>/anti-IL-10R-treated mice, we examined the expression of CD49b and LAG-3 on FoxP3-negative LP CD4<sup>+</sup> T cells. The gating strategy used for the analysis is shown in **Figure 5.12C**. Our results showed that although there was an increase in the frequency of both Tr1 cells (FoxP3<sup>-</sup>LAG-3<sup>+</sup>CD49b<sup>+</sup>) and effector LAG-3<sup>+</sup>CD4<sup>+</sup> T cells (FoxP3<sup>-</sup>LAG-3<sup>+</sup>CD49b<sup>-</sup>) in both *Hh*<sup>+</sup> and *Hh*<sup>+</sup>/anti-IL-10R-treated mice, compared to uninfected controls, it was only significant in the colitic group (**Figure 5.12D, upper panel**). Furthermore, examination of numbers revealed that both the CD49b<sup>-</sup> LAG-3<sup>+</sup> FoxP3<sup>-</sup> cells and the CD49b<sup>+</sup> LAG-3<sup>+</sup> FoxP3<sup>-</sup> cells expanded in both *Hh*<sup>+</sup> and *Hh*<sup>+</sup>/anti-IL-10R-treated mice compare to uninfected controls (**Figure 5.12D, lower panel**). Together, the results in **Figure 5.12** demonstrated that the expansion in LAG-3<sup>+</sup> FoxP3-negative cells in *Hh*<sup>+</sup> and *Hh*<sup>+</sup>/anti-IL-10R-treated mice was partly due to an expansion in Tr1 cells but primarily due to an increase in either exhausted CD4<sup>+</sup> T cells or LAG-3<sup>+</sup> effector CD4<sup>+</sup> T cells or a combination of the two.

### 5.2.7 Simultaneous detection of Helios and GFP is impossible with current fixation and permeabilisation protocols

We next wanted to examine the phenotype of IL-10-producing CD4<sup>+</sup> T cells in the *Tiger* mice *ex vivo* based on GFP signal. One of the markers we wanted to use to phenotype IL-10-producing CD4<sup>+</sup> T cells was Helios. Unfortunately we were unable to optimize a fixation and permeabilisation protocol that would enable us to simultaneously detect IL-10 by GFP signal and Helios. As a result, we were unable to examine the extent to which pTregs/tTregs constitute the IL-10<sup>+</sup> FoxP3<sup>+</sup> pool in the three experimental groups. It is unclear why 2% PFA/eBio perm worked for FoxP3 but not for Helios. We tried two alternative protocols to try and improve Helios staining. Data from the literature suggests that pre-fixing the cells with 2% PFA for 30 minutes, followed by a 30 minute fixation with the eBio fix-perm and subsequent permeabilisation with eBio perm buffer allows simultaneous detection of YFP signal and FoxP3 and Helios (Grupillo et al., 2011). To examine whether this method worked in our hands, we isolated LP cells from 2-wk *Hh*<sup>+</sup>/anti-IL-10R-treated IL-17A-eYFP mice and stained them for surface markers followed by fixation, permeabilisation and intracellular staining using the following combinations using the following combinations of fixation and permeabilising reagents: i) eBio fix-perm/eBio perm, ii) 2% PFA/eBio perm, and iii) 2% PFA followed by eBio fix-perm/eBio perm. The results showed that while eBio fix-perm/eBio perm was effective at detecting FoxP3 and Helios, it quenched the eYFP signal (**Figure 5.13A, left panel**). 2% PFA/eBio perm retained eYFP, showed similar frequencies of FoxP3<sup>+</sup> cells but yielded poor Helios staining compared to eBio fix-perm/eBio perm (**Figure 5.13A, middle panel**). Using 2% PFA followed by eBio fix-perm/eBio perm retained eYFP, but resulted in poor FoxP3 and Helios staining compared to eBio fix-perm/eBio perm (**Figure 5.13A, right panel**).

Another study found that the use of 2% formaldehyde (FA), containing less than 3% methanol as a fixative was sufficient to detect eYFP and FoxP3 (Heinen et al., 2014), however Helios expression was not examined by this protocol. To examine whether this protocol would work for detection of Helios, we isolated LP cells from 2-wk *Hh*<sup>+</sup>/anti-IL-10R-treated IL-17A-eYFP mice and stained them for surface markers followed by fixation, permeabilisation and intracellular staining using the following combinations of fixatives and permeabilising reagents: i) eBio fix-perm/eBio perm, ii) 2% PFA/eBio perm and iii) 2% FA/eBio perm. The results showed that although fixing cells with 2% FA retained eYFP, both FoxP3 and Helios staining were poor compared to the staining obtained with eBio fix-perm/eBio perm buffers (**Figure 5.13B**). These results demonstrated that the only protocol that worked to detect Helios was eBio fix-perm/eBio perm, and because this protocol was inefficient at retaining YFP signal, it made it difficult to simultaneously detect both Helios and YFP. Thus, it was impossible to differentiate FoxP3<sup>+</sup> IL-10-GFP<sup>+</sup> cells into tTregs and pTregs.

### 5.2.8 In both $Hh^+$ and $Hh^+$ /anti-IL-10R-treated mice, the majority of IL-10-producing $CD4^+$ T cells are of a regulatory phenotype

We next examined the phenotype of IL-10-producing  $CD4^+$  T cells in a non-inflammatory immune response to  $Hh$  ( $Hh^+$  *Tiger* mice) and compared it to the phenotype observed in an inflammatory immune response to  $Hh$  ( $Hh^+$ /anti-IL-10R-treated *Tiger* mice). To do so, we isolated LP cells from the large intestine of uninfected and 2-wk  $Hh^+$  and  $Hh^+$ /anti-IL-10R-infected *Tiger* mice, and then characterised the phenotype of IL-10<sup>+</sup>  $CD4^+$  T cells by flow cytometry. The gating strategy used for the analysis is depicted in **Figure 5.14A**. From the results, both  $Hh^+$  and  $Hh^+$ /anti-IL-10R-infected mice showed a decrease in the frequency of IL-10<sup>+</sup> FoxP3<sup>+</sup> cells compared to uninfected mice, however this decrease was only significant in the colitic setting (**Figure 5.14B**) suggesting that in the colitic setting in particular, there is an expansion in the proportion of IL-10<sup>+</sup>  $CD4^+$  T cells that are FoxP3-negative.

To examine whether the expansion in the proportion of FoxP3-negative IL-10-producing  $CD4^+$  T cells in the colitic setting was due to an expansion in Tr1 cells, we next examined the phenotype of IL-10-producing  $CD4^+$  T cells based on co-expression of CD49b and LAG-3. The gating strategy used is depicted in **Figure 5.15A**. Examination of LAG-3 expression alone by IL-10-GFP<sup>+</sup> cells revealed that the frequency of LAG-3-expressing IL-10-GFP<sup>+</sup> cells increased significantly in both  $Hh^+$  and  $Hh^+$ /anti-IL-10R-infected mice compared to uninfected controls (**Figure 5.15B, left panel**). In terms of numbers, there was an increase in LAG-3<sup>+</sup> IL-10-GFP<sup>+</sup> cells in both  $Hh^+$  and  $Hh^+$ /anti-IL-10R-infected mice compared to uninfected controls, however, this increase was only significant in the colitic setting (**Figure 5.15B, right panel**). A representative staining of CD49b and LAG-3 from the  $Hh^+$  group of each experiment, when gated on IL-10-GFP<sup>+</sup>  $CD4^+$  T cells is shown in **Figure 5.15C**. Although the CD49b/LAG-3 staining looked different in the three experiments, we set the gates based on the staining obtained with either the isotype controls or (Fluorescence-1) controls in case of experiment three, and thus considered the staining of CD49b/LAG-3 we observed to be true (**Figure 5.15C**). The results showed that in both  $Hh^+$  and  $Hh^+$ /anti-IL-10R-infected mice, there was no significant difference in the frequency of Tr1 cells (IL-10<sup>+</sup> CD49b<sup>+</sup> LAG-3<sup>+</sup>) compared to uninfected mice (**Figure 5.15D, left panel**). When examining the total numbers of Tr1 cells (IL-10<sup>+</sup> CD49b<sup>+</sup> LAG-3<sup>+</sup>) we found that there was a slight increase in the  $Hh^+$  mice, but a significant increase in the colitic group (**Figure 5.15D, right panel**). Examination of the fold change in the numbers of IL-10<sup>+</sup> Tr1 cells and IL-10<sup>+</sup> FoxP3<sup>+</sup> cells compared to those in uninfected controls revealed that in  $Hh^+$  mice, there was a slight but not significant expansion of IL-10<sup>+</sup> Tr1 cells, whereas in the colitic setting both the IL-10<sup>+</sup> Tr1 cells and IL-10<sup>+</sup> FoxP3<sup>+</sup> expanded, with the IL-10<sup>+</sup> Tr1 cells showing the greatest expansion (**Figure 5.15E**).

Together, the results in **Figures 5.14-5.15** showed that together, the IL-10<sup>+</sup> Tr1 cells and IL-10<sup>+</sup> FoxP3<sup>+</sup> cells account for approximately 98% of IL-10-producing  $CD4^+$  T cells in

uninfected mice, 76% in *Hh*<sup>+</sup> mice and 68% in colitic mice suggesting that following infection with *Hh*, there is an expansion of IL-10-producing CD4<sup>+</sup> T cells from effector T cells.

### **5.2.9 In both *Hh*<sup>+</sup> and *Hh*<sup>+</sup>/anti-IL-10R-treated mice, the majority of IL-10-producing CD4<sup>+</sup> T cells express CD25**

We have previously shown using the *Hh* CD4<sup>+</sup> T-cell transfer model of colitis that the CD45RB<sup>low</sup> CD25<sup>-</sup> population is more protective than the CD45RB<sup>low</sup> CD25<sup>+</sup> cells (Kullberg et al., 2002). As protection in the *Hh* CD4<sup>+</sup> T cell transfer model of colitis is dependent on IL-10 (Kullberg et al., 2002), this suggested that the CD45RB<sup>low</sup> CD25<sup>-</sup> population either produces greater amounts of IL-10 on a per cell basis or contains greater numbers of IL-10-producing CD4<sup>+</sup> T cells compared to the CD45RB<sup>low</sup> CD25<sup>+</sup> cells. Here, to examine whether the numbers of IL-10<sup>+</sup> CD25<sup>-</sup> cells were greater than IL-10<sup>+</sup> CD25<sup>+</sup> cells following infection with *Hh*, we isolated LP cells from the large intestine of uninfected and 2-wk *Hh*<sup>+</sup> and *Hh*<sup>+</sup>/anti-IL-10R-treated IL-17A-eYFP mice, stimulated the cells with PMA and ionomycin in the presence of Brefeldin A. Following surface and intracellular staining, we examined the expression of CD25 in IL-10 producing CD4<sup>+</sup> T cells. The gating strategy used to analyse the results is shown in **Figure 5.16A**. The results showed that compared to uninfected controls, there was an expansion in both IL-10<sup>+</sup> CD25<sup>-</sup> cells and IL-10<sup>+</sup> CD25<sup>+</sup> cells in *Hh*<sup>+</sup> and *Hh*<sup>+</sup>/anti-IL-10R-treated mice, however, in both these groups, the number of IL-10<sup>+</sup> CD25<sup>+</sup> cells was far greater than the IL-10<sup>+</sup> CD25<sup>-</sup> cells (**Figure 5.16B**).

The CD45RB<sup>low</sup> CD25<sup>+/-</sup> cells used in our previous studies were done using cells sorted from MLNs of *Hh*<sup>+</sup> WT mice and transferred into *Hh*<sup>+</sup> RAG KO mice (Kullberg et al., 2002). The CD4<sup>+</sup> CD45RB<sup>low</sup> cells contain Treg populations and antigen-experienced cells (Toms and Powrie, 2001). In the large intestine, most cells are antigen-experienced and therefore express CD45RB<sup>low</sup> (Asigbetse et al., 2010). Furthermore, although CD25 is constitutionally expressed by Tregs, it is up-regulated on effector CD4<sup>+</sup> T cells upon activation (McNeill et al., 2007; Sakaguchi et al., 1995). Thus using CD45RB<sup>low</sup> and CD25 to distinguish Treg populations was not feasible in the LP. Therefore, to determine whether the increase in IL-10<sup>+</sup> CD25<sup>+</sup> cells we saw was comprised of effector T cells expressing CD25, or Tregs expressing CD25, we examined the phenotype of IL-10-producing CD4<sup>+</sup> T cells based on co-expression of FoxP3 and CD25. Although CD25 is constitutionally expressed by tTregs (McNeill et al., 2007; Sakaguchi et al., 1995), it may or may not be expressed on pTregs and Tr1 cells and is up-regulated on effector CD4<sup>+</sup> T cells upon activation. The results showed that in all three experimental groups, the majority of the IL-10<sup>+</sup> cells co-expressed FoxP3 and CD25, although the frequency of these cells dropped from 65% in the uninfected and *Hh*<sup>+</sup> mice to 56% in the colitic group (**Figure 5.16C**). Furthermore, the CD25<sup>-</sup> cells constituted between 28-31% of the IL-10-producing CD4<sup>+</sup> T cells in the three experimental groups (**Figure 5.16C**). The results in **Figure 5.16C** showed that the proportion of IL-10<sup>+</sup> FoxP3<sup>+</sup> CD25<sup>+</sup> Tregs were more than the IL-10<sup>+</sup> CD25<sup>-</sup> cells, suggesting that if indeed the CD25<sup>-</sup> cells are more protective, it is most likely because of a

greater amount of IL-10 secreted on a per cell basis rather than an increased frequency of these cells.

The majority of all the IL-10-producing CD4<sup>+</sup> T cells in the three experimental groups were FoxP3<sup>+</sup>, with the frequency of IL-10<sup>+</sup> FoxP3<sup>+</sup> cells dropping from about 80% in uninfected and *Hh*<sup>+</sup> mice to about 61% in the colitic group (**Figure 5.16C**). The IL-10<sup>+</sup> CD25-single positive cells constituted the smallest proportion of IL-10<sup>+</sup> CD4<sup>+</sup> T cells in uninfected and *Hh*<sup>+</sup> mice, however the frequency of these cells increased significantly in the colitic setting (**Figure 5.16C**), suggesting an expansion of IL-10-producing CD4<sup>+</sup> T cells that may be from effector T cells.

#### **5.2.10 In both *Hh*<sup>+</sup> and *Hh*<sup>+</sup>/anti-IL-10R-treated mice, there is an expansion in IL-10-producing CD4<sup>+</sup> T cells that co-express inflammatory cytokines IL-17A and IFN- $\gamma$ .**

Data published in the literature show that effector Th1 and Th17 cells can also produce IL-10 (Esplugues et al., 2011; Saraiva et al., 2009). Because inflammation in the *Hh* colitis model is characterised by an increase in cells expressing inflammatory cytokines IL-17A and/or IFN- $\gamma$ , we decided to examine whether IL-10-producing CD4<sup>+</sup> T cells would co-express these cytokines. To do so, we isolated LP cells from the large intestine of uninfected and 2-wk *Hh*<sup>+</sup> and *Hh*<sup>+</sup>/anti-IL-10R-treated *Tiger* mice and stimulated the cells with PMA and ionomycin in the presence of Brefeldin A. Following surface and intracellular staining, we examined the phenotype of cells producing IL-10 by flow cytometry. We began by comparing the phenotype of IL-10-producing CD4<sup>+</sup> T cells detected by GFP signal with that of IL-10 protein detected by ICS. Representative staining of IL-10-GFP and co-expression of IL-10-GFP and IL-17A and/or IFN- $\gamma$  in the three experimental groups is depicted in **Figure 5.17A**. When gating on IL-10-GFP<sup>+</sup> cells, the results showed that in uninfected mice most of the IL-10 producing CD4<sup>+</sup> T cells were from cells that do not co-express IL-17A and/or IFN- $\gamma$  (**Figure 5.17B**). In the *Hh*<sup>+</sup> *Tiger* mice, there was a slight expansion in the IL-10-GFP<sup>+</sup> cells that co-expressed IL-17A and/or IFN- $\gamma$  (**Figure 5.17B**), however in the *Hh*<sup>+</sup>/anti-IL-10R-treated *Tiger* mice, the IL-10-GFP<sup>+</sup> cells that co-expressed IL-17A and/or IFN- $\gamma$  constituted approximately 40% of the IL-10-producing CD4<sup>+</sup> T cells (**Figure 5.17B**). Representative staining of IL-10 detected by ICS and co-expression of IL-10 and IL-17A and/or IFN- $\gamma$  in the three experimental groups is depicted in **Figure 5.17C**. Similar to the results obtained when gating on IL-10-GFP<sup>+</sup> cells, when gating on IL-10<sup>+</sup> cells detected by ICS, there was an expansion in IL-10<sup>+</sup> CD4<sup>+</sup> T cells that co-expressed IL-17A and or IFN- $\gamma$  in the *Hh*<sup>+</sup> and *Hh*<sup>+</sup>/anti-IL-10R-treated *Tiger* mice compared to uninfected controls, particularly in the colitic setting where these cells constituted slightly more than half of the IL-10<sup>+</sup> LP CD4<sup>+</sup> T cells (**Figure 5.17D**). Together, these results (**Figure 5.17**) showed that following infection with *Hh*, there was an expansion in IL-10-producing CD4<sup>+</sup> T cells that co-express IL-17A and/or IFN- $\gamma$  both by ICS and GFP signal, particularly so in colitic

mice where these cells constitute approximately 40% of the IL-10-GFP<sup>+</sup> LP CD4<sup>+</sup> T cells or slightly more than half of the IL-10<sup>+</sup> LP CD4<sup>+</sup> T cells detected by ICS.

### **5.2.11 Ex-Th17 cells contribute to a small proportion of the IL-10<sup>+</sup> IFN- $\gamma$ <sup>+</sup> cells in the colitic setting.**

Given that between 13% of the IL-10-producing CD4<sup>+</sup> T cells in the colitis *Tiger* mice co-expressed IFN- $\gamma$  (**Figure 5.17 B and D**), we next examined the extent to which the ex-Th17 cells contributed to this population. To do so, we used the IL-17A-eYFP mice, so that we could track the ex-Th17 cells. Thus we isolated LP cells from the large intestine of uninfected and 2-wk *Hh*<sup>+</sup> and *Hh*<sup>+</sup>/anti-IL-10R-treated IL-17A-eYFP mice and stimulated the cells with PMA and ionomycin in the presence of Brefeldin A. Following surface and intracellular staining, we examined the phenotype of cells producing IL-10 by flow cytometry. The gating strategy used is shown in **Figure 5.18A**. The results showed that compared to uninfected controls, the *Hh*<sup>+</sup> mice showed a slight expansion in the IL-10<sup>+</sup> IL-17A<sup>+</sup> cells whereas in the colitic setting, approximately 40% of the IL-10-producing CD4<sup>+</sup> T cells co-expressed IL-17A and/or IFN- $\gamma$  (**Figure 5.18B**). In addition these results demonstrated that in the colitic setting alone, the ex-Th17 cells constituted 4% of the IL-10-producing CD4<sup>+</sup> T cells (**Figure 5.18B**). Interestingly, in both *Hh*<sup>+</sup> and *Hh*<sup>+</sup>/anti-IL-10R-treated mice, there was an expansion in IL-10<sup>+</sup> eYFP<sup>+</sup> IL-17A<sup>-</sup>IFN- $\gamma$ <sup>-</sup> cells (**Figure 5.18B**) demonstrating that at some point, these IL-10<sup>+</sup> cells produced IL-17A, but have since switched off IL-17A production. Fold change comparison of the numbers of IL-10-producing CD4<sup>+</sup> T cells that co-expressed eYFP, IL-17A and/or IFN- $\gamma$  in *Hh*<sup>+</sup> IL-17A-eYFP mice compared to uninfected controls revealed that the highest fold increase was observed in the IL-10<sup>+</sup> IL-17A<sup>+</sup> and IL-10<sup>+</sup> eYFP<sup>+</sup> IL-17A<sup>-</sup>IFN- $\gamma$ <sup>-</sup> cells (**Figure 5.18C, left panel**). In the *Hh*<sup>+</sup>/anti-IL-10R-treated mice, all the IL-10-producing CD4<sup>+</sup> T cells that co-expressed eYFP, IL-17A and/or IFN- $\gamma$  showed a similar high fold increases mice compared to uninfected controls (**Figure 5.18C**).

### **5.2.12 At least half the IL-10-producing CD4<sup>+</sup> T cells that co-express IL-17A and/or IFN- $\gamma$ also express Foxp3.**

In the current study we found that in the colitic setting, approximately 40-50% of the IL-10-producing CD4<sup>+</sup> T cells also co-expressed inflammatory cytokines IL-17A and/or IFN- $\gamma$  (**Figure 5.17C-D** and **Figure 5.18B**). At the same time, we also found that approximately 60-75% of the IL-10-producing CD4<sup>+</sup> T cells were of a regulatory phenotype i.e. 50-60% were FoxP3<sup>+</sup> (**Figure 5.14B** and **Figure 5.16C**) and 16% were Tr1 cells (**Figure 5.15D**). These results suggested the possibility that there might be an overlap between these two subsets. As FoxP3<sup>+</sup> cells that co-express IL-17A or IFN- $\gamma$  have been described in the literature (Bhaskaran et al., 2015; Koch et al., 2009), we next examined whether the IL-10-producing CD4<sup>+</sup> T cells that co-express either eYFP, IL-17A and/or IFN- $\gamma$  also express FoxP3. The gating strategy used is shown in **Figure 5.19A**. The results showed that in the uninfected mice, most of IL-10<sup>+</sup> cells

were from cells that were eYFP<sup>+</sup>IL-17A<sup>-</sup>IFN- $\gamma$ <sup>-</sup> and most of these cells expressed FoxP3 (**Figure 5.19B, left panel**). In *Hh*<sup>+</sup> mice, there was a slight expansion in the IL-10<sup>+</sup> IL-17A<sup>+</sup> cells and IL-10<sup>+</sup>eYFP<sup>+</sup>IL-17A<sup>-</sup>IFN- $\gamma$ <sup>-</sup> cells and most of these cells also expressed FoxP3 (**Figure 5.19B, middle panel**). In the colitic setting, approximately half the cells in all the IL-10<sup>+</sup> subsets that co-expressed IL-17A and/or IFN- $\gamma$  also expressed FoxP3 (**Figure 5.19B, right panel**). Additionally, most of the IL-10<sup>+</sup>eYFP<sup>+</sup>IL-17A<sup>-</sup>IFN- $\gamma$ <sup>-</sup> cells in the colitic setting co-expressed FoxP3 (**Figure 5.19B, right panel**). These results demonstrated that following infection with *Hh*, there is an expansion of a population of IL-10<sup>+</sup> cells that share phenotypic characteristics of both effector T cells and regulatory T cells in that they express inflammatory cytokines like IFN- $\gamma$  and IL-17A, but also express the regulatory transcription factor FoxP3 and produce anti-inflammatory cytokine IL-10. Furthermore, the expansion of eYFP<sup>+</sup> FoxP3<sup>+</sup> cells that do not express IL-17A or IFN- $\gamma$  following infection with *Hh*, also suggests the possibility of Th17 cells changing phenotype to become regulatory.

### **5.2.13 In a non-inflammatory immune response to *Hh*, a greater proportion of IL-17A and/or IFN- $\gamma$ -expressing cells also co-express FoxP3 and IL-10, compared to the colitic setting.**

Given that in the *Hh*<sup>+</sup> and *Hh*<sup>+</sup>/anti-IL-10R-treated mice there was an expansion in intestinal IL-10<sup>+</sup> CD4<sup>+</sup> T cells co-expressed eYFP, IL-17A and/or IFN- $\gamma$ , we next examined the proportion of the effector T cell-subsets that express FoxP3 or IL-10 in uninfected, *Hh*<sup>+</sup> and *Hh*<sup>+</sup>/anti-IL-10R-treated IL-17A-eYFP mice. The gating strategy used is shown in **Figure 5.20A**. The results showed that a significantly higher proportion of Th17, IL-17A<sup>+</sup>IFN- $\gamma$ <sup>+</sup>, Th1 and eYFP<sup>+</sup>IL-17A<sup>-</sup>IFN- $\gamma$ <sup>-</sup> cells expressed IL-10 in *Hh*<sup>+</sup> mice compared to uninfected and *Hh*<sup>+</sup>/anti-IL-10R-treated IL-17A-eYFP mice (**Figure 5.20B**). Conversely, the colitic mice only showed a significant increase in the proportion of IL-10<sup>+</sup> IL-17A<sup>+</sup>IFN- $\gamma$ <sup>+</sup> and IL-10<sup>+</sup> ex-Th17 compared to the uninfected controls by virtue of the ex-Th17 cells and IL-17A<sup>+</sup>IFN- $\gamma$ <sup>+</sup> being virtually absent in the latter (**Figure 5.20B**).

Examination of FoxP3 expression revealed that the *Hh*<sup>+</sup> IL-17A-eYFP mice showed a significantly higher proportion of Th17, IL-17A<sup>+</sup>IFN- $\gamma$ <sup>+</sup> and eYFP<sup>+</sup>IL-17A<sup>-</sup>IFN- $\gamma$ <sup>-</sup> cells expressed FoxP3 compared to uninfected and *Hh*<sup>+</sup>/anti-IL-10R-treated IL-17A-eYFP mice (**Figure 5.20C**). While the frequency of FoxP3<sup>+</sup> Th1 cells was similar in all three experimental groups, the highest frequency was observed in the *Hh*<sup>+</sup> group (**Figure 5.20C**). The colitic mice only showed a significant increase in the proportion of FoxP3<sup>+</sup> ex-Th17 compared to the uninfected controls by virtue of the ex-Th17 cells and IL-17A<sup>+</sup>IFN- $\gamma$ <sup>+</sup> being virtually absent in the latter (**Figure 5.20C**).

Taken together, these results show in the non-inflammatory immune response to *Hh*, a greater proportion of IL-17A and/or IFN- $\gamma$ -expressing CD4<sup>+</sup> T cells also co-express FoxP3 or IL-10 compared to the inflammatory immune response to *Hh*.

### 5.3 DISCUSSION

Here, we provide the first extensive characterisation of different Treg subsets as well as the phenotype of IL-10-producing CD4<sup>+</sup> T cells at the site of *Hh* colonisation in the large intestine during two different immune responses to *Hh*; a non-inflammatory immune response observed in *Hh*<sup>+</sup> *Tiger*/IL-17A-eYFP mice, and an inflammatory immune response observed in *Hh*<sup>+</sup>/anti-IL-10R-treated *Tiger*/IL-17A-eYFP mice. The LP CD4<sup>+</sup> T cells were characterised as Tregs based on expression of tTreg/pTreg marker FoxP3, tTreg marker Helios and Tr1 markers CD49b and LAG-3. The IL-10-producing CD4<sup>+</sup> T cells were characterised based on co-expression CD49b and LAG-3, FoxP3 and co-expression of inflammatory cytokines IL-17A and/or IFN- $\gamma$ .

In this study, we found that in the non-inflammatory response to *Hh*, there were more FoxP3 and IL-10-producing CD4<sup>+</sup> T cells compared to those producing inflammatory cytokines IL-17A and IFN- $\gamma$  (**Figure 5.21A**). Conversely, the opposite was true in the inflammatory immune response to *Hh* (**Figure 5.21A**). This suggests that in order to maintain intestinal homeostasis, the number of FoxP3 and IL-10-expressing cells must be greater than effector T cells expressing IL-17A and IFN- $\gamma$ . In the inflammatory immune response to *Hh*, while there was an expansion of IL-10<sup>+</sup> and FoxP3<sup>+</sup> T cells, the inflammatory T cells expanded to a greater extent. Given that mice have to be concomitantly infected with *Hh* and treated with a blocking antibody to the IL-10R in order to develop intestinal inflammation, this suggests that IL-10R-signaling plays an important role in maintaining the balance between effector T cells and Tregs. Aside from the tolerogenic effects that IL-10 signaling elicits in DCs, the Th17 and IL-17A<sup>+</sup> IFN- $\gamma$ <sup>+</sup> cells have also been shown to express the IL-10R and can be directly suppressed by IL-10 (Huber et al., 2011). Furthermore, another study found that IL-10R-signaling is necessary for Treg-mediated Th17 suppression and that IL-10R signaling potentiates IL-10 production by FoxP3<sup>+</sup> Tregs (Chaudhry et al., 2011).

In the current study, we used co-expression of Helios and FoxP3 to differentiate tTregs from pTregs. Although both NRP1 and Helios have been identified as markers that are expressed on tTregs but not pTregs, we could not use NRP1 in our study as we found that NRP1 was destroyed by the liberase digestion we used to obtain large intestine LP cells. Recent studies have called to question the reliability of Helios as a marker of tTregs. The basis of suggesting that Helios is a marker of tTregs was centered on three findings. Firstly, the first FoxP3<sup>+</sup> Tregs to populate the thymus of 3 day old mice and the spleen of 4 day old mice are exclusively Helios<sup>+</sup> and the appearance of Helios<sup>-</sup> cells only began to appear in the spleen in 12 day old mice (Thornton et al., 2010). Secondly, *in vitro* induction of iTregs from CD4<sup>+</sup> FoxP3<sup>-</sup> cells are Helios<sup>-</sup> and thirdly, *in vivo* induction of pTregs in a model of oral tolerance revealed that these pTregs did not express Helios (Thornton et al., 2010). Since then, a few studies have shown that Helios can be expressed by pTregs. One study showed that *in vitro* Helios

expression could be induced on iTregs depending on the method by which the cells are stimulated (Verhagen and Wraith, 2010). Helios expression was observed in pTregs derived from RAG KO TCR T4 Tg CD4<sup>+</sup> FoxP3<sup>-</sup> cells stimulated with their cognate antigen in the presence of APCs but not when these cells were stimulated with plate bound anti-CD3 and anti-CD28 (Verhagen and Wraith, 2010). A subsequent study reported that Helios is also up-regulated by other CD4<sup>+</sup> T cell subsets upon activation and proliferation (Akimova et al., 2011). In a communication to the editor of the Journal of Immunology Thornton et al argue that all the studies where Helios was up-regulated on cells other than tTregs (Akimova et al., 2011; Verhagen and Wraith, 2010) were in studies where cells were stimulated *in vitro*. Further, in a review, Thornton and Shevach state that the method of stimulating cells affects Helios expression and also argued that in the study by Akimova et al, Helios expression was examined at the 3 day time point in suppression co-culture cells and at this time point, very few, if any responder T cells would have remained due to Treg-mediated depletion of IL-2 (Shevach and Thornton, 2014). Since then, a number of groups have used Helios to differentiate tTregs from pTregs (Daniel et al., 2015; Muller et al., 2015; Sanin et al., 2015; Smith et al., 2015). Thus to limit any scope for error, we examined Helios expression in FoxP3<sup>+</sup> CD4<sup>+</sup> T cells directly *ex vivo*, without stimulating the cells in any way.

Here, we characterized, for the first time, the proportions of tTregs, pTregs and Tr1 cells in the large intestine LP in uninfected, *Hh*<sup>+</sup> and *Hh*<sup>+</sup>/anti-IL-10R-treated mice. We found that in uninfected *Tiger* mice, the proportion of FoxP3<sup>+</sup> Tregs was far greater than the proportion of Tr1 cells, suggesting that at steady state, in the large intestine, the dominant Treg population is the FoxP3<sup>+</sup> Tregs (**Figure 5.21A**). This finding concurs with that of another study (Maynard et al., 2007). We found that this phenomenon of greater numbers of FoxP3<sup>+</sup> Tregs compared to Tr1 cells in the large intestine LP was seen in both *Hh*<sup>+</sup> and *Hh*<sup>+</sup>/anti-IL-10R-treated *Tiger* mice. Characterization of the FoxP3<sup>+</sup> Tregs into tTregs and pTregs (based on expression of Helios by tTregs but not pTregs) revealed that in uninfected mice, these cells were present in equal numbers in the large intestine LP (**Figure 5.21A**). This finding is similar to results obtained by other groups who used NRP1 expression to differentiate tTregs from pTregs (Weiss et al., 2012; Yadav et al., 2012). Following infection with *Hh*, the tTregs and pTregs expanded slightly in the non-inflamed mice and maintained the relative proportions seen in the uninfected mice i.e. similar proportion of pTregs to tTregs (**Figure 5.21A**). Conversely, in the inflamed mice the tTregs and pTregs expanded significantly and furthermore, the proportion of pTregs was slightly greater than tTregs (**Figure 5.21A**). When examining the proportions of Tr1 cells, we found that although there was a slight expansion in the number of Tr1 cells in *Hh*<sup>+</sup> mice and a significant expansion in the colitic setting, the frequency of Tr1 cells in both groups remained similar to that of uninfected mice. Although tTregs (Uhlir et al., 2006), pTregs (Mucida et al., 2007) and Tr1 (Groux et al., 1997) cells are effective at preventing CD4<sup>+</sup> T cell transfer colitis, it is unclear *in vivo* which subset might play a more important role in preventing *Hh*-induced

colitis. There are a number of studies that suggest that pTregs may be superior to tTregs in preventing autoimmune disease. In a model of autoimmune gastritis, iTregs and not tTregs were able to suppress Th17 responses (Huter et al., 2008). Another study involving adoptive transfer of tTregs alone or in combination with conventional T cells into newborn FoxP3-deficient mice showed that transfer of tTregs alone was able to prevent disease lethality but was unable to suppress chronic inflammation (Haribhai et al., 2011). Conversely, transfer of conventional T cells along with tTregs was able to reconstitute the pTreg pool and establish tolerance, highlighting a superior role for pTregs in preventing autoimmune and inflammatory responses (Haribhai et al., 2011). It has been established that *Hh* priming is necessary for the generation of disease protective Tregs (Kullberg et al., 2002), thus it is tempting to speculate that the pTregs and Tr1 cells might play a more important role than tTregs in preventing *Hh*-induced colitis. Further comparison of the suppressive capacities of these three populations of Tregs using the modified *Hh*/RAG KO T cell transfer model of colitis will help to resolve this question.

In this study, we also examined the expression of regulatory protein LAG-3. LAG-3 has been shown to play an important role in preventing autoimmune and inflammatory diseases (Okamura et al., 2009; Okazaki et al., 2011). LAG-3 deficiency accelerated onset of Type 1 diabetes in non-obese diabetic mice (Okazaki et al., 2011). In the CD4<sup>+</sup> T cell transfer model of colitis, co-transfer of IL-10 KO CD25<sup>-</sup> LAG-3<sup>+</sup> (which were FoxP3<sup>-</sup>) cells along with naïve CD4<sup>+</sup> T cells decreased the severity of colitis, however transfer of IL-10 sufficient CD25<sup>-</sup> LAG-3<sup>+</sup> cells completely prevented colitis (Okamura et al., 2009), suggesting that while LAG-3 on its own can limit colitis development to an extent, maximal protection is dependent on IL-10. In the current study, we found that in the uninfected and *Hh*<sup>+</sup> mice, most of the LAG-3 was expressed by pTregs, tTregs and Tr1 cells whereas in the colitic setting, although there was an expansion in the numbers of LAG-3<sup>+</sup> pTregs, tTregs and Tr1 cells, most of the LAG-3 was expressed by cells negative for Treg markers (i.e. CD4<sup>+</sup> FoxP3<sup>-</sup> CD49b<sup>-</sup>). These LAG-3<sup>+</sup> FoxP3<sup>-</sup> CD49b<sup>-</sup> might represent exhausted T cells, which reportedly arise during chronic inflammation (Wherry, 2011), or more intriguingly, represent a population of effector T cells with regulatory potential. Exhausted CD4<sup>+</sup> T cells express a host of inhibitory receptors such as TIM-3 and PD-1 (Wherry, 2011). Further examination of these markers in the LAG-3<sup>+</sup> CD49b<sup>-</sup> FoxP3<sup>-</sup> population would help delineate whether the LAG-3-expressing effector T cells represented exhausted T cells. In the current study, in both *Hh* and *Hh*<sup>+</sup>/anti-IL-10R-treated mice, there were higher numbers of LAG-3-expressing pTregs compared to LAG-3-expressing tTregs. Given that LAG-3 is upregulated on antigen-activated cells (Workman et al., 2002), these results suggest that the LAG-3<sup>+</sup> FoxP3<sup>+</sup> Tregs are the Tregs specific for colitogenic antigens. LAG-3 has also been shown to be required for maximal suppressive capacity of CD4<sup>+</sup> CD25<sup>+</sup> FoxP3<sup>+</sup> Tregs (Do et al., 2015; Huang et al., 2004), thus it is tempting to speculate that the LAG3<sup>+</sup> pTregs/tTregs

observed in *Hh* and *Hh*<sup>+</sup>/anti-IL-10R-treated mice may be more suppressive than LAG3<sup>-</sup> pTregs/tTregs.

In the current study, we found that both *Hh*<sup>+</sup> and *Hh*<sup>+</sup>/anti-IL-10R-treated *Tiger*/IL-17A-eYFP mice showed an expansion in IL-10-producing CD4<sup>+</sup> T cells compared to uninfected controls. Examination of the phenotype of the IL-10-GFP<sup>+</sup> cells *ex vivo* based on tTreg/pTreg marker FoxP3 and Tr1 markers CD49b and LAG-3 revealed that following infection with *Hh*, both IL-10<sup>+</sup> FoxP3<sup>+</sup> cells and IL-10<sup>+</sup> Tr1 cells expanded slightly in *Hh*<sup>+</sup> mice and significantly in colitic mice compared to uninfected controls. Furthermore, the majority of IL-10<sup>+</sup> cells in all three experimental groups expressed FoxP3 and a small proportion were Tr1-derived. Together, the FoxP3<sup>+</sup> Tregs and Tr1 cells contributed to 98% of IL-10-producing CD4<sup>+</sup> T cells in uninfected mice, 76% in *Hh*<sup>+</sup> mice and 68% in the colitic setting, suggesting an expansion in effector T cells producing IL-10 following infection with *Hh*.

Classifying the FoxP3<sup>+</sup> IL-10 GFP<sup>+</sup> cells further into tTregs and pTregs based on Helios expression proved to be challenging as we were unable to optimise the fixation and permeabilisation protocol to simultaneously detect IL-10-GFP and Helios. It is unclear why using the combination of 2% PFA/0.1% saponin to fix the cells was efficient at detecting FoxP3 but ineffective at detecting Helios. Grupillo et al., 2011 published a protocol claiming that fixing cells with a combination of 2% PFA and eBio fix-perm followed by permeabilisation with eBio perm was effective at detecting Helios. However, in their results, they never showed positive staining for Helios using eBio fix-perm/eBio perm (Grupillo et al., 2011) and although we obtained similar Helios staining to Grupillo et al using their protocol of 2% PFA/eBio fix-perm/eBio perm, we found that compared to the positive staining obtained with eBio fix-perm/eBio perm, the Helios staining was very poor. To date, all the published literature in which Helios has been examined has been done using eBio fix-perm/eBio perm (Akimova et al., 2011; Muller et al., 2015; Singh et al., 2015; Thornton et al., 2010) and to our knowledge, nobody has successfully managed to simultaneously detect Helios and GFP/eYFP expressed by some transgenic mouse strains.

Using the T-cell transfer model of colitis, findings in Fiona Powrie's lab showed that the CD4<sup>+</sup> CD25<sup>+</sup> cells mediate cure of colitis in an IL-10-dependent manner (Uhlir et al., 2006). Research in our lab, using a modified *Hh*<sup>+</sup> CD4<sup>+</sup> T-cell transfer model of colitis, showed that both CD25<sup>+</sup> and CD25<sup>-</sup> CD45RB<sup>low</sup> cells were protected against the development of *Hh*-induced colitis in an IL-10-dependent manner (Kullberg et al., 2002). However, in contrast to findings by Uhlir et al, in the study by Kullberg et al, it was found that at a higher ratio of CD45RB<sup>high</sup> : CD45RB<sup>low</sup> cells, the CD45RB<sup>low</sup> CD25<sup>-</sup> cells were more protective than CD45RB<sup>low</sup> CD25<sup>+</sup> cells (Kullberg et al., 2002). The main difference between the studies by Uhlir et al and Kullberg et al was the fact that the development of colitis in the latter model is dependent on *Hh*. Therefore the difference in the results between these two studies could be attributed to the fact that *Hh*

might modulate the immune response and result in the generation of either a greater frequency of IL-10-producing CD4<sup>+</sup> T cells in the CD4<sup>+</sup>CD45RB<sup>low</sup>CD25<sup>-</sup> fraction or a greater amount of IL-10 being produced by the CD4<sup>+</sup>CD45RB<sup>low</sup>CD25<sup>-</sup> fraction. The previous study by Kullberg et al used CD4<sup>+</sup>CD45RB<sup>low</sup>CD25<sup>-</sup> cells from the MLNs of *Hh*<sup>+</sup> WT mice and transferring them at different ratios along with naïve CD4<sup>+</sup> T cells from *Hh*<sup>+</sup> IL-10 KO mice into *Hh*<sup>+</sup> RAG KO mice. In the current study, we assessed the expression of CD25 on IL-10<sup>+</sup> cells in the large intestine LP CD4<sup>+</sup> T cells from uninfected, *Hh*<sup>+</sup> and *Hh*<sup>+</sup>/anti-IL-10R-treated mice. We found that in all three groups, the frequency of IL-10<sup>+</sup> FoxP3<sup>+</sup>CD25<sup>+</sup> cells was higher than IL-10<sup>+</sup> CD25<sup>-</sup> cells in the large intestine, suggesting that the greater suppressive nature of the IL-10<sup>+</sup> CD25<sup>-</sup> cells observed previously was likely due to higher amounts of IL-10 being produced on a per cell basis.

Our results thus far had indicated that the majority of IL-10-producing CD4<sup>+</sup> T cells in uninfected, *Hh*<sup>+</sup> and *Hh*<sup>+</sup>/anti-IL-10R treated mice were of a Treg phenotype (either FoxP3<sup>+</sup> Treg or Tr1) (**Figure 5.21B**). In both *Hh*<sup>+</sup> and *Hh*<sup>+</sup>/anti-IL-10R-treated mice, there was an expansion in the proportion of IL-10 coming from cells that were negative for markers of Tregs and could therefore be effector T cells producing IL-10. The effector CD4<sup>+</sup> T cell response in *Hh*<sup>+</sup> mice was characterised by a slight increase in the IL-17A<sup>+</sup> and IFN- $\gamma$ <sup>+</sup> cells, whereas, in *Hh*<sup>+</sup>/anti-IL-10R-treated mice, there was a significant expansion in IL-17A<sup>+</sup>, IL-17A<sup>+</sup> IFN- $\gamma$ <sup>+</sup> and IFN- $\gamma$ <sup>+</sup> CD4<sup>+</sup> T cells compared to uninfected controls (**Figure 5.21A**). Some studies have shown that effector Th1 and Th17 cells can produce IL-10 (Esplugues et al., 2011; Saraiva et al., 2009). In the current study, examination of the phenotype of IL-10<sup>+</sup> CD4<sup>+</sup> T cells based on co-expression of IL-17A and IFN- $\gamma$  revealed that interestingly, following infection with *Hh* alone, there was an expansion in the IL-10<sup>+</sup> IL-17A<sup>+</sup> cells, however, in the colitic setting, there was an expansion in IL-10<sup>+</sup> IL-17A<sup>+</sup>, IL-10<sup>+</sup> IL-17A<sup>+</sup> IFN- $\gamma$ <sup>+</sup> and IL-10<sup>+</sup> IFN- $\gamma$ <sup>+</sup> cells (**Figure 5.21B**). Furthermore, in the colitic setting, IL-10<sup>+</sup> CD4<sup>+</sup> T cells that co-expressed IL-17A and/or IFN- $\gamma$  constituted almost half of the IL-10 producing CD4<sup>+</sup> T cells (**Figure 5.21B**). These results were reproducible when examined by IL-10-GFP signal and IL-10 detected by intracellular staining. We also found that in the colitic setting alone, where ex-Th17 cells are enriched, a small proportion of IL-10-producing CD4<sup>+</sup> T cells were ex-Th17-derived (**Figure 5.21B**). These findings are interesting because they suggest that the expansion of an effector T cell subset is accompanied by an expansion in a proportion of that particular effector T cell population that also co-expresses IL-10 in both the inflammatory and non-inflammatory immune response to *Hh*. The exact mechanisms driving IL-10-production by CD4<sup>+</sup> effector T cells is not clearly understood. Data from the literature suggests that different microbes and parasites, as well as the cytokine environments play a role in influencing IL-10 production by CD4<sup>+</sup> effector T cells. IL-10 producing Th1 cells were first seen in the broncho-alveolar lavage in patients with active tuberculosis (Gerosa et al., 1999). Since then, Th1 cells have also been shown to be a major source of IL-10 in murine models of two different parasitic infections;

cutaneous *Leishmania major* (Anderson et al., 2007) and *Toxoplasma gondii* (Jankovic et al., 2007). Furthermore, Th1 cells can acquire the ability to produce IL-10 in environments where they undergo repeated antigenic stimulation, such as inflammation (Saraiva et al., 2009). IL-10-producing Th17 cells have also been described in the literature. IL-10<sup>+</sup> IL-17A<sup>+</sup> cells have been observed in humans suffering from rheumatoid arthritis (Guggino et al., 2015) and psoriasis vulgaris (Antiga et al., 2012). *In vitro* studies show that the cytokine environment determines whether Th17 cells produce IL-10. One such *in vitro* study showed that *C.albicans* elicits IL-1 $\beta$  production, which in turn stimulated human Th17 cells to produce IFN- $\gamma$  whereas *S.aureus* elicits IL-2 production and induced Th17 cells to produce IL-10 (Zielinski et al., 2012). Another study showed that *in vitro* derived Th17 cells, cultured in the presence of TGF- $\beta$  and IL-6, but not IL-23 and IL-6 also co-express IL-10 (Singh et al., 2013). Although all these studies corroborate the existence of cells that co-express IL-10 and IL-17A or IFN- $\gamma$ , we show here for the first time the extent to which these cells contribute to the total IL-10-producing CD4<sup>+</sup> T cells in the large intestine during colitis. Furthermore, this study also demonstrated for the first time that ex-Th17 cells produce IL-10. Although both Th1 and ex-Th17 cells express T-bet, produce IFN- $\gamma$  and are present in comparable numbers in the large intestine of colitic mice (Morrison et al., 2013), these results also showed that a smaller proportion of ex-Th17 cells produce IL-10 compared to the Th1 cells, highlighting another difference between these two cell types.

We also found that in the non-inflammatory response to *Hh*, most of the IL-10-producing CD4<sup>+</sup> T cells that co-expressed IL-17A and/or IFN- $\gamma$  also expressed FoxP3 whereas in the inflammatory response to *Hh*, half or slightly less than half of IL-10-producing CD4<sup>+</sup> T cells that co-expressed IL-17A and/or IFN- $\gamma$  also expressed FoxP3. These findings demonstrated that these cells share phenotypic characteristics of effector and regulatory CD4<sup>+</sup> T cells (**Figure 5.21B**). Another study, using IL-17A-eYFP mice to examine Th17 plasticity during EAE found that similar to our model, Th17 cells changed phenotype to become ex-Th17 cells (Hirota et al., 2011). However, in this model, Hirota et al found negligible FoxP3 expression in the eYFP expressing cells in the draining lymph node and CNS cells of 12-15 day EAE mice (Hirota et al., 2011). One reason for the differences in FoxP3 expression in their model and ours could be explained by the fact that they examined FoxP3 in eYFP<sup>+</sup> cells from the spleen and CNS, whereas our studies were done on large intestinal LP cells and the local tissue environment may play a role in the immune responses elicited. Secondly, *Hh* may also modulate the immune response to induce slightly different phenotypes to those seen in EAE. Cells co-expressing FoxP3 and inflammatory cytokines have been observed previously. Suppressive IL-17A<sup>+</sup> FoxP3<sup>+</sup> (Hovhannisyan et al., 2011) cells have been isolated from the LP of patients with active CD. FoxP3<sup>+</sup> pTregs but not tTregs have been shown to produce IL-17A and IFN- $\gamma$  (Thornton et al., 2010). Another study involving fate mapping of FoxP3<sup>+</sup> Tregs in autoimmune arthritis showed that FoxP3<sup>+</sup> Tregs transdifferentiate to become pathogenic Th17

cells, and that FoxP3<sup>+</sup> IL-17A<sup>+</sup> cells may represent an intermediate phenotype of these cells (Komatsu et al., 2014). FoxP3<sup>+</sup> cells have been shown to start producing IFN- $\gamma$  during the induction of intestinal inflammation in a microbiota-dependent colitis model and these cells were suppressive in nature (Feng et al., 2011b). Another study showed that some FoxP3<sup>+</sup> CD4<sup>+</sup> T cells express the Th1 transcription factor T-bet, which in turn enabled them to express CXCR3, and accumulate at the same site as Th1 cells and suppress them (Koch et al., 2009). In light of all these studies, it is unclear whether the IL-10<sup>+</sup> FoxP3<sup>+</sup> CD4<sup>+</sup> T cells that co-expressed IL-17A and/or IFN- $\gamma$  originate from effector T cells or FoxP3<sup>+</sup> Tregs and furthermore, whether these cells are protective or pathogenic. In the current study, we observed IL-10<sup>+</sup> IL-17A<sup>+</sup> FoxP3<sup>+/-</sup> cells in the non-inflammatory immune response to *Hh*, making it tempting to speculate that these cells may play protective roles. As these IL-10<sup>+</sup> IL-17A<sup>+</sup> FoxP3<sup>+/-</sup> cells were also observed in the inflammatory response to *Hh* of the current study, it is plausible that they may be protective in this setting as well. Further work examining the suppressive capacity of the IL-10<sup>+</sup> FoxP3<sup>+</sup> CD4<sup>+</sup> T cells that co-express IL-17A and/or IFN- $\gamma$  needs to be done.

Interestingly, the current study also identified a population of IL-10<sup>+</sup> cells that were eYFP<sup>+</sup>IL-17A<sup>-</sup> IFN- $\gamma$ <sup>-</sup> that expanded in both *Hh*<sup>+</sup> and *Hh*<sup>+</sup>/anti-IL-10R-treated mice, demonstrating that following infection with *Hh*, a population of cells that once produced IL-17A had switched off IL-17A production, were IFN- $\gamma$ <sup>-</sup> and secreted IL-10. Furthermore, most of the IL-10<sup>+</sup>eYFP<sup>+</sup>IL-17A<sup>-</sup> IFN- $\gamma$ <sup>-</sup> cells in both *Hh*<sup>+</sup> and *Hh*<sup>+</sup>/anti-IL-10R-treated IL-17A-eYFP mice co-expressed FoxP3, suggesting two possible scenarios: i) a proportion of FoxP3<sup>+</sup> Tregs transiently express IL-17A before switching off IL-17A production, ii) a proportion of Th17 cells are switching phenotype to become regulatory in both the inflammatory and the non-inflammatory immune response to *Hh*. Using IL-17A-eYFP mice, Hirota et al found that following *C.albicans* infection, eYFP<sup>+</sup>IL-17A<sup>-</sup> IFN- $\gamma$ <sup>-</sup> CD4<sup>+</sup> T cells were observed in the skin, but these cells were quiescent and produced little IL-17F, IL-22 and GM-CSF (Hirota et al., 2011). Of note, IL-10 expression was not examined in these cells so it is unclear if they produced IL-10 or not (Hirota et al., 2011). One reason that could account for the differences in the phenotype of eYFP<sup>+</sup>IL-17A<sup>-</sup> IFN- $\gamma$ <sup>-</sup> between the skin and the large intestine LP aside from the fact that they are different tissues, is that both the studies examined the effect of immune responses to different microbes i.e. Hirota et al examined the response to *C.albicans* and we examined the immune response to *Hh*. Different microbes have been shown to modulate CD4<sup>+</sup> T-cell responses (Atarashi et al., 2011; Geuking et al., 2011; Zielinski et al., 2012). Some microbes promote FoxP3<sup>+</sup> Tregs in the colon (Atarashi et al., 2011). Another study showed that *C.albicans* elicits IL-1 $\beta$  production, which in turn stimulated human Th17 cells to produce IFN- $\gamma$  whereas *S.aureus* elicits IL-2 production and induced Th17 cells to produce IL-10 (Zielinski et al., 2012). These studies give credence to the theory that the IL-10<sup>+</sup>eYFP<sup>+</sup>IL-17A<sup>-</sup> IFN- $\gamma$ <sup>-</sup> observed in the current study could be microbially-induced. A recent study examined Th17

plasticity in a resolving immune response observed during *N. brasiliensis* and *S.aureus* infection and non-resolving immune response observed in DNIL-10R mice treated with anti-CD3, where mortality is Th17 associated (Gagliani et al., 2015). Gagliani et al showed that during a non-resolving immune response a greater proportion of the Th17 cells switched phenotype to become IFN- $\gamma$ -producing ex-Th17 cells (Gagliani et al., 2015). Conversely, during the resolution of inflammation, Th17 cells in the small intestine transdifferentiate to a cell termed as Tr1<sup>ex-Th17</sup> (Gagliani et al., 2015). The Tr1<sup>ex-Th17</sup> cells are thought to be Tr1-like because a significant proportion of these cells expressed IL-10 and LAG-3 but negligible amounts of FoxP3 (Gagliani et al., 2015). The current study suggests that in both the inflammatory and non-inflammatory immune response to *Hh*, the majority of IL-10<sup>+</sup>eYFP<sup>+</sup>IL-17A<sup>-</sup>IFN- $\gamma$ <sup>-</sup> cells were FoxP3<sup>+</sup> suggesting that in the large intestine, if a proportion of Th17 cells are switching to a regulatory phenotype, they seem to be switching to a FoxP3<sup>+</sup> Treg phenotype rather than a Tr1 phenotype. The fact we may be seeing a switch from Th17 to FoxP3<sup>+</sup> phenotype in the large intestine whereas Gagliani et al saw a switch from Th17 to Tr1<sup>ex-Th17</sup> in the small intestine (Gagliani et al., 2015) could be explained by the fact that at steady state, the large intestine harbours greater numbers of FoxP3<sup>+</sup> Tregs compared to Tr1 cells (Uhlir et al., 2006) whereas the opposite is true in the small intestine (Maynard et al., 2007). Thus it is possible that local factors influence Th17 cells in the small intestine to become Tr1-like, whereas in the large intestine, to become FoxP3<sup>+</sup>. In this study, we only examined the phenotype of the IL-10-producing CD4<sup>+</sup> T cells at the peak of *Hh*-induced inflammation and the proportion of IL-10<sup>+</sup>eYFP<sup>+</sup>IL-17A<sup>-</sup>IFN- $\gamma$ <sup>-</sup>FoxP3<sup>+</sup> was relatively small compared to the ex-Th17 cells. *Hh*-induced inflammation does eventually resolve at about 90 days pi (Morrison et al., 2013). We know from previous work in the lab that during the resolution of *Hh*-induced inflammation, there is a drastic decrease in the number of ex-Th17 cells, and the CD4<sup>+</sup> T cell response becomes more Th17 oriented (although the numbers of Th17 cells also drop). Thus it is tempting to speculate that perhaps inflammation resolves toward the later timepoints post *Hh*-infection because Th17 cells switch to FoxP3<sup>+</sup> Tregs or Tr1 cells rather than ex-Th17 cells. A kinetic experiment carried out in *Hh*<sup>+</sup>/anti-IL-10R-treated IL-17A-eYFP mice over a 90 day period and tracking IL-17A, IFN- $\gamma$ , FoxP3 and LAG-3 expression in the LP CD4<sup>+</sup> T cells will help to address this question.

### 5.3.1 Summary

The similarities and differences in CD4<sup>+</sup> T-cell responses, Treg profile and the phenotype of IL-10-producing CD4<sup>+</sup> T cells in the large intestine LP in a non-inflammatory immune response compared to an inflammatory immune response to *Hh* are summarised in **Table 5.2**.

Briefly, the experiments carried out in this chapter showed that in both *Tiger* and IL-17A-eYFP mice, the primary CD4<sup>+</sup> T cell response in *Hh*<sup>+</sup> mice was a non-inflammatory response characterized by a higher frequency of FoxP3 and IL-10-expressing CD4<sup>+</sup> T cells compared to those expressing IL-17A and/or IFN- $\gamma$  (**Table 5.2**). In the *Hh*<sup>+</sup>/anti-IL-10R-treated mice, the primary CD4<sup>+</sup> T cell response was an inflammatory response, characterized by a higher frequency of IL-17A and/or IFN- $\gamma$ -producing cells compared to those producing IL-10 and FoxP3 (**Table 5.2**).

*Ex-vivo* characterisation of the Treg profile using *Tiger* mice revealed that in all three experimental groups, there were greater numbers of FoxP3<sup>+</sup> Tregs compared to Tr1 cells in the large intestine (**Table 5.2**). Examination of Helios expression in the FoxP3<sup>+</sup> Tregs revealed that in uninfected and *Hh*<sup>+</sup> mice, there were equal proportions of pTregs and tTregs (**Table 5.2**). In contrast, in the colitic setting, there were slightly higher numbers of pTregs compared to tTregs (**Table 5.2**).

Examination of the phenotype of IL-10<sup>+</sup> LP CD4<sup>+</sup> T cells based on Treg markers revealed that in all three experimental groups, the majority of IL-10<sup>+</sup> LP CD4<sup>+</sup> T cells expressed FoxP3 and a small proportion were Tr1 cells (**Table 5.2**). The major difference in the phenotype of the IL-10<sup>+</sup> CD4<sup>+</sup> T cells when compared to uninfected controls was that in the non-inflammatory response, there was a slight expansion in the IL-10<sup>+</sup> IL-17A<sup>+</sup> cells and most of these cells also co-expressed FoxP3 whereas in the colitic setting, almost half the IL-10<sup>+</sup> CD4<sup>+</sup> T cells co-expressed IL-17A and/or IFN- $\gamma$  and half or slightly less than half of these cells also co-expressed FoxP3 (**Table 5.2**).

In the colitic setting alone, a small proportion of ex-Th17 cells produced IL-10 (**Table 5.2**).

**Table 5.2 The similarities and differences in CD4<sup>+</sup> T-cell responses and the phenotype of IL-10-producing CD4<sup>+</sup> T cells in the large intestine LP of uninfected and 2-wk *Hh*<sup>+</sup> and *Hh*<sup>+</sup>/aati-IL-10R-treated mice**

	<b>Uninfected mice</b>	<b>Non-inflammatory immune response to <i>Hh</i> (<i>Hh</i><sup>+</sup> mice)</b>	<b>Inflammatory immune response to <i>Hh</i> (<i>Hh</i><sup>+</sup> mice/anti-IL-10R-treated mice)</b>
<b>CD4<sup>+</sup>T-CELL RESPONSES</b>	Primarily regulatory IL-10 <sup>+</sup> and FoxP3 <sup>+</sup> cells > IL-17A <sup>+</sup> and/or IFN-γ <sup>+</sup> cells	Primarily regulatory IL-10 <sup>+</sup> and FoxP3 <sup>+</sup> cells > IL-17A <sup>+</sup> and/or IFN-γ <sup>+</sup> cells	Primarily inflammatory IL-17A <sup>+</sup> and/or IFN-γ <sup>+</sup> cells > IL-10 <sup>+</sup> and FoxP3 <sup>+</sup> cells
<b>FOXP3<sup>+</sup> TREGS AND TR1 CELLS</b>	FoxP3 <sup>+</sup> Treg > Tr1 cells	FoxP3 <sup>+</sup> Treg > Tr1 cells	FoxP3 <sup>+</sup> Treg > Tr1 cells
	No. of pTregs = No. of tTregs	No. of pTregs = No. of tTregs	No. of pTregs > No. of tTregs
<b>LAG-3 EXPRESSING CELLS</b>	Majority were FoxP3 <sup>+</sup> Tregs and Tr1 cells	Majority were FoxP3 <sup>+</sup> Tregs and Tr1 cells	Majority were effector T cells
<b>PHENOTYPE OF IL-10<sup>+</sup> CD4<sup>+</sup> T CELLS</b>	80% FoxP3 <sup>+</sup>	60-80% FoxP3 <sup>+</sup>	50-60% FoxP3 <sup>+</sup>
	15% Tr1	16% Tr1	18% Tr1
	About 5% co-expressed IL-17A and/or IFN-γ of which most expressed FoxP3.	About 25% co-expressed IL-17A and/or IFN-γ of which most expressed FoxP3.	About 40% co-expressed IL-17A and/or IFN-γ of which half or slightly less than half of these cells also expressed FoxP3.

## 5.4 FIGURES

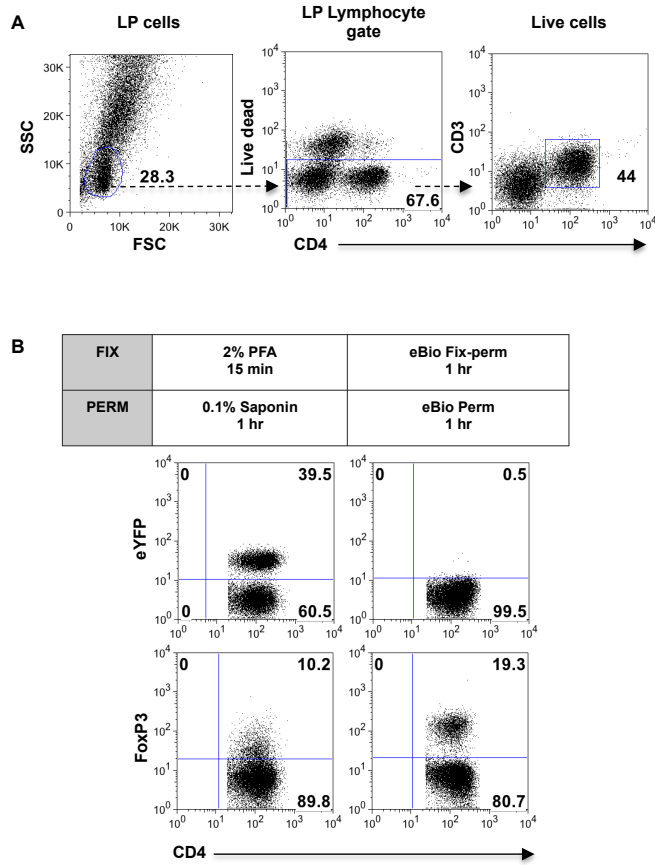


**Figure 5.1 Analysis of eYFP and FoxP3 expression using different fixation and permeabilisation buffers.**

A female *Il17a<sup>cre</sup>R26R<sup>eYFP</sup>* mouse was inoculated with *Hh* and treated with anti-IL-10R mAb on days 0 and 7 pi. At 2 wks pi, large intestinal LP cells were isolated, surface stained with mAb specific for CD3, CD4 and a live dead exclusion dye, fixed and intracellularly stained for FoxP3 and analysed by flow cytometry. (A) Gating strategy used for analysis of the results. (B) Dot plots depicting eYFP and FoxP3 staining after the use of different combinations of fixatives and permeabilisation buffers (as indicated). Dot plots are gated on live CD4<sup>+</sup> T cells. The data shown are from a single experiment.

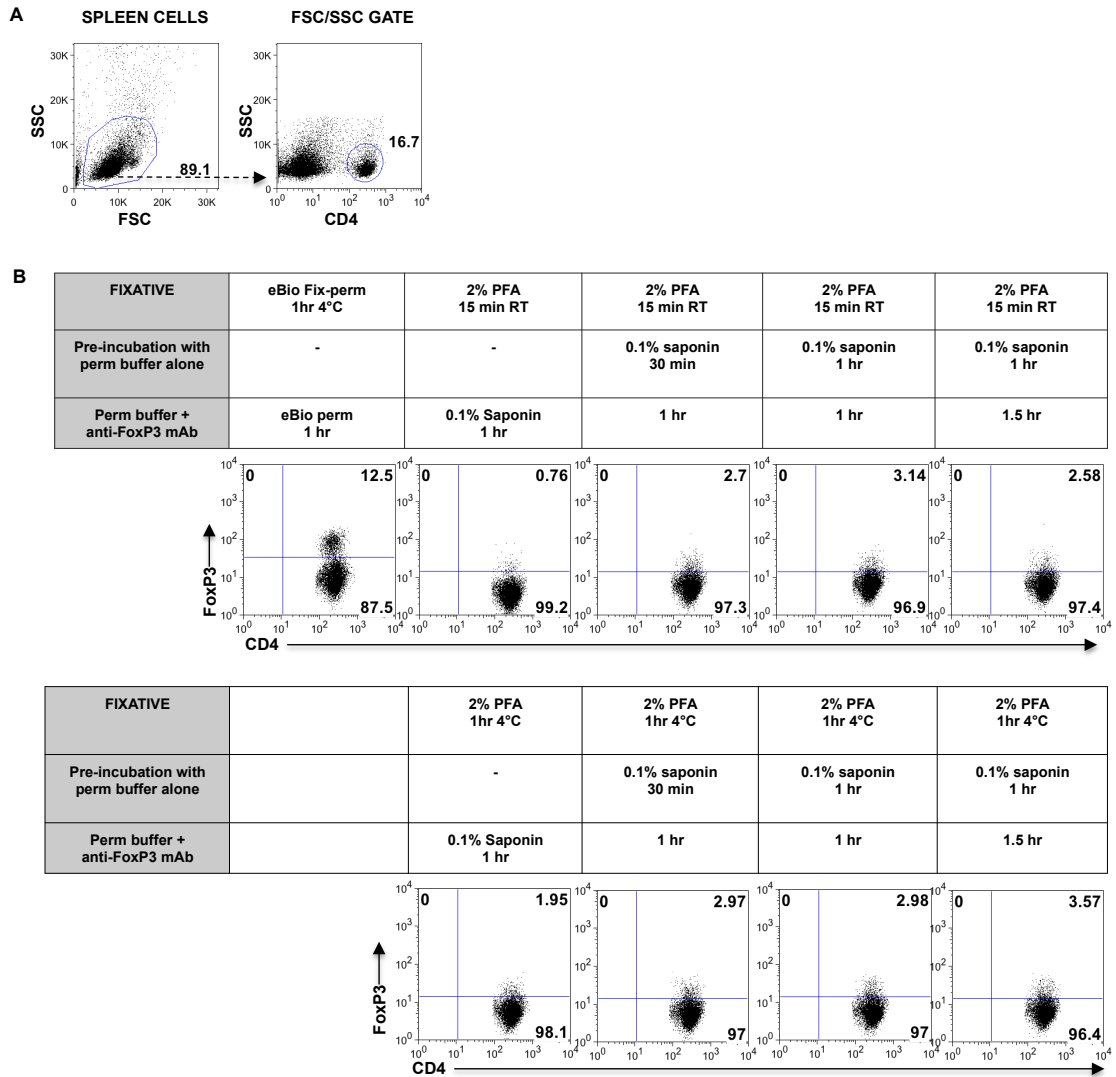


**Figure 5.2 Altering the fixation and permeabilisation time when using the combination of 2% PFA fix/0.1% saponin perm does not improve FoxP3 staining.** Splenocytes were isolated from a female WT mouse, surface stained with a mAb to CD4, fixed and then intracellularly stained for FoxP3 and analyzed by flow cytometry. (A) Gating strategy used for the analysis (B) FoxP3 expression after different incubation times for fixation, permeabilisation and intracellular staining steps (as indicated). Dot plots are gated on CD4<sup>+</sup> cells. The figure shows data from a single experiment.

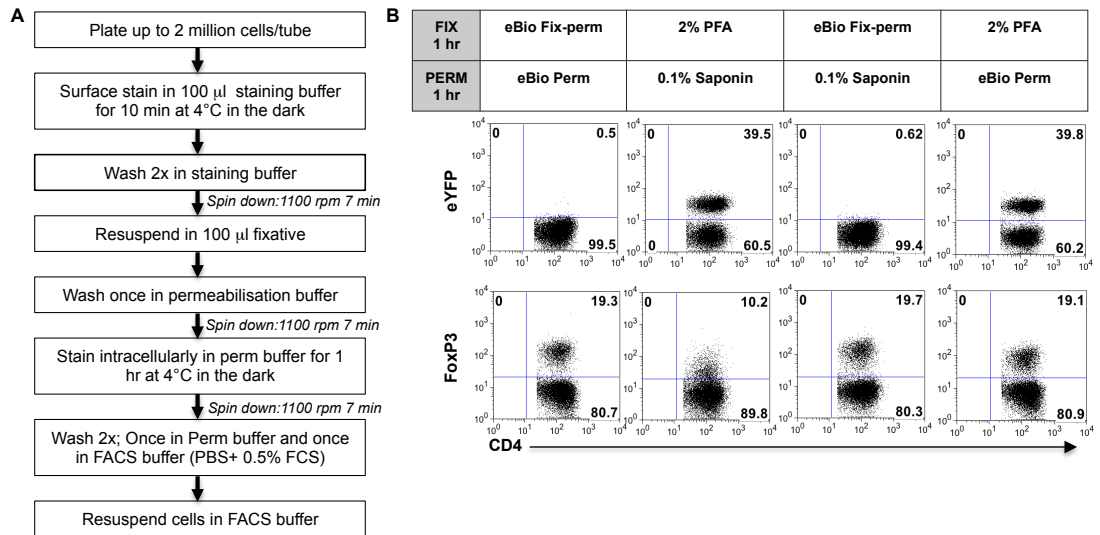


**Figure 5.3 Simultaneous detection of eYFP and FoxP3 expression using 2% PFA and eBioscience permeabilisation buffer.**

*I117a<sup>cre</sup>R26R<sup>eYFP</sup>* mice were inoculated with *Hh* and treated with anti-IL-10R mAb on days 0 and 7 pi. At 2 wks pi, large intestinal LP cells were isolated, surface stained with mAb specific for CD3 and CD4 and a live dead exclusion dye, fixed and intracellularly stained for FoxP3 and analysed by flow cytometry. (A) Protocol used for the intracellular staining of transcription factors. (B) Dot plots depicting eYFP and FoxP3 staining after the use of different combinations of fixatives and permeabilisation buffers (as indicated). Dot plots are gated on live CD4<sup>+</sup> T cells and show data from one experiment where LP cells from a single *I117a<sup>cre</sup>R26R<sup>eYFP</sup>* female mouse were used.

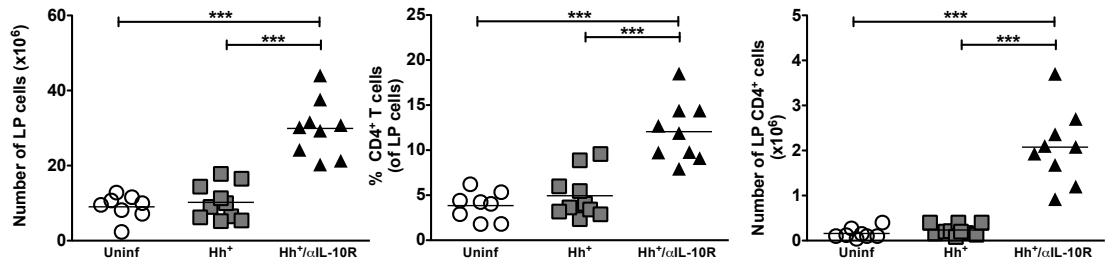


**Figure 5.4 LP cell numbers and percentage and number of LP CD4<sup>+</sup> T cells in the large intestine of *Tiger* mice following infection with *Hh*.**

LP cells were isolated from the large intestine of uninfected, *Hh*<sup>+</sup> and *Hh*<sup>+</sup>/anti-IL-10R-treated female *Tiger* mice at 2 wks pi. The cells were surface stained with mAb specific for CD45, CD3, CD4 and a live dead exclusion dye, fixed with 2% PFA and then examined by flow cytometry. Scatter plots depicting the total number of LP cells (left panel), percentage of LP CD4<sup>+</sup> T cells (middle panel) and total number of LP CD4<sup>+</sup> T cells (right panel) in the large intestine. Horizontal bars show the mean. Each symbol represents an individual mouse. Data shown are pooled from three independent experiments. \*\*\*P<0.001 as determined by one-way Anova.

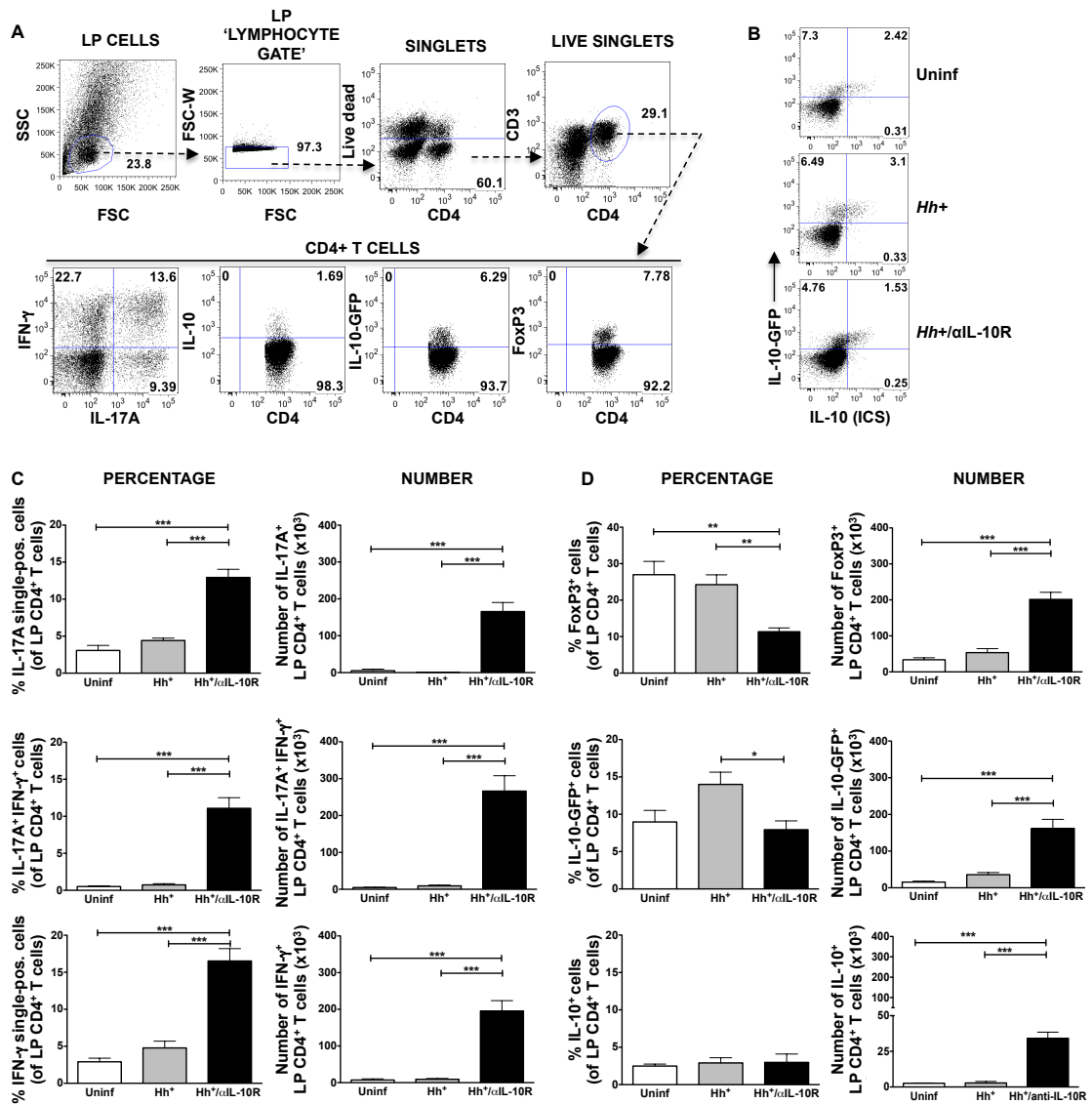


**Figure 5.5 CD4<sup>+</sup> T cell responses in the large intestine of *Tiger* mice following infection with *Hh*.**

LP cells were isolated from the large intestine of uninfected, *Hh*<sup>+</sup> and *Hh*<sup>+</sup>/anti-IL-10R-treated female *Tiger* mice at 2 wks pi. Half the LP cells were left unstimulated and the other half stimulated with PMA and ionomycin in the presence of Brefeldin A. Both the stimulated and unstimulated cells surface stained with mAb specific for CD3, CD4 and a live dead exclusion dye, fixed with 2% PFA, permeabilised with ebio perm buffer. The unstimulated cells were then intracellularly stained for FoxP3 and the stimulated cells stained for IL-10, IL-17A and IFN-γ. (A) Dot plots depicting the gating strategy used for the analysis. (B) Dot plots showing representative staining of IL-10 GFP and IL-10 detected by ICS in the three experimental groups. Dot plots are gated on live CD4<sup>+</sup> T cells. Data shown are from a single experiment where where n ≥ 3 mice/group. (C) Graphs depicting the frequency of LP CD4<sup>+</sup> T cells that are IL-17A single-positive, IL-17A<sup>+</sup> IFN-γ<sup>+</sup> and IFN-γ single-positive. Data shown are pooled from two independent experiments where n ≥ 5 mice/group in total. (D) Graphs depicting the frequency and number of LP CD4<sup>+</sup> T cells that express FoxP3 (top panel), IL-10-GFP (middle panel) and IL-10 by ICS (bottom panel). Data shown are pooled from three independent experiments where n ≥ 8 mice/group in total for FoxP3 and IL-10-GFP and from a single experiment where n ≥ 3 mice/group for IL-10 detected by ICS. Bars in (C) and (D) show means + s.e.m. of either n ≥ 8 mice/group in total (FoxP3 and IL-10-GFP) or n ≥ 3 mice/group for IL-10 detected by ICS. \*P<0.05 \*\*P<0.01 and \*\*\*P<0.001 as determined by one-way Anova.

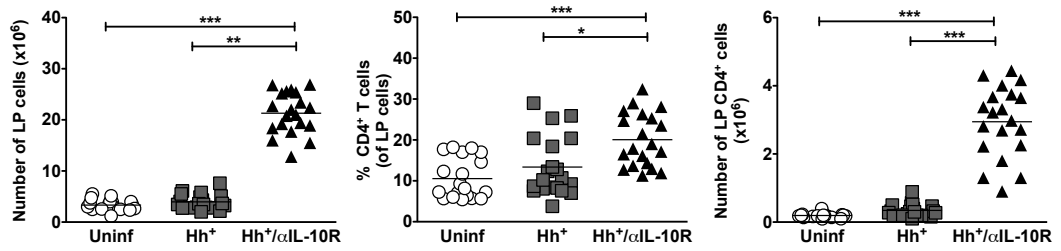


**Figure 5.6 LP cell numbers and percentage and number of LP CD4<sup>+</sup> T cells in the large intestine of *IL-17A<sup>cre</sup>Rosa26<sup>eYFP</sup>* mice following infection with *Hh*.**

LP cells were isolated from the large intestine of uninfected, *Hh*<sup>+</sup> and *Hh*<sup>+</sup>/anti-IL-10R-treated female *Il17a<sup>cre</sup>R26R<sup>eYFP</sup>* mice at 2 wks pi. The cells were surface stained with mAb specific for CD45, CD3, CD4 and a live dead exclusion dye, fixed with 2% PFA and then examined by flow cytometry. Scatter plots depicting the total number of LP cells (left panel), percentage of LP CD4<sup>+</sup> T cells (middle panel) and total number of LP CD4<sup>+</sup> T cells (right panel) in the large intestine. Horizontal bars show the mean. Each symbol represents an individual mouse. Except for the plot showing the number of CD4<sup>+</sup> T cells, which is pooled from four independent experiments, data shown are pooled from five independent experiments. \*P<0.05 \*\*P<0.01 and \*\*\*P<0.001 as determined by one-way Anova.

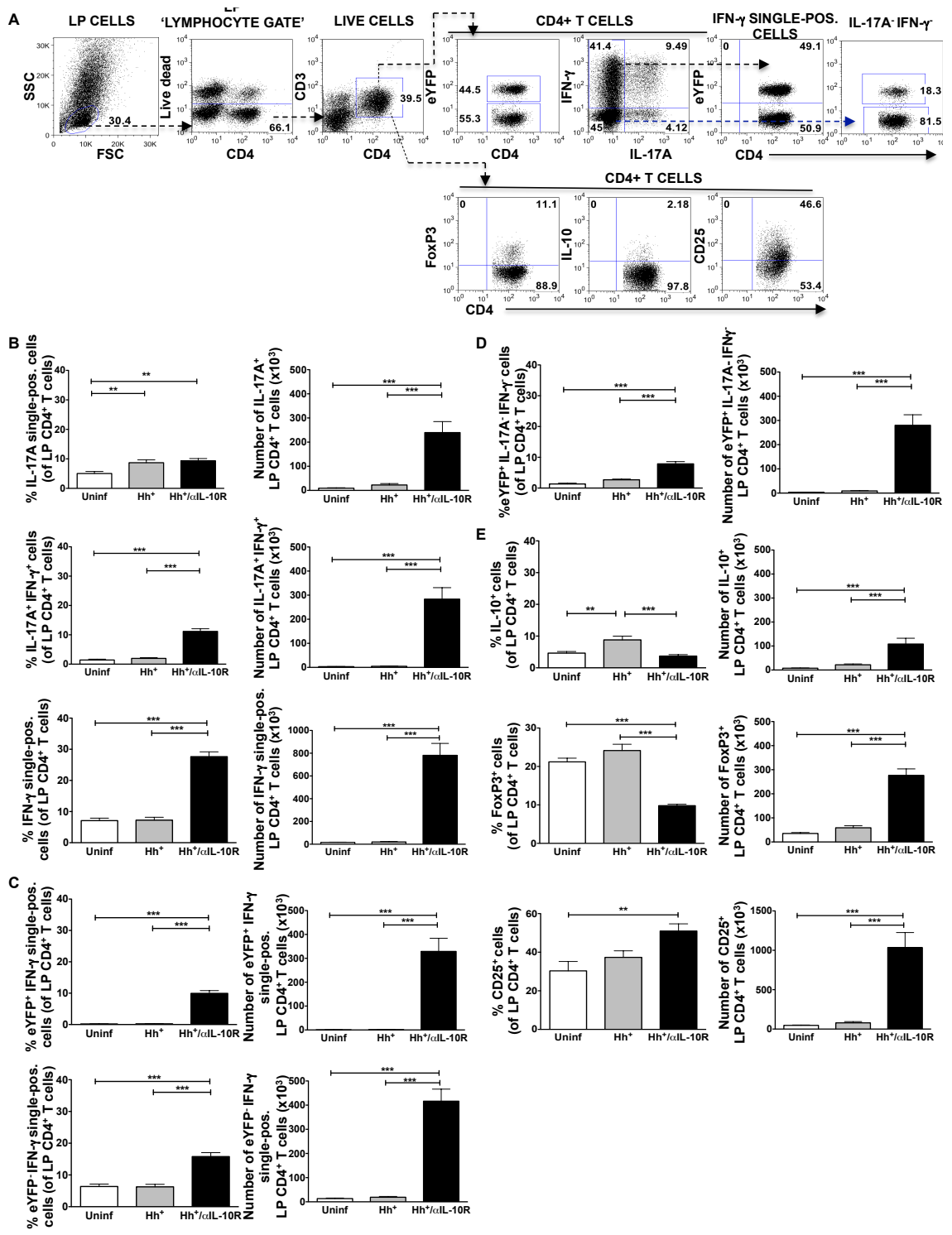


**Figure 5.7. CD4<sup>+</sup> T-cell responses in the large intestine of *Il17a<sup>cre</sup>R26R<sup>eYFP</sup>* mice following infection with *Hh*.** LP cells were isolated from the large intestine of uninfected, *Hh*<sup>+</sup> and *Hh*<sup>+</sup>/anti-IL-10R-treated female *Il17a<sup>cre</sup>R26R<sup>eYFP</sup>* mice at 2 wks pi. The cells were stimulated with PMA and ionomycin in the presence of Brefeldin A. The cells were then surface stained with mAbs specific for CD3, CD4, CD25 and a live dead exclusion dye, fixed and then intracellularly stained for FoxP3, IL-10, IL-17A and IFN- $\gamma$ . With the exception of one experiment, which was fixed and permeabilised with 2% PFA/0.1% saponin, all the other experiments were fixed and permeabilised with the combination of 2% PFA/eBio perm. (A) Dot plots depicting the gating strategy used for the analysis. (B) Graphs depicting the frequency (left panel) and number (right panel) of LP CD4<sup>+</sup> T cells that are IL-17A single-positive (Th17), IL-17A<sup>+</sup> IFN- $\gamma$ <sup>+</sup>, IFN- $\gamma$ -single positive in the three experimental groups. (C) Graphs depicting the frequency (left panel) and number (right panel) of LP CD4<sup>+</sup> T cells that are IFN- $\gamma$ -single positive eYFP<sup>+</sup> (ex-Th17), IFN- $\gamma$ -single positive eYFP<sup>-</sup> (Th1) (D) Graphs depicting the frequency (left panel) and number (right panel) of LP CD4<sup>+</sup> T cells that are eYFP<sup>+</sup>IL-17A<sup>-</sup> IFN- $\gamma$ <sup>-</sup>. Data shown in (B), (C) and (D) are pooled from five independent experiments where  $n \geq 3$  mice/group/experiment. (E) Graphs depicting the frequency (left panel) and number (right panel) of LP CD4<sup>+</sup> T cells that express IL-10 (upper panel), FoxP3 (middle panel) and CD25 (lower panel). Data shown are pooled from five independent experiments where  $n \geq 3$  mice/group/experiment for IL-10, four independent experiments where  $n \geq 3$  mice/group/experiment for FoxP3 and CD25 two independent experiments where  $n \geq 5$  mice/group in total for CD25. Bars in (B) and (C) show means + s.e.m. of  $n \geq 5$  mice/group in total \* $P < 0.05$  \*\* $P < 0.01$  and \*\*\* $P < 0.001$  as determined by one-way Anova.

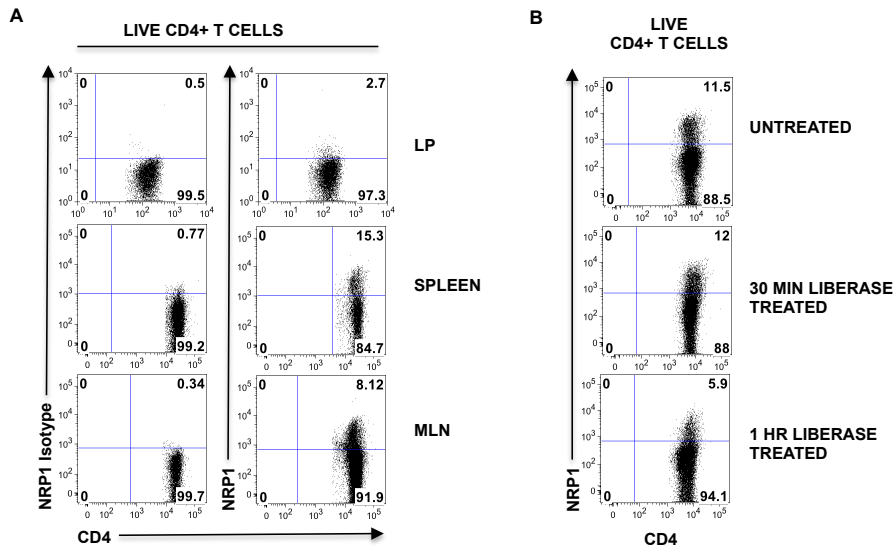


**Figure 5.8 NRP1 expression is lost following digestion of tissues with liberase.**

LP, MLN and spleen cells were isolated from WT female mice, surface stained with mAb specific for CD3, CD4, NRP1 or an isotype control for NRP1 and a live dead exclusion dye, fixed with 2% PFA and analyzed by flow cytometry. (A) Dot plots depicting NRP1 expression in the LP (upper panel), spleen (middle panel) and MLN (lower panel). (B) Dot plots showing NRP1 expression in spleen cells that were either untreated (upper panel) or liberase treated for 30 minutes (middle panel) or 1hr (lower panel). Dot plots in (A) and (B) are gated on live CD4<sup>+</sup> T cells. Data shown are from individual experiments carried out once.

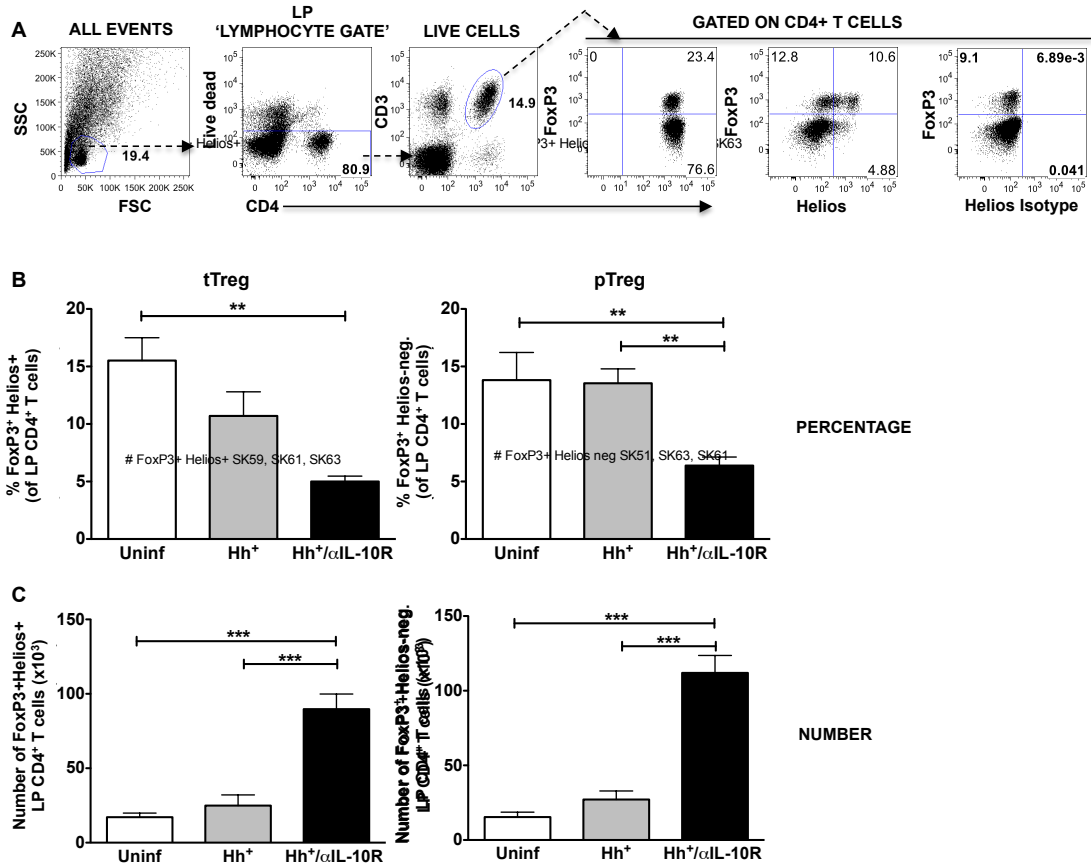


**Figure 5.9 Co-expression of Helios and FoxP3 in LP CD4<sup>+</sup> T cells.**

Large intestinal LP cells were isolated from uninfected, *Hh*<sup>+</sup> and *Hh*<sup>+</sup>/anti-IL-10R-treated male and female *Tiger* mice at 2 wks pi. Cells were surface stained with mAb specific for CD3, CD4 and a live dead exclusion dye, fixed with 2% PFA, permeabilised with eBio perm and then intracellularly stained for Foxp3 and either Helios or an isotype control for Helios (A) Dot plots depicting the gating strategy used for the analysis. (B) Frequency of LP CD4<sup>+</sup> T cells that are FoxP3<sup>+</sup>Helios<sup>+</sup> (left panel) and FoxP3<sup>+</sup>Helios<sup>-</sup> (right panel). (C) Number of LP CD4<sup>+</sup> T cells that are FoxP3<sup>+</sup>Helios<sup>+</sup> (left panel) and FoxP3<sup>+</sup>Helios<sup>-</sup> (right panel). Data shown in (B) and (C) are a pool of three independent experiments. Bars show means + s.e.m. where  $n \geq 8$  mice/group in total. \*\* $P < 0.01$  and \*\*\* $P < 0.001$  as determined by one-way Anova.

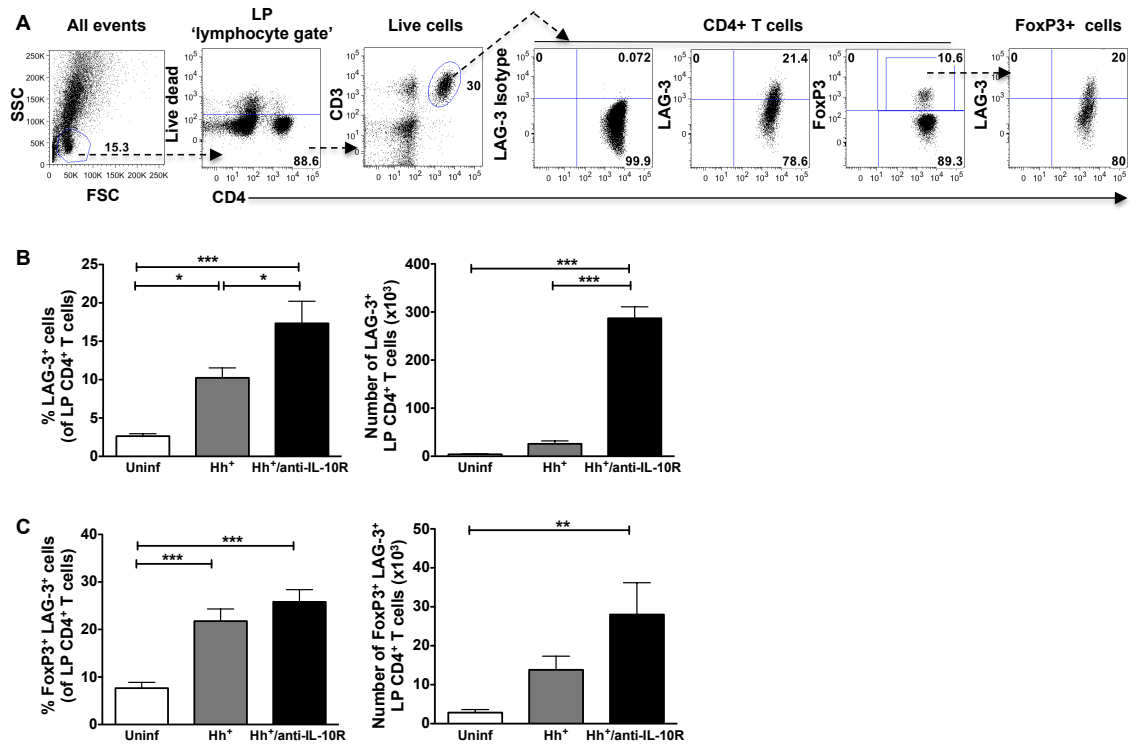


**Figure 5.10 Expression of LAG-3 in LP CD4<sup>+</sup> T cells and FoxP3<sup>+</sup> LP CD4<sup>+</sup> T cell.**

Large intestinal LP cells were isolated from uninfected, *Hh*<sup>+</sup> and *Hh*<sup>+</sup>/anti-IL-10R-treated *Tiger* mice at 2 wks pi. Cells were surface stained with mAb specific for CD3, CD4, LAG-3, CD49b and a live dead exclusion dye, fixed with eBio fix-perm and then permeabilised with eBio perm and intracellularly stained for Foxp3 and Helios. (A) Dot plots depicting the gating strategy used for the analysis of LAG-3 and FoxP3 expression. (B) Frequency (left panel) and number (right panel) of LAG-3<sup>+</sup> LP CD4<sup>+</sup> T cells. (C) Frequency (left panel) and number (right panel) of FoxP3<sup>+</sup> LAG-3<sup>+</sup> LP CD4<sup>+</sup> T cells. Data shown in B-C are pooled from three independent experiments. Bars show means + s.e.m of n ≥ 8 mice/group in total. \*\*P<0.01 and \*\*\*P<0.001 as determined by one-way Anova.

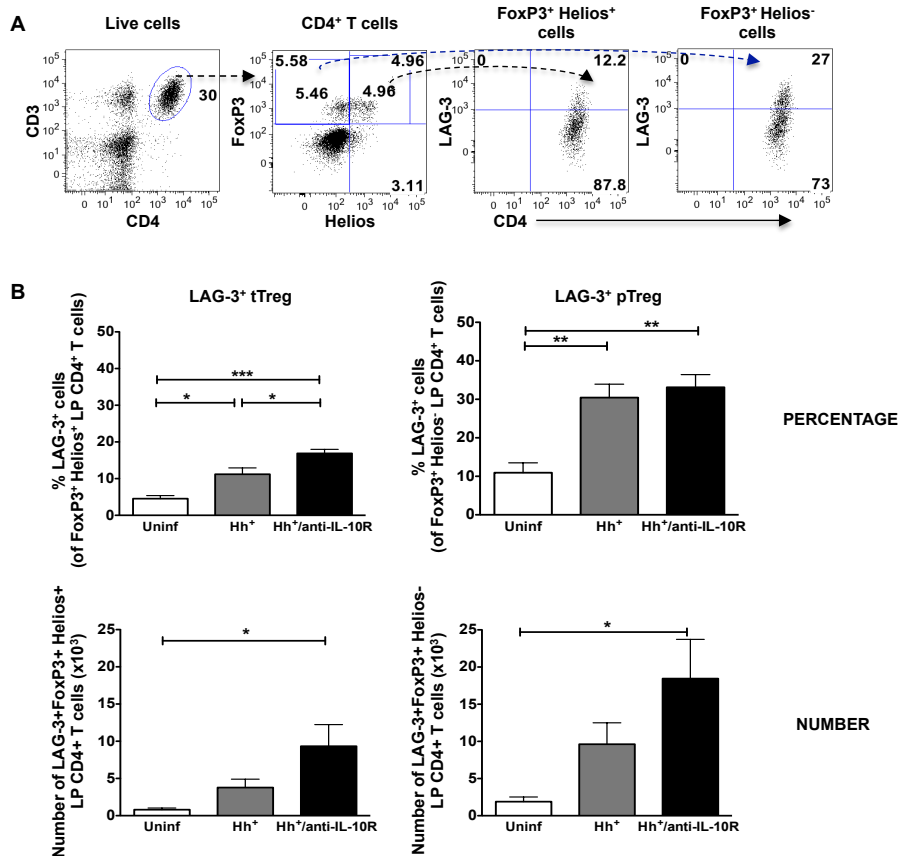


**Figure 5.11 Expression of LAG-3 in FoxP3<sup>+</sup> tTregs and pTregs.**

Large intestinal LP cells were isolated from uninfected, *Hh*<sup>+</sup> and *Hh*<sup>+</sup>/anti-IL-10R-treated *Tiger* mice at 2 wks pi. Cells were surface stained with mAb specific for CD3, CD4, LAG-3 or LAG-3 isotype control and a live dead exclusion dye, fixed with eBio fix-perm and then permeabilised with eBio perm and intracellularly stained for Foxp3 and Helios or their respective isotype controls. (A) Gating strategy used for analysis of LAG-3 expression in FoxP3<sup>+</sup> Helios<sup>+</sup> and FoxP3<sup>+</sup> Helios<sup>-</sup> LP CD4<sup>+</sup> T cells. (B) Upper panels: Frequency of LAG-3 expression in FoxP3<sup>+</sup> Helios<sup>+</sup> (left panel) and FoxP3<sup>+</sup> Helios<sup>-</sup> (right panel) LP CD4<sup>+</sup> T cells. Lower panels: Number of FoxP3<sup>+</sup> Helios<sup>+</sup> LAG-3<sup>+</sup> (left panel) and FoxP3<sup>+</sup> Helios<sup>-</sup> LAG-3<sup>+</sup> (right panel) LP CD4<sup>+</sup> T cells. Data shown are pooled from three independent experiments. Bars show means + s.e.m of n ≥ 8 mice/group in total. \*\*P < 0.01 and \*\*\*P < 0.001 as determined by one-way Anova.

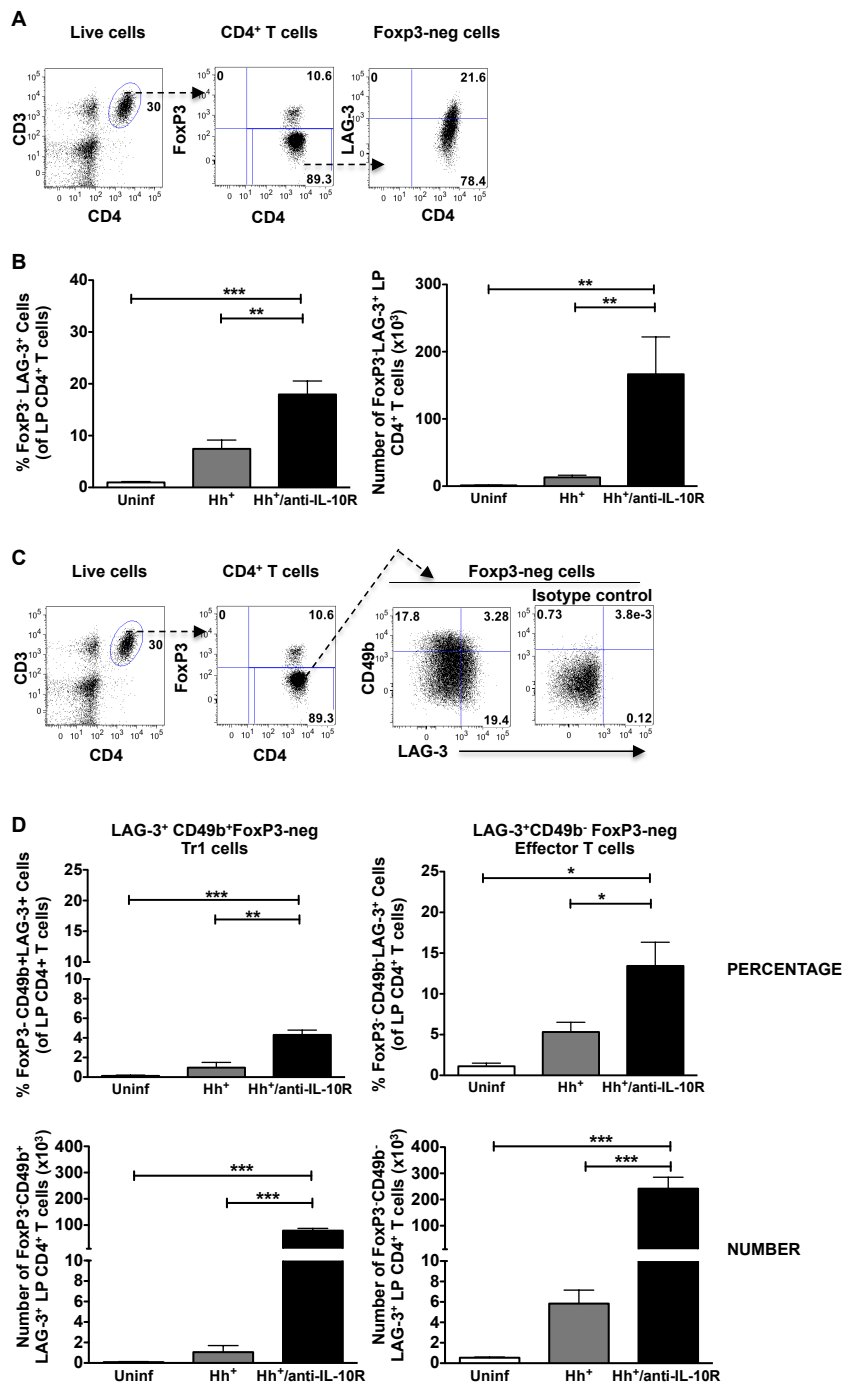
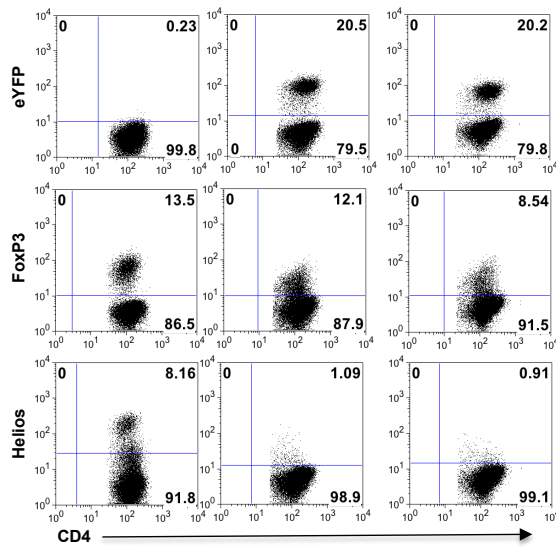


**Figure 5.12 Expression of LAG-3 in FoxP3<sup>-</sup> LP CD4<sup>+</sup> T cells.**

Large intestinal LP cells were isolated from uninfected, *Hh*<sup>+</sup> and *Hh*<sup>+</sup>/anti-IL-10R-treated *Tiger* mice at 2 wks pi. Cells were surface stained with mAb specific for CD3, CD4, LAG-3, CD49b and a live dead exclusion dye, fixed with 2% PFA, permeabilised with eBio perm and then intracellularly stained for Foxp3 and Helios. (A) Gating strategy for the analysis of LAG-3 in the FoxP3<sup>-</sup> LP CD4<sup>+</sup> T cells. (B) Frequency (left panel) and number (right panel) of LAG-3<sup>+</sup> FoxP3<sup>-</sup> LP CD4<sup>+</sup> T cells. Data shown are pooled from three independent experiments. Bars show means + s.e.m of  $n \geq 8$  mice/group in total. (C) Gating strategy for the analysis of LAG-3 and CD49b in the FoxP3<sup>-</sup> LP CD4<sup>+</sup> T cells. (D) Upper panel: Frequency of FoxP3<sup>-</sup> CD49b<sup>+</sup> LAG-3<sup>+</sup> (left panel) and FoxP3<sup>-</sup> CD49b<sup>-</sup> LAG-3<sup>+</sup> (right panel) LP CD4<sup>+</sup> T cells. Lower panel: Number of Frequency of FoxP3<sup>-</sup> CD49b<sup>+</sup> LAG-3<sup>+</sup> (left panel) and FoxP3<sup>-</sup> CD49b<sup>-</sup> LAG-3<sup>+</sup> (right panel) LP CD4<sup>+</sup> T cells. Data shown are pooled from two independent experiments. Bars in (B) and (D) show means + s.e.m of  $n \geq 6$  mice/group in total. \*\* $P < 0.01$  and \*\*\* $P < 0.001$  as determined by one-way Anova.

FIX	eBio Fix-perm 1 hr	2% PFA 1 hr	30 min 2% PFA 30 min eBio Fix
	PERM	eBio Perm 1 hr	eBio Perm 1 hr



FIX	eBio Fix-perm 1 hr	2% PFA 1 hr	2% FA 1 hr
	PERM	eBio Perm 1 hr	eBio Perm 1 hr

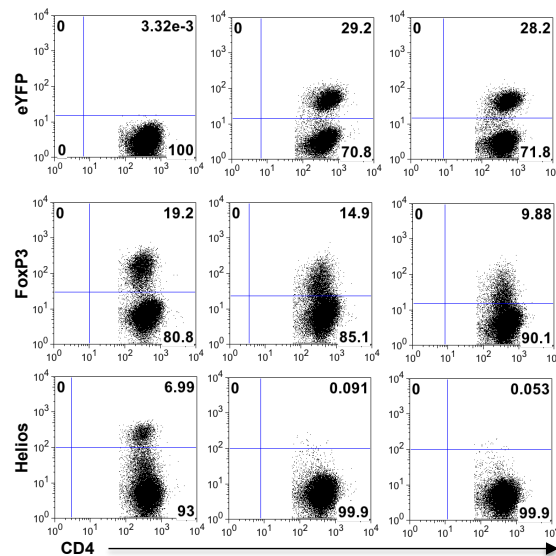


**Figure 5.13 Effect of different fixation protocols on Helios staining.**

*Il17a<sup>cre</sup>R26R<sup>eYFP</sup>* mice were inoculated with *Hh* and treated with anti-IL-10R mAb on days 0 and 7 pi. At 2 wks pi, large intestinal LP cells were isolated, surface stained with mAb specific for CD3 and CD4 and a live dead exclusion dye, fixed and intracellularly stained for FoxP3 and Helios and analysed by flow cytometry. Dot plots in (A) and (B) depict the expression of eYFP, FoxP3 and Helios after the use of different fixatives (as indicated) and are gated on live CD4<sup>+</sup> T cells. Data shown in (A) and (B) are from a single experiment in each case where cells from a single *Il17a<sup>cre</sup>R26R<sup>eYFP</sup>* female mouse were used.

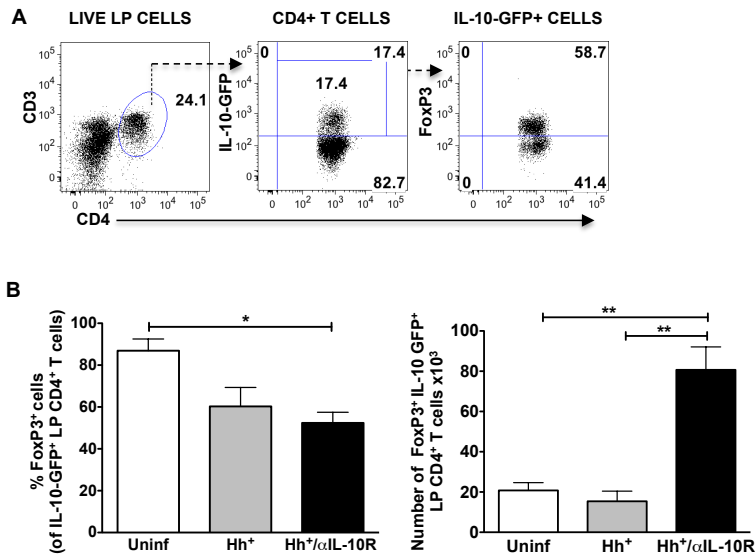


**Figure 5.14 Phenotype of IL-10-producing CD4<sup>+</sup> T cells based on expression of FoxP3.**

LP cells were isolated from the large intestine of uninfected, *Hh*<sup>+</sup> and *Hh*<sup>+</sup>/anti-IL-10R-treated male and female *Tiger* mice at 2 wks pi. The cells were stimulated with PMA and ionomycin in the presence of Brefeldin A and the other half left untreated. The cells were fixed with 2% PFA, surface stained with mAb specific for CD3, CD4 and a live dead exclusion dye, and then permeabilised with eBio perm and intracellularly stained for FoxP3. (A) Dot plots depicting the gating strategy used for the analysis. (B) Frequency (left panel) and number (right panel) of IL-10-GFP<sup>+</sup> FoxP3<sup>+</sup> LP CD4<sup>+</sup> T cells. Data shown are from a single experiment. Bars in (B) show means + s.e.m of n ≥ 3 mice/group in total. \*P<0.01 \*\*P<0.001 and as determined by one-way Anova.

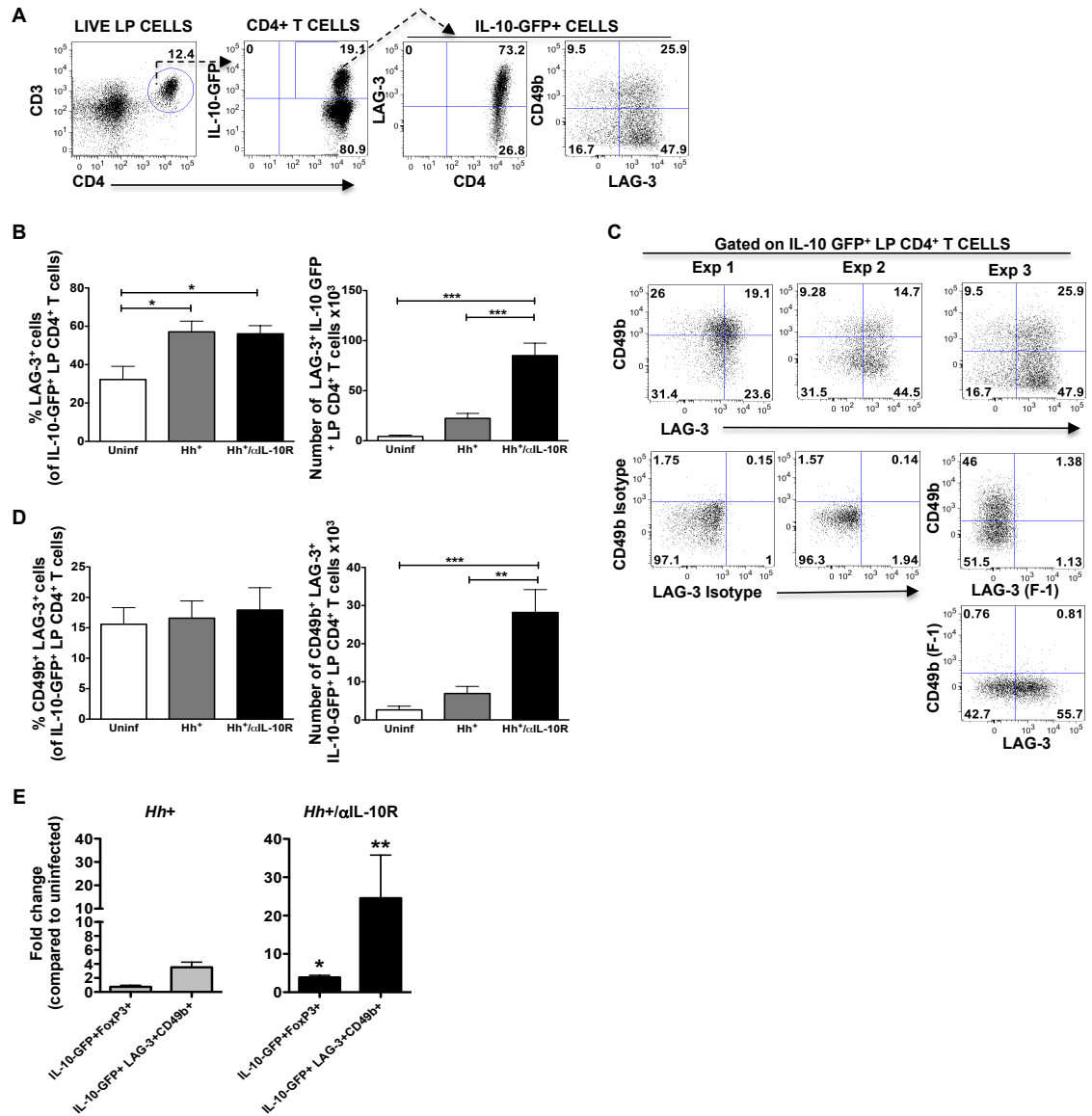


**Figure 5.15 Phenotype of IL-10-producing CD4<sup>+</sup> T cells based on LAG-3 and/or CD49b.** LP cells were isolated from the large intestine of uninfected, *Hh*<sup>+</sup> and *Hh*<sup>+</sup>/anti-IL-10R-treated male and female *Tiger* mice at 2 wks pi. The cells were fixed with 2% PFA, surface stained *ex vivo* with mAb specific for CD3, CD4, CD49b and LAG-3 and a live dead exclusion dye and analysed by flow cytometry. (A) Dot plots depicting the gating strategy used for the analysis of CD49b and LAG-3 expression in IL-10-GFP<sup>+</sup> LP CD4<sup>+</sup> T cells. (B) Frequency (left panel) and number (right panel) of LAG-3<sup>+</sup> IL-10-GFP<sup>+</sup> LP CD4<sup>+</sup> T cells. (C) Dot plots showing representative staining of CD49b and LAG-3 expression. Dot plots shown are from the *Hh*<sup>+</sup> group and are gated on live IL-10-GFP<sup>+</sup> LP CD4<sup>+</sup> T cells. (D) Frequency (left panel) and number (right panel) of CD49b<sup>+</sup> LAG-3<sup>+</sup> IL-10-GFP<sup>+</sup> LP CD4<sup>+</sup> T cells. Data shown in (B) and (D) are pooled from three independent experiments. (E) Fold change of the number of CD4<sup>+</sup> T cells and different subsets of IL-10-GFP expressing cells (as indicated in the figure) in *Hh*<sup>+</sup> mice (left panel) and *Hh*<sup>+</sup>/anti-IL-10R -treated mice (right panel) compared to uninfected controls. Data shown are pooled from three independent experiments. Bars in (B), (D) and (E) show means + s.e.m of n ≥ 8 mice/group in total. \*P<0.01 \*\*P<0.001 and \*\*\*P<0.0001 as determined by one-way Anova for (B) and (D) and Mann-Whitney test for (E).

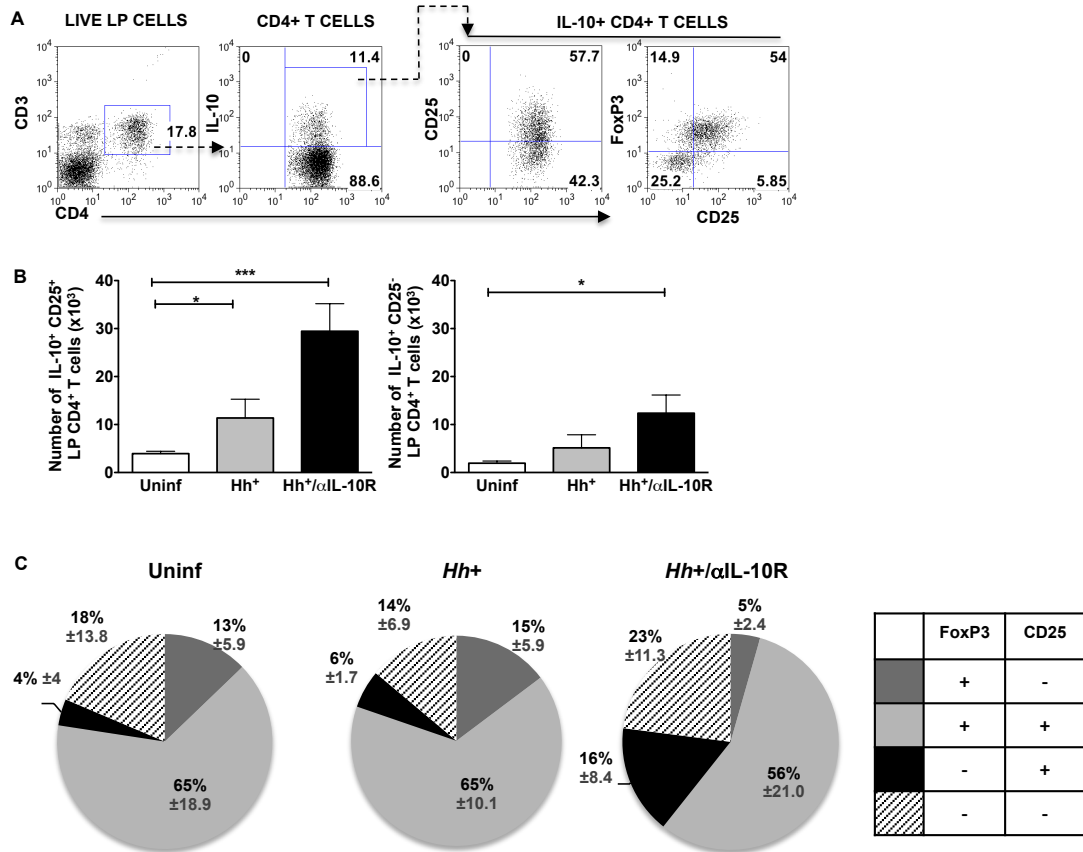


**Figure 5.16** Following infection with *Hh*, the majority of IL-10-producing CD4<sup>+</sup> T cells express CD25.

LP cells were isolated from the large intestine of uninfected, *Hh*<sup>+</sup> and *Hh*<sup>+</sup>/anti-IL-10R-treated female *I117a<sup>cre</sup>R26R<sup>eYFP</sup>* mice at 2 wks pi. The cells were stimulated with PMA and ionomycin in the presence of Brefeldin A. The cells were then surface stained with mAb specific for CD3, CD4, CD25 and a live dead exclusion dye, fixed with 2% PFA, permeabilised with eBio perm buffer and then intracellularly stained for FoxP3. (A) Gating strategy used for the analysis. (B) Graphs depicting the number of LP CD4<sup>+</sup> T cells that are IL-10<sup>+</sup>CD25<sup>+</sup> (left panel) and IL-10<sup>+</sup>CD25<sup>-</sup> (right panel). (C) Distribution of IL-10-producing CD4<sup>+</sup> T cells based on the expression of FoxP3 and/or CD25. Values shown represent average frequencies  $\pm$  standard deviation of  $n \geq 6$  mice/group in total. Data shown in (B) and (C) are pooled from two independent experiments. \* $P < 0.01$  \*\* $P < 0.001$  and \*\*\* $P < 0.0001$  as determined by one-way Anova.

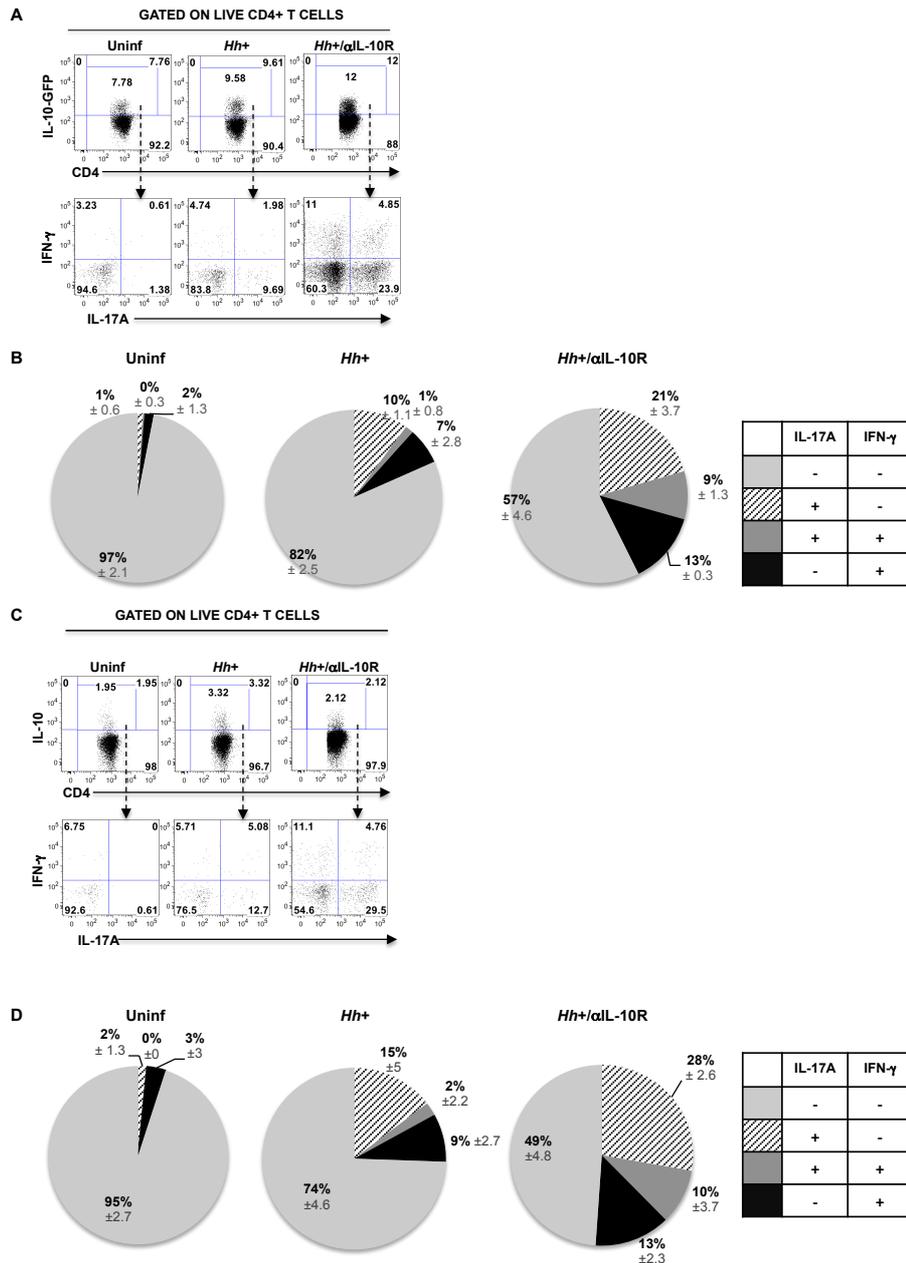


**Figure 5.17** In the colitic setting, there is an expansion of IL-10-producing CD4<sup>+</sup> T cells that co-express IL-17A and/or IFN-γ.

LP cells were isolated from the large intestine of uninfected, *Hh*<sup>+</sup> and *Hh*<sup>+</sup>/anti-IL-10R-treated male and female *Tiger* mice at 2 wks pi and stimulated with PMA and ionomycin in the presence of Brefeldin A. The cells were surface stained with mAb specific for CD3, CD4 and a live dead exclusion dye, fixed with 2% PFA, permeabilised with eBio perm buffer and then intracellularly stained for IL-17A, IFN-γ and IL-10 and analysed by flow cytometry. (A) Dot plots showing representative staining of IL-10-GFP (upper panel) and distribution of IL-10 GFP<sup>+</sup> cells based on co-expression of IL-17A and/or IFN-γ (lower panel) in uninfected, *Hh*<sup>+</sup> and *Hh*<sup>+</sup>/anti-IL-10R-treated *Tiger* mice. Dot plots are gated on live LP CD4<sup>+</sup> T cells. (B) Distribution of IFN-γ and IL-17A expression in each group when gated on LP CD4<sup>+</sup> IL-10-GFP<sup>+</sup> cells. Data shown are representative of one of two experiments. (C) Dot plots showing representative staining of IL-10 detected by ICS (upper panel) and distribution of IL-10<sup>+</sup> cells (detected by ICS) based on co-expression of IL-17A and/or IFN-γ (lower panel) in uninfected, *Hh*<sup>+</sup> and *Hh*<sup>+</sup>/anti-IL-10R-treated *Tiger* mice. Dot plots are gated on live LP CD4<sup>+</sup> T cells. (D) Distribution of IFN-γ and IL-17A expression in each group when gated on LP CD4<sup>+</sup> IL-10<sup>+</sup> cells (detected by ICS). Data shown are from a single experiment. In (B) and (D), figures depict the frequency ± standard deviation of n ≥ 3 mice/group.

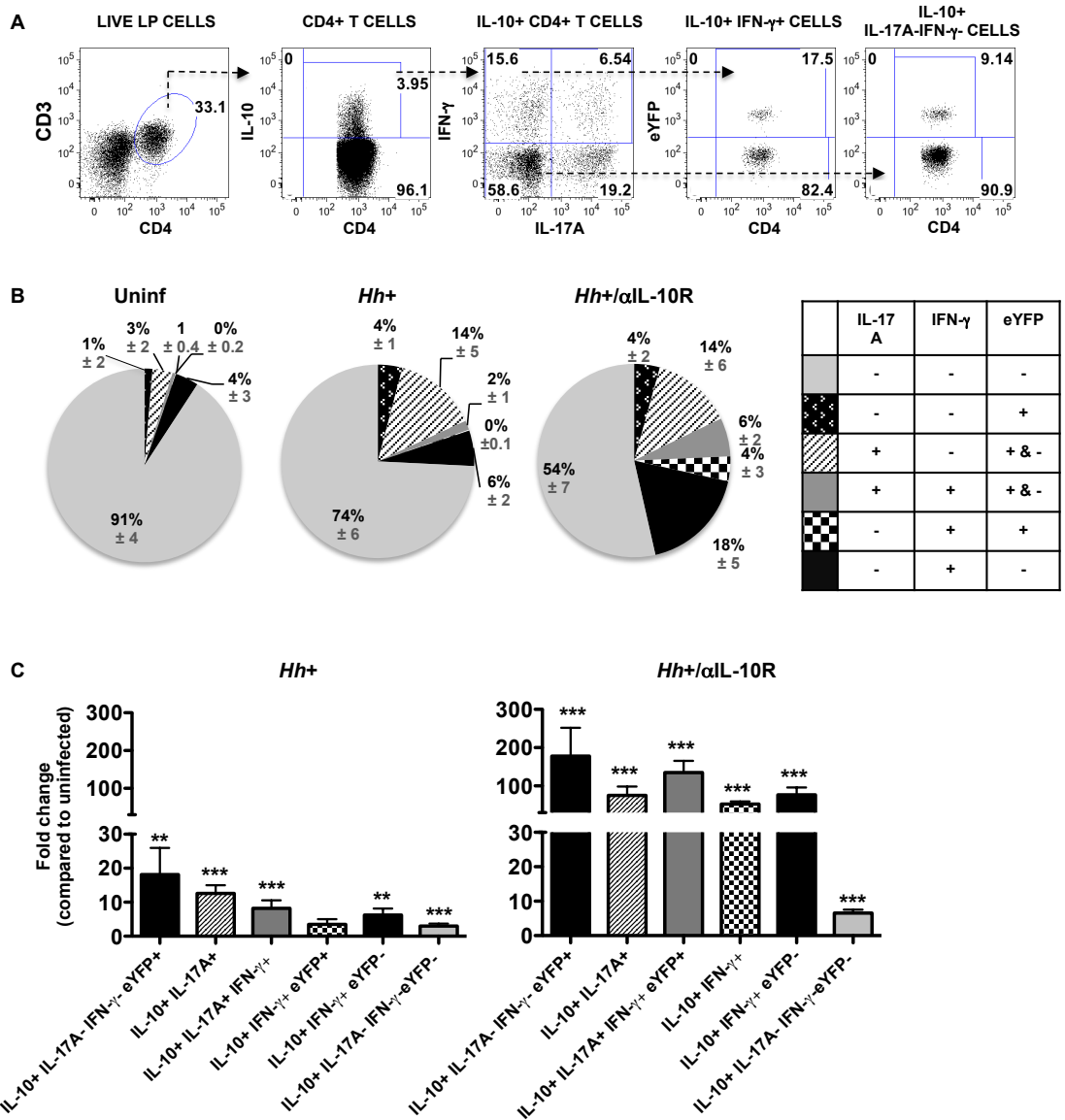


**Figure 5.18** A small proportion of IL-10<sup>+</sup> IFN- $\gamma$ <sup>+</sup> cells in the colitic setting are derived from ex-Th17 cells.

LP cells were isolated from the large intestine of uninfected, *Hh*<sup>+</sup> and *Hh*<sup>+</sup>/anti-IL-10R-treated female *Il17a<sup>cre</sup>R26R<sup>eYFP</sup>* mice at 2 wks pi. The cells were stimulated with PMA and ionomycin in the presence of Brefeldin A. The cells were then surface stained with mAb specific for CD3, CD4, and a live dead exclusion dye, fixed and then intracellularly stained for FoxP3, IL-17A and IFN- $\gamma$ . In one experiment in which the cells were fixed and permeabilised with 2% PFA/0.1% saponin and in the other four experiments, the cells were fixed and permeabilised with 2% PFA/eBio perm. (A) Gating strategy used for the analysis of IL-10-producing CD4<sup>+</sup> T cells that co-express eYFP, IL-17A and/or IFN- $\gamma$ . (B) Distribution of IL-10-producing CD4<sup>+</sup> T cells based on the expression of eYFP, IL-17A and/or IFN- $\gamma$  in the three experimental groups. Data shown are pooled from five independent experiments. Values shown represent average frequencies  $\pm$  standard deviation of  $n \geq 18$  mice/group in total. (C) Fold change of the number of IL-10<sup>+</sup> CD4<sup>+</sup> T cells expressing either eYFP, IL-17A and/or IFN- $\gamma$  (as indicated in the figure) in *Hh*<sup>+</sup> mice (left panel) or *Hh*<sup>+</sup>/anti-IL-10R-treated mice (right panel) when compared to uninfected controls. Data shown are pooled from four independent experiments. Bars show means + s.e.m. of  $n \geq 15$  mice/group in total. \* $P < 0.05$  \*\* $P < 0.01$  and \*\*\* $p < 0.001$  as determined by Mann-Whitney test.

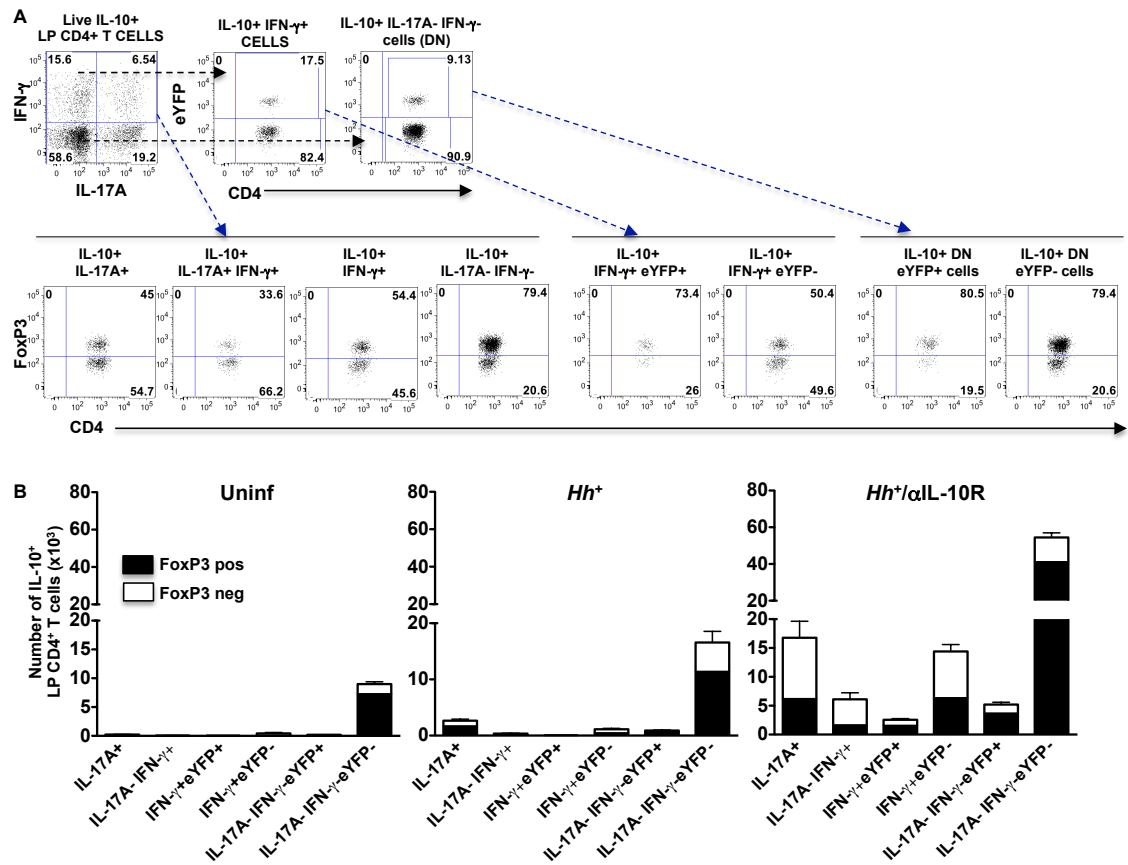


**Figure 5.19 FoxP3 expression in IL-10-producing CD4<sup>+</sup> T cells that co-express IL-17A and/or IFN- $\gamma$ .**

LP cells were isolated from the large intestine of uninfected, *Hh*<sup>+</sup> and *Hh*<sup>+</sup>/anti-IL-10R-treated female *Il17a<sup>cre</sup>R26R<sup>eYFP</sup>* mice at 2 wks pi. The cells were stimulated with PMA and ionomycin in the presence of brefeldin A. The cells were then surface stained with mAb specific for CD3, CD4, and a live dead exclusion dye, fixed with 2% PFA, permeabilised with eBio perm buffer and then intracellularly stained for FoxP3, IL-17A and IFN- $\gamma$ . (A) Gating strategy used for the analysis of FoxP3 expression within each of the IL-10-producing CD4<sup>+</sup> T-cell subsets that co-express eYFP, IL-17A and/or IFN- $\gamma$ . (B) Bars depict the number of FoxP3-positive (filled bars) and FoxP3-negative (open bars) cells in the LP IL-10-producing CD4<sup>+</sup> T cells that co-express eYFP, IL-17A and/or IFN- $\gamma$  in the three experimental groups. Data shown are pooled from three independent experiments. Bars show means + s.e.m of  $n \geq 11$  mice/group in total.

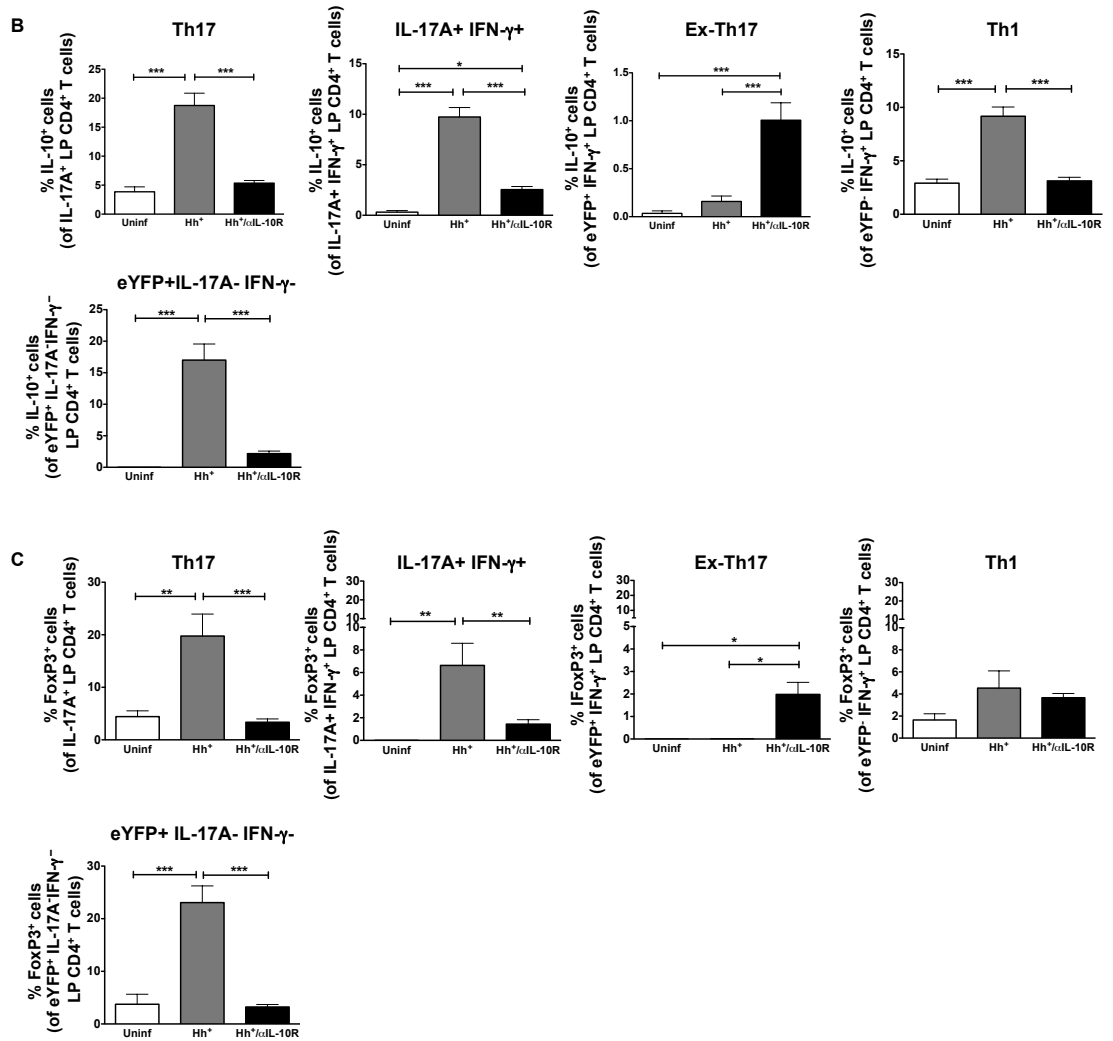
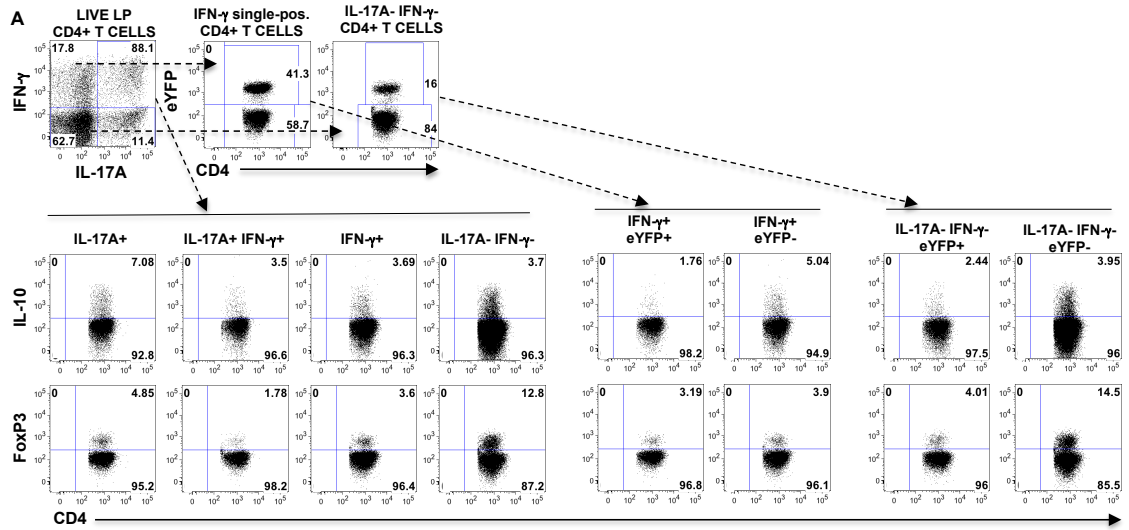
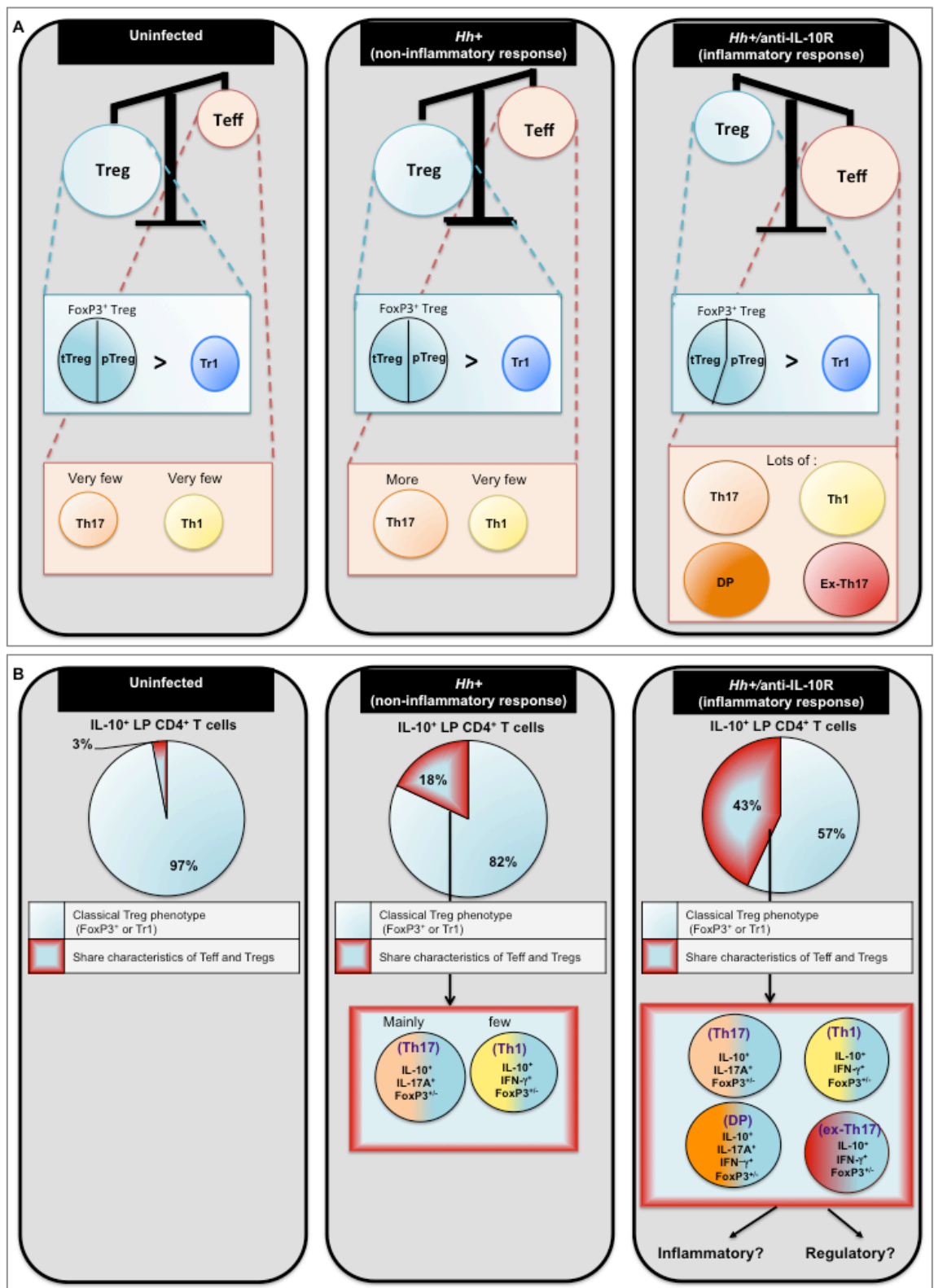


Figure 5.20 A proportion of ex-Th17 cells express IL-10 and FoxP3.

**Figure 5.20. A proportion of ex-Th17 cells express IL-10 and FoxP3.** LP cells were isolated from the large intestine of uninfected, *Hh*<sup>+</sup> and *Hh*<sup>+</sup>/anti-IL-10R-treated female *Il17a<sup>cre</sup>R26R<sup>eYFP</sup>* mice at 2 wks pi. The cells were stimulated with PMA and ionomycin in the presence of Brefeldin A. The cells were then surface stained with mAb specific for CD3, CD4, and a live dead exclusion dye, fixed and then intracellularly stained with mAb specific for FoxP3, IL-17A and IFN- $\gamma$ . (A) Gating strategy used for the analysis of IL-10 and FoxP3 expression in CD4<sup>+</sup> T cell-subsets that express eYFP, IL-17A and/or IFN- $\gamma$ . Frequency of (B) IL-10<sup>+</sup> cells and (C) FoxP3<sup>+</sup> cells in IL-17A<sup>+</sup>, IL-17A<sup>+</sup> IFN- $\gamma$ <sup>+</sup>, IFN- $\gamma$ <sup>+</sup> eYFP<sup>+</sup>, IFN- $\gamma$ <sup>+</sup>eYFP<sup>-</sup> and IL-17A<sup>-</sup> IFN- $\gamma$ <sup>-</sup>eYFP<sup>+</sup> CD4<sup>+</sup> T cells in the three experimental groups. Data shown in (B) are pooled from five independent experiments and data shown in (C) are pooled from three independent experiments. With the exception of one experiment in (B), in which the LP cells were fixed and permeabilised with 2% PFA/0.1% saponin, in all the other experiments in (B) and (C), the LP cells were fixed and permeabilised with the combination of 2% PFA/eBio perm. Bars show mean + s.e.m of  $n \geq 11$  mice/group in total. \*P<0.05 \*\*P<0.01 and \*\*\*P<0.001 as determined by one-way Anova.



**Figure 5.21 Schematic depicting the main findings of chapter 5.**

The balance in the figure depicts the fact that in uninfected and Hh<sup>+</sup> mice, the Treg response dominates over the effector CD4<sup>+</sup> T-cell response. Conversely, in inflamed mice, the effector response dominates over the Treg response. The pale blue box linked by dotted blue lines to the Treg circle on the balance depicts the proportions of different Tregs examined, while the pale orange box linked by dotted orange lines to the Teff circle on the balance depicts the effector T cell populations present in each group. (B) The pie chart depicts the distribution of the IL-10<sup>+</sup> LP CD4<sup>+</sup> T cells in each experimental group as described in the figure. The phenotypic characteristics of the cells that make up the IL-10<sup>+</sup> cells that share characteristic of effector T cells and Tregs are depicted in the blue box with the red border.

## CHAPTER 6. GENERAL DISCUSSION

Intestinal inflammation is thought to occur because of a breakdown in the regulatory mechanisms that keep effector CD4<sup>+</sup> T-cell responses in check. Although previous studies in our lab have extensively characterised the pathogenic effector CD4<sup>+</sup> T-cell response in *Hh* colitis (Morrison et al., 2013), the alteration in regulatory mechanisms is less well understood. The work carried out in this thesis sought to examine whether two types of regulatory mechanisms are altered in colitic mice compared to uninfected controls. At a cell-intrinsic level, we examined whether the profile of microRNAs, which are post-transcriptional gene regulators, are altered at the tissue level and CD4<sup>+</sup> T-cell level in the large intestine of colitic IL-10 KO mice compared to uninfected controls. The anti-inflammatory cytokine IL-10 has been shown to be important for preventing intestinal inflammation in the *Hh* model (Kullberg et al., 2002), as well as other models of colitis (Asseman et al., 1999; Carthew and Sontheimer, 2009) and represents one of the cell-extrinsic mechanisms of keeping pathogenic immune responses in check. Furthermore, we have also shown previously that priming with *Hh* is necessary to generate disease-protective IL-10<sup>+</sup> cells as Tregs from *Hh*<sup>+</sup> WT but not uninfected WT mice were able to protect RAG KO mice from developing colitis upon co-transfer with naïve CD4<sup>+</sup> T cells (Kullberg et al., 2002). Although previous work in the lab has shown that protection against *Hh*-induced inflammation is dependent on IL-10, the phenotype of these cells has not been examined before. Here, we examined the phenotype of IL-10<sup>+</sup> CD4<sup>+</sup> T cells in a non-inflammatory and an inflammatory immune response to *Hh* to determine whether these cells exhibit an altered phenotype in the colitic setting. Briefly, the work carried out in this thesis has shown that the profile of microRNAs and IL-10<sup>+</sup> CD4<sup>+</sup> T cells is markedly altered in the colitic setting suggesting that the alteration observed in both these regulatory mechanisms may play a role in driving the inflammatory response.

In Chapter 4, we focused on examining microRNA expression in the large intestine of *Hh*<sup>+</sup> IL-10 KO mice and compared it to that of uninfected controls. Although differential microRNA expression has been observed in tissues from humans with active UC or CD compared to healthy controls (Wu et al., 2011; Wu et al., 2010; Wu et al., 2008), and altered microRNA expression has been shown to potentiate colitis in several animal models of colitis (Brain et al., 2013; Koukos et al., 2013; Xue et al., 2011; Zhang et al., 2010), the role of microRNAs in *Hh*-induced colitis has not been examined before. The current study revealed that microRNAs are differentially expressed at the tissue-level and CD4<sup>+</sup> T-cell level in colitic mice compared to uninfected controls. Kinetic examination of microRNA expression at the tissue level revealed that the change in expression of microRNAs coincided with the development of intestinal inflammation. We next profiled microRNA expression by means of a microRNA microarray in LP CD4<sup>+</sup> T cells. To our knowledge, this is the first time microRNAs have been profiled on ex vivo isolated LP CD4<sup>+</sup> T cells in any colitis model. The microarray

revealed that two microRNAs (miR-21a and miR-31) were significantly up-regulated and seven microRNAs (miR-181a, miR-125a, miR-125b, miR-30a, miR-192, miR-467c and miR-139) were significantly down-regulated in LP CD4<sup>+</sup> T cells from 2-wk *Hh*<sup>+</sup> IL-10 KO mice compared to uninfected controls. A further 105 microRNAs showed a fold change greater than two in LP CD4<sup>+</sup> T cells from 2-wk *Hh*<sup>+</sup> IL-10 KO mice compared to uninfected controls of which miR-210 and miR-96 showed the greatest fold increase. The differential expression of microRNAs in inflamed tissue and in LP CD4<sup>+</sup> T cells from colitic mice compared to those from uninfected controls suggests the possibility of a change in microRNA expression modulating the inflammatory response in *Hh* colitis, and perhaps potentiating pathology through excessive suppression (in case of up-regulated microRNAs) or loss of suppression (in case of down-regulated microRNAs) of their target mRNAs. From the microRNAs identified from the microarray, we examined the expression of miR-21a, miR-31, miR-210, miR-96 and miR-181a further and found that compared to naïve CD4<sup>+</sup> T cells, miR-21a, miR-31, miR-210 and miR-96 were up-regulated and miR-181a was down-regulated in *in vitro* polarized Th1 and Th17 cells. A number of predicted and experimentally validated mRNA targets of these microRNAs were identified whose microRNA-mediated change in expression could potentiate the inflammatory CD4<sup>+</sup> T cell response in *Hh* colitis. Of these predicted and experimentally validated mRNA targets, the most promising targets to investigate further, in my opinion, are miR-31 predicted target Twist 1, miR-31 and miR-210 validated target FoxP3 and the experimentally validated target for miR-21 but predicted target for miR-181a, Smad7.

In the current study, we found that miR-31 was progressively up-regulated in *in vitro* polarized Th1 and Th17 cells following activation with anti-CD3. If Twist 1 proves to be a target of miR-31, miR-31-mediated repression of Twist 1 could augment the Th1, Th17 and perhaps the ex-Th17 response in a number of ways. Twist 1 is a transcriptional repressor that prevents the expression of IFN- $\gamma$ , TNF $\alpha$  and IL-2 by Th1 cells (Niesner et al., 2008). Twist 1 prevents T-bet and Runx3 from binding to the *Ifng* locus and prevents IFN- $\gamma$  production (Pham et al., 2012). Twist 1 also limits Th17 development by directly repressing IL-6R $\alpha$  (Pham et al., 2013). Given the current knowledge of the role of Twist 1, it is tempting to speculate that increased miR-31 expression suppresses Twist 1 and allows expression of IFN- $\gamma$ . Whether Twist 1 is also important for IFN- $\gamma$  expression by ex-Th17 cells remains to be seen.

FoxP3 is a validated target of both miR-31 and miR-210 (Rouas et al., 2009; Zhao et al., 2014). Given that FoxP3 is necessary for the suppressive capacity of Tregs (Fontenot et al., 2003; Khattry et al., 2003), overexpression of both miR-31 and miR-210 in the colitic setting might result in decreased FoxP3 expression and thus a decrease in the suppressive capacity of the Tregs.

Smad7 is a validated target of miR-21 but a predicted target of miR-181a. In the current study, we saw an up-regulation of miR-21 and a down-regulation of miR-181a in LP CD4<sup>+</sup> T

cells from 2-wk *Hh*<sup>+</sup> IL-10 KO mice compared to those from uninfected controls. Thus it is unclear whether Smad7 expression is suppressed due to increased miR-21a levels or whether it is overexpressed due to decreased miR-181a levels. It might also be that loss of miR-181a-mediated suppression of Smad7 might be partially or completely compensated by miR-21-mediated suppression of Smad7. Smad7 itself plays a very important role in IBD and colitis, where inhibition of Smad7 was found to ameliorate disease (Boirivant et al., 2006; Fantini et al., 2009). Smad7 is found to be highly up-regulated in patients with CD, and high Smad7 expression makes effector CD4<sup>+</sup> T cells resistant to suppression by Tregs (Fantini et al., 2009). Blocking Smad7 expression in CD4<sup>+</sup> T cells dramatically improved disease in TNBS and oxazolone colitis but not T cell transfer colitis (Boirivant et al., 2006) and antisense nucleotides targeting Smad7 are currently in clinical trials for treatment of CD (Monteleone et al., 2012). In contrast to its role in colitis, in EAE, miR-21-mediated knockdown of Smad7 promoted Th17 differentiation and potentiated disease (Murugaiyan et al., 2015).

To examine whether miR-31, miR-21a, miR-210 and miR-181a and their predicted/validated targets play any role in augmenting the pathogenic Th1 and Th17 response in *Hh* colitis, it would be necessary to first examine whether predicted targets Smad7 and Twist 1 are actually targets of miR-181a and miR-31 respectively by doing a luciferase assay to determine whether miR-181a and miR-31 are able to bind to Smad7 and Twist 1 and inhibit their expression. In a luciferase assay, the 3' UTR of the mRNA of interest is cloned immediately downstream of luciferase (*Photinus* or *Renilla*) contained in the reporter plasmid (Jin et al., 2013; Kuhn et al., 2008). The reporter plasmid and miRNA of interest are then transfected into a cell line such as HeLa cell or Jurkat cell and luciferase activity measured after 24-48 hrs (Jin et al., 2013; Kuhn et al., 2008). A decrease in luciferase activity implies that the microRNA has bound to its mRNA target and prevented luciferase protein expression (Jin et al., 2013; Kuhn et al., 2008). The luciferase assay only verifies whether a microRNA can bind to its mRNA target, not whether this miR/mRNA interaction actually takes place in the cell of interest (in our case CD4<sup>+</sup> T cells). Therefore, once a particular mRNA is validated as a target of a given microRNA, *in vitro* proof of principle studies can be carried out whereby the effect of overexpressing or inhibiting a microRNA on its target mRNA expression can be examined. Naïve CD4<sup>+</sup> T cells can be transfected with microRNA mimics/inhibitors and then polarized to a Th1, Th17 or iTreg phenotype and the effect of microRNA overexpression or inhibition on its target mRNA expression, phenotype of the cell and cytokine production examined.

Based on the results of the *in vitro* studies, *in vivo* studies could then be carried out to determine whether altering microRNA expression levels has any functional effect on disease severity in *Hh*-induced colitis. For microRNAs that were overexpressed in LP CD4<sup>+</sup> T cells from 2-wk *Hh*<sup>+</sup> IL-10 KO compared to uninfected controls, i.e. miR-21a, miR-31 and miR-210, the functional effect of these microRNAs on *Hh* colitis would be assessed by silencing them. There are three methods that are currently used to carry out *in vivo* studies to deplete

microRNAs: i) MicroRNA sponges (Ebert and Sharp, 2010), ii) Anti-sense oligonucleotides (Stenvang et al., 2012) and iii) Genetic knockouts (Stenvang et al., 2012). MicroRNA sponges are designed to act as decoy targets for a particular microRNA of interest and in essence deplete the microRNA by ‘soaking it up’ (Ebert and Sharp, 2010). Anti-sense oligonucleotides bind to the microRNA and prevent it from binding to its target mRNA (Stenvang et al., 2012). Finally, genetic knockouts can be generated for a particular microRNA (Stenvang et al., 2012). If possible, my preference would be to use genetically modified mice for the microRNAs that were overexpressed i.e. miR-31, miR-21a and miR-210, primarily because genetic knockouts ensure complete deletion of the microRNA of interest (Stenvang et al., 2012). In contrast, antisense oligonucleotides and sponges do not achieve complete depletion of the microRNA of interest and it is unclear how effective they are for long-term depletion of a microRNA (Ebert and Sharp, 2010; Stenvang et al., 2012). Thus by breeding mice that conditionally knockout miR-31, miR-21a or miR-210 in CD4<sup>+</sup> T cells alone, and infecting these mice with *Hh* and concomitantly treating them anti-IL-10R, the effect of these microRNAs on the CD4<sup>+</sup> T-cell response, and on disease severity in *Hh* colitis could be assessed *in vivo*. We know from previous work in the lab that transfer of naïve CD4<sup>+</sup> T cells from uninfected WT mice into *Hh*<sup>+</sup> RAG KO mice results in intestinal inflammation (Kullberg et al., 2002). This model of *Hh* colitis could also be used to assess the effect of the miRNA/mRNA pathway *in vivo* by sorting naïve CD45RB<sup>high</sup> CD4<sup>+</sup> T cells from miR-31 KO and miR-210 KO mice and adoptively transferring them into *Hh*<sup>+</sup> RAG KO. This would not only enable us to assess effect of knocking out of these microRNAs on colitis severity, but also whether CD4<sup>+</sup> T cells deficient in miR-31, miR-21 or miR-210 are defective in their ability to develop into Th1 and Th17 cells.

For microRNAs that were down-regulated in LP CD4<sup>+</sup> T cells from 2-wk *Hh*<sup>+</sup> IL-10 KO compared to uninfected controls, i.e. miR-181a, the functional effect of these microRNAs on *Hh* colitis would be assessed by overexpressing them. To do so, naïve CD4<sup>+</sup> T cells could be sorted from uninfected IL-10 KO mice, transfected with synthetic miR-181a mimics, and transferred into *Hh*<sup>+</sup> RAG KO mice to determine the effect of overexpressing miR-181a levels on colitis severity and on the development of the Th1 and Th17 cells.

The experiments carried out in chapter 4 have provided very promising early results for future projects examining the roles that the microRNAs that were differentially expressed in LP CD4<sup>+</sup> T cells isolated from colitic mice compared to uninfected controls play in modulating the CD4<sup>+</sup> T-cell response during intestinal inflammation. Further delineation of the mRNA targets of these microRNAs, and examining whether these targets have any functional role in disease pathogenesis will help to shed more light on the molecular mechanisms underlying the pathogenesis of intestinal inflammation and will hopefully also identify potential novel therapeutic strategies to treat intestinal inflammation. With a number of microRNAs now emerging as biomarkers and being tested in clinical trials for use as therapeutic agents (Alevizos and Illei, 2010; Dong et al., 2014; Guay and Regazzi, 2013; van Rooij et al., 2012), the potential

clinical significance of microRNAs in CD, a disease which currently has few effective treatments, is important and needs to be examined further.

In Chapter 5, we focused on examining the phenotype of IL-10-producing CD4<sup>+</sup> T cells in the large intestine LP in a non-inflammatory immune response seen in *Hh*<sup>+</sup> mice and an inflammatory immune response seen in *Hh*<sup>+</sup>/anti-IL-10R-treated mice. Our key finding was that in uninfected mice and mice exhibiting a non-inflammatory immune response to *Hh*, most of the IL-10-producing CD4<sup>+</sup> T cells were of a purely Treg phenotype whereas in the colitic setting, almost half the IL-10-producing CD4<sup>+</sup> T cells shared phenotypic characteristics of effector T cells (co-expressed IL-17A and/or IFN- $\gamma$ ) and regulatory T cells (expressed FoxP3). Furthermore, we also show in this study for the first time, that a small proportion of ex-Th17 cells produce IL-10 and express FoxP3. Although IL-10<sup>+</sup> cells that share effector and regulatory cell phenotypes have been observed in different diseases including human CD and murine colitis models, this study shows for the first time the extent to which these cells constitute the total IL-10<sup>+</sup> CD4<sup>+</sup> T-cell pool during colitis. These findings raise three important questions; 1) How does the phenotype of IL-10-producing LP CD4<sup>+</sup> T cells change over time 2) Are the IL-10<sup>+</sup> CD4<sup>+</sup> T cells that share characteristics of regulatory and inflammatory cells pathogenic or protective, and 3) Do these cells originate from an effector T cell or a regulatory T cell. The implications of the answers to these questions and the experiments that could be done to address them have been expanded upon in the next few paragraphs.

### **1) How does the phenotype of IL-10<sup>+</sup> CD4<sup>+</sup> T cells change over time?**

In the current study, in both *Hh*<sup>+</sup> and *Hh*<sup>+</sup>/anti-IL-10R-treated mice, the phenotype of IL-10-producing LP CD4<sup>+</sup> T cells was only examined at 2 wks pi and seemed to mirror, at much smaller frequencies, the phenotype effector CD4<sup>+</sup> T cells subsets that were present in that particular experimental group at this timepoint (with the exception that some of the IL-10<sup>+</sup> cells also expressed FoxP3). This finding suggests that there is a possibility that there are specialised Treg subsets that evolve alongside the effector T cells that keep them in check. We know from previous work in the lab, that *Hh*-induced inflammation peaks at 2wks pi and resolves at about 14 wks pi and during the resolution of inflammation, the frequencies of IFN- $\gamma$ <sup>+</sup> and IL-17A<sup>+</sup>IFN- $\gamma$ <sup>+</sup> LP CD4<sup>+</sup> T cells decrease but the frequency of Th17 cells increase (Morrison et al., 2013). A recent study showed that small intestinal Th17 cells have been shown to change phenotype to become Tr1<sup>ex-Th17</sup> cells that primarily secrete IL-10 during the resolution of inflammation (Gagliani et al., 2015). Thus it would be interesting to examine whether the skewing of the immune response to a Th17 response at the later stages of *Hh*-infection that we have previously observed is accompanied by a phenotype shift to become IL-17A<sup>+</sup> IL-10<sup>+</sup> FoxP3<sup>+/-</sup> cells phenotype rather than an ex-Th17 cell phenotype, and if this shift might play a role in the resolution of the *Hh*-induced intestinal inflammation (**Figure 6.1**). To examine whether this is the case, a kinetic study could be done to examine whether the phenotype of IL-

IL-10-producing CD4<sup>+</sup> T cells follows a similar change in expression pattern as the effector CD4<sup>+</sup> T cells over time in uninfected, *Hh*<sup>+</sup> and *Hh*<sup>+</sup>/anti-IL-10R-treated IL-17A-eYFP mice, and whether, during the resolution of *Hh*-induced intestinal inflammation, the Th17/Th17 IL-10<sup>+</sup> FoxP3<sup>+</sup> switch dominates over the Th17/ex-Th17 switch.

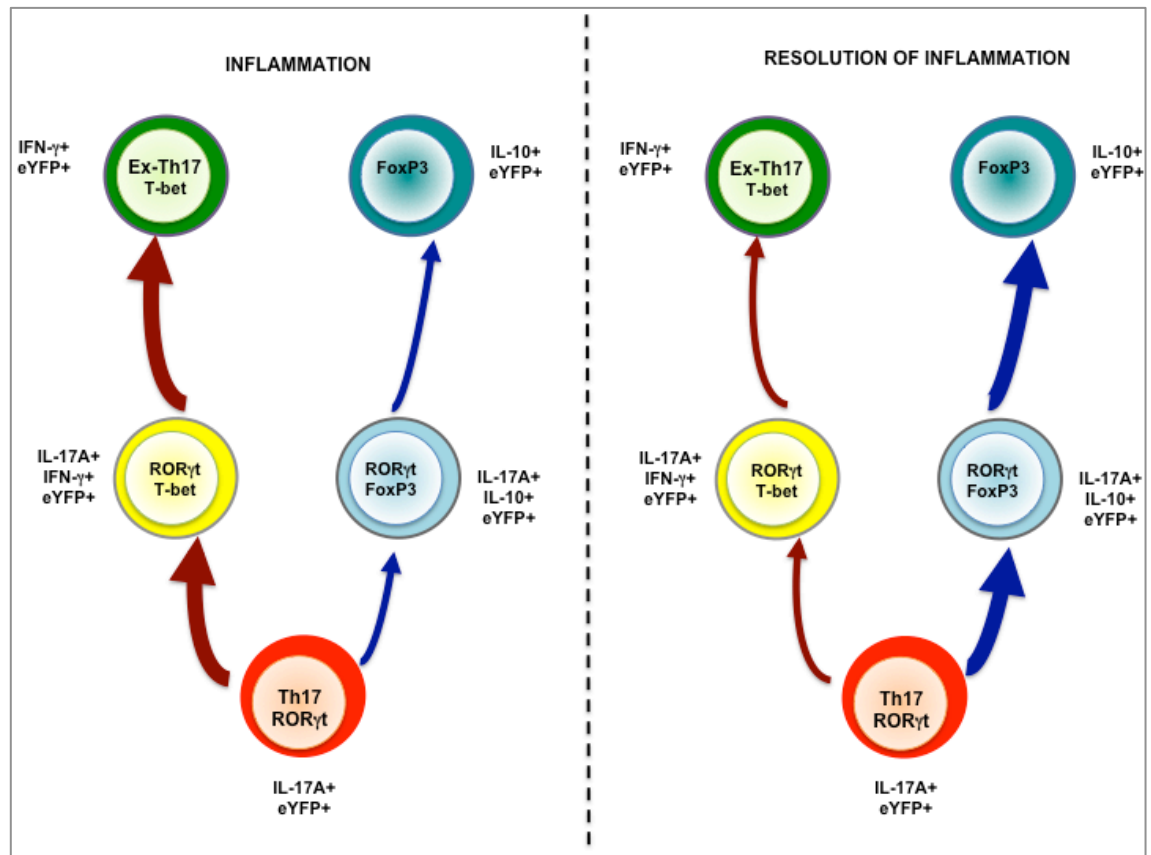


**Figure 6.1 Th17-phenotype shifting during inflammation and the resolution of inflammation.**

The figure depicts the hypothesis that during inflammation, the Th17 to ex-Th17 pathway dominates (indicated by thick red arrows) whereas during the resolution of inflammation, the Th17 to a FoxP3<sup>+</sup> Treg phenotype might dominate (indicated by thick blue arrows).

**2) Are the IL-10<sup>+</sup> CD4<sup>+</sup> T cells that share characteristics of regulatory and inflammatory cells pathogenic or protective?**

Another question that needs to be addressed is whether the IL-10-producing CD4<sup>+</sup> T cells that co-express inflammatory cytokines are protective or pathogenic. Similar to the phenotype of cells we observed in *Hh*<sup>+</sup> and *Hh*<sup>+</sup>/anti-IL-10R-treated mice, IL-17A<sup>+</sup>IL-10<sup>+</sup> FoxP3<sup>-</sup> (Esplugues et al., 2011) and IL-17A<sup>+</sup> FoxP3<sup>+</sup> (Hovhannisyanyan et al., 2011) cells have been isolated from the LP of patients with active CD. Although the IL-17A<sup>+</sup>IL-10<sup>+</sup> FoxP3<sup>-</sup> (Esplugues et al., 2011) and IL-17A<sup>+</sup> FoxP3<sup>+</sup> (Hovhannisyanyan et al., 2011) examined in humans suffering from CD were suppressive in nature, it is unclear whether the IL-10-producing CD4<sup>+</sup> T cells that co-express inflammatory cytokines that we observed in *Hh*<sup>+</sup> and *Hh*<sup>+</sup>/anti-IL-10R-treated mice are suppressive or inflammatory. *In vitro* and *in vivo* suppression assays could be used to address this question. For both assays, IL-10-producing CD4<sup>+</sup> T cells that co-express IL-17A and/or IFN-γ can be sorted either by means of triple reporter mice that are FoxP3-RFP, IL-10-GFP and

either IFN- $\gamma$  or IL-17A-eYFP, or by means of a cytokine secretion assay that we have previously used to sort like IFN- $\gamma^+$ , IL-17A<sup>+</sup>IFN- $\gamma^+$  and IL-17A<sup>+</sup> cells (Morrison et al., 2013). *In vitro* suppression assays would involve labelling responder CD4<sup>+</sup> T cells (CD4<sup>+</sup>CD25<sup>-</sup>), with a dye such as CellTrace Violet (CTV) and culturing the CTV-labelled cells alone or in combination with the IL-10-producing CD4<sup>+</sup> T cells that co-express IL-17A and/or IFN- $\gamma$ . Following stimulation with anti-CD3/anti-CD28 for 3 days, the ability of the IL-10-producing CD4<sup>+</sup> T cells that co-express IL-17A and/or IFN- $\gamma$  to limit the proliferation of responder cells could be examined by flow cytometry using the dilution of CTV signal as a read out of proliferative capacity. To examine whether the IL-10-producing CD4<sup>+</sup> T cells that co-express IL-17A and/or IFN- $\gamma$  are pathogenic, these cells could be sorted from *Hh*<sup>+</sup>/anti-IL-10R-treated WT mice, transferred into *Hh*<sup>+</sup> RAG KO mice and the effect on colitis development determined.

### **3) Do the IL-10<sup>+</sup> CD4<sup>+</sup> T cells that share characteristics of effector and regulatory cells originate from effector T cells or regulatory T cells?**

Finally, and perhaps the more difficult question to address is the origin of the IL-10-producing CD4<sup>+</sup> T cells that co-express IL-17A and/or IFN- $\gamma$  that we observed in *Hh*<sup>+</sup> and *Hh*<sup>+</sup>/anti-IL-10R-treated mice. These cells could arise from i) effector T cells, ii) FoxP3<sup>+</sup> Tregs and/or Tr1 cells, iii) represent a hybrid Treg/effector subset that differentiates directly from naive CD4<sup>+</sup> T cells or iv) a combination of two or more of these scenarios. The fact that the phenotype of the IL-10<sup>+</sup>FoxP3<sup>+/-</sup> CD4<sup>+</sup> T cells that co-express IL-17A and/or IFN- $\gamma$  seem to mirror, at smaller frequencies, the effector T cells that expand in that particular experimental group, seems to suggest that perhaps these cells originate from effector T cells. However, in the literature, aside from one study which showed that during the resolution of inflammation, small intestinal Th17 cells have been shown to transdifferentiate into Tr1-like regulatory T cells (Gagliani et al., 2015), most studies suggest that IL-10-producing CD4<sup>+</sup> T cells that co-express IL-17A and/or IFN- $\gamma$  might arise from FoxP3<sup>+</sup> Tregs or Tr1 cells. Although Tr1 cells primarily produce IL-10, they have been shown to produce small amount of IL-17A and variable amount of IFN- $\gamma$  (Gagliani et al., 2013; Roncarolo et al., 2011). In all the studies where FoxP3 was co-expressed with Th1 or Th17 signature cytokines or transcription factors, these cells originally arose from Foxp3<sup>+</sup> Tregs (Feng et al., 2011a; Koch et al., 2009; Komatsu et al., 2014; McPherson et al., 2015). FoxP3<sup>+</sup> cells have been shown to start producing IFN- $\gamma$  during the induction of intestinal inflammation in a microbiota-dependent colitis model and these cells were suppressive in nature (Feng et al., 2011b). In the EAE model, FoxP3<sup>+</sup> Tregs were shown to start expressing T-bet, which in turn enabled them to express CXCR3 and accumulate at the same site as Th1 cells to suppress them (Koch et al., 2009). In autoimmune arthritis, fate mapping of FoxP3<sup>+</sup> Tregs showed that these cells transdifferentiate to become pathogenic Th17 cells, and that FoxP3<sup>+</sup> IL-17A<sup>+</sup> cells may represent an intermediate phenotype of these cells

(Komatsu et al., 2014). One study showed that when highly purified FoxP3<sup>+</sup> Tregs were cultured in the presence of anti-CD3/CD28 and IL-1 $\beta$  and IL-2, it resulted in a significant proportion of these cells secreting IL-17A, and these IL-17A<sup>+</sup> FoxP3<sup>+</sup> cells were termed Tr17 cells (Li et al., 2012). Tr17 cells were found to express similar levels of FoxP3, CTLA-4 and GITR to FoxP3<sup>+</sup> IL-17<sup>-</sup> Tregs (Li et al., 2012). In contrast to FoxP3<sup>+</sup> IL-17<sup>-</sup> Tregs, the Tr17 cells expressed significantly higher levels of ICOS, Runx1 and Runx3 (Li et al., 2012). Runx1 is reportedly important for the sustained expression of FoxP3 and IL-17A in the Tr17 cells and Runx3 enables the Tr17 cells to express higher levels of perforin and Granzyme B (Li et al., 2012). Interestingly, Runx1 and Runx3 are also required for the generation of IFN- $\gamma$ -producing ex-Th17 cells (Wang et al., 2014d). In the current study, if the IL-10<sup>+</sup> IL-17A<sup>+</sup> FoxP3<sup>+</sup> cells observed in *Hh*<sup>+</sup> and *Hh*<sup>+</sup>/anti-IL-10R-treated mice are actually Tr17 cells, it might be that in the colitic setting, whatever stimuli trigger Runx1 and Runx3 expression in Th17 cells and cause them to change phenotype to become ex-Th17 cells, might trigger a similar switch in IL-10<sup>+</sup> IL-17A<sup>+</sup> FoxP3<sup>+</sup> Tr17 cells and enable them to switch alongside the effector T cells and thus express similar cytokines (**Figure 6.2**). Further analysis of GITR, CTLA-4 and ICOS in the IL-10-producing CD4<sup>+</sup> T cells that co-express FoxP3 and IFN- $\gamma$  and/or IL-17A will give us further insight into whether these cells resemble the Tr17 cells and in fact constitute a Treg population rather than an effector T cell population.

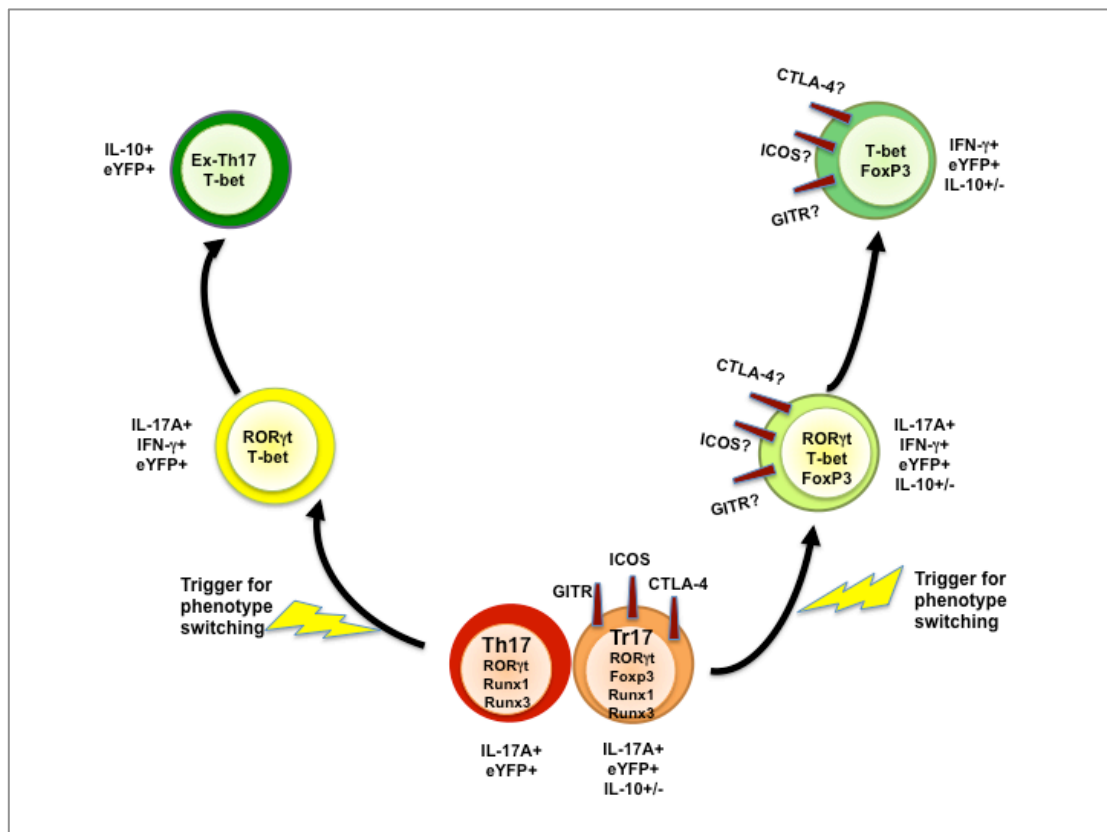


**Figure 6.2 Cartoon depicting hypothesis that Tr17 and Th17 cells switch alongside each other during *Hh*-induced intestinal inflammation.**

The schematic depicts the hypothesis that during *Hh*-induced colitis, Tr17 cells, and Th17 cells switch alongside each other. Tr17 cells are regulatory cells that resemble effector Th17 cells in that they express ROR $\gamma$ t and Runx1 and Runx3, but differ from Th17 cells in that they express regulatory-cell associated factors like FoxP3, ICOS, GITR and CTLA-4 (Li et al., 2012). Since the induction of Runx1 and Runx3 has been shown to trigger Th17 phenotype shifting to an ex-Th17 phenotype (Wang et al., 2014d), it is plausible that if Tr17 cells are present during *Hh*-induced colitis, that these Runx1 and Runx3-expressing cells might switch alongside the Th17 cells, resulting in a regulatory cell population that phenotypically expresses similar cytokines and transcription factors to the effector T cells present, but at the same time, also expresses regulatory-cell associated cytokines and transcription factors such as IL-10 and FoxP3.

To determine whether FoxP3<sup>+</sup> Tregs become pathogenic effector T cells during *Hh*-induced colitis, FoxP3 reporter mice such as those used by Komatsu et al, can be infected with *Hh* and concomitantly treated with anti-IL-10R and analysing the expression of IFN- $\gamma$ , IL-17A and IL-10 at different time points pi with *Hh* by flow cytometry. Komatsu et al bred a FoxP3 reporter mouse by crossing *Foxp3* bacterial artificial chromosome transgenic mice expressing the GFP-Cre recombinase fusion protein with ROSA26-YFP reporter mice to generate a mouse in which cells that are expressing or previously expressed FoxP3 are permanently labelled with YFP, whereas those currently expressing FoxP3 are labelled with GFP (Komatsu et al., 2014). Thus ex-Foxp3<sup>+</sup> cells will be GFP<sup>-</sup> YFP<sup>+</sup>, enabling one to identify whether the ex-FoxP3 cells (if any) express inflammatory cytokines. To determine whether effector T cells have the potential to become Treg-like, one could use triple reporter mice that are IL-10-GFP, FoxP3-RFP and IL-17A or IFN- $\gamma$ -RFP such as those used by Gagliani et al (Gagliani et al., 2015). Different effector T-cell subsets that are negative for FoxP3 and IL-10 could be sorted from *Hh*<sup>+</sup>/anti-IL-10R-

treated triple reporter mice and adoptively transferred into *Hh*<sup>+</sup> RAG KO mice to determine whether these cells start expressing IL-10 and/or FoxP3.

### **Importance of the findings of this thesis to the IBD field**

IBD is a complex group of diseases that is caused by a mix of genetic and environmental factors. This infers that the underlying trigger factors for development of IBD are different in each individual, and therefore it is not a disease where one treatment will fit all the cases. Indeed, this is illustrated by the fact that a third of patients remain refractory to TNF- $\alpha$  treatment and that treatment with recombinant IL-10 is only efficacious in patients who had a defect in IL-10 production. The current understanding is that IBD occurs either because of a breakdown in the regulatory mechanisms that keep immune cells in check, or because effector T cells become resistant to the suppressive effects of the Tregs or a combination of both these factors. Thus understanding the roles that different regulatory mechanisms play in modulating the inflammatory response might lead to the development of new therapies. For example, one of the findings of the work in this thesis was that miR-21, miR-31 and miR-210 were significantly increased in LP CD4<sup>+</sup> T cells from colitic mice compared to uninfected controls. It is plausible that these microRNAs work in concert to promote the inflammatory T-cell response by rendering effector T cells refractory to Treg suppression and inhibiting the Treg response itself. Both miR-31 and miR-210 have been found to inhibit Treg generation, as both these microRNAs repress FoxP3 and miR-31 also represses Retinoic acid-inducible protein 3, an important factor for pTreg generation (Fayyad-Kazan et al., 2012; Rouas et al., 2009; Zhang et al., 2015a). MiR-21 has been shown to repress Peli1 (Marquez et al., 2010). Peli1 is an ubiquitin ligase abundantly expressed in T cells and has been shown to inhibit NF- $\kappa$ B signaling (Chang et al., 2011). Peli1 KO mice show multiorgan autoimmunity and the T cells in these mice are resistant to suppression by Tregs (Chang et al., 2011). Thus an increase in miR-21 could inhibit Peli1 expression in effector T cells and make them resistant to Treg-mediated suppression. If this is also the case in patients suffering from IBD, then inhibiting these microRNAs may restore intestinal homeostasis. MicroRNA therapy could also potentially be used in combination with other therapeutic agents to improve or speed up recovery.

Another very important finding of the work carried out in this thesis is that a significant proportion of IL-10<sup>+</sup> LP CD4<sup>+</sup> T cells in the colitic setting share phenotypic characteristics of both inflammatory and regulatory T cells. Given the important role of IL-10 in preventing intestinal inflammation, IL-10 as a therapeutic tool has been an area of active investigation. Unfortunately, although animal models of colitis showed great promise for IL-10 therapy (Asseman et al., 1999; Lindsay et al., 2002; Sasaki et al., 2005), clinical trials in humans with IBD showed little efficacy (Buruiana et al., 2010; Herfarth and Scholmerich, 2002). There are several possible explanations for this. Firstly, it is possible that recombinant IL-10 is not very stable. Secondly, it is also possible that the dose of IL-10 is too low to elicit a response.

Thirdly, as explained previously, different individuals have different disease phenotypes/severity of disease. Patients with inherently low IL-10-levels benefited more from IL-10 supplementation (Colombel et al., 2001). Furthermore, patients with very severe disease benefited from IL-10-supplementation compared to patients with less severe disease (Schreiber et al., 2000). Finally, IL-10 alone may fail to suppress all the pro-inflammatory mediators. Supporting this theory, previous studies from our lab using the *Hh*<sup>+</sup>/RAG KO T-cell transfer model of colitis have shown that IL-10<sup>+</sup> T cells from *Hh*<sup>+</sup> WT mice but not uninfected WT mice protected *Hh*<sup>+</sup> RAG KO mice from developing colitis suggesting that antigen-priming is necessary to generate disease protective cells (Kullberg et al., 2002). This protective effect was lost when the mice were treated with a blocking antibody to the IL-10R (Kullberg et al., 2002). Thus it is tempting to speculate that although protection from colitis is dependent on IL-10, perhaps the antigen-primed Tregs utilize other mechanisms that are dependent on IL-10 to keep effector T cells in check. Thus using Tregs expanded from the patient's own serum to treat IBD is another area that is now an important area of research. Using Tregs as therapy will not only overcome the problem of stability and dosage issues of recombinant-IL-10, as these cells can produce IL-10 endogenously at the site of inflammation, but they may also be more effective at limiting effector T cell responses by other mechanisms. The work carried out in this thesis has shown that a large proportion of IL-10<sup>+</sup> LP CD4<sup>+</sup> T cells seen in *Hh*-induced colitis share phenotypic characteristics of regulatory and inflammatory T cells. If these cells are of Treg origin and are pathogenic, then they are a cause for grave concern, as it highlights the possibility that Tregs may be unstable in the inflammatory environment and precludes their use to treat IBD. Equally, if the IL-10-producing CD4<sup>+</sup> T cells that co-express IL-17A and/or IFN- $\gamma$  and/or FoxP3 are suppressive, and actually represent a highly specialised subset of Treg cells that are more effective at suppressing a particular effector T cell, then understanding the factors that trigger the development of these cells could lead to the development of more effective immunotherapies. In order to use Tregs as therapy, it is important to ensure that these cells are stable and do not become pathogenic themselves when introduced into an inflammatory environment. Recent clinical trial data of Treg therapy in other diseases has proved promising. Treatment of humanised mice with *in vitro* expanded Tregs was found to prevent transplant rejection (Issa et al., 2010; Sagoo et al., 2011) and graft versus host disease (GVHD) (Ermann et al., 2005; Scotta et al., 2013). Furthermore, phase I trials in patients with GVHD and type 1 diabetes showed that Treg therapy is safe (Marek-Trzonkowska et al., 2012; Trzonkowski et al., 2009). Using Tregs as cell based therapies for CD is an attractive proposition, and a proof-of-principle study showed that it is possible to expand CD45RA<sup>+</sup> regulatory cells from the blood of patients with CD *in vitro* and that these cells homed to the human small bowel and were stable and did not express inflammatory cytokines when transferred into C.B-17 SCID mice bearing human small intestine xenotransplants (Canavan et al., 2015). Furthermore, *in vitro* CD45RA<sup>+</sup> Tregs suppressed Tconv cells isolated from patients with active CD (Canavan et al., 2015). In

an earlier phase 1/2a trial, CD patients refractive to other therapy were sensitised to ova and ovalbumin-specific Tregs (Ova-Tregs) subsequently isolated from CD patients' peripheral blood mononuclear cells, expanded *in vitro* and administered intravenously to the same patients (Desreumaux et al., 2012). Desreumaux et al's study demonstrated that while Ova-Treg therapy was safe and well tolerated in most of the patients, 3 of the 20 participants suffered from severe adverse events related to the Ova-Tregs (mainly gastrointestinal and related to underlying CD) (Desreumaux et al., 2012). Although early results are promising, more comprehensive studies are required to ensure efficacy of Treg therapy for CD, primarily because of the diversity of mucosal environments and the significant influence the resident microbiota has in shaping immune responses in the gut.

In conclusion, the data presented in this thesis highlight changes in the expression profile of two important regulatory factors in LP CD4<sup>+</sup> T cells from colitic mice compared to those from uninfected controls; microRNAs and IL-10. Further studies should focus on whether the change in microRNA expression and/or the phenotype of IL-10-producing CD4<sup>+</sup> T cells in the colitic setting potentiates inflammation in any way, and whether these factors may be manipulated to decrease the severity or prevent intestinal inflammation.

## APPENDICES

### APPENDIX 1 MICRORNA MICROARRAY RAW DATA

	microRNAs up-regulated $\geq 2$ fold
	microRNAs with fold difference $< 2$ fold Only 3 of 1133 miRs (miR-155, miR-326 and miR-132) are shown as these microRNAs were examined at the tissue level in Chapter 4
	microRNAs down-regulated $\geq 2$ fold

**Table A1.1 Raw data of microRNA microarray carried out on LP CD4<sup>+</sup> T cells from uninfected and 2-wk *Hh*<sup>+</sup> IL-10 KO mice**

MicroRNA	Fluorescence Intensity of sample <sup>a</sup> (normalised to negative control) (log scale)							Average uninf <sup>b</sup> (A1-A3)	Average <i>Hh</i> -inf <sup>c</sup> (B1-B4)	Expression in uninf control <sup>d</sup> (2 <sup>^</sup> value)	Expression in <i>Hh</i> -inf mice <sup>e</sup> (2 <sup>^</sup> value)	Upreg Fold change (ratio of Inf/Uninf)	Downreg Fold change (ratio of uninf/inf)
	A1	A2	A3	B1	B2	B3	B4						
<b>Blank/neg control value:</b>	-5.1	-5.4	-6.3	-5.1	-5.1	-5.7	-5.0						
<b>mmu-miR-210-3p</b>	0.0	0.0	4.5	6.3	6.7	6.4	5.5	1.5	6.2	2.8	74.0	26.35	0.04
<b>mmu-miR-96-5p</b>	0.0	0.0	4.8	6.4	5.3	6.2	6.4	1.6	6.1	3.0	68.5	22.83	0.04
<b>mmu-miR-182-5p</b>	0.0	0.0	5.3	6.0	5.5	5.7	5.7	1.8	5.7	3.4	53.3	15.82	0.06
<b>mmu-miR-18a-5p</b>	0.0	0.0	4.9	5.4	5.1	5.4	5.6	1.6	5.4	3.1	41.0	13.15	0.08
<b>mmu-miR-148a-3p</b>	0.0	0.0	4.8	5.0	5.1	5.2	5.0	1.6	5.1	3.0	34.0	11.26	0.09
<b>mmu-miR-301a-3p</b>	0.0	0.0	0.0	0.0	0.0	5.1	4.9	0.0	2.5	1.0	5.6	5.59	0.18
<b>mmu-miR-188-5p</b>	0.0	3.4	6.2	5.2	6.0	6.2	4.4	3.2	5.4	9.1	43.4	4.78	0.21
<b>mmu-miR-370-3p</b>	0.0	0.0	5.7	4.4	5.9	6.0	0.0	1.9	4.1	3.7	16.9	4.53	0.22
<b>mmu-miR-185-5p</b>	4.4	0.0	5.6	5.4	5.2	5.8	5.5	3.3	5.5	10.2	43.9	4.31	0.23
<b>mmu-miR-31-5p</b>	4.7	4.4	6.0	7.0	6.9	7.1	7.0	5.0	7.0	32.8	131.0	4.00	0.25
<b>mmu-miR-21a-5p</b>	12.0	11.3	12.7	13.7	13.8	14.0	13.8	12.0	13.8	4096.7	14365.3	3.51	0.29
<b>mmu-miR-135a-1-3p</b>	0.0	0.0	0.0	0.0	3.7	3.4	0.0	0.0	1.8	1.0	3.4	3.42	0.29
<b>mmu-miR-532-5p</b>	0.0	4.3	5.6	4.9	4.9	5.0	4.9	3.3	4.9	9.8	30.1	3.07	0.33
<b>mmu-miR-202-3p</b>	5.7	0.0	6.3	4.6	5.8	6.0	5.8	4.0	5.6	15.8	47.2	2.99	0.33
<b>mmu-miR-27b-3p</b>	6.3	5.5	7.5	7.9	7.8	7.9	8.0	6.5	7.9	87.6	238.2	2.72	0.37

MicroRNA	Fluorescence Intensity of sample <sup>a</sup> (normalised to negative control) (log scale)							Average uninf <sup>b</sup> (A1-A3)	Average <i>Hh</i> -inf <sup>c</sup> (B1-B4)	Expression in uninf control <sup>d</sup> (2 <sup>^</sup> value)	Expression in <i>Hh</i> -inf mice <sup>e</sup> (2 <sup>^</sup> value)	Upreg Fold change (ratio of Inf/Uninf)	Downreg Fold change (ratio of uninf/inf)
	A1	A2	A3	B1	B2	B3	B4						
Blank/neg control value:	-5.1	-5.4	-6.3	-5.1	-5.1	-5.7	-5.0						
<i>mmu</i> -miR-652-5p	0.0	0.0	0.0	0.0	0.0	5.7	0.0	1.4	1.0	2.7	2.70	0.37	
<i>mmu</i> -miR-466h-3p	0.0	0.0	0.0	0.0	4.7	0.0	0.0	1.2	1.0	2.3	2.26	0.44	
<i>mmu</i> -miR-3096b-5p	0.0	5.2	5.6	4.6	5.4	4.8	3.6	4.8	12.1	27.4	2.26	0.44	
<i>mmu</i> -miR-6538	0.0	4.4	6.4	4.4	4.5	5.7	3.6	4.8	12.1	27.2	2.25	0.45	
<i>mmu</i> -miR-19a-3p	0.0	0.0	0.0	0.0	0.0	4.6	0.0	1.2	1.0	2.2	2.24	0.45	
<i>mmu</i> -miR-6354	0.0	0.0	0.0	0.0	4.6	0.0	0.0	1.1	1.0	2.2	2.21	0.45	
<i>mmu</i> -miR-3096a-5p	0.0	5.1	6.1	4.8	5.0	5.0	3.7	4.9	13.1	28.9	2.20	0.45	
<i>mmu</i> -miR-668-3p	0.0	0.0	0.0	0.0	0.0	4.5	0.0	1.1	1.0	2.2	2.17	0.46	
<i>mmu</i> -miR-183-5p	5.0	4.4	5.8	6.4	5.5	6.4	5.0	6.2	33.1	71.8	2.17	0.46	
<i>mmu</i> -miR-1306-3p	0.0	0.0	0.0	0.0	0.0	4.4	0.0	1.1	1.0	2.1	2.13	0.47	
<i>mmu</i> -miR-130b-3p	5.9	5.9	7.4	7.6	7.4	7.4	6.4	7.5	85.8	182.3	2.12	0.47	
<i>mmu</i> -miR-146a-5p	9.2	8.7	9.7	10.4	10.0	10.4	9.2	10.3	587.0	1243.2	2.12	0.47	
<i>mmu</i> -miR-223-3p	7.0	7.9	10.2	9.1	9.3	9.8	8.4	9.4	331.1	675.4	2.04	0.49	
<i>mmu</i> -miR-3102-5p	5.9	6.1	7.6	7.4	7.8	8.1	6.6	7.6	95.0	190.6	2.01	0.50	
<i>mmu</i> -miR-155-3p	8.8	8.4	9.2	9.1	8.8	9.4	8.8	9.1	439.5	540	1.23	0.81	
<i>mmu</i> -miR-326-5p	0.0	0.0	0.0	0.0	0.0	0.0	0.0	0.0	1.0	1.0	1.00	1.00	
<i>mmu</i> -miR-132-5p	0.0	0.0	0.0	0.0	0.0	0.0	0.0	0.0	1.0	1.0	1.00	1.00	
<i>mmu</i> -miR-126-3p	6.7	0.0	7.3	0.0	4.7	4.8	4.7	3.7	25.7	12.7	0.49	2.03	
<i>mmu</i> -miR-3070b-3p	6.7	6.7	6.5	5.8	5.9	5.8	6.7	5.6	101.2	49.5	0.49	2.05	
<i>mmu</i> -miR-5121	5.1	6.1	6.4	0.0	9.6	5.2	5.9	4.8	57.7	27.9	0.48	2.07	
<i>mmu</i> -miR-30b-3p	0.0	0.0	3.3	0.0	0.0	0.0	1.1	0.0	2.2	1.0	0.46	2.15	
<i>mmu</i> -miR-710	0.0	0.0	3.3	0.0	0.0	0.0	1.1	0.0	2.2	1.0	0.46	2.15	
<i>mmu</i> -miR-298-5p	0.0	0.0	3.3	0.0	0.0	0.0	1.1	0.0	2.2	1.0	0.46	2.17	
<i>mmu</i> -miR-504-3p	7.7	7.7	7.2	6.4	6.7	6.6	7.6	6.4	188.2	86.2	0.46	2.18	
<i>mmu</i> -miR-1839-3p	5.9	6.5	6.7	5.1	4.8	5.6	6.4	5.2	82.7	37.6	0.45	2.20	
<i>mmu</i> -miR-191-3p	0.0	0.0	3.4	0.0	0.0	0.0	1.1	0.0	2.2	1.0	0.45	2.21	
<i>mmu</i> -miR-302c-5p	3.4	0.0	0.0	0.0	0.0	0.0	1.1	0.0	2.2	1.0	0.45	2.21	
<i>mmu</i> -miR-1947-3p	4.5	5.7	5.9	5.6	0.0	5.6	5.4	4.2	41.2	17.8	0.43	2.31	

MicroRNA	Fluorescence Intensity of sample <sup>a</sup> (normalised to negative control) (log scale)							Average uninf <sup>b</sup> (A1-A3)	Average <i>Hh</i> -inf <sup>c</sup> (B1-B4)	Expression in uninf control <sup>d</sup> (2 <sup>^</sup> value)	Expression in <i>Hh</i> -inf mice <sup>e</sup> (2 <sup>^</sup> value)	Upreg Fold change (ratio of Inf/Uninf)	Downreg Fold change (ratio of uninf/inf)
	A1	A2	A3	B1	B2	B3	B4						
Blank/neg control value:	-5.1	-5.4	-6.3	-5.1	-5.1	-5.7	-5.0						
mmu-miR-342-3p	10.9	10.8	11.8	9.9	9.7	10.4	9.8	11.2	10.0	2304.2	993.3	0.43	2.32
mmu-miR-378d	6.7	6.5	7.4	5.1	6.1	6.3	5.0	6.9	5.6	116.6	49.5	0.42	2.35
mmu-miR-877-3p	5.1	5.8	5.9	5.7	0.0	6.1	5.5	5.6	4.3	48.6	20.3	0.42	2.40
mmu-miR-671-5p	0.0	3.3	3.5	0.0	0.0	3.6	0.0	2.3	0.9	4.9	1.9	0.39	2.59
mmu-miR-196b-5p	0.0	0.0	4.2	0.0	0.0	0.0	0.0	1.4	0.0	2.7	1.0	0.38	2.67
mmu-miR-221-3p	0.0	0.0	4.2	0.0	0.0	0.0	0.0	1.4	0.0	2.7	1.0	0.37	2.67
mmu-miR-149-3p	0.0	0.0	4.3	0.0	0.0	0.0	0.0	1.4	0.0	2.7	1.0	0.37	2.68
mmu-miR-1934-3p	0.0	0.0	4.3	0.0	0.0	0.0	0.0	1.4	0.0	2.7	1.0	0.37	2.70
mmu-miR-3107-5p	0.0	0.0	4.3	0.0	0.0	0.0	0.0	1.4	0.0	2.7	1.0	0.37	2.71
mmu-miR-181d-5p	0.0	0.0	4.3	0.0	0.0	0.0	0.0	1.4	0.0	2.7	1.0	0.37	2.71
mmu-miR-130a-3p	0.0	0.0	4.3	0.0	0.0	0.0	0.0	1.4	0.0	2.7	1.0	0.37	2.71
mmu-miR-3473c	0.0	4.3	0.0	0.0	0.0	0.0	0.0	1.4	0.0	2.7	1.0	0.37	2.71
mmu-miR-7a-1-3p	0.0	0.0	4.4	0.0	0.0	0.0	0.0	1.5	0.0	2.8	1.0	0.36	2.77
mmu-miR-30e-3p	0.0	0.0	4.4	0.0	0.0	0.0	0.0	1.5	0.0	2.8	1.0	0.36	2.77
mmu-miR-3069-3p	0.0	0.0	4.4	0.0	0.0	0.0	0.0	1.5	0.0	2.8	1.0	0.36	2.79
mmu-let-7c-5p	11.4	10.6	12.0	10.0	9.4	10.1	10.0	11.3	9.9	2598.1	930.3	0.36	2.79
mmu-miR-5117-3p	4.1	3.4	5.4	3.4	0.0	4.0	3.8	4.3	2.8	19.6	7.0	0.36	2.80
mmu-miR-378a-5p	0.0	0.0	4.5	0.0	0.0	0.0	0.0	1.5	0.0	2.8	1.0	0.36	2.81
mmu-miR-1196-3p	4.5	0.0	0.0	0.0	0.0	0.0	0.0	1.5	0.0	2.8	1.0	0.35	2.82
mmu-miR-200a-3p	0.0	0.0	4.5	0.0	0.0	0.0	0.0	1.5	0.0	2.8	1.0	0.35	2.83
mmu-miR-5046	4.5	0.0	0.0	0.0	0.0	0.0	0.0	1.5	0.0	2.9	1.0	0.35	2.85
mmu-miR-3473e	0.0	0.0	4.5	0.0	0.0	0.0	0.0	1.5	0.0	2.9	1.0	0.35	2.85
mmu-miR-146b-5p	0.0	0.0	4.6	0.0	0.0	0.0	0.0	1.5	0.0	2.9	1.0	0.35	2.89
mmu-miR-511-3p	0.0	0.0	4.6	0.0	0.0	0.0	0.0	1.5	0.0	2.9	1.0	0.34	2.91
mmu-miR-99b-5p	0.0	0.0	4.6	0.0	0.0	0.0	0.0	1.5	0.0	2.9	1.0	0.34	2.92
mmu-miR-324-5p	0.0	0.0	4.6	0.0	0.0	0.0	0.0	1.5	0.0	2.9	1.0	0.34	2.92
mmu-miR-100-5p	0.0	0.0	4.7	0.0	0.0	0.0	0.0	1.6	0.0	3.0	1.0	0.34	2.95
mmu-let-7b-5p	11.7	11.1	12.2	10.1	9.7	10.3	10.3	11.7	10.1	3253.7	1100.6	0.34	2.96

MicroRNA	Fluorescence Intensity of sample <sup>a</sup> (normalised to negative control) (log scale)							Average uninf <sup>b</sup> (A1-A3)	Average <i>Hh</i> -inf <sup>c</sup> (B1-B4)	Expression in uninf control <sup>d</sup> (2 <sup>^</sup> value)	Expression in <i>Hh</i> -inf mice <sup>e</sup> (2 <sup>^</sup> value)	Upreg Fold change (ratio of Inf/Uninf)	Downreg Fold change (ratio of uninf/inf)
	A1	A2	A3	B1	B2	B3	B4						
Blank/neg control value:	-5.1	-5.4	-6.3	-5.1	-5.1	-5.7	-5.0						
mmu-miR-345-5p	0.0	0.0	4.7	0.0	0.0	0.0	0.0	1.6	0.0	3.0	1.0	0.34	2.96
mmu-miR-328-5p	0.0	0.0	4.7	0.0	0.0	0.0	0.0	1.6	0.0	3.0	1.0	0.33	2.99
mmu-miR-129-1-3p	4.8	0.0	0.0	0.0	0.0	0.0	0.0	1.6	0.0	3.0	1.0	0.33	3.00
mmu-let-7b-3p	4.6	5.5	5.5	4.5	0.0	4.5	5.5	5.2	3.6	37.2	12.1	0.33	3.06
mmu-miR-331-3p	0.0	0.0	4.9	0.0	0.0	0.0	0.0	1.6	0.0	3.1	1.0	0.33	3.07
mmu-miR-5099	0.0	0.0	4.9	0.0	0.0	0.0	0.0	1.6	0.0	3.1	1.0	0.32	3.13
mmu-miR-5627-3p	5.0	0.0	0.0	0.0	0.0	0.0	0.0	1.7	0.0	3.2	1.0	0.32	3.17
mmu-miR-10b-5p	0.0	0.0	5.1	0.0	0.0	0.0	0.0	1.7	0.0	3.2	1.0	0.31	3.21
mmu-miR-181c-5p	0.0	0.0	5.2	0.0	0.0	0.0	0.0	1.7	0.0	3.3	1.0	0.30	3.31
mmu-miR-3544-3p	6.7	5.9	5.9	5.4	0.0	6.1	6.0	6.1	4.4	70.5	20.6	0.29	3.43
mmu-miR-1897-5p	0.0	0.0	5.3	0.0	0.0	0.0	0.0	1.8	0.0	3.4	1.0	0.29	3.43
mmu-miR-195a-5p	5.0	0.0	7.0	0.0	0.0	4.4	4.4	4.0	2.2	15.9	4.6	0.29	3.45
mmu-miR-5107-5p	4.4	4.7	6.3	4.4	0.0	4.6	4.3	5.2	3.3	35.8	10.1	0.28	3.56
mmu-miR-5620-3p	4.8	0.0	4.2	0.0	0.0	0.0	4.3	3.0	1.1	8.0	2.1	0.26	3.82
mmu-miR-1892	5.8	0.0	0.0	0.0	0.0	0.0	0.0	1.9	0.0	3.8	1.0	0.26	3.84
mmu-miR-181b-5p	0.0	0.0	5.8	0.0	0.0	0.0	0.0	1.9	0.0	3.8	1.0	0.26	3.84
mmu-miR-497-5p	0.0	0.0	5.8	0.0	0.0	0.0	0.0	1.9	0.0	3.8	1.0	0.26	3.85
mmu-miR-3099-3p	6.4	6.3	6.0	5.5	5.6	5.6	0.0	6.2	4.2	74.9	18.2	0.24	4.12
mmu-miR-322-5p	0.0	0.0	6.2	0.0	0.0	0.0	0.0	2.1	0.0	4.2	1.0	0.24	4.19
mmu-miR-199b-5p	0.0	0.0	6.3	0.0	0.0	0.0	0.0	2.1	0.0	4.3	1.0	0.23	4.30
mmu-let-7e-5p	7.3	6.4	8.7	5.3	4.7	5.6	5.3	7.5	5.2	177.9	37.7	0.21	4.73
mmu-miR-6401	6.2	5.8	5.8	4.4	5.6	4.5	0.0	5.9	3.6	59.7	12.3	0.21	4.84
mmu-miR-199a-3p	0.0	0.0	7.1	0.0	0.0	0.0	0.0	2.4	0.0	5.1	1.0	0.19	5.13
mmu-miR-5119	0.0	4.0	4.0	0.0	0.0	0.0	0.0	2.7	0.0	6.3	1.0	0.16	6.29
mmu-miR-705	4.3	0.0	3.7	0.0	0.0	0.0	0.0	2.7	0.0	6.4	1.0	0.16	6.37
mmu-miR-1196-5p	5.8	5.9	6.6	0.0	0.0	6.0	5.6	6.1	2.9	68.8	7.5	0.11	9.17
mmu-miR-467e-5p	4.8	0.0	4.8	0.0	0.0	0.0	0.0	3.2	0.0	9.3	1.0	0.11	9.32
mmu-miR-290-3p	0.0	5.5	4.3	0.0	0.0	0.0	0.0	3.3	0.0	9.7	1.0	0.10	9.66

MicroRNA	Fluorescence Intensity of sample <sup>a</sup> (normalised to negative control) (log scale)							Average uninf <sup>b</sup> (A1-A3)	Average <i>Hh</i> -inf <sup>c</sup> (B1-B4)	Expression in uninf control <sup>d</sup> (2 <sup>^</sup> value)	Expression in <i>Hh</i> -inf mice <sup>e</sup> (2 <sup>^</sup> value)	Upreg Fold change (ratio of Inf/Uninf)	Downreg Fold change (ratio of uninf/inf)
	A1	A2	A3	B1	B2	B3	B4						
Blank/neg control value:	-5.1	-5.4	-6.3	-5.1	-5.1	-5.7	-5.0						
mmu-miR-467b-5p	5.5	5.1	6.4	0.0	4.6	4.6	0.0	5.7	2.3	50.6	4.9	0.10	10.26
mmu-miR-194-5p	0.0	4.8	5.3	0.0	0.0	0.0	0.0	3.4	0.0	10.4	1.0	0.10	10.41
mmu-let-7f-1-3p	3.5	5.5	5.4	0.0	0.0	5.4	0.0	4.8	1.4	27.6	2.6	0.09	10.81
mmu-miR-1897-3p	4.5	4.4	5.8	0.0	0.0	5.6	0.0	4.9	1.4	30.1	2.7	0.09	11.31
mmu-miR-375-3p	0.0	5.2	5.3	0.0	0.0	0.0	0.0	3.5	0.0	11.3	1.0	0.09	11.34
mmu-miR-342-5p	4.3	4.1	5.1	0.0	0.0	3.6	0.0	4.5	0.9	22.1	1.9	0.08	11.84
mmu-miR-151-5p	4.5	0.0	6.2	0.0	0.0	0.0	0.0	3.6	0.0	11.9	1.0	0.08	11.87
mmu-miR-99a-5p	0.0	4.3	6.5	0.0	0.0	0.0	0.0	3.6	0.0	12.1	1.0	0.08	12.07
mmu-miR-34a-5p	5.1	5.7	7.9	0.0	4.7	4.9	0.0	6.2	2.4	75.2	5.3	0.07	14.21
mmu-miR-429-3p	0.0	6.1	6.5	0.0	0.0	0.0	0.0	4.2	0.0	18.3	1.0	0.05	18.32
mmu-miR-467c-5p	4.5	4.2	4.8	0.0	0.0	0.0	0.0	4.5	0.0	22.7	1.0	0.04	22.73
mmu-miR-451a	6.8	5.9	8.2	4.3	0.0	0.0	5.2	7.0	2.4	125.6	5.3	0.04	23.91
mmu-miR-139-5p	4.7	4.2	5.6	0.0	0.0	0.0	0.0	4.8	0.0	28.7	1.0	0.03	28.72
mmu-miR-200c-3p	4.9	6.2	6.7	0.0	0.0	0.0	4.3	5.9	1.1	60.8	2.1	0.03	29.04
mmu-miR-125a-5p	4.5	4.3	5.8	0.0	0.0	0.0	0.0	4.9	0.0	29.5	1.0	0.03	29.46
mmu-miR-30a-5p	4.1	4.3	6.4	0.0	0.0	0.0	0.0	4.9	0.0	30.5	1.0	0.03	30.52
mmu-miR-200b-3p	5.8	7.3	7.5	0.0	0.0	0.0	4.6	6.9	1.2	116.6	2.2	0.02	52.24
mmu-miR-192-5p	5.0	6.5	7.1	0.0	0.0	0.0	0.0	6.2	0.0	71.5	1.0	0.01	71.51
mmu-miR-125b-5p	5.4	5.0	8.1	0.0	0.0	0.0	0.0	6.2	0.0	72.6	1.0	0.01	72.59
mmu-miR-181a-5p	6.1	6.3	7.2	0.0	0.0	0.0	0.0	6.5	0.0	91.9	1.0	0.01	91.86

<sup>a</sup> Samples A1-A3 denote samples from uninfected IL-10 KO mice and samples B1-B4 denote samples from 2-wk *Hh*<sup>+</sup> IL-10 KO mice

<sup>b</sup> Average normalised fluorescence intensities of samples from uninfected mice

<sup>c</sup> Average normalised fluorescence intensities of samples from 2-wk *Hh*<sup>+</sup> IL-10 KO mice

<sup>d</sup> Average microRNA expression in samples from uninfected mice

<sup>e</sup> Average microRNA expression in samples from 2-wk *Hh*<sup>+</sup> IL-10 KO mice

## APPENDIX 2 MRNA TARGETS PREDICTED BY MIRWALK

	Gene plays a role in CD4 <sup>+</sup> T-cell development and function. Altered regulation of gene by miR in question could have an inflammatory role in <i>Hh</i> colitis
	Gene plays a role in CD4 <sup>+</sup> T-cell development and function. Altered regulation of gene could have an anti-inflammatory role in <i>Hh</i> colitis

**Table A2.1 Predicted mRNA targets of miR-31**

Mouse miR	Gene	Sum of target prediction programs <sup>a</sup>	Gene function <sup>b</sup>
MiR-31	Unc93b1	7	Plays a role in TLR signalling
	Narg1	7	Mainly involved in retinopathy and blood vessel development
	Kank1	7	No literature available on function
	Slc25a28	7	No literature available on function
	Hip2	7	No literature available on function
	Sugt1	7	Involved in neurogenesis
	Topbp1	7	Growth factor/ Involved in neurogenesis, vdj recombination in lymphocyte development
	Ppp6c	7	No literature available on function
	Stx12	7	No literature available on function
	Ctnnd2	6	Maintenance of neural structure and synapses
	Ppl	6	Part of the cornified envelop of the epidermis
	Snx16	6	Sorting nexin thought to be involved in trafficking of proteins between early and late endosomal compartments
	Twist1	6	Deficiency of Twist1 promotes Th17 cell development. Involved in a feedback loop with STAT3 to repress IL-6 production. Negative regulatory factor that inhibits the expression of T-bet, Runx3 and IL-12Rβ2 (Niesner et al., 2008; Pham et al., 2012; Pham et al., 2013)
	Heatr5a	6	No literature available on function
	Khdrbs3	6	Involved in spermatogenesis
Herpud2	6	No literature available on function	

Mouse miR	Gene	Sum of target prediction programs <sup>a</sup>	Gene function <sup>b</sup>
MiR-31	Irf4	6	T-bet represses IRF4 to inhibit Th17 cells. IRF4 deficiency promotes Th1 response (Gokmen et al., 2013)
	Srpr	6	No literature available on function
	Orc5l	6	No literature available on function
	Nup153	6	No literature available on function
	Pou2f3	6	Expressed mainly in the skin. Epidermis and keratinocytes. No function in the literature
	Supt16h	6	No literature available on function. Highly expressed in the thymus but can't access paper. No mechanism mentioned in title'
	Sh2d1a/SAP	6	SAP is mainly involved in promoting T-cell dependent humoral immunity. It is shown to promote Th2 development and suppress Th1 cells (Cannons et al., 2006).
	Zfand3	6	No literature available on function
	Dpagt1	6	No literature available on function. Papers last published in 1999>1994>1982
	Jazf1	6	Lipid metabolism.
	Hyou1	6	Involved in anti-tumour response. Facilitates Ag cross presentation, CD8 tumour-specific response and increased IFN- $\gamma$ and IL-12 from NK cells (Yu et al., 2013).
	Snx4	6	Involved in endocytosis and intracellular trafficking
	Jph4	6	Part of Junctionophilin family of transmembrane proteins. Involved in formation of junctional membrane structures in excitable cells by interacting with plasma membrane and spanning the ER.
	Xpnpep3	6	No literature available on function
	Usp28	6	No literature available on function
	Lats2	6	Core Kinase of Hippo pathway and plays an important role in cell proliferation as seen in adipocytes
	Nup50	6	Part of nucleopore complex that allows flow of macromolecules between nucleus and cytoplasm. Mutations in Nup50 associated with autoimmune hepatitis
	Grhpr	6	No literature available on function
	B3gnt2	6	Involved in olfactory discrimination
	Tmem117	6	Involved in spermatogenesis
Tnrc4	6	Regulate pre-mRNA alternative splicing	

Mouse miR	Gene	Sum of target prediction programs <sup>a</sup>	Gene function <sup>b</sup>
MiR-31	Dnajb1	6	Anti-Inflammatory in rheumatoid arthritis patients. Inhibited CD4 <sup>+</sup> T cells and stimulated PBMCs to produce IL-10. Together with chaperone protein Schlafen 1 induces cell cycle arrest in T cells (Zhang et al., 2008).
	Nipsnap3a	6	No literature available on function
	Asb3	6	No literature available on function
	Fbxw11	6	Involved in down-regulation of CD4
	Ubac1	6	No literature available on function
	Gabrp	6	GABA, a major inhibitory neurotransmitter binds to Gabrp to open an integral chloride channel and inhibit synaptic transmission
	Prpf40b	6	No literature available on function
	Fzr1	6	Involved in mitosis and meiosis
	Rsb1	6	Exclusively expressed in spermatids
	Pwp1	6	No literature available on function
	Tppp3	6	Binds to tubulin. May be involved in cell proliferation
	Plekha6	6	No literature available on function
	Acad11	6	Mutation results in polycystic kidney disease. Deletion in embryonic lethality and congenital heart defects
	Ppp3ca	6	Calcineurin promotes degradation of STAT3 in neurons. Plays an important role in TCR signaling in mature cells and promotes production of IFN- $\gamma$ and IL-2 (Chan et al., 2002).
	Zc3h18	6	No literature available on function
	Ube3b	6	Neuronal development and functions
	Tmem9b	6	No literature available on function
	Ccr2	6	Receptor for monocyte chemoattractant CCL2
	D430039N05 Rik	6	No literature available on function
	Ppp2r5a	6	Involved in negative control of cell growth and division
Tacc2	6	Member of TACC family of proteins. Involved in stabilizing of microtubules	
Lin7c	6	Mainly involved in CNS functions in the synapse, metastasis of HSSC	

<b>Mouse miR</b>	<b>Gene</b>	<b>Sum of target prediction programs<sup>a</sup></b>	<b>Gene function<sup>b</sup></b>
MiR-31	Spred1	6	Inhibition of Ras/MAPK pathway, inhibition of cell motility and metastasis, tumour suppressor, suppressor of IL-3 induced late phase hematopoiesis.
	Ppp1r9b	6	Scaffold protein. Mostly localized in dendrite spines. Thought to be involved in info transfer at the immunological synapse in DCs.
	Cops2/cop9	6	Cop9 signalosome is required for survival and proliferation of T cells (Menon et al., 2007).
	Fermt1/Kindlin	6	Mainly expressed in epithelial cells in lung cancer and UC

<sup>a</sup> Sum of target prediction programs that predict that miR-31 will bind to a given gene. Target prediction programs taken into account: miRanda, miRDB, miRWalk, RNA Hybrid, PICTAR5, PITA, RNA22 and Targetscan.

<sup>b</sup> Gene function as per NCBI Gene cards and where referenced, primary literature.

**Table A2.2 Predicted mRNA targets of miR-21a**

<b>Mouse miR</b>	<b>Gene</b>	<b>Sum of target prediction programs<sup>a</sup></b>	<b>Gene function<sup>b</sup></b>
MiR-21	Wwp1	7	Inhibits differentiation of stem cells/osteoblasts etc.
	Aspn	7	Modulates TGF beta signalling pathway.
	Stag2	7	Cell cycle, meiosis, mitosis.
	Peli1	7	Validated target of miR-21 in proliferation phase of liver regeneration. Inhibits NF-kB signaling. Necessary for maintaining T cell tolerance in the periphery (Marquez et al., 2010).
	Trim33	7	differentiation of hematopoietic cells. Smads/TGFbeta signalling
	Dnajb4	7	No literature available on function
	Zfp704	6	No literature available on function
	Tssk2	6	Important for spermatogenesis
	Xk	6	Regulates ion transport in erythrocytes.
	Elf2/NERF	6	Interacts with Runx1 (Cho et al., 2004).
	Tnrc6b	6	Key component of RISC. Disruption in yolk sac resulted in gene disruption and apoptosis.
	Tgfb1	6	TGF beta signalling? Found to regulate bone mass and size in mice.
	Xkr6	6	No literature on function.
	Stc1	6	anti-inflammatory. Inhibits ROS formation. Negative feedback loop for ERK1/2 signalling during oxidative stress
	Mrpl9	6	No literature on function.
	Spata9	6	Involved in spermatogenesis
	Bhlhb2/DEC1	6	DEC1 is a transcription factor that is necessary for T cell autoreactive response in EAE. Promotes production of GM-CSF, IFN- $\gamma$ and IL-2 (Martinez-Llordella et al., 2013).
	B230380D07 Rik	6	No literature on function.
	Nfib	6	Coregulation of genetic programs with STAT5
	Ntf3	6	Growth factor involved in neurogenesis. Produced by Th1 cells in spinal cord to aid in wound healing.
Wdr78	6	No literature on function.	

Mouse miR	Gene	Sum of target prediction programs <sup>a</sup>	Gene function <sup>b</sup>
MiR-21	Acvr2a	6	Th17 specific gene thought to play a role in differentiation of naïve T cells to Th17 cells. Induced by TGFβ and IL-6 (Ihn et al., 2011).
	Sox5	6	Transcription factor involved in embryonic development. No T cell specific function in the literature.
	Klhdc5	6	Seems to be involved mainly in mitosis
	Eif2ak4	6	Amino acid-starvation response component (Bunpo et al., 2010). Anti-inflammatory. Involved in remission of EAE (Orsini et al., 2014). Involved in pathway of inhibition of Th17 pathway following Halofuginone treatment (Sundrud et al., 2009). Promotes IDO and thereby promotes Tregs (Wang et al., 2009a).

<sup>a</sup> Sum of target prediction programs that predict that miR-21 will bind to a given gene. Target prediction programs taken into account: miRanda, miRDB, miRWalk, RNA Hybrid, PICTAR5, PITA, RNA22 and Targetscan.

<sup>b</sup> Gene function as per NCBI Gene cards and where referenced, primary literature.

**Table A2.3 Predicted mRNA targets of miR-210**

Mouse miR	Gene	Sum of target prediction programs <sup>a</sup>	Gene function <sup>b</sup>
MiR-210	<b>Zmiz1</b>	6	Susceptibility loci for IBD, T1D, and vitilago. Collaborates with Notch to promote cute lymphocytic leukemia. ZimZ1 is involved in IL-23 pathway and is a transcriptional co-activator of protein inhibitor of Stat signaling (PIAS) family (Lees et al., 2011; Li et al., 2006b).
	Foxa1	6	Transcription factor thought to define a new class of Tregs in the CNS in MS and EAE. Also seen to promote cancer metastasis.
	Htr7	6	Serotonon receptor. Colitis severity is less in KO mice. Expressed by DCs.
	Hhip	6	Part of hedgehog signaling. Polymorphisms associated with COPD and lung function.
	Dnajc15	6	Negative regulator of mitochondrial membrane potential and ATP production
	<b>Nfkb1</b>	6	Validated target (Qi et al., 2012). Regulates T cell homeostasis and prevents chronic colonic inflammation (Chang et al., 2009).
	<b>Coro1c</b>	6	Not much literature on coronin1c. Actin binding protein. Coronin 1 KO mice are resistant to AI and lack peripheral T cells. Coronin1a is only expressed on hematopoeitic cells and is an activation marker of T cells. Suggested as a therapeutic target for T-cell mediated autoimmune diseases (Pieters et al., 2013).
	Setd8	6	Histone methyl tranferase involved in cell cycle regulation, breast cancer and regulating adipogenesis
	Sertad4	6	No literature available
	Galk1	6	Deficiency causes development of cataracts
	C330002I19 Rik	5	Necessary for sustained ERK signaling in T cells, regulates T cell motility
	Tssc1	5	Not much literature. Runx2 induces bone osteolysis via Tssc1 in breast cancer
	Lamp1	5	Lysosome associated membrane protein. Necessary for infection of T-cruzi into host.
	<b>Lair1</b>	5	Collagen receptor widely expressed by immune cells. Immune inhibitory receptor, down-regulated on T cells in Rheumatoid arthritis. Shown to inhibit proliferation and induce apoptosis of T cells (Meyaard, 2008; Zhang et al., 2014c).
	Pld1	5	May play a role in signal transduction and subcellular trafficking
	Zmat3	5	No literature available
	<b>Ctgf</b>	5	Connective tissue growth factor. Shown to promote Th17 differentiation in renal tissue. Seen in Rheumatoid arthritis as well (Nozawa et al., 2013; Rodrigues-Diez et al., 2015)
	Aldh5a1	5	Involved in lipid and myelin regulation
	Txndc9	5	Not much literature. Expression correlates with tumour size and invasion in colorectal cancer

Mouse miR	Gene	Sum of target prediction programs <sup>a</sup>	Gene function <sup>b</sup>
MiR-210	Rtn1	5	Bind to Bcl2 and reduce Bcl2,s anti-apototic activity.
	Gsr	5	Glutathione reductase is an important anti-oxidant and makes cells resistant to oxidative stress
	Necab1	5	Calcium binding protein expressed in the hippocampus
	Epha7	5	Mainly involved in cancer. Marker of metastasis
	AC125535.4	5	Not much let on function. Required for cranofacial and eye developmeno in frogs
	Xpnpep3	5	NO literature on function
	<b>Dapk1</b>	5	Controls Stat3 Activation in IELs and prevents TNF-induced Stat3 activation. It inhibits NF-Kb activation in T cells and thereby limits T-cell proliferation and IL-2 production (Chakilam et al., 2013; Chuang et al., 2008).
	<b>Ppp2r5c</b>	5	Inhibits NFkB activation in t cells and thereby inhibits T cell proliferation (Breuer et al., 2014).
	Drd5	5	Doapmine receptor D5. Expressed on DC and potentiates Th17 response
	Tpm3	5	Involved in wound healing. Promotes Th2 response
	Syt10	5	No literature on function
	<b>Sin3a</b>	5	Validated target. Repressor of IFN- $\gamma$ gene expression. T-bet antagonizes Sin3a recruitment to promote IFN- $\gamma$ expression (Chang et al., 2008; Shang et al., 2014; Tong et al., 2005).
	Tppp	5	Critical for oligodendrocyte differentiation
	Dpy1913	5	No literature on function
	Txnip	5	Oxidative stress mediator
	Enpp5	5	No literature on function
	Rbpms2	5	No literature on function
	<b>Acvr1b</b>	5	Validated target of miR-210 (Mizuno et al., 2009). Suppresses Acvr1b to inhibit osteoblast differentiation. Belongs to TGF $\beta$ superfamily. Activin receptor is necessary for signaling. Mutations associated with pitiutary tumours
	Rad50	5	Essential for Th2 cytokine response
	Eml4	5	Stabilizes microtubules
Wdr38	5	No literature on function	
Slc3a1	5	No literature on function	

Mouse miR	Gene	Sum of target prediction programs <sup>a</sup>	Gene function <sup>b</sup>
MiR-210	Rab3b	5	Neuronal Rab3 required for long-term suppression of hippocampal inhibitory synapse. Required for normal function of calcium-triggered synaptic vesicle exocytosis
	Iscu	5	Validated miR-210 target. Represses ISCU to control mitochondrial metabolism during hypoxia (McCormick et al., 2013).
	Rab6ip1	5	No literature on function
	Cdcp1	5	Stem cell marker. Involved in cancer metastasis and tumour progression
	Hhat	5	Involved in hedgehog signaling
	Ctbp2	5	Transcription factor Zeb1, co-operates with CtBP2 and HDAC1 to suppress IL-2 gene function in T cells. Also contributes to cancer metastasis (Wang et al., 2009b)
	ErbB2	5	Growth factor receptor located on epithelial cells. Involved in breast cancer metastasis
	Chd6	5	Essential for motor co-ordination as deletion of CHD6 affects motor co-ordination
	Neur12	5	No literature on function
	Nptx1	5	Involved in neuropathic pain and hypoxic-ischemic neuronal death

<sup>a</sup> Sum of target prediction programs that predict that miR-210 will bind to a given gene. Target prediction programs taken into account: miRanda, miRDB, miRWalk, RNA Hybrid, PICTAR5, PITA, RNA22 and Targetscan.

<sup>b</sup> Gene function as per NCBI Gene cards and where referenced, primary literature.

**Table A2.4 Predicted mRNA targets of miR-96**

<b>Mouse miR</b>	<b>Gene</b>	<b>Sum of target prediction programs<sup>a</sup></b>	<b>Gene function<sup>b</sup></b>
MiR-96	Tcf712	8	Key regulator of glucose metabolism. Tcf712 KO mice are less susceptible to diabetes
	Ezr	7	Protein that mediates interactions between plasma and actin cytoskeleton. Implicated in amplification of B-cell signaling and homeostasis
	E2f5	7	Validated miR 181a target. Promotes hepatocellular cancer and gastric cancer. Involved in cell cycle and embryogenesis
	0910001A06Rik	7	No literature on function
	Rev1	7	Deoxycytidyl transferase involved in DNA repair. Transfers a dCMP residue from dCTP to the 3'-end of a DNA primer in a template-dependent reaction
	Cdh20	7	Cadherin (calcium dependent cell adhesion molecule). Involved in mouse embryogenesis
	Klh18	7	No literature on function
	<b>Itpr2</b>	7	Inositol Triphosphate receptor forms a ligand gated ion channel act by calcium and IP3. Controls CD4 <sup>+</sup> T cell cytokine program (Nagaleekar et al., 2008).
	Mkx	6	Regulator of Tendon development. Suppresses SIN3a (miR-201a target in fibroblasts. No studies on T cells).
	Cables1	6	Critical for neuronal development. Positively affects neuron growth. Tumour suppressor in the intestine
	Xkr4	6	Mainly bovine studies. Associated with increased rump fat
	Map3k7ip2	6	Involved in innate immune signaling. Adaptor protein with MAP3K7 and TAK1 and TRAF6. Promotes IL-1 signaling
	Vcl	6	actin filament binding protein. Regulates cell-matrix and cell-cell adhesion
	Amph	6	Involved in synaptic recycling machinery as well as has a role in macrophage survival
	Grhl2	6	TF that promotes breast cancer tumour growth and proliferation f cells
	Meox2	6	Role in mesoderm induction and its earliest regional specification, somitogenesis, and myogenic and sclerotomal differentiation
	Heatr5a	6	No literature available on function
	Zhx1	6	Transcriptional repressor. No function a such with T cells
	Tacc1	6	No literature available on function
	<b>Fyn</b>	6	Protein tyrosine kinase. Promotes Th17 differentiation observed in lamina propria and T-cell transfer colitis model (Ueda et al., 2012).
Gphn	6	Microtubule-associated protein involved in membrane protein-cytoskeleton interactions. It is thought to	

<b>Mouse miR</b>	<b>Gene</b>	<b>Sum of target prediction programs<sup>a</sup></b>	<b>Gene function<sup>b</sup></b>
MiR-96	Klhl7	6	No literature available on function
	Fut9	6	Involved in anxiety disorders. Shown to maintain stem cell populations
	Galnt7	6	Plays a role in osteoblast differentiation
	Hoxa5	6	Plays a role in intestinal maturation and organogenesis
	Smek1	6	Involved in stem cell pluripotency maintenance in embryos
	Fgf13	6	Fibroblast growth factor 13
	Cobl	6	Critical for neuromorphogenesis processes
	Gad2	6	Islet antigen in T1D
	Ube2q2	6	No literature available on function
	Ptpn9	6	Plays a role in negative regulation of hepatic insulin signaling
	Rhpn2	6	No literature available on function
	Chmp2b	6	Not much literature on function. Plays a role in neurodegeneration
	Actr1a	6	No literature available on function
	Map2k1	6	
	Snx30	6	No literature available on function
	Pcdh8	6	Calcium-dependent cell-adhesion protein (By similarity). May play a role in activity-induced synaptic reorganization underlying long term memory
	Farp1	6	Involved in synapse formation
	Herpud1	6	Membrane protein that is expressed during cellular stress. Not much literature available on function
	Wdr47	6	No literature available on function
	Dus21	6	No literature available on function
AC140392.3	6	Component of the NuA4 histone acetyltransferase (HAT) complex that is involved in transcriptional activation of select genes principally by acetylation of nucleosomal histones H4 and H2A.	
Plod2	6	Essential for stability of intermolecular collagen	
Epb4.113	6	Tumor suppressor that inhibits cell proliferation and promotes apoptosis.	

Mouse miR	Gene	Sum of target prediction programs <sup>a</sup>	Gene function <sup>b</sup>
MiR-96	D3Bwg0562e	6	Hydrolyzes lysophosphatidic acid (LPA). Facilitates axonal outgrowth during development and regenerative sprouting
	Yipf4	6	No literature available on function
	Frs2	6	Fibroblast growth factor receptor
	Zcchc11	6	Suppresses miRNA biogenesis thru uridylation of pre-microRNAs.
	Rab35	6	The small GTPases Rab are key regulators of intracellular membrane trafficking, from the formation of
	<b>Ptger3</b>	6	Transport vesicles to their fusion with membranes (Sakata et al., 2010).
	Ppfibp2	6	No literature available on function
	Gpm6b	6	No literature available on function
	Ube2g1	6	No literature available on function
	Zdhhc5	6	Palmitoyl acyltransferase for the G-protein coupled receptor SSTR5
	Dock1	6	Involved in cytoskeletal rearrangements required for phagocytosis of apoptotic cells and cell motility.
	Unc45b	6	Acts as a co-chaperone for HSP90 and is required for proper folding of the myosin motor domain. Plays a role in sarcomere formation during muscle cell development
	Vat1	6	The protein encoded by this gene is an abundant integral membrane protein of cholinergic synaptic vesicles and is thought to be involved in vesicular transport.
	Pgs1	6	No literature available on function

<sup>a</sup> Sum of target prediction programs that predict that miR-96 will bind to a given gene. Target prediction programs taken into account: miRanda, miRDB, miRWalk, RNA Hybrid, PICTAR5, PITA, RNA22 and Targetscan.

<sup>b</sup> Gene function as per NCBI Gene cards and where referenced, primary litera

**Table A2.5 Predicted mRNA targets of miR-181a**

Mouse miR	Gene	Sum of target prediction programs <sup>a</sup>	Gene function <sup>b</sup>
MiR-181a	Smad7	7	Growth inhibitor. Inhibits proliferation and TGFβ signaling. Expression of Smad7 shown to promote IL-17A <sup>+</sup> IFN-γ <sup>+</sup> cells (Rizzo et al., 2014). Smad7 knockdown in clinical trials for patients with active CD. Drives Th1 response in EAE and MS (Kleiter et al., 2010; Zorzi et al., 2013).
	Kank1	7	Involved in regulation of actin polymerization and cell motility.
	Lmo3	7	Oncoprotein and plays a role in adipogenesis
	Npepps	7	Limits MHC class I presentation in DCs. Impedes development of neuropathology by inhibiting TAU-induced neurodegeneration.
	Rnf145	7	No literature available
	Zic3	7	Involved in cardiac gene expression, development of the inner ear and converts fibroblasts to neural progenitor-like cells
	Btbd3	7	Controls dendrite orientation towards active axons
	Bcl6b	6	Required for activation of naive CD4 <sup>+</sup> T cells by TCR triggering (Takamori et al., 2004). Bazf deficient mice show aberrant regulation of hematopoiesis by T cells mediates magnitude of secondary response from CD8 <sup>+</sup> T cells (Broxmeyer et al., 2007).
	Dazap2	6	Not much lit. down-regulated in multiple myeloma. May be associated with cell cycle and proliferation
	Fkbp1a	6	Regulates notch1 to facilitate cell communication between endocardium and myocardium
	Ywhag	6	Proto-oncogene. Overexpressed in various cancers.
	Abcd3	6	Likely plays an important role in peroxisome biogenesis
	Id2	6	ID2 knockdown in GVHD led to aberrant IL-10 prod by effector T cells. Necessary for development of EAE (Lin et al., 2012). ID2-deficient T cells results increased expression of SOCS3 and BIM on activated cells (Lin et al., 2012). Furthermore, CD4 <sup>+</sup> T cells deficient in ID2 show decreased proliferation and increased cell death (Lin et al., 2012).
	Cttnbp2nl	6	No literature available
	Tnfrsf11b	6	Involved in production of osteoprotegerin, a protein important for bone remodelling
	Plcl2	6	Not much literature. Modulates pain behavior in neuropathic pain model in mice
	Adcy1	6	Potentiates insulin secretion from MIN6 cells, mutations cause severe hearing impairment.
	Atp1b1	6	Required for blastocyst formation and cardiac contractility. Plays a role in renal handling of fluid balance
	Tgfbi	6	Anti-adhesion protein that reduces metastatic potential of cancers
	Prdm4	6	Critical mediator of cell death, mitosis and differentiation of neural stem cells

<b>Mouse miR</b>	<b>Gene</b>	<b>Sum of target prediction programs<sup>a</sup></b>	<b>Gene function<sup>b</sup></b>
MiR-181a	Hmgb2	6	Promotes cell viability metastatic and chemotherapeutic resistance in cancers
	Unc5a	6	Tumour suppressor in bladder cancer. Promotes neuronal apoptosis during spinal cord development
	Klhl8	6	No literature available
	Trspap1	6	No literature available
	Fbxl3	6	Role in circadian rhythm
	Mgat3	6	Biomarker for prognosis and therapy of alzheimers
	Arhgef3	6	Involved in iron uptake and implicated in osteoporosis
	Tox	6	Role in thymocyte selection. Required for CD4 <sup>+</sup> Lineage commitment
	Klf15	6	Pro-adipogenic transcription factor.
	Wsb1	6	Binds to IL-21 and enhances it's maturation. Increased survival of neuroblastoma (Nara et al., 2011).
	Baz2b	6	Not much literature available
	Etv6	6	Forms a fusion gene with Runx1. Susceptibility loci for ALL.
	Cpd	6	Role in intracellular trafficking. Thought to play a role in TGF beta signaling
	Crebl2	6	Involved in adipogenesis
	Ppp3r1	6	Involved in cardiac contractility, beta cell formation and bone formation
	Lmbrd2	6	No literature available
	Esr1	6	Estrogen receptor 1. Shown to induce Tregs in EAE and inhibit inflammatory cytokine production
	Tmem116	6	No literature available
	Psmf1	6	Selective modulator of proteasome mediated MHC class I Ag presentation
	Afap1	6	Actin filament associated protein 1. Not a lot of specific literature on Afap1 but other Afaps involved in modulation of actin cytoskeleton
	Yipf4	6	No literature available
	Lin28	6	Neurogenesis, tissue repair, oncogene
	Mlf1	6	Regulates Runx Protein levels (drosophilla.). Plays a role in cell proliferation (Bras et al., 2012).
Wnk1	6	Plays a role in maintaining blood pressure	

Mouse miR	Gene	Sum of target prediction programs <sup>a</sup>	Gene function <sup>b</sup>
MiR-181a	Eif4a2	6	No literature on function
	Ibtk	6	No literature available
	AC121108.12	6	Involved in lipid mobilisation in adipocytes.
	Ddx55	6	No literature available
	Illa	6	Not T cells intrinsic
	Cpne2	6	Calcium binding protein expressed by neutrophils. Thought to play a role in their differentiation
	Fbxo11	6	Suppresses p53 function. Thought to be involved in TGF beta signalling. Not much lit available
	Tbpl1	6	Involved in spermatogenesis
	Napg	6	No specific lit on function. Gene variants are implicated in bipolar disorder
	Mkrn1	6	Controls cells cycle arrest and apoptosis.
	Ssx2ip	6	Promotes metastasis and chemoresistance of hepatocellular carcinoma
	Tbc1d15	6	No literature on function
	Hoxa11	6	Control chondrocyte differentiation upstream of Runx2
	Jazf1	6	Susceptibility loci for T2D
	Gatm	6	No literature on function
	Atp5l	6	ATP Synthase
	Ghitm	6	Transmembrane protein. Found to be differentially expressed in Jurkat T cells when stim with CXCL10/CXCL12. No literature on function
	Fign	6	No literature on function
	Slc39a8	6	Solute carrier family 39.
	Heatr5a	6	No literature on function
<b>Tgfb1</b>	6	Validated target of miR-181a. Activated TGFβR1 phosphorylates Smad2, results in Smad2-Smad4 complex translocating to the nucleus and modulating expression of TGFβ associated genes (Liu et al., 2012).	
Dock4	6	GTPase activator. It regulates dendrite development in neurones and promotes cancer cell migration	
Pak7	6	Promotes gastric cancer by promoting cell proliferation. It can promote neurite outgrowth and stabilise microtubule formation	

Mouse miR	Gene	Sum of target prediction programs <sup>a</sup>	Gene function <sup>b</sup>
MiR-181a	Nol4	6	No literature on function
	Ss1811	6	No literature on function
	Mtmr12	6	No literature on function
	Spire1	6	Involved in vesicle transport processes
	St8sia4	6	Required for synthesis of Polysialic acid, a modulator of neural adhesion molecule NCAM1
	Sgpp1	6	Regulates Sphingolipid metabolism and apoptosis
	Hck	6	Belongs to Src family of tyrosine kinases. Acts downstream of IFNG, IL-2, IL-6, IL-8 and Fc Receptors
	Itga2	6	Regulates neutrophil recruitment during DSS colitis. Marker of Tr1 cells
	Fos	6	Together with JUN, C-fos forms the TF AP-1. Blocking of AP-1 results in diminishes Th1/Th17 differentiation and increased FoxP3 in GVHD (Park et al., 2014). AP-1 also shown to promote expression of IL-23p19 in macrophages (Liu et al., 2009).
	<b>Prkcd</b>	6	Validated miR-181a target (Chen et al., 2014). Lack of PKRCD leads to autoreactive B cells.
	Plk4	6	Involved in spindle formation during cell cycle
	Lmo1	6	Oncogene. Promotes T cell lymphocytic leukaemia
	Ddx3x	6	RNA helicase. Not much literature on function
	Hoxa1	6	Promotes tumour growth.
	Zfand5	6	Involved in osteoclast differentiation
	Wasl	6	Highly expressed in neural tissues. Associates with signaling molecules to alter actin cytoskeleton
	Spata9	6	Involved in spermatogenesis
	Gabra1	6	GABA A receptor. Involved in neuronal signaling. Implicated in epilepsy
	Pdhx	6	No literature on function
	Ddit4	6	Regulates cell growth, proliferation and survival via inhibition of mTORC1
	Spry4	6	Inhibitor of MAPK signaling pathway
Il6	6	IL-6 promotes Th17 cell development	
Sel1l	6	Regulates beta cell function and growth	
Tanc2	6	Regulation of dendritic spines and spinal memory and cytoskeletal rearrangements	

<b>Mouse miR</b>	<b>Gene</b>	<b>Sum of target prediction programs<sup>a</sup></b>	<b>Gene function<sup>b</sup></b>
MiR-181a	Aftph	6	No literature on function
	Zyg11b	6	No literature on function
	Gpr22	6	G-protein coupled receptor involved in cardiovascular function
	<b>E2f5</b>	6	Validated miR-181a target. Promotes hepatocellular cancer and gastric cancer. Involved in cell cycle and embryogenesis (Zou et al., 2014)
	Epc2	6	No literature on function
	Nr6a1	6	Receptor involved in germ cell development and neurogenesis
	Rad21	6	Involved in mitosis

<sup>a</sup> Sum of target prediction programs that predict that miR-181a will bind to a given gene. Target prediction programs taken into account: miRanda, miRDB, miRWalk, RNA Hybrid, PICTAR5, PITA, RNA22 and Targetscan.

<sup>b</sup> Gene function as per NCBI Gene cards and where referenced, primary literature.

## ABBREVIATIONS

ABTS	2,2'-azino-bis(3-ethylbenzothiazoline-6-sulphonic acid)
ADP	Adenosine diphosphate
AE	Accessibility energy
AHR	Aryl hydrocarbon receptor
ANOVA	Analysis of variance
APC	Allophycocyanin (fluorochrome)
APCs	Antigen-presenting cells
ARGM	Acetylnithine aminotransferase
ATG16L1	Autophagy related 16-like 1
ATP	Adenosine triphosphate
B6	C57BL/6 mouse
BCL2	B-cell CLL/Lymphoma 2
BCR	B-cell receptor
BMDC	Bone-marrow-derived dendritic cell
BSA	Bovine serum albumin
BV	Brilliant violet
c-Myb	C-Myb Avian myeloblastosis viral oncogene homolog
CD	Cluster of differentiation
CD	Crohn's disease
CDH4	Adherin 4, Type 1, R-cadherin (retinal)
CDK2	Cyclin-dependent kinase 2
cDNA	Complimentary deoxyribonucleic acids
CLL	Chronic lymphocytic leukemia
Cre	Cre recombinase
CTLA-4	Cytotoxic T lymphocyte antigen-4
CXCL12 $\beta$	Chemokine (C-X-C motif) ligand 12 $\beta$
CXCR3	Chemokine (C-X-C motif) receptor 3
DAP	Death-associated protein

Dapk1	Death-associated protein kinase 1
DC	Dendritic cell
DEPC	Diethylpyrocarbonate
DGCR8	Di George Syndrome Critical Region 8
DNA	Deoxyribonucleic acids
dNTP	Deoxynucleotide triphosphate
DSS	Dextran sodium sulphate
DTT	Dithiothreitol
DUSP5/6	Dual specificity phosphatase 5/6
EAE	Experimental autoimmune encephalomyelitis
eBio	eBioscience
ECM1	Extracellular matrix protein 1
EDTA	Ethylenediaminetetraacetic acid
ELF4	E74-like Factor 4 (Ets domain transcription factor)
ELISA	Enzyme-linked immunosorbant assay
Ets-1	V-ets avian erythroblastosis virus E26 oncogene homolog 1
eYFP	Enhanced yellow fluorescent protein
FACS	Fluorescence activated cell sorting
FBS	Fetal bovine serum
FCS	Fetal calf serum
FDR	False discovery rate
FGFR2	Fibroblast growth factor receptor 2
FITC	Fluorescein Isothiocyanate
FOXO3a	Forkhead box O3
FoxP3	Forkhead box P3
GFP	Green fluorescent protein
GI	Gastro-intestinal
GM-CSF	Granulocyte macrophage-colony stimulating factor
GVHD	Graft versus host disease

GWAS	Genome-wide association studies
HC	Hematopoietic cells
HCV	Hepatitis C virus
<i>Hh</i>	<i>Helicobacter hepaticus</i>
<i>Hh</i> <sup>+</sup>	<i>Helicobacter hepaticus</i> -infected
HIF-1 $\alpha$	Hypoxia-inducible factor 1, alpha subunit
HNF4A	Hepatocyte nuclear factor 4, alpha
HPRT	Hypoxanthine guanine phosphoribosyl transferase
HRP	Horseradish peroxidase
IBD	Inflammatory bowel disease
ICS	Intracellular cytokine staining
IEC	Intestinal epithelial cells
IFN- $\gamma$	Interferon-gamma
Ig	Immunoglobulin
IL	Interleukin
IL-10R	IL-10 receptor
IRAK1	Interleukin-1 receptor-associated kinase 1
IRES	Internal ribosomal entry site
IRF4	Interferon regulatory factor 4
IRF5	Interferon regulatory factor 5
iTreg	<i>In vitro</i> -induced Treg
KLF13	Kruppel-Like factor 13
KO	Knock out
KRAS	Kirsten rat sarcoma viral oncogene homolog
KSR2	Kinase suppressor of Ras2
LAG-3	Lymphocyte activation gene 3
Lair1	Leukocyte-associated immunoglobulin-like receptor 1
LP	Lamina propria
M	Molar

mAb	Monoclonal antibody
MCL-1	Myeloid cell leukemia 1
MCP-1	Monocyte chemoattractant protein-1
ME	Mercaptoethanol
mg	Milligram
MHC	Major histocompatibility complex
miR	MicroRNA
MiRISC	MicroRNA loaded onto RNA-induced silencing complex
ml	Millilitre
MLNs	Mesenteric lymph nodes
mM	Millimolar
MMP-9	Matrix metalloprotease 9
mRNA	Messenger RNA
NCAM-1	Neural cell adhesion molecule 1
NEAA	Non-essential amino acids
NF- $\kappa$ B	Nuclear Factor kappa-light-chain enhancer of activated B cells
NFAT	Nuclear factor of activated T-cells
NOD2	Nucleotide-binding oligomerization domain containing 2
NRP1	Neuropilin-1
OD	Optical density
OVA	Ovalbumin
p-bodies	Processing bodies
PAMPs	Pathogen-associated molecular patterns
PBMCs	Peripheral blood mononuclear cells
PBS	Phosphate buffered saline
PCA	Principal component analysis
PCR	Polymerase chain reaction
PDCD4	Programmed cell death 4
PE	Phytoertherin

PE-Cy7	Phycoertherin-cyanine 7
Peli1	Pellino 1
PerCP	Perdinin chlorophyll protein
Perm	Permeabilisation buffer
PFA	Paraformaldehyde
PIAS3	Protein inhibitor of activated stat, 3
PMA	Phorbol 12-myristate 13-acetate
Ppp2r5c	Protein phosphatase 2, regulatory subunit B
Pre-miRNA	Precursor-microRNA
Pri-miRNA	Primary microRNA
PRKC $\epsilon$	Protein Kinase C epsilon
PRRs	Pathogen recognition receptors
PTPN22	Protein tyrosine phosphatase, non-receptor type 22
pTreg	Peripherally-derived Treg
PV	Polycystic Vulgaris
qRT-PCR	Quantitative real-time polymerase chain reaction
rad	Radiation absorbed dose
RAG	Recombination activating gene
RANTES	Regulated on activation, normal T expressed and secreted
Rhoa	Ras homolog family member A
RhoB	Ras homolog family member B
RIN	RNA integrity number
RISC	RNA-induced silencing complex
RNA	Ribonucleic acid
RNU6	RNA, U6 small nuclear 6
ROR $\gamma$ t	Retinoic-acid related orphan receptor- $\gamma$ t
rpm	Revolutions per minute
RPMI	Roswell Park memorial institute
RT	Reverse transcription

Runx1	Runt-related transcription factor-1
Runx3	Runt-related transcription factor-3
SCID	Severe combined immunodeficiency
SDS	Sodium dodecyl sulphate
SEM	Standard error of the mean
ShelAg	Soluble <i>H. hepaticus</i> antigen preparation
SHIP-1	Src homology-2 domain-containing inositol5-phosphatase 1
SHP-2	Src homology-2 domain-containing protein tyrosine phosphatase 2
Siah2	Siah E3 Ubiquitin protein ligase 2
SIN3A	Sin3 transcription regulator family member A
siRNA	Silencing ribonucleic acids
SLE	Systemic Lupus Erythematosus
Smad7	Mothers against decapentaplegic homolog 7
SOCS1	Suppressor of cytokine signaling 1
SPF	Specific pathogen free
STAT	Signal transducer and activator of transcription
T-bet	T-box transcription factor T
TCR	T-cell receptor
TGF- $\beta$	Transforming growth factor $\beta$
Th	T-helper
<i>Tiger</i>	Interleukin-ten ires gfp-enhanced reporter
TIGIT	T-cell immune-receptor with immunoglobulin and ITIM domain
TLR	Toll-like receptor
TNBS	Tri-nitro benzene sulphonic acid
TNF- $\alpha$	Tumour necrosis factor $\alpha$
Tr1	T regulatory 1
TRAF6	TNF Receptor-associated factor 6
Treg	T regulatory cell
tTreg	Thymically-derived Treg

U	Units
UC	Ulcerative colitis
UTR	Untranslated region
UV	Ultra violet
Wk	Week
WT	Wild-type
x g	Times gravity
XIAP	X-linked inhibitor of apoptosis
ZMIZ1	Zinc-finger, MIZ-type containing 1
µg	Microgram
µl	Microlitre
µM	Micromolar

## REFERENCES

- Abbas, A.K., Benoist, C., Bluestone, J.A., Campbell, D.J., Ghosh, S., Hori, S., Jiang, S., Kuchroo, V.K., Mathis, D., Roncarolo, M.G., *et al.* (2013). Regulatory T cells: recommendations to simplify the nomenclature. *Nat Immunol* *14*, 307-308.
- Afkarian, M., Sedy, J.R., Yang, J., Jacobson, N.G., Cereb, N., Yang, S.Y., Murphy, T.L., and Murphy, K.M. (2002). T-bet is a STAT1-induced regulator of IL-12R expression in naive CD4<sup>+</sup> T cells. *Nat Immunol* *3*, 549-557.
- Aggarwal, S., Ghilardi, N., Xie, M.H., de Sauvage, F.J., and Gurney, A.L. (2003). Interleukin-23 promotes a distinct CD4 T cell activation state characterized by the production of interleukin-17. *J Biol Chem* *278*, 1910-1914.
- Ahlfors, H., Morrison, P.J., Duarte, J.H., Li, Y., Biro, J., Tolaini, M., Di Meglio, P., Potocnik, A.J., and Stockinger, B. (2014). IL-22 fate reporter reveals origin and control of IL-22 production in homeostasis and infection. *J Immunol* *193*, 4602-4613.
- Akimova, T., Beier, U.H., Wang, L., Levine, M.H., and Hancock, W.W. (2011). Helios expression is a marker of T cell activation and proliferation. *PLoS One* *6*, e24226.
- Alevizos, I., and Illei, G.G. (2010). MicroRNAs as biomarkers in rheumatic diseases. *Nat Rev Rheumatol* *6*, 391-398.
- Altwegg, R., and Vincent, T. (2014). TNF blocking therapies and immunomonitoring in patients with inflammatory bowel disease. *Mediators Inflamm* *2014*, 172821.
- Aluwihare, P., Mu, Z., Zhao, Z., Yu, D., Weinreb, P.H., Horan, G.S., Violette, S.M., and Munger, J.S. (2009). Mice that lack activity of alphavbeta6- and alphavbeta8-integrins reproduce the abnormalities of Tgfb1- and Tgfb3-null mice. *J Cell Sci* *122*, 227-232.
- Ambros, V. (2004). The functions of animal microRNAs. *Nature* *431*, 350-355.
- Amiot, A., and Peyrin-Biroulet, L. (2015). Current, new and future biological agents on the horizon for the treatment of inflammatory bowel diseases. *Therap Adv Gastroenterol* *8*, 66-82.
- Amsen, D., Antov, A., Jankovic, D., Sher, A., Radtke, F., Souabni, A., Busslinger, M., McCright, B., Gridley, T., and Flavell, R.A. (2007). Direct regulation of Gata3 expression determines the T helper differentiation potential of Notch. *Immunity* *27*, 89-99.
- Anderson, C.A., Boucher, G., Lees, C.W., Franke, A., D'Amato, M., Taylor, K.D., Lee, J.C., Goyette, P., Imielinski, M., Latiano, A., *et al.* (2011). Meta-analysis identifies 29 additional ulcerative colitis risk loci, increasing the number of confirmed associations to 47. *Nat Genet* *43*, 246-252.
- Anderson, C.F., Oukka, M., Kuchroo, V.J., and Sacks, D. (2007). CD4(+)CD25(-)Foxp3(-) Th1 cells are the source of IL-10-mediated immune suppression in chronic cutaneous leishmaniasis. *J Exp Med* *204*, 285-297.
- Annes, J.P., Munger, J.S., and Rifkin, D.B. (2003). Making sense of latent TGFbeta activation. *J Cell Sci* *116*, 217-224.

- Annunziato, F., Cosmi, L., Santarlasci, V., Maggi, L., Liotta, F., Mazzinghi, B., Parente, E., Fili, L., Ferri, S., Frosali, F., *et al.* (2007). Phenotypic and functional features of human Th17 cells. *J Exp Med* 204, 1849-1861.
- Antiga, E., Volpi, W., Cardilicchia, E., Maggi, L., Fili, L., Manuelli, C., Parronchi, P., Fabbri, P., and Caproni, M. (2012). Etanercept downregulates the Th17 pathway and decreases the IL-17+/IL-10+ cell ratio in patients with psoriasis vulgaris. *J Clin Immunol* 32, 1221-1232.
- Apostolou, I., and von Boehmer, H. (2004). In vivo instruction of suppressor commitment in naive T cells. *J Exp Med* 199, 1401-1408.
- Araya, J., Cambier, S., Morris, A., Finkbeiner, W., and Nishimura, S.L. (2006). Integrin-mediated transforming growth factor-beta activation regulates homeostasis of the pulmonary epithelial-mesenchymal trophic unit. *Am J Pathol* 169, 405-415.
- Arpaia, N., Campbell, C., Fan, X., Dikiy, S., van der Veecken, J., deRoos, P., Liu, H., Cross, J.R., Pfeffer, K., Coffey, P.J., and Rudensky, A.Y. (2013). Metabolites produced by commensal bacteria promote peripheral regulatory T-cell generation. *Nature* 504, 451-455.
- Arvey, A., Larsson, E., Sander, C., Leslie, C.S., and Marks, D.S. (2010). Target mRNA abundance dilutes microRNA and siRNA activity. *Mol Syst Biol* 6, 363.
- Asangani, I.A., Rasheed, S.A., Nikolova, D.A., Leupold, J.H., Colburn, N.H., Post, S., and Allgayer, H. (2008). MicroRNA-21 (miR-21) post-transcriptionally downregulates tumor suppressor Pcd4 and stimulates invasion, intravasation and metastasis in colorectal cancer. *Oncogene* 27, 2128-2136.
- Asigbetse, K.E., Eigenmann, P.A., and Frossard, C.P. (2010). Intestinal lamina propria TcR $\gamma$ delta+ lymphocytes selectively express IL-10 and IL-17. *J Investig Allergol Clin Immunol* 20, 391-401.
- Askenasy, N. (2013). Enhanced killing activity of regulatory T cells ameliorates inflammation and autoimmunity. *Autoimmun Rev* 12, 972-975.
- Asseman, C., Mauze, S., Leach, M.W., Coffman, R.L., and Powrie, F. (1999). An essential role for interleukin 10 in the function of regulatory T cells that inhibit intestinal inflammation. *J Exp Med* 190, 995-1004.
- Asseman, C., and von Herrath, M. (2003). Regulation of viral and autoimmune responses. *Novartis Found Symp* 252, 239-253; discussion 253-267.
- Atarashi, K., Tanoue, T., Oshima, K., Suda, W., Nagano, Y., Nishikawa, H., Fukuda, S., Saito, T., Narushima, S., Hase, K., *et al.* (2013). Treg induction by a rationally selected mixture of Clostridia strains from the human microbiota. *Nature* 500, 232-236.
- Atarashi, K., Tanoue, T., Shima, T., Imaoka, A., Kuwahara, T., Momose, Y., Cheng, G., Yamasaki, S., Saito, T., Ohba, Y., *et al.* (2011). Induction of colonic regulatory T cells by indigenous Clostridium species. *Science* 331, 337-341.
- Aujla, S.J., Chan, Y.R., Zheng, M., Fei, M., Askew, D.J., Pociask, D.A., Reinhart, T.A., McAllister, F., Edeal, J., Gaus, K., *et al.* (2008). IL-22 mediates mucosal host defense against Gram-negative bacterial pneumonia. *Nat Med* 14, 275-281.

- Aung, L.L., Mouradian, M.M., Dhib-Jalbut, S., and Balashov, K.E. (2015). MMP-9 expression is increased in B lymphocytes during multiple sclerosis exacerbation and is regulated by microRNA-320a. *J Neuroimmunol* 278, 185-189.
- Awasthi, A., Carrier, Y., Peron, J.P., Bettelli, E., Kamanaka, M., Flavell, R.A., Kuchroo, V.K., Oukka, M., and Weiner, H.L. (2007). A dominant function for interleukin 27 in generating interleukin 10-producing anti-inflammatory T cells. *Nat Immunol* 8, 1380-1389.
- Bacchetta, R., Passerini, L., Gambineri, E., Dai, M., Allan, S.E., Perroni, L., Dagna-Bricarelli, F., Sartirana, C., Matthes-Martin, S., Lawitschka, A., *et al.* (2006). Defective regulatory and effector T cell functions in patients with FOXP3 mutations. *J Clin Invest* 116, 1713-1722.
- Bader, A.G., Brown, D., and Winkler, M. (2010). The promise of microRNA replacement therapy. *Cancer Res* 70, 7027-7030.
- Bakdash, G., Vogelpoel, L.T., van Capel, T.M., Kapsenberg, M.L., and de Jong, E.C. (2015). Retinoic acid primes human dendritic cells to induce gut-homing, IL-10-producing regulatory T cells. *Mucosal Immunol* 8, 265-278.
- Barbara, G., Xing, Z., Hogaboam, C.M., Gauldie, J., and Collins, S.M. (2000). Interleukin 10 gene transfer prevents experimental colitis in rats. *Gut* 46, 344-349.
- Barner, M., Mohrs, M., Brombacher, F., and Kopf, M. (1998). Differences between IL-4R alpha-deficient and IL-4-deficient mice reveal a role for IL-13 in the regulation of Th2 responses. *Curr Biol* 8, 669-672.
- Bartel, D.P. (2004). MicroRNAs: genomics, biogenesis, mechanism, and function. *Cell* 116, 281-297.
- Basu, R., O'Quinn, D.B., Silberberger, D.J., Schoeb, T.R., Fouser, L., Ouyang, W., Hatton, R.D., and Weaver, C.T. (2012). Th22 cells are an important source of IL-22 for host protection against enteropathogenic bacteria. *Immunity* 37, 1061-1075.
- Behm-Ansmant, I., Rehwinkel, J., Doerks, T., Stark, A., Bork, P., and Izaurralde, E. (2006). mRNA degradation by miRNAs and GW182 requires both CCR4:NOT deadenylase and DCP1:DCP2 decapping complexes. *Genes Dev* 20, 1885-1898.
- Benjamini, Y., Drai, D., Elmer, G., Kafkafi, N., and Golani, I. (2001). Controlling the false discovery rate in behavior genetics research. *Behav Brain Res* 125, 279-284.
- Bergman, P., James, T., Kular, L., Ruhrmann, S., Kramarova, T., Kvist, A., Supic, G., Gillett, A., Pivarski, A., and Jagodic, M. (2013). Next-generation sequencing identifies microRNAs that associate with pathogenic autoimmune neuroinflammation in rats. *J Immunol* 190, 4066-4075.
- Bettelli, E., Carrier, Y., Gao, W., Korn, T., Strom, T.B., Oukka, M., Weiner, H.L., and Kuchroo, V.K. (2006). Reciprocal developmental pathways for the generation of pathogenic effector TH17 and regulatory T cells. *Nature* 441, 235-238.
- Bevan, M.J. (2004). Helping the CD8(+) T-cell response. *Nat Rev Immunol* 4, 595-602.

- Bhaskaran, N., Cohen, S., Zhang, Y., Weinberg, A., and Pandiyan, P. (2015). TLR-2 Signaling Promotes IL-17A Production in CD4<sup>+</sup>CD25<sup>+</sup>Foxp3<sup>+</sup> Regulatory Cells during Oropharyngeal Candidiasis. *Pathogens* 4, 90-110.
- Bibiloni, R., Mangold, M., Madsen, K.L., Fedorak, R.N., and Tannock, G.W. (2006). The bacteriology of biopsies differs between newly diagnosed, untreated, Crohn's disease and ulcerative colitis patients. *J Med Microbiol* 55, 1141-1149.
- Boirivant, M., Pallone, F., Di Giacinto, C., Fina, D., Monteleone, I., Marinaro, M., Caruso, R., Colantoni, A., Palmieri, G., Sanchez, M., *et al.* (2006). Inhibition of Smad7 with a specific antisense oligonucleotide facilitates TGF-beta1-mediated suppression of colitis. *Gastroenterology* 131, 1786-1798.
- Bonilla, F.A., and Oettgen, H.C. (2010). Adaptive immunity. *J Allergy Clin Immunol* 125, S33-40.
- Borsellino, G., Kleinewietfeld, M., Di Mitri, D., Sternjak, A., Diamantini, A., Giometto, R., Hopner, S., Centonze, D., Bernardi, G., Dell'Acqua, M.L., *et al.* (2007). Expression of ectonucleotidase CD39 by Foxp3<sup>+</sup> Treg cells: hydrolysis of extracellular ATP and immune suppression. *Blood* 110, 1225-1232.
- Brain, O., Owens, B.M., Pichulik, T., Allan, P., Khatamzas, E., Leslie, A., Steevels, T., Sharma, S., Mayer, A., Catuneanu, A.M., *et al.* (2013). The intracellular sensor NOD2 induces microRNA-29 expression in human dendritic cells to limit IL-23 release. *Immunity* 39, 521-536.
- Bras, S., Martin-Lannere, S., Gobert, V., Auge, B., Breig, O., Sanial, M., Yamaguchi, M., Haenlin, M., Plessis, A., and Waltzer, L. (2012). Myeloid leukemia factor is a conserved regulator of RUNX transcription factor activity involved in hematopoiesis. *Proc Natl Acad Sci U S A* 109, 4986-4991.
- Brennecke, J., Stark, A., Russell, R.B., and Cohen, S.M. (2005). Principles of microRNA-target recognition. *PLoS Biol* 3, e85.
- Breuer, R., Becker, M.S., Brechmann, M., Mock, T., Arnold, R., and Krammer, P.H. (2014). The protein phosphatase 2A regulatory subunit B56gamma mediates suppression of T cell receptor (TCR)-induced nuclear factor-kappaB (NF-kappaB) activity. *J Biol Chem* 289, 14996-15004.
- Broxmeyer, H.E., Sehra, S., Cooper, S., Toney, L.M., Kusam, S., Aloor, J.J., Marchal, C.C., Dinauer, M.C., and Dent, A.L. (2007). Aberrant regulation of hematopoiesis by T cells in BAZF-deficient mice. *Mol Cell Biol* 27, 5275-5285.
- Brucklacher-Waldert, V., Carr, E.J., Linterman, M.A., and Veldhoen, M. (2014). Cellular Plasticity of CD4<sup>+</sup> T Cells in the Intestine. *Front Immunol* 5, 488.
- Brustle, A., Heink, S., Huber, M., Rosenplanter, C., Stadelmann, C., Yu, P., Arpaia, E., Mak, T.W., Kamradt, T., and Lohoff, M. (2007). The development of inflammatory T(H)-17 cells requires interferon-regulatory factor 4. *Nat Immunol* 8, 958-966.
- Bunpo, P., Cundiff, J.K., Reinert, R.B., Wek, R.C., Aldrich, C.J., and Anthony, T.G. (2010). The eIF2 kinase GCN2 is essential for the murine immune system to adapt to amino acid deprivation by asparaginase. *J Nutr* 140, 2020-2027.

- Burchill, M.A., Yang, J., Vang, K.B., Moon, J.J., Chu, H.H., Lio, C.W., Vegoe, A.L., Hsieh, C.S., Jenkins, M.K., and Farrar, M.A. (2008). Linked T cell receptor and cytokine signaling govern the development of the regulatory T cell repertoire. *Immunity* 28, 112-121.
- Burger, D., and Travis, S. (2011). Conventional medical management of inflammatory bowel disease. *Gastroenterology* 140, 1827-1837 e1822.
- Buruiana, F.E., Sola, I., and Alonso-Coello, P. (2010). Recombinant human interleukin 10 for induction of remission in Crohn's disease. *Cochrane Database Syst Rev*, CD005109.
- Busk, M., Pytela, R., and Sheppard, D. (1992). Characterization of the integrin alpha v beta 6 as a fibronectin-binding protein. *J Biol Chem* 267, 5790-5796.
- Calin, G.A., and Croce, C.M. (2006). MicroRNA signatures in human cancers. *Nat Rev Cancer* 6, 857-866.
- Campbell, D.J., and Butcher, E.C. (2002). Rapid acquisition of tissue-specific homing phenotypes by CD4(+) T cells activated in cutaneous or mucosal lymphoid tissues. *J Exp Med* 195, 135-141.
- Canavan, J.B., Scotta, C., Vossenkamper, A., Goldberg, R., Elder, M.J., Shoval, I., Marks, E., Stolarczyk, E., Lo, J.W., Powell, N., *et al.* (2015). Developing in vitro expanded CD45RA+ regulatory T cells as an adoptive cell therapy for Crohn's disease. *Gut*.
- Cannons, J.L., Yu, L.J., Jankovic, D., Crotty, S., Horai, R., Kirby, M., Anderson, S., Cheever, A.W., Sher, A., and Schwartzberg, P.L. (2006). SAP regulates T cell-mediated help for humoral immunity by a mechanism distinct from cytokine regulation. *J Exp Med* 203, 1551-1565.
- Cao, X., Cai, S.F., Fehniger, T.A., Song, J., Collins, L.I., Piwnica-Worms, D.R., and Ley, T.J. (2007). Granzyme B and perforin are important for regulatory T cell-mediated suppression of tumor clearance. *Immunity* 27, 635-646.
- Carrier, Y., Yuan, J., Kuchroo, V.K., and Weiner, H.L. (2007). Th3 cells in peripheral tolerance. I. Induction of Foxp3-positive regulatory T cells by Th3 cells derived from TGF-beta T cell-transgenic mice. *J Immunol* 178, 179-185.
- Carthew, R.W., and Sontheimer, E.J. (2009). Origins and Mechanisms of miRNAs and siRNAs. *Cell* 136, 642-655.
- Cebula, A., Seweryn, M., Rempala, G.A., Pabla, S.S., McIndoe, R.A., Denning, T.L., Bry, L., Kraj, P., Kisielow, P., and Ignatowicz, L. (2013). Thymus-derived regulatory T cells contribute to tolerance to commensal microbiota. *Nature* 497, 258-262.
- Chakilam, S., Gandesiri, M., Rau, T.T., Agaimy, A., Vijayalakshmi, M., Ivanovska, J., Wirtz, R.M., Schulze-Luehrmann, J., Benderska, N., Wittkopf, N., *et al.* (2013). Death-associated protein kinase controls STAT3 activity in intestinal epithelial cells. *Am J Pathol* 182, 1005-1020.

- Chan, V.S., Wong, C., and Ohashi, P.S. (2002). Calcineurin Aalpha plays an exclusive role in TCR signaling in mature but not in immature T cells. *Eur J Immunol* *32*, 1223-1229.
- Chang, H.C., Sehra, S., Goswami, R., Yao, W., Yu, Q., Stritesky, G.L., Jabeen, R., McKinley, C., Ahyi, A.N., Han, L., *et al.* (2010). The transcription factor PU.1 is required for the development of IL-9-producing T cells and allergic inflammation. *Nat Immunol* *11*, 527-534.
- Chang, M., Jin, W., Chang, J.H., Xiao, Y., Brittain, G.C., Yu, J., Zhou, X., Wang, Y.H., Cheng, X., Li, P., *et al.* (2011). The ubiquitin ligase Peli1 negatively regulates T cell activation and prevents autoimmunity. *Nat Immunol* *12*, 1002-1009.
- Chang, M., Lee, A.J., Fitzpatrick, L., Zhang, M., and Sun, S.C. (2009). NF-kappa B1 p105 regulates T cell homeostasis and prevents chronic inflammation. *J Immunol* *182*, 3131-3138.
- Chang, P.V., Hao, L., Offermanns, S., and Medzhitov, R. (2014). The microbial metabolite butyrate regulates intestinal macrophage function via histone deacetylase inhibition. *Proc Natl Acad Sci U S A* *111*, 2247-2252.
- Chang, S., Collins, P.L., and Aune, T.M. (2008). T-bet dependent removal of Sin3A-histone deacetylase complexes at the *Ifng* locus drives Th1 differentiation. *J Immunol* *181*, 8372-8381.
- Chaplin, D.D. (2010). Overview of the immune response. *J Allergy Clin Immunol* *125*, S3-23.
- Chatila, T.A., Blaeser, F., Ho, N., Lederman, H.M., Voulgaropoulos, C., Helms, C., and Bowcock, A.M. (2000). JM2, encoding a fork head-related protein, is mutated in X-linked autoimmunity-allergic dysregulation syndrome. *J Clin Invest* *106*, R75-81.
- Chau, B.N., Xin, C., Hartner, J., Ren, S., Castano, A.P., Linn, G., Li, J., Tran, P.T., Kaimal, V., Huang, X., *et al.* (2012). MicroRNA-21 promotes fibrosis of the kidney by silencing metabolic pathways. *Sci Transl Med* *4*, 121ra118.
- Chaudhry, A., Samstein, R.M., Treuting, P., Liang, Y., Pils, M.C., Heinrich, J.M., Jack, R.S., Wunderlich, F.T., Bruning, J.C., Muller, W., and Rudensky, A.Y. (2011). Interleukin-10 signaling in regulatory T cells is required for suppression of Th17 cell-mediated inflammation. *Immunity* *34*, 566-578.
- Chen, B., She, S., Li, D., Liu, Z., Yang, X., Zeng, Z., and Liu, F. (2013a). Role of miR-19a targeting TNF-alpha in mediating ulcerative colitis. *Scand J Gastroenterol* *48*, 815-824.
- Chen, Y., Ke, G., Han, D., Liang, S., Yang, G., and Wu, X. (2014). MicroRNA-181a enhances the chemoresistance of human cervical squamous cell carcinoma to cisplatin by targeting PRKCD. *Exp Cell Res* *320*, 12-20.
- Chen, Y., Xiao, Y., Ge, W., Zhou, K., Wen, J., Yan, W., Wang, Y., Wang, B., Qu, C., Wu, J., *et al.* (2013b). miR-200b inhibits TGF-beta1-induced epithelial-mesenchymal transition and promotes growth of intestinal epithelial cells. *Cell Death Dis* *4*, e541.

Chendrimada, T.P., Finn, K.J., Ji, X., Baillat, D., Gregory, R.I., Liebhaber, S.A., Pasquinelli, A.E., and Shiekhattar, R. (2007). MicroRNA silencing through RISC recruitment of eIF6. *Nature* 447, 823-828.

Chendrimada, T.P., Gregory, R.I., Kumaraswamy, E., Norman, J., Cooch, N., Nishikura, K., and Shiekhattar, R. (2005). TRBP recruits the Dicer complex to Ago2 for microRNA processing and gene silencing. *Nature* 436, 740-744.

Cho, J.Y., Akbarali, Y., Zerbini, L.F., Gu, X., Boltax, J., Wang, Y., Oettgen, P., Zhang, D.E., and Libermann, T.A. (2004). Isoforms of the Ets transcription factor NERF/ELF-2 physically interact with AML1 and mediate opposing effects on AML1-mediated transcription of the B cell-specific blk gene. *J Biol Chem* 279, 19512-19522.

Chuang, Y.T., Fang, L.W., Lin-Feng, M.H., Chen, R.H., and Lai, M.Z. (2008). The tumor suppressor death-associated protein kinase targets to TCR-stimulated NF-kappa B activation. *J Immunol* 180, 3238-3249.

Chung, Y., Chang, S.H., Martinez, G.J., Yang, X.O., Nurieva, R., Kang, H.S., Ma, L., Watowich, S.S., Jetten, A.M., Tian, Q., and Dong, C. (2009). Critical regulation of early Th17 cell differentiation by interleukin-1 signaling. *Immunity* 30, 576-587.

Cobb, B.S., Nesterova, T.B., Thompson, E., Hertweck, A., O'Connor, E., Godwin, J., Wilson, C.B., Brockdorff, N., Fisher, A.G., Smale, S.T., and Merckenschlager, M. (2005). T cell lineage choice and differentiation in the absence of the RNase III enzyme Dicer. *J Exp Med* 201, 1367-1373.

Colombel, J.F., Rutgeerts, P., Malchow, H., Jacyna, M., Nielsen, O.H., Rask-Madsen, J., Van Deventer, S., Ferguson, A., Desreumaux, P., Forbes, A., *et al.* (2001). Interleukin 10 (Tenovil) in the prevention of postoperative recurrence of Crohn's disease. *Gut* 49, 42-46.

Cong, Y., Brandwein, S.L., McCabe, R.P., Lazenby, A., Birkenmeier, E.H., Sundberg, J.P., and Elson, C.O. (1998). CD4+ T cells reactive to enteric bacterial antigens in spontaneously colitic C3H/HeJBir mice: increased T helper cell type 1 response and ability to transfer disease. *J Exp Med* 187, 855-864.

Consortium, U.I.G., Barrett, J.C., Lee, J.C., Lees, C.W., Prescott, N.J., Anderson, C.A., Phillips, A., Wesley, E., Parnell, K., Zhang, H., *et al.* (2009). Genome-wide association study of ulcerative colitis identifies three new susceptibility loci, including the HNF4A region. *Nat Genet* 41, 1330-1334.

Coombes, J.L., Siddiqui, K.R., Arancibia-Carcamo, C.V., Hall, J., Sun, C.M., Belkaid, Y., and Powrie, F. (2007). A functionally specialized population of mucosal CD103+ DCs induces Foxp3+ regulatory T cells via a TGF-beta and retinoic acid-dependent mechanism. *J Exp Med* 204, 1757-1764.

Cosmi, L., Maggi, L., Santarlasci, V., Capone, M., Cardilicchia, E., Frosali, F., Querci, V., Angeli, R., Matucci, A., Fambrini, M., *et al.* (2010). Identification of a novel subset of human circulating memory CD4(+) T cells that produce both IL-17A and IL-4. *J Allergy Clin Immunol* 125, 222-230 e221-224.

Cosmi, L., Maggi, L., Santarlasci, V., Liotta, F., and Annunziato, F. (2014). T helper cells plasticity in inflammation. *Cytometry A* 85, 36-42.

- Cummings, J.H., Pomare, E.W., Branch, W.J., Naylor, C.P., and Macfarlane, G.T. (1987). Short chain fatty acids in human large intestine, portal, hepatic and venous blood. *Gut* 28, 1221-1227.
- Dai, Y., Huang, Y.S., Tang, M., Lv, T.Y., Hu, C.X., Tan, Y.H., Xu, Z.M., and Yin, Y.B. (2007). Microarray analysis of microRNA expression in peripheral blood cells of systemic lupus erythematosus patients. *Lupus* 16, 939-946.
- Daniel, V., Trojan, K., Adamek, M., and Opelz, G. (2015). IFN $\gamma$ + Treg in-vivo and in-vitro represent both activated nTreg and peripherally induced aTreg and remain phenotypically stable in-vitro after removal of the stimulus. *BMC Immunol* 16, 45.
- Dardalhon, V., Awasthi, A., Kwon, H., Galileos, G., Gao, W., Sobel, R.A., Mitsdoerffer, M., Strom, T.B., Elyaman, W., Ho, I.C., *et al.* (2008). IL-4 inhibits TGF-beta-induced Foxp3+ T cells and, together with TGF-beta, generates IL-9+ IL-10+ Foxp3(-) effector T cells. *Nat Immunol* 9, 1347-1355.
- Desreumaux, P., Foussat, A., Allez, M., Beaugerie, L., Hebuterne, X., Bouhnik, Y., Nachury, M., Brun, V., Bastian, H., Belmonte, N., *et al.* (2012). Safety and efficacy of antigen-specific regulatory T-cell therapy for patients with refractory Crohn's disease. *Gastroenterology* 143, 1207-1217 e1201-1202.
- Dhodapkar, M.V., Steinman, R.M., Krasovsky, J., Munz, C., and Bhardwaj, N. (2001). Antigen-specific inhibition of effector T cell function in humans after injection of immature dendritic cells. *J Exp Med* 193, 233-238.
- Dieleman, L.A., Arends, A., Tonkonogy, S.L., Goerres, M.S., Craft, D.W., Grenther, W., Sellon, R.K., Balish, E., and Sartor, R.B. (2000). Helicobacter hepaticus does not induce or potentiate colitis in interleukin-10-deficient mice. *Infect Immun* 68, 5107-5113.
- Djuretic, I.M., Levanon, D., Negreanu, V., Groner, Y., Rao, A., and Ansel, K.M. (2007). Transcription factors T-bet and Runx3 cooperate to activate Ifng and silence Il4 in T helper type 1 cells. *Nat Immunol* 8, 145-153.
- Do, J.S., Visperas, A., Sanogo, Y.O., Bechtel, J.J., Dvorina, N., Kim, S., Jang, E., Stohlman, S.A., Shen, B., Fairchild, R.L., *et al.* (2015). An IL-27/Lag3 axis enhances Foxp3 regulatory T cell-suppressive function and therapeutic efficacy. *Mucosal Immunol*.
- Dong, Y., Yu, J., and Ng, S.S. (2014). MicroRNA dysregulation as a prognostic biomarker in colorectal cancer. *Cancer Manag Res* 6, 405-422.
- Du, C., Liu, C., Kang, J., Zhao, G., Ye, Z., Huang, S., Li, Z., Wu, Z., and Pei, G. (2009). MicroRNA miR-326 regulates TH-17 differentiation and is associated with the pathogenesis of multiple sclerosis. *Nat Immunol* 10, 1252-1259.
- Duchmann, R., Kaiser, I., Hermann, E., Mayet, W., Ewe, K., and Meyer zum Buschenfelde, K.H. (1995). Tolerance exists towards resident intestinal flora but is broken in active inflammatory bowel disease (IBD). *Clin Exp Immunol* 102, 448-455.
- Duhen, T., Geiger, R., Jarrossay, D., Lanzavecchia, A., and Sallusto, F. (2009). Production of interleukin 22 but not interleukin 17 by a subset of human skin-homing memory T cells. *Nat Immunol* 10, 857-863.

Durant, L., Watford, W.T., Ramos, H.L., Laurence, A., Vahedi, G., Wei, L., Takahashi, H., Sun, H.W., Kanno, Y., Powrie, F., and O'Shea, J.J. (2010). Diverse targets of the transcription factor STAT3 contribute to T cell pathogenicity and homeostasis. *Immunity* 32, 605-615.

Dwyer, K.M., Hanidziar, D., Putheti, P., Hill, P.A., Pommey, S., McRae, J.L., Winterhalter, A., Doherty, G., Deaglio, S., Koulmanda, M., *et al.* (2010). Expression of CD39 by human peripheral blood CD4<sup>+</sup> CD25<sup>+</sup> T cells denotes a regulatory memory phenotype. *Am J Transplant* 10, 2410-2420.

Ebert, M.S., and Sharp, P.A. (2010). MicroRNA sponges: progress and possibilities. *RNA* 16, 2043-2050.

Ebert, P.J., Jiang, S., Xie, J., Li, Q.J., and Davis, M.M. (2009). An endogenous positively selecting peptide enhances mature T cell responses and becomes an autoantigen in the absence of microRNA miR-181a. *Nat Immunol* 10, 1162-1169.

Elson, C.O., Cong, Y., and Sundberg, J. (2000). The C3H/HeJBir mouse model: a high susceptibility phenotype for colitis. *Int Rev Immunol* 19, 63-75.

Ermann, J., Hoffmann, P., Edinger, M., Dutt, S., Blankenberg, F.G., Higgins, J.P., Negrin, R.S., Fathman, C.G., and Strober, S. (2005). Only the CD62L<sup>+</sup> subpopulation of CD4<sup>+</sup>CD25<sup>+</sup> regulatory T cells protects from lethal acute GVHD. *Blood* 105, 2220-2226.

Ermann, J., Szanya, V., Ford, G.S., Paragas, V., Fathman, C.G., and Lejon, K. (2001). CD4<sup>(+)</sup>CD25<sup>(+)</sup> T cells facilitate the induction of T cell anergy. *J Immunol* 167, 4271-4275.

Esplugues, E., Huber, S., Gagliani, N., Hauser, A.E., Town, T., Wan, Y.Y., O'Connor, W., Jr., Rongvaux, A., Van Rooijen, N., Haberman, A.M., *et al.* (2011). Control of TH17 cells occurs in the small intestine. *Nature* 475, 514-518.

Eulalio, A., Huntzinger, E., and Izaurralde, E. (2008). Getting to the root of miRNA-mediated gene silencing. *Cell* 132, 9-14.

Fabian, M.R., and Sonenberg, N. (2012). The mechanics of miRNA-mediated gene silencing: a look under the hood of miRISC. *Nat Struct Mol Biol* 19, 586-593.

Fahlen, L., Read, S., Gorelik, L., Hurst, S.D., Coffman, R.L., Flavell, R.A., and Powrie, F. (2005). T cells that cannot respond to TGF-beta escape control by CD4<sup>(+)</sup>CD25<sup>(+)</sup> regulatory T cells. *J Exp Med* 201, 737-746.

Fan, W., Liang, D., Tang, Y., Qu, B., Cui, H., Luo, X., Huang, X., Chen, S., Higgs, B.W., Jallal, B., *et al.* (2012). Identification of microRNA-31 as a novel regulator contributing to impaired interleukin-2 production in T cells from patients with systemic lupus erythematosus. *Arthritis Rheum* 64, 3715-3725.

Fantini, M.C., Rizzo, A., Fina, D., Caruso, R., Sarra, M., Stolfi, C., Becker, C., Macdonald, T.T., Pallone, F., Neurath, M.F., and Monteleone, G. (2009). Smad7 controls resistance of colitogenic T cells to regulatory T cell-mediated suppression. *Gastroenterology* 136, 1308-1316, e1301-1303.

Faulkner, H., Renauld, J.C., Van Snick, J., and Grecis, R.K. (1998). Interleukin-9 enhances resistance to the intestinal nematode *Trichuris muris*. *Infect Immun* *66*, 3832-3840.

Fayyad-Kazan, H., Hamade, E., Rouas, R., Najar, M., Fayyad-Kazan, M., El Zein, N., ElDirani, R., Hussein, N., Fakhry, M., Al-Akoum, C., *et al.* (2014). Downregulation of microRNA-24 and -181 parallels the upregulation of IFN-gamma secreted by activated human CD4 lymphocytes. *Hum Immunol* *75*, 677-685.

Fayyad-Kazan, H., Rouas, R., Fayyad-Kazan, M., Badran, R., El Zein, N., Lewalle, P., Najar, M., Hamade, E., Jebbawi, F., Merimi, M., *et al.* (2012). MicroRNA profile of circulating CD4-positive regulatory T cells in human adults and impact of differentially expressed microRNAs on expression of two genes essential to their function. *J Biol Chem* *287*, 9910-9922.

Feagan, B.G., Greenberg, G.R., Wild, G., Fedorak, R.N., Pare, P., McDonald, J.W., Dube, R., Cohen, A., Steinhart, A.H., Landau, S., *et al.* (2005). Treatment of ulcerative colitis with a humanized antibody to the alpha4beta7 integrin. *N Engl J Med* *352*, 2499-2507.

Fedorak, R.N., Gangl, A., Elson, C.O., Rutgeerts, P., Schreiber, S., Wild, G., Hanauer, S.B., Kilian, A., Cohard, M., LeBeaut, A., and Feagan, B. (2000). Recombinant human interleukin 10 in the treatment of patients with mild to moderately active Crohn's disease. The Interleukin 10 Inflammatory Bowel Disease Cooperative Study Group. *Gastroenterology* *119*, 1473-1482.

Feng, T., Cao, A.T., Weaver, C.T., Elson, C.O., and Cong, Y. (2011a). Interleukin-12 converts Foxp3+ regulatory T cells to interferon-gamma-producing Foxp3+ T cells that inhibit colitis. *Gastroenterology* *140*, 2031-2043.

Feng, T., Qin, H., Wang, L., Benveniste, E.N., Elson, C.O., and Cong, Y. (2011b). Th17 cells induce colitis and promote Th1 cell responses through IL-17 induction of innate IL-12 and IL-23 production. *J Immunol* *186*, 6313-6318.

Fitzgerald, D.C., Zhang, G.X., El-Behi, M., Fonseca-Kelly, Z., Li, H., Yu, S., Saris, C.J., Gran, B., Ciric, B., and Rostami, A. (2007). Suppression of autoimmune inflammation of the central nervous system by interleukin 10 secreted by interleukin 27-stimulated T cells. *Nat Immunol* *8*, 1372-1379.

Fletcher, J.M., Lonergan, R., Costelloe, L., Kinsella, K., Moran, B., O'Farrelly, C., Tubridy, N., and Mills, K.H. (2009). CD39+Foxp3+ regulatory T Cells suppress pathogenic Th17 cells and are impaired in multiple sclerosis. *J Immunol* *183*, 7602-7610.

Fontana, L., Pelosi, E., Greco, P., Racanicchi, S., Testa, U., Liuzzi, F., Croce, C.M., Brunetti, E., Grignani, F., and Peschle, C. (2007). MicroRNAs 17-5p-20a-106a control monocytopoiesis through AML1 targeting and M-CSF receptor upregulation. *Nat Cell Biol* *9*, 775-787.

Fontenot, J.D., Gavin, M.A., and Rudensky, A.Y. (2003). Foxp3 programs the development and function of CD4+CD25+ regulatory T cells. *Nat Immunol* *4*, 330-336.

- Fontenot, J.D., Rasmussen, J.P., Williams, L.M., Dooley, J.L., Farr, A.G., and Rudensky, A.Y. (2005). Regulatory T cell lineage specification by the forkhead transcription factor foxp3. *Immunity* 22, 329-341.
- Fox, J.G., Dewhirst, F.E., Tully, J.G., Paster, B.J., Yan, L., Taylor, N.S., Collins, M.J., Jr., Gorelick, P.L., and Ward, J.M. (1994). *Helicobacter hepaticus* sp. nov., a microaerophilic bacterium isolated from livers and intestinal mucosal scrapings from mice. *J Clin Microbiol* 32, 1238-1245.
- Fox, J.G., Yan, L., Shames, B., Campbell, J., Murphy, J.C., and Li, X. (1996). Persistent hepatitis and enterocolitis in germfree mice infected with *Helicobacter hepaticus*. *Infect Immun* 64, 3673-3681.
- Frank, D.N., Amand, A.L.S., Feldman, R.A., Boedeker, E.C., Harpaz, N., and Pace, N.R. (2007). Molecular-phylogenetic characterization of microbial community imbalances in human inflammatory bowel diseases. *Proc Natl Acad Sci U S A* 104, 13780-13785.
- Freeman, G.J., and Sharpe, A.H. (2012). A new therapeutic strategy for malaria: targeting T cell exhaustion. *Nat Immunol* 13, 113-115.
- Friedman, R.C., Farh, K.K., Burge, C.B., and Bartel, D.P. (2009). Most mammalian mRNAs are conserved targets of microRNAs. *Genome Res* 19, 92-105.
- Furusawa, Y., Obata, Y., Fukuda, S., Endo, T.A., Nakato, G., Takahashi, D., Nakanishi, Y., Uetake, C., Kato, K., Kato, T., *et al.* (2013). Commensal microbe-derived butyrate induces the differentiation of colonic regulatory T cells. *Nature* 504, 446-450.
- Gagliani, N., Magnani, C.F., Huber, S., Gianolini, M.E., Pala, M., Licona-Limon, P., Guo, B., Herbert, D.R., Bulfone, A., Trentini, F., *et al.* (2013). Coexpression of CD49b and LAG-3 identifies human and mouse T regulatory type 1 cells. *Nat Med* 19, 739-746.
- Gagliani, N., Vesely, M.C., Iseppon, A., Brockmann, L., Xu, H., Palm, N.W., de Zoete, M.R., Licona-Limon, P., Paiva, R.S., Ching, T., *et al.* (2015). Th17 cells transdifferentiate into regulatory T cells during resolution of inflammation. *Nature*.
- Gao, Y.C., and Wu, J. (2015). MicroRNA-200c and microRNA-141 as potential diagnostic and prognostic biomarkers for ovarian cancer. *Tumour Biol*.
- Garchow, B.G., Bartulos Encinas, O., Leung, Y.T., Tsao, P.Y., Eisenberg, R.A., Caricchio, R., Obad, S., Petri, A., Kauppinen, S., and Kiriakidou, M. (2011). Silencing of microRNA-21 in vivo ameliorates autoimmune splenomegaly in lupus mice. *EMBO Mol Med* 3, 605-615.
- Gerosa, F., Nisii, C., Righetti, S., Micciolo, R., Marchesini, M., Cazzadori, A., and Trinchieri, G. (1999). CD4(+) T cell clones producing both interferon-gamma and interleukin-10 predominate in bronchoalveolar lavages of active pulmonary tuberculosis patients. *Clin Immunol* 92, 224-234.
- Geuking, M.B., Cahenzli, J., Lawson, M.A., Ng, D.C., Slack, E., Hapfelmeier, S., McCoy, K.D., and Macpherson, A.J. (2011). Intestinal bacterial colonization induces mutualistic regulatory T cell responses. *Immunity* 34, 794-806.

- Gionchetti, P., Rizzello, F., Helwig, U., Venturi, A., Lammers, K.M., Brigidi, P., Vitali, B., Poggioli, G., Miglioli, M., and Campieri, M. (2003). Prophylaxis of pouchitis onset with probiotic therapy: a double-blind, placebo-controlled trial. *Gastroenterology* *124*, 1202-1209.
- Girard, M., Jacquemin, E., Munnich, A., Lyonnet, S., and Henrion-Caude, A. (2008). miR-122, a paradigm for the role of microRNAs in the liver. *J Hepatol* *48*, 648-656.
- Git, A., Dvinge, H., Salmon-Divon, M., Osborne, M., Kutter, C., Hadfield, J., Bertone, P., and Caldas, C. (2010). Systematic comparison of microarray profiling, real-time PCR, and next-generation sequencing technologies for measuring differential microRNA expression. *RNA* *16*, 991-1006.
- Globig, A.M., Hennecke, N., Martin, B., Seidl, M., Ruf, G., Hasselblatt, P., Thimme, R., and Bengsch, B. (2014). Comprehensive intestinal T helper cell profiling reveals specific accumulation of IFN-gamma+IL-17+coproducing CD4+ T cells in active inflammatory bowel disease. *Inflamm Bowel Dis* *20*, 2321-2329.
- Glocker, E.O., Kotlarz, D., Boztug, K., Gertz, E.M., Schaffer, A.A., Noyan, F., Perro, M., Diestelhorst, J., Allroth, A., Murugan, D., *et al.* (2009). Inflammatory bowel disease and mutations affecting the interleukin-10 receptor. *N Engl J Med* *361*, 2033-2045.
- Gokmen, M.R., Dong, R., Kanhere, A., Powell, N., Perucha, E., Jackson, I., Howard, J.K., Hernandez-Fuentes, M., Jenner, R.G., and Lord, G.M. (2013). Genome-wide regulatory analysis reveals that T-bet controls Th17 lineage differentiation through direct suppression of IRF4. *J Immunol* *191*, 5925-5932.
- Gomez, G.D., and Balcazar, J.L. (2008). A review on the interactions between gut microbiota and innate immunity of fish. *FEMS Immunol Med Microbiol* *52*, 145-154.
- Gondek, D.C., Lu, L.F., Quezada, S.A., Sakaguchi, S., and Noelle, R.J. (2005). Cutting edge: contact-mediated suppression by CD4+CD25+ regulatory cells involves a granzyme B-dependent, perforin-independent mechanism. *J Immunol* *174*, 1783-1786.
- Goswami, R., Jabeen, R., Yagi, R., Pham, D., Zhu, J., Goenka, S., and Kaplan, M.H. (2012). STAT6-dependent regulation of Th9 development. *J Immunol* *188*, 968-975.
- Grenningloh, R., Kang, B.Y., and Ho, I.C. (2005). Ets-1, a functional cofactor of T-bet, is essential for Th1 inflammatory responses. *J Exp Med* *201*, 615-626.
- Grimson, A., Farh, K.K., Johnston, W.K., Garrett-Engele, P., Lim, L.P., and Bartel, D.P. (2007). MicroRNA targeting specificity in mammals: determinants beyond seed pairing. *Mol Cell* *27*, 91-105.
- Groom, J.R., Richmond, J., Murooka, T.T., Sorensen, E.W., Sung, J.H., Bankert, K., von Andrian, U.H., Moon, J.J., Mempel, T.R., and Luster, A.D. (2012). CXCR3 chemokine receptor-ligand interactions in the lymph node optimize CD4+ T helper 1 cell differentiation. *Immunity* *37*, 1091-1103.
- Grossman, W.J., Verbsky, J.W., Barchet, W., Colonna, M., Atkinson, J.P., and Ley, T.J. (2004). Human T regulatory cells can use the perforin pathway to cause autologous target cell death. *Immunity* *21*, 589-601.

- Groux, H., O'Garra, A., Bigler, M., Rouleau, M., Antonenko, S., de Vries, J.E., and Roncarolo, M.G. (1997). A CD4<sup>+</sup> T-cell subset inhibits antigen-specific T-cell responses and prevents colitis. *Nature* 389, 737-742.
- Grupillo, M., Lakomy, R., Geng, X., Styche, A., Rudert, W.A., Trucco, M., and Fan, Y. (2011). An improved intracellular staining protocol for efficient detection of nuclear proteins in YFP-expressing cells. *Biotechniques* 51, 417-420.
- Guay, C., and Regazzi, R. (2013). Circulating microRNAs as novel biomarkers for diabetes mellitus. *Nat Rev Endocrinol* 9, 513-521.
- Guggino, G., Giardina, A., Ferrante, A., Giardina, G., Schinocca, C., Sireci, G., Dieli, F., Ciccia, F., and Triolo, G. (2015). The in vitro addition of methotrexate and/or methylprednisolone determines peripheral reduction in Th17 and expansion of conventional Treg and of IL-10 producing Th17 lymphocytes in patients with early rheumatoid arthritis. *Rheumatol Int* 35, 171-175.
- Guo, G., Kang, Q., Zhu, X., Chen, Q., Wang, X., Chen, Y., Ouyang, J., Zhang, L., Tan, H., Chen, R., *et al.* (2014). A long noncoding RNA critically regulates Bcr-Abl-mediated cellular transformation by acting as a competitive endogenous RNA. *Oncogene*.
- Haas, J.D., Nistala, K., Petermann, F., Saran, N., Chennupati, V., Schmitz, S., Korn, T., Wedderburn, L.R., Forster, R., Krueger, A., and Prinz, I. (2011). Expression of miRNAs miR-133b and miR-206 in the *Il17a/f* locus is co-regulated with IL-17 production in alphabeta and gammadelta T cells. *PLoS One* 6, e20171.
- Hampe, J., Franke, A., Rosenstiel, P., Till, A., Teuber, M., Huse, K., Albrecht, M., Mayr, G., De La Vega, F.M., Briggs, J., *et al.* (2007). A genome-wide association scan of nonsynonymous SNPs identifies a susceptibility variant for Crohn disease in *ATG16L1*. *Nat Genet* 39, 207-211.
- Han, J., Lee, Y., Yeom, K.H., Nam, J.W., Heo, I., Rhee, J.K., Sohn, S.Y., Cho, Y., Zhang, B.T., and Kim, V.N. (2006). Molecular basis for the recognition of primary microRNAs by the Drosha-DGCR8 complex. *Cell* 125, 887-901.
- Hara, M., Kingsley, C.I., Niimi, M., Read, S., Turvey, S.E., Bushell, A.R., Morris, P.J., Powrie, F., and Wood, K.J. (2001). IL-10 is required for regulatory T cells to mediate tolerance to alloantigens in vivo. *J Immunol* 166, 3789-3796.
- Haribhai, D., Williams, J.B., Jia, S., Nickerson, D., Schmitt, E.G., Edwards, B., Ziegelbauer, J., Yassai, M., Li, S.H., Relland, L.M., *et al.* (2011). A requisite role for induced regulatory T cells in tolerance based on expanding antigen receptor diversity. *Immunity* 35, 109-122.
- Heinen, A.P., Wanke, F., Moos, S., Attig, S., Luche, H., Pal, P.P., Budisa, N., Fehling, H.J., Waisman, A., and Kurschus, F.C. (2014). Improved method to retain cytosolic reporter protein fluorescence while staining for nuclear proteins. *Cytometry A* 85, 621-627.
- Heldin, C.H., Miyazono, K., and ten Dijke, P. (1997). TGF-beta signalling from cell membrane to nucleus through SMAD proteins. *Nature* 390, 465-471.

- Herfarth, H., and Scholmerich, J. (2002). IL-10 therapy in Crohn's disease: at the crossroads. Treatment of Crohn's disease with the anti-inflammatory cytokine interleukin 10. *Gut* 50, 146-147.
- Herfarth, H.H., Bocker, U., Janardhanam, R., and Sartor, R.B. (1998). Subtherapeutic corticosteroids potentiate the ability of interleukin 10 to prevent chronic inflammation in rats. *Gastroenterology* 115, 856-865.
- Hill, J.A., Hall, J.A., Sun, C.M., Cai, Q., Ghyselinck, N., Chambon, P., Belkaid, Y., Mathis, D., and Benoist, C. (2008). Retinoic acid enhances Foxp3 induction indirectly by relieving inhibition from CD4<sup>+</sup>CD44<sup>hi</sup> Cells. *Immunity* 29, 758-770.
- Hirota, K., Duarte, J.H., Veldhoen, M., Hornsby, E., Li, Y., Cua, D.J., Ahlfors, H., Wilhelm, C., Tolaini, M., Menzel, U., *et al.* (2011). Fate mapping of IL-17-producing T cells in inflammatory responses. *Nat Immunol* 12, 255-263.
- Hovhannisyan, Z., Treatman, J., Littman, D.R., and Mayer, L. (2011). Characterization of interleukin-17-producing regulatory T cells in inflamed intestinal mucosa from patients with inflammatory bowel diseases. *Gastroenterology* 140, 957-965.
- Hu, R., Huffaker, T.B., Kagele, D.A., Runtsch, M.C., Bake, E., Chaudhuri, A.A., Round, J.L., and O'Connell, R.M. (2013). MicroRNA-155 confers encephalogenic potential to Th17 cells by promoting effector gene expression. *J Immunol* 190, 5972-5980.
- Huang, C.T., Workman, C.J., Flies, D., Pan, X., Marson, A.L., Zhou, G., Hipkiss, E.L., Ravi, S., Kowalski, J., Levitsky, H.I., *et al.* (2004). Role of LAG-3 in regulatory T cells. *Immunity* 21, 503-513.
- Huang, S., Apasov, S., Koshiba, M., and Sitkovsky, M. (1997). Role of A2a extracellular adenosine receptor-mediated signaling in adenosine-mediated inhibition of T-cell activation and expansion. *Blood* 90, 1600-1610.
- Huang, Z., Shi, T., Zhou, Q., Shi, S., Zhao, R., Shi, H., Dong, L., Zhang, C., Zeng, K., Chen, J., and Zhang, J. (2014). miR-141 Regulates colonic leukocytic trafficking by targeting CXCL12beta during murine colitis and human Crohn's disease. *Gut* 63, 1247-1257.
- Huber, S., Gagliani, N., Esplugues, E., O'Connor, W., Jr., Huber, F.J., Chaudhry, A., Kamanaka, M., Kobayashi, Y., Booth, C.J., Rudensky, A.Y., *et al.* (2011). Th17 cells express interleukin-10 receptor and are controlled by Foxp3(-) and Foxp3+ regulatory CD4+ T cells in an interleukin-10-dependent manner. *Immunity* 34, 554-565.
- Hugot, J.P., Chamaillard, M., Zouali, H., Lesage, S., Cezard, J.P., Belaiche, J., Almer, S., Tysk, C., O'Morain, C.A., Gassull, M., *et al.* (2001). Association of NOD2 leucine-rich repeat variants with susceptibility to Crohn's disease. *Nature* 411, 599-603.
- Hullinger, T.G., Montgomery, R.L., Seto, A.G., Dickinson, B.A., Semus, H.M., Lynch, J.M., Dalby, C.M., Robinson, K., Stack, C., Latimer, P.A., *et al.* (2012). Inhibition of miR-15 Protects Against Cardiac Ischemic Injury. *Circ Res* 110, 71-81.
- Huter, E.N., Stummvoll, G.H., DiPaolo, R.J., Glass, D.D., and Shevach, E.M. (2008). Cutting edge: antigen-specific TGF beta-induced regulatory T cells suppress Th17-mediated autoimmune disease. *J Immunol* 181, 8209-8213.

- Ihn, H.J., Kim, D.H., Oh, S.S., Moon, C., Chung, J.W., Song, H., and Kim, K.D. (2011). Identification of *Acvr2a* as a Th17 cell-specific gene induced during Th17 differentiation. *Biosci Biotechnol Biochem* 75, 2138-2141.
- Iliopoulos, D., Kavousanaki, M., Ioannou, M., Boumpas, D., and Verginis, P. (2011). The negative costimulatory molecule PD-1 modulates the balance between immunity and tolerance via miR-21. *Eur J Immunol* 41, 1754-1763.
- Inobe, J., Slavin, A.J., Komagata, Y., Chen, Y., Liu, L., and Weiner, H.L. (1998). IL-4 is a differentiation factor for transforming growth factor-beta secreting Th3 cells and oral administration of IL-4 enhances oral tolerance in experimental allergic encephalomyelitis. *Eur J Immunol* 28, 2780-2790.
- Isaacs, K.L., and Sartor, R.B. (2004). Treatment of inflammatory bowel disease with antibiotics. *Gastroenterol Clin North Am* 33, 335-345, x.
- Issa, F., Hester, J., Goto, R., Nadig, S.N., Goodacre, T.E., and Wood, K. (2010). Ex vivo-expanded human regulatory T cells prevent the rejection of skin allografts in a humanized mouse model. *Transplantation* 90, 1321-1327.
- Ivanov, II, McKenzie, B.S., Zhou, L., Tadokoro, C.E., Lepelley, A., Lafaille, J.J., Cua, D.J., and Littman, D.R. (2006). The orphan nuclear receptor ROR $\gamma$  directs the differentiation program of proinflammatory IL-17+ T helper cells. *Cell* 126, 1121-1133.
- Iwata, M., Hirakiyama, A., Eshima, Y., Kagechika, H., Kato, C., and Song, S.Y. (2004). Retinoic acid imprints gut-homing specificity on T cells. *Immunity* 21, 527-538.
- Jager, A., Dardalhon, V., Sobel, R.A., Bettelli, E., and Kuchroo, V.K. (2009). Th1, Th17, and Th9 effector cells induce experimental autoimmune encephalomyelitis with different pathological phenotypes. *J Immunol* 183, 7169-7177.
- Jankovic, D., Kullberg, M.C., Feng, C.G., Goldszmid, R.S., Collazo, C.M., Wilson, M., Wynn, T.A., Kamanaka, M., Flavell, R.A., and Sher, A. (2007). Conventional T-bet(+)/Foxp3(-) Th1 cells are the major source of host-protective regulatory IL-10 during intracellular protozoan infection. *J Exp Med* 204, 273-283.
- Janssen, H.L., Reesink, H.W., Lawitz, E.J., Zeuzem, S., Rodriguez-Torres, M., Patel, K., van der Meer, A.J., Patick, A.K., Chen, A., Zhou, Y., *et al.* (2013). Treatment of HCV infection by targeting microRNA. *N Engl J Med* 368, 1685-1694.
- Janssens, W., Carlier, V., Wu, B., VanderElst, L., Jacquemin, M.G., and Saint-Remy, J.M. (2003). CD4+CD25+ T cells lyse antigen-presenting B cells by Fas-Fas ligand interaction in an epitope-specific manner. *J Immunol* 171, 4604-4612.
- Jin, Y., Chen, Z., Liu, X., and Zhou, X. (2013). Evaluating the microRNA targeting sites by luciferase reporter gene assay. *Methods Mol Biol* 936, 117-127.
- Johansson-Lindbom, B., Svensson, M., Pabst, O., Palmqvist, C., Marquez, G., Forster, R., and Agace, W.W. (2005). Functional specialization of gut CD103+ dendritic cells in the regulation of tissue-selective T cell homing. *J Exp Med* 202, 1063-1073.
- Johansson-Lindbom, B., Svensson, M., Wurbel, M.A., Malissen, B., Marquez, G., and Agace, W. (2003). Selective generation of gut tropic T cells in gut-associated lymphoid

tissue (GALT): requirement for GALT dendritic cells and adjuvant. *J Exp Med* 198, 963-969.

Johnson, S.M., Grosshans, H., Shingara, J., Byrom, M., Jarvis, R., Cheng, A., Labourier, E., Reinert, K.L., Brown, D., and Slack, F.J. (2005). RAS is regulated by the let-7 microRNA family. *Cell* 120, 635-647.

Jonuleit, H., Schmitt, E., Schuler, G., Knop, J., and Enk, A.H. (2000). Induction of interleukin 10-producing, nonproliferating CD4(+) T cells with regulatory properties by repetitive stimulation with allogeneic immature human dendritic cells. *J Exp Med* 192, 1213-1222.

Jopling, C.L., Yi, M., Lancaster, A.M., Lemon, S.M., and Sarnow, P. (2005). Modulation of hepatitis C virus RNA abundance by a liver-specific MicroRNA. *Science* 309, 1577-1581.

Kamanaka, M., Kim, S.T., Wan, Y.Y., Sutterwala, F.S., Lara-Tejero, M., Galan, J.E., Harhaj, E., and Flavell, R.A. (2006). Expression of interleukin-10 in intestinal lymphocytes detected by an interleukin-10 reporter knockin tiger mouse. *Immunity* 25, 941-952.

Kang, S.G., Lim, H.W., Andrisani, O.M., Broxmeyer, H.E., and Kim, C.H. (2007). Vitamin A metabolites induce gut-homing FoxP3+ regulatory T cells. *J Immunol* 179, 3724-3733.

Kaplan, M.H., Schindler, U., Smiley, S.T., and Grusby, M.J. (1996). Stat6 is required for mediating responses to IL-4 and for development of Th2 cells. *Immunity* 4, 313-319.

Kaser, A., Zeissig, S., and Blumberg, R.S. (2010). Genes and environment: how will our concepts on the pathophysiology of IBD develop in the future? *Dig Dis* 28, 395-405.

Kawano, S., and Nakamachi, Y. (2011). miR-124a as a key regulator of proliferation and MCP-1 secretion in synoviocytes from patients with rheumatoid arthritis. *Ann Rheum Dis* 70 Suppl 1, i88-91.

Kelsall, B. (2008). Recent progress in understanding the phenotype and function of intestinal dendritic cells and macrophages. *Mucosal Immunol* 1, 460-469.

Kertesz, M., Iovino, N., Unnerstall, U., Gaul, U., and Segal, E. (2007). The role of site accessibility in microRNA target recognition. *Nat Genet* 39, 1278-1284.

Kerzerho, J., Maazi, H., Speak, A.O., Szely, N., Lombardi, V., Khoo, B., Geryak, S., Lam, J., Soroosh, P., Van Snick, J., and Akbari, O. (2013). Programmed cell death ligand 2 regulates TH9 differentiation and induction of chronic airway hyperreactivity. *J Allergy Clin Immunol* 131, 1048-1057, 1057 e1041-1042.

Khan, S., Lakhe-Reddy, S., McCarty, J.H., Sorenson, C.M., Sheibani, N., Reichardt, L.F., Kim, J.H., Wang, B., Sedor, J.R., and Schelling, J.R. (2011). Mesangial cell integrin alphavbeta8 provides glomerular endothelial cell cytoprotection by sequestering TGF-beta and regulating PECAM-1. *Am J Pathol* 178, 609-620.

- Khattari, R., Cox, T., Yasayko, S.A., and Ramsdell, F. (2003). An essential role for Scurfin in CD4+CD25+ T regulatory cells. *Nat Immunol* *4*, 337-342.
- Kim, S.C., Tonkonogy, S.L., Albright, C.A., Tsang, J., Balish, E.J., Braun, J., Huycke, M.M., and Sartor, R.B. (2005). Variable phenotypes of enterocolitis in interleukin 10-deficient mice monoassociated with two different commensal bacteria. *Gastroenterology* *128*, 891-906.
- Kittl, S., Korczak, B.M., Niederer, L., Baumgartner, A., Buettner, S., Overesch, G., and Kuhnert, P. (2013). Comparison of genotypes and antibiotic resistances of *Campylobacter jejuni* and *Campylobacter coli* on chicken retail meat and at slaughter. *Appl Environ Microbiol* *79*, 3875-3878.
- Kleiter, I., Song, J., Lukas, D., Hasan, M., Neumann, B., Croxford, A.L., Pedre, X., Hovelmeyer, N., Yogeve, N., Mildner, A., *et al.* (2010). Smad7 in T cells drives T helper 1 responses in multiple sclerosis and experimental autoimmune encephalomyelitis. *Brain* *133*, 1067-1081.
- Koch, M.A., Tucker-Heard, G., Perdue, N.R., Killebrew, J.R., Urdahl, K.B., and Campbell, D.J. (2009). The transcription factor T-bet controls regulatory T cell homeostasis and function during type 1 inflammation. *Nat Immunol* *10*, 595-602.
- Kojima, A., Tanaka-Kojima, Y., Sakakura, T., and Nishizuka, Y. (1976). Spontaneous development of autoimmune thyroiditis in neonatally thymectomized mice. *Lab Invest* *34*, 550-557.
- Komatsu, N., Okamoto, K., Sawa, S., Nakashima, T., Oh-hora, M., Kodama, T., Tanaka, S., Bluestone, J.A., and Takayanagi, H. (2014). Pathogenic conversion of Foxp3+ T cells into TH17 cells in autoimmune arthritis. *Nat Med* *20*, 62-68.
- Kondkar, A.A., and Abu-Amero, K.K. (2015). Utility of Circulating MicroRNAs as Clinical Biomarkers for Cardiovascular Diseases. *Biomed Res Int* *2015*, 821823.
- Koralov, S.B., Muljo, S.A., Galler, G.R., Krek, A., Chakraborty, T., Kanellopoulou, C., Jensen, K., Cobb, B.S., Merkenschlager, M., Rajewsky, N., and Rajewsky, K. (2008). Dicer ablation affects antibody diversity and cell survival in the B lymphocyte lineage. *Cell* *132*, 860-874.
- Korn, T., Bettelli, E., Gao, W., Awasthi, A., Jager, A., Strom, T.B., Oukka, M., and Kuchroo, V.K. (2007). IL-21 initiates an alternative pathway to induce proinflammatory T(H)17 cells. *Nature* *448*, 484-487.
- Kotlarz, D., Beier, R., Murugan, D., Diestelhorst, J., Jensen, O., Boztug, K., Pfeifer, D., Kreipe, H., Pfister, E.D., Baumann, U., *et al.* (2012). Loss of interleukin-10 signaling and infantile inflammatory bowel disease: implications for diagnosis and therapy. *Gastroenterology* *143*, 347-355.
- Koukos, G., Polytaichou, C., Kaplan, J.L., Morley-Fletcher, A., Gras-Miralles, B., Kokkotou, E., Baril-Dore, M., Pothoulakis, C., Winter, H.S., and Iliopoulos, D. (2013). MicroRNA-124 regulates STAT3 expression and is down-regulated in colon tissues of pediatric patients with ulcerative colitis. *Gastroenterology* *145*, 842-852 e842.
- Kozomara, A., and Griffiths-Jones, S. (2011). miRBase: integrating microRNA annotation and deep-sequencing data. *Nucleic Acids Res* *39*, D152-157.

Kretschmer, K., Apostolou, I., Hawiger, D., Khazaie, K., Nussenzweig, M.C., and von Boehmer, H. (2005). Inducing and expanding regulatory T cell populations by foreign antigen. *Nat Immunol* *6*, 1219-1227.

Krichevsky, A.M., King, K.S., Donahue, C.P., Khrapko, K., and Kosik, K.S. (2003). A microRNA array reveals extensive regulation of microRNAs during brain development. *RNA* *9*, 1274-1281.

Krissansen, G.W., Yang, Y., McQueen, F.M., Leung, E., Peek, D., Chan, Y.C., Print, C., Dalbeth, N., Williams, M., and Fraser, A.G. (2015). Overexpression of miR-595 and miR-1246 in the Sera of Patients with Active Forms of Inflammatory Bowel Disease. *Inflamm Bowel Dis* *21*, 520-530.

Kuhn, D.E., Martin, M.M., Feldman, D.S., Terry, A.V., Jr., Nuovo, G.J., and Elton, T.S. (2008). Experimental validation of miRNA targets. *Methods* *44*, 47-54.

Kuhn, R., Lohler, J., Rennick, D., Rajewsky, K., and Muller, W. (1993). Interleukin-10-deficient mice develop chronic enterocolitis. *Cell* *75*, 263-274.

Kullberg, M.C., Andersen, J.F., Gorelick, P.L., Caspar, P., Suerbaum, S., Fox, J.G., Cheever, A.W., Jankovic, D., and Sher, A. (2003). Induction of colitis by a CD4<sup>+</sup> T cell clone specific for a bacterial epitope. *Proc Natl Acad Sci U S A* *100*, 15830-15835.

Kullberg, M.C., Hay, V., Cheever, A.W., Mamura, M., Sher, A., Letterio, J.J., Shevach, E.M., and Piccirillo, C.A. (2005). TGF-beta1 production by CD4<sup>+</sup> CD25<sup>+</sup> regulatory T cells is not essential for suppression of intestinal inflammation. *Eur J Immunol* *35*, 2886-2895.

Kullberg, M.C., Jankovic, D., Feng, C.G., Hue, S., Gorelick, P.L., McKenzie, B.S., Cua, D.J., Powrie, F., Cheever, A.W., Maloy, K.J., and Sher, A. (2006). IL-23 plays a key role in *Helicobacter hepaticus*-induced T cell-dependent colitis. *J Exp Med* *203*, 2485-2494.

Kullberg, M.C., Jankovic, D., Gorelick, P.L., Caspar, P., Letterio, J.J., Cheever, A.W., and Sher, A. (2002). Bacteria-triggered CD4(+) T regulatory cells suppress *Helicobacter hepaticus*-induced colitis. *J Exp Med* *196*, 505-515.

Kullberg, M.C., Rothfuchs, A.G., Jankovic, D., Caspar, P., Wynn, T.A., Gorelick, P.L., Cheever, A.W., and Sher, A. (2001). *Helicobacter hepaticus*-induced colitis in interleukin-10-deficient mice: cytokine requirements for the induction and maintenance of intestinal inflammation. *Infect Immun* *69*, 4232-4241.

Kullberg, M.C., Ward, J.M., Gorelick, P.L., Caspar, P., Hieny, S., Cheever, A., Jankovic, D., and Sher, A. (1998). *Helicobacter hepaticus* triggers colitis in specific-pathogen-free interleukin-10 (IL-10)-deficient mice through an IL-12- and gamma interferon-dependent mechanism. *Infect Immun* *66*, 5157-5166.

Kumar, H., Kawai, T., and Akira, S. (2011). Pathogen recognition by the innate immune system. *Int Rev Immunol* *30*, 16-34.

Lanford, R.E., Hildebrandt-Eriksen, E.S., Petri, A., Persson, R., Lindow, M., Munk, M.E., Kauppinen, S., and Orum, H. (2010). Therapeutic silencing of microRNA-122 in primates with chronic hepatitis C virus infection. *Science* *327*, 198-201.

- Langrish, C.L., Chen, Y., Blumenschein, W.M., Mattson, J., Basham, B., Sedgwick, J.D., McClanahan, T., Kastelein, R.A., and Cua, D.J. (2005). IL-23 drives a pathogenic T cell population that induces autoimmune inflammation. *J Exp Med* 201, 233-240.
- Lappas, C.M., Rieger, J.M., and Linden, J. (2005). A2A adenosine receptor induction inhibits IFN-gamma production in murine CD4+ T cells. *J Immunol* 174, 1073-1080.
- Lathrop, S.K., Bloom, S.M., Rao, S.M., Nutsch, K., Lio, C.W., Santacruz, N., Peterson, D.A., Stappenbeck, T.S., and Hsieh, C.S. (2011). Peripheral education of the immune system by colonic commensal microbiota. *Nature* 478, 250-254.
- Lazarevic, V., Chen, X., Shim, J.H., Hwang, E.S., Jang, E., Bolm, A.N., Oukka, M., Kuchroo, V.K., and Glimcher, L.H. (2011). T-bet represses T(H)17 differentiation by preventing Runx1-mediated activation of the gene encoding RORgammat. *Nat Immunol* 12, 96-104.
- Lee, R.C., Feinbaum, R.L., and Ambros, V. (1993). The *C. elegans* heterochronic gene *lin-4* encodes small RNAs with antisense complementarity to *lin-14*. *Cell* 75, 843-854.
- Lee, Y., Kim, M., Han, J., Yeom, K.H., Lee, S., Baek, S.H., and Kim, V.N. (2004). MicroRNA genes are transcribed by RNA polymerase II. *EMBO J* 23, 4051-4060.
- Lees, C.W., Barrett, J.C., Parkes, M., and Satsangi, J. (2011). New IBD genetics: common pathways with other diseases. *Gut* 60, 1739-1753.
- Levy, D.E., and Darnell, J.E., Jr. (2002). Stats: transcriptional control and biological impact. *Nat Rev Mol Cell Biol* 3, 651-662.
- Li, L., Miao, X., Ni, R., Miao, X., Wang, L., Gu, X., Yan, L., Tang, Q., and Zhang, D. (2015). Epithelial-specific ETS-1 (ESE1/ELF3) regulates apoptosis of intestinal epithelial cells in ulcerative colitis via accelerating NF-kappaB activation. *Immunol Res.*
- Li, L., Patsoukis, N., Petkova, V., and Boussiotis, V.A. (2012). Runx1 and Runx3 are involved in the generation and function of highly suppressive IL-17-producing T regulatory cells. *PLoS One* 7, e45115.
- Li, M.O., Wan, Y.Y., Sanjabi, S., Robertson, A.K., and Flavell, R.A. (2006a). Transforming growth factor-beta regulation of immune responses. *Annu Rev Immunol* 24, 99-146.
- Li, Q., Zhang, D., Wang, Y., Sun, P., Hou, X., Larner, J., Xiong, W., and Mi, J. (2013a). MiR-21/Smad 7 signaling determines TGF-beta1-induced CAF formation. *Sci Rep* 3, 2038.
- Li, Q.J., Chau, J., Ebert, P.J., Sylvester, G., Min, H., Liu, G., Braich, R., Manoharan, M., Soutschek, J., Skare, P., *et al.* (2007). miR-181a is an intrinsic modulator of T cell sensitivity and selection. *Cell* 129, 147-161.
- Li, X., Thyssen, G., Beliakov, J., and Sun, Z. (2006b). The novel PIAS-like protein hZimp10 enhances Smad transcriptional activity. *J Biol Chem* 281, 23748-23756.

- Li, X., Tian, F., and Wang, F. (2013b). Rheumatoid arthritis-associated microRNA-155 targets SOCS1 and upregulates TNF-alpha and IL-1beta in PBMCs. *Int J Mol Sci* *14*, 23910-23921.
- Li, Z., and Rana, T.M. (2014). Therapeutic targeting of microRNAs: current status and future challenges. *Nat Rev Drug Discov* *13*, 622-638.
- Liang, S.C., Tan, X.Y., Luxenberg, D.P., Karim, R., Dunussi-Joannopoulos, K., Collins, M., and Fouser, L.A. (2006). Interleukin (IL)-22 and IL-17 are coexpressed by Th17 cells and cooperatively enhance expression of antimicrobial peptides. *J Exp Med* *203*, 2271-2279.
- Lin, J., Welker, N.C., Zhao, Z., Li, Y., Zhang, J., Reuss, S.A., Zhang, X., Lee, H., Liu, Y., and Bronner, M.P. (2014). Novel specific microRNA biomarkers in idiopathic inflammatory bowel disease unrelated to disease activity. *Mod Pathol* *27*, 602-608.
- Lin, Y.Y., Jones-Mason, M.E., Inoue, M., Lasorella, A., Iavarone, A., Li, Q.J., Shinohara, M.L., and Zhuang, Y. (2012). Transcriptional regulator Id2 is required for the CD4 T cell immune response in the development of experimental autoimmune encephalomyelitis. *J Immunol* *189*, 1400-1405.
- Lindsay, J., Van Montfrans, C., Brennan, F., Van Deventer, S., Drillenburger, P., Hodgson, H., Te Velde, A., and Sol Rodriguez Pena, M. (2002). IL-10 gene therapy prevents TNBS-induced colitis. *Gene Ther* *9*, 1715-1721.
- Lio, C.W., and Hsieh, C.S. (2008). A two-step process for thymic regulatory T cell development. *Immunity* *28*, 100-111.
- Liu, C., Kelnar, K., Liu, B., Chen, X., Calhoun-Davis, T., Li, H., Patrawala, L., Yan, H., Jeter, C., Honorio, S., *et al.* (2011). The microRNA miR-34a inhibits prostate cancer stem cells and metastasis by directly repressing CD44. *Nat Med* *17*, 211-215.
- Liu, L., Wang, Y., Fan, H., Zhao, X., Liu, D., Hu, Y., Kidd, A.R., 3rd, Bao, J., and Hou, Y. (2012). MicroRNA-181a regulates local immune balance by inhibiting proliferation and immunosuppressive properties of mesenchymal stem cells. *Stem Cells* *30*, 1756-1770.
- Liu, W., Ouyang, X., Yang, J., Liu, J., Li, Q., Gu, Y., Fukata, M., Lin, T., He, J.C., Abreu, M., *et al.* (2009). AP-1 activated by toll-like receptors regulates expression of IL-23 p19. *J Biol Chem* *284*, 24006-24016.
- Lu, C., Chen, J., Xu, H.G., Zhou, X., He, Q., Li, Y.L., Jiang, G., Shan, Y., Xue, B., Zhao, R.X., *et al.* (2014). MIR106B and MIR93 prevent removal of bacteria from epithelial cells by disrupting ATG16L1-mediated autophagy. *Gastroenterology* *146*, 188-199.
- Lu, Y., Hong, S., Li, H., Park, J., Hong, B., Wang, L., Zheng, Y., Liu, Z., Xu, J., He, J., *et al.* (2012). Th9 cells promote antitumor immune responses in vivo. *J Clin Invest* *122*, 4160-4171.
- Luo, X., Zhang, L., Li, M., Zhang, W., Leng, X., Zhang, F., Zhao, Y., and Zeng, X. (2013). The role of miR-125b in T lymphocytes in the pathogenesis of systemic lupus erythematosus. *Clin Exp Rheumatol* *31*, 263-271.

- Lv, B., Liu, Z., Wang, S., Liu, F., Yang, X., Hou, J., Hou, Z., and Chen, B. (2014). miR-29a promotes intestinal epithelial apoptosis in ulcerative colitis by down-regulating Mcl-1. *Int J Clin Exp Pathol* 7, 8542-8552.
- Macpherson, A., Khoo, U.Y., Forgacs, I., Philpott-Howard, J., and Bjarnason, I. (1996). Mucosal antibodies in inflammatory bowel disease are directed against intestinal bacteria. *Gut* 38, 365-375.
- Madabusi, L.V., Latham, G.J., and Andruss, B.F. (2006). RNA extraction for arrays. *Methods Enzymol* 411, 1-14.
- Male, D., Brostoff, J., Roth, D.B., and Roitt, I. (2006). *Immunology Seventh Edition* edn (Philadelphia: Mosby Elsevier).
- Malmhall, C., Alawieh, S., Lu, Y., Sjostrand, M., Bossios, A., Eldh, M., and Radinger, M. (2014). MicroRNA-155 is essential for T(H)2-mediated allergen-induced eosinophilic inflammation in the lung. *J Allergy Clin Immunol* 133, 1429-1438, 1438 e1421-1427.
- Marek-Trzonkowska, N., Mysliwiec, M., Dobyszuk, A., Grabowska, M., Techmanska, I., Juscinska, J., Wujtewicz, M.A., Witkowski, P., Mlynarski, W., Balcerska, A., *et al.* (2012). Administration of CD4+CD25highCD127- regulatory T cells preserves beta-cell function in type 1 diabetes in children. *Diabetes Care* 35, 1817-1820.
- Marquez, R.T., Wendlandt, E., Galle, C.S., Keck, K., and McCaffrey, A.P. (2010). MicroRNA-21 is upregulated during the proliferative phase of liver regeneration, targets Pellino-1, and inhibits NF-kappaB signaling. *Am J Physiol Gastrointest Liver Physiol* 298, G535-541.
- Martinez-Llordella, M., Esensten, J.H., Bailey-Bucktrout, S.L., Lipsky, R.H., Marini, A., Chen, J., Mughal, M., Mattson, M.P., Taub, D.D., and Bluestone, J.A. (2013). CD28-inducible transcription factor DEC1 is required for efficient autoreactive CD4+ T cell response. *J Exp Med* 210, 1603-1619.
- Maslowski, K.M., Vieira, A.T., Ng, A., Kranich, J., Sierro, F., Yu, D., Schilter, H.C., Rolph, M.S., Mackay, F., Artis, D., *et al.* (2009). Regulation of inflammatory responses by gut microbiota and chemoattractant receptor GPR43. *Nature* 461, 1282-1286.
- Mathonnet, G., Fabian, M.R., Svitkin, Y.V., Parsyan, A., Huck, L., Murata, T., Biffo, S., Merrick, W.C., Darzynkiewicz, E., Pillai, R.S., *et al.* (2007). MicroRNA inhibition of translation initiation in vitro by targeting the cap-binding complex eIF4F. *Science* 317, 1764-1767.
- Mathur, A.N., Chang, H.C., Zisoulis, D.G., Stritesky, G.L., Yu, Q., O'Malley, J.T., Kapur, R., Levy, D.E., Kansas, G.S., and Kaplan, M.H. (2007). Stat3 and Stat4 direct development of IL-17-secreting Th cells. *J Immunol* 178, 4901-4907.
- Matsumoto, S., Okabe, Y., Setoyama, H., Takayama, K., Ohtsuka, J., Funahashi, H., Imaoka, A., Okada, Y., and Umesaki, Y. (1998). Inflammatory bowel disease-like enteritis and caecitis in a senescence accelerated mouse P1/Yit strain. *Gut* 43, 71-78.
- Mattes, J., Collison, A., Plank, M., Phipps, S., and Foster, P.S. (2009). Antagonism of microRNA-126 suppresses the effector function of TH2 cells and the development of allergic airways disease. *Proc Natl Acad Sci U S A* 106, 18704-18709.

- Maynard, C.L., Harrington, L.E., Janowski, K.M., Oliver, J.R., Zindl, C.L., Rudensky, A.Y., and Weaver, C.T. (2007). Regulatory T cells expressing interleukin 10 develop from Foxp3<sup>+</sup> and Foxp3<sup>-</sup> precursor cells in the absence of interleukin 10. *Nat Immunol* 8, 931-941.
- Mazmanian, S.K., Liu, C.H., Tzianabos, A.O., and Kasper, D.L. (2005). An immunomodulatory molecule of symbiotic bacteria directs maturation of the host immune system. *Cell* 122, 107-118.
- McCormick, R.I., Blick, C., Ragoussis, J., Schoedel, J., Mole, D.R., Young, A.C., Selby, P.J., Banks, R.E., and Harris, A.L. (2013). miR-210 is a target of hypoxia-inducible factors 1 and 2 in renal cancer, regulates ISCU and correlates with good prognosis. *Br J Cancer* 108, 1133-1142.
- McMurchy, A.N., Di Nunzio, S., Roncarolo, M.G., Bacchetta, R., and Levings, M.K. (2009). Molecular regulation of cellular immunity by FOXP3. *Adv Exp Med Biol* 665, 30-46.
- McNeill, A., Spittle, E., and Backstrom, B.T. (2007). Partial depletion of CD69<sup>low</sup>-expressing natural regulatory T cells with the anti-CD25 monoclonal antibody PC61. *Scand J Immunol* 65, 63-69.
- McPherson, R.C., Turner, D.G., Mair, I., O'Connor, R.A., and Anderton, S.M. (2015). T-bet Expression by Foxp3(+) T Regulatory Cells is Not Essential for Their Suppressive Function in CNS Autoimmune Disease or Colitis. *Front Immunol* 6, 69.
- Meisgen, F., Xu, N., Wei, T., Janson, P.C., Obad, S., Broom, O., Nagy, N., Kauppinen, S., Kemeny, L., Stahle, M., *et al.* (2012). MiR-21 is up-regulated in psoriasis and suppresses T cell apoptosis. *Exp Dermatol* 21, 312-314.
- Meng, F., Henson, R., Wehbe-Janek, H., Ghoshal, K., Jacob, S.T., and Patel, T. (2007). MicroRNA-21 regulates expression of the PTEN tumor suppressor gene in human hepatocellular cancer. *Gastroenterology* 133, 647-658.
- Menon, S., Chi, H., Zhang, H., Deng, X.W., Flavell, R.A., and Wei, N. (2007). COP9 signalosome subunit 8 is essential for peripheral T cell homeostasis and antigen receptor-induced entry into the cell cycle from quiescence. *Nat Immunol* 8, 1236-1245.
- Meyaard, L. (2008). The inhibitory collagen receptor LAIR-1 (CD305). *J Leukoc Biol* 83, 799-803.
- Milner, R., Frost, E., Nishimura, S., Delcommenne, M., Streuli, C., Pytela, R., and Ffrench-Constant, C. (1997). Expression of alpha vbeta3 and alpha vbeta8 integrins during oligodendrocyte precursor differentiation in the presence and absence of axons. *Glia* 21, 350-360.
- Min, M., Peng, L., Yang, Y., Guo, M., Wang, W., and Sun, G. (2014). MicroRNA-155 is involved in the pathogenesis of ulcerative colitis by targeting FOXO3a. *Inflamm Bowel Dis* 20, 652-659.
- Mitchell, P.S., Parkin, R.K., Kroh, E.M., Fritz, B.R., Wyman, S.K., Pogosova-Agadjanyan, E.L., Peterson, A., Noteboom, J., O'Briant, K.C., Allen, A., *et al.* (2008). Circulating microRNAs as stable blood-based markers for cancer detection. *Proc Natl Acad Sci U S A* 105, 10513-10518.

- Miyazaki, Y., Li, R., Rezk, A., Misirliyan, H., Moore, C., Farooqi, N., Solis, M., Goiry, L.G., de Faria Junior, O., Dang, V.D., *et al.* (2014). A novel microRNA-132-surtuin-1 axis underlies aberrant B-cell cytokine regulation in patients with relapsing-remitting multiple sclerosis. *PLoS One* *9*, e105421.
- Mizuno, Y., Tokuzawa, Y., Ninomiya, Y., Yagi, K., Yatsuka-Kanesaki, Y., Suda, T., Fukuda, T., Katagiri, T., Kondoh, Y., Amemiya, T., *et al.* (2009). miR-210 promotes osteoblastic differentiation through inhibition of AcvR1b. *FEBS Lett* *583*, 2263-2268.
- Mohnle, P., Schutz, S.V., van der Heide, V., Hubner, M., Luchting, B., Sedlbauer, J., Limbeck, E., Hinske, L.C., Briegel, J., and Kreth, S. (2015). MicroRNA-146a controls Th1-cell differentiation of human CD4+ T lymphocytes by targeting PRKCepsilon. *Eur J Immunol* *45*, 260-272.
- Monteleone, G., Fantini, M.C., Onali, S., Zorzi, F., Sancesario, G., Bernardini, S., Calabrese, E., Viti, F., Monteleone, I., Biancone, L., and Pallone, F. (2012). Phase I clinical trial of Smad7 knockdown using antisense oligonucleotide in patients with active Crohn's disease. *Mol Ther* *20*, 870-876.
- Morris, G.P., Beck, P.L., Herridge, M.S., Depew, W.T., Szewczuk, M.R., and Wallace, J.L. (1989). Hapten-induced model of chronic inflammation and ulceration in the rat colon. *Gastroenterology* *96*, 795-803.
- Morrison, P.J., Bending, D., Fouser, L.A., Wright, J.F., Stockinger, B., Cooke, A., and Kullberg, M.C. (2013). Th17-cell plasticity in *Helicobacter hepaticus*-induced intestinal inflammation. *Mucosal Immunol* *6*, 1143-1156.
- Morrissey, P.J., Charrier, K., Braddy, S., Liggitt, D., and Watson, J.D. (1993). CD4+ T cells that express high levels of CD45RB induce wasting disease when transferred into congenic severe combined immunodeficient mice. Disease development is prevented by cotransfer of purified CD4+ T cells. *J Exp Med* *178*, 237-244.
- Mosmann, T.R., Cherwinski, H., Bond, M.W., Giedlin, M.A., and Coffman, R.L. (1986). Two types of murine helper T cell clone. I. Definition according to profiles of lymphokine activities and secreted proteins. *J Immunol* *136*, 2348-2357.
- Mucida, D., Park, Y., Kim, G., Turovskaya, O., Scott, I., Kronenberg, M., and Cheroutre, H. (2007). Reciprocal TH17 and regulatory T cell differentiation mediated by retinoic acid. *Science* *317*, 256-260.
- Mucida, D., Pino-Lagos, K., Kim, G., Nowak, E., Benson, M.J., Kronenberg, M., Noelle, R.J., and Cheroutre, H. (2009). Retinoic acid can directly promote TGF-beta-mediated Foxp3(+) Treg cell conversion of naive T cells. *Immunity* *30*, 471-472; author reply 472-473.
- Muljo, S.A., Ansel, K.M., Kanellopoulou, C., Livingston, D.M., Rao, A., and Rajewsky, K. (2005). Aberrant T cell differentiation in the absence of Dicer. *J Exp Med* *202*, 261-269.
- Muller, M., Herrath, J., and Malmstrom, V. (2015). IL-1R1 is expressed on both Helios and Helios FoxP3 CD4 T cells in the rheumatic joint. *Clin Exp Immunol*.

- Muralimanoharan, S., Guo, C., Myatt, L., and Maloyan, A. (2015). Sexual dimorphism in miR-210 expression and mitochondrial dysfunction in the placenta with maternal obesity. *Int J Obes (Lond)*.
- Murugaiyan, G., da Cunha, A.P., Ajay, A.K., Joller, N., Garo, L.P., Kumaradevan, S., Yosef, N., Vaidya, V.S., and Weiner, H.L. (2015). MicroRNA-21 promotes Th17 differentiation and mediates experimental autoimmune encephalomyelitis. *J Clin Invest* *125*, 1069-1080.
- Mycko, M.P., Cichalewska, M., Machlanska, A., Cwiklinska, H., Mariasiewicz, M., and Selmaj, K.W. (2012). MicroRNA-301a regulation of a T-helper 17 immune response controls autoimmune demyelination. *Proc Natl Acad Sci U S A* *109*, E1248-1257.
- Nagaleekar, V.K., Diehl, S.A., Juncadella, I., Charland, C., Muthusamy, N., Eaton, S., Haynes, L., Garrett-Sinha, L.A., Anguita, J., and Rincon, M. (2008). IP3 receptor-mediated Ca<sup>2+</sup> release in naive CD4 T cells dictates their cytokine program. *J Immunol* *181*, 8315-8322.
- Nakahama, T., Hanieh, H., Nguyen, N.T., Chinen, I., Ripley, B., Millrine, D., Lee, S., Nyati, K.K., Dubey, P.K., Chowdhury, K., *et al.* (2013). Aryl hydrocarbon receptor-mediated induction of the microRNA-132/212 cluster promotes interleukin-17-producing T-helper cell differentiation. *Proc Natl Acad Sci U S A* *110*, 11964-11969.
- Nakasa, T., Miyaki, S., Okubo, A., Hashimoto, M., Nishida, K., Ochi, M., and Asahara, H. (2008). Expression of microRNA-146 in rheumatoid arthritis synovial tissue. *Arthritis Rheum* *58*, 1284-1292.
- Nara, H., Onoda, T., Rahman, M., Araki, A., Juliana, F.M., Tanaka, N., and Asao, H. (2011). WSB-1, a novel IL-21 receptor binding molecule, enhances the maturation of IL-21 receptor. *Cell Immunol* *269*, 54-59.
- Nata, T., Fujiya, M., Ueno, N., Moriichi, K., Konishi, H., Tanabe, H., Ohtake, T., Ikuta, K., and Kohgo, Y. (2013). MicroRNA-146b improves intestinal injury in mouse colitis by activating nuclear factor-kappaB and improving epithelial barrier function. *J Gene Med* *15*, 249-260.
- Niederer, F., Trenkmann, M., Ospelt, C., Karouzakis, E., Neidhart, M., Stanczyk, J., Kolling, C., Gay, R.E., Detmar, M., Gay, S., *et al.* (2012). Down-regulation of microRNA-34a\* in rheumatoid arthritis synovial fibroblasts promotes apoptosis resistance. *Arthritis Rheum* *64*, 1771-1779.
- Niesner, U., Albrecht, I., Janke, M., Doebis, C., Loddenkemper, C., Lexberg, M.H., Eulenburg, K., Kreher, S., Koeck, J., Baumgrass, R., *et al.* (2008). Autoregulation of Th1-mediated inflammation by twist1. *J Exp Med* *205*, 1889-1901.
- Nishizuka, Y., and Sakakura, T. (1969). Thymus and reproduction: sex-linked dysgenesis of the gonad after neonatal thymectomy in mice. *Science* *166*, 753-755.
- Noguchi, M., Hiwatashi, N., Liu, Z., and Toyota, T. (1995). Enhanced interferon-gamma production and B7-2 expression in isolated intestinal mononuclear cells from patients with Crohn's disease. *J Gastroenterol* *30 Suppl 8*, 52-55.
- Nozawa, K., Fujishiro, M., Kawasaki, M., Yamaguchi, A., Ikeda, K., Morimoto, S., Iwabuchi, K., Yanagida, M., Ichinose, S., Morioka, M., *et al.* (2013). Inhibition of

connective tissue growth factor ameliorates disease in a murine model of rheumatoid arthritis. *Arthritis Rheum* 65, 1477-1486.

O'Connell, R.M., Kahn, D., Gibson, W.S., Round, J.L., Scholz, R.L., Chaudhuri, A.A., Kahn, M.E., Rao, D.S., and Baltimore, D. (2010). MicroRNA-155 promotes autoimmune inflammation by enhancing inflammatory T cell development. *Immunity* 33, 607-619.

O'Connell, R.M., Taganov, K.D., Boldin, M.P., Cheng, G., and Baltimore, D. (2007). MicroRNA-155 is induced during the macrophage inflammatory response. *Proc Natl Acad Sci U S A* 104, 1604-1609.

Ogura, Y., Bonen, D.K., Inohara, N., Nicolae, D.L., Chen, F.F., Ramos, R., Britton, H., Moran, T., Karaliuskas, R., Duerr, R.H., *et al.* (2001). A frameshift mutation in NOD2 associated with susceptibility to Crohn's disease. *Nature* 411, 603-606.

Okamura, T., Fujio, K., Shibuya, M., Sumitomo, S., Shoda, H., Sakaguchi, S., and Yamamoto, K. (2009). CD4<sup>+</sup>CD25<sup>+</sup>LAG3<sup>+</sup> regulatory T cells controlled by the transcription factor Egr-2. *Proc Natl Acad Sci U S A* 106, 13974-13979.

Okayasu, I., Hatakeyama, S., Yamada, M., Ohkusa, T., Inagaki, Y., and Nakaya, R. (1990). A novel method in the induction of reliable experimental acute and chronic ulcerative colitis in mice. *Gastroenterology* 98, 694-702.

Okazaki, T., Okazaki, I.M., Wang, J., Sugiura, D., Nakaki, F., Yoshida, T., Kato, Y., Fagarasan, S., Muramatsu, M., Eto, T., *et al.* (2011). PD-1 and LAG-3 inhibitory co-receptors act synergistically to prevent autoimmunity in mice. *J Exp Med* 208, 395-407.

Oppmann, B., Lesley, R., Blom, B., Timans, J.C., Xu, Y., Hunte, B., Vega, F., Yu, N., Wang, J., Singh, K., *et al.* (2000). Novel p19 protein engages IL-12p40 to form a cytokine, IL-23, with biological activities similar as well as distinct from IL-12. *Immunity* 13, 715-725.

Orsini, H., Araujo, L.P., Maricato, J.T., Guerreschi, M.G., Mariano, M., Castilho, B.A., and Basso, A.S. (2014). GCN2 kinase plays an important role triggering the remission phase of experimental autoimmune encephalomyelitis (EAE) in mice. *Brain Behav Immun* 37, 177-186.

Owyang, A.M., Zaph, C., Wilson, E.H., Guild, K.J., McClanahan, T., Miller, H.R., Cua, D.J., Goldschmidt, M., Hunter, C.A., Kastelein, R.A., and Artis, D. (2006). Interleukin 25 regulates type 2 cytokine-dependent immunity and limits chronic inflammation in the gastrointestinal tract. *J Exp Med* 203, 843-849.

Pandiyan, P., Zheng, L., Ishihara, S., Reed, J., and Lenardo, M.J. (2007). CD4<sup>+</sup>CD25<sup>+</sup>Foxp3<sup>+</sup> regulatory T cells induce cytokine deprivation-mediated apoptosis of effector CD4<sup>+</sup> T cells. *Nat Immunol* 8, 1353-1362.

Parikh, A., Leach, T., Wyant, T., Scholz, C., Sankoh, S., Mould, D.R., Ponich, T., Fox, I., and Feagan, B.G. (2012). Vedolizumab for the treatment of active ulcerative colitis: a randomized controlled phase 2 dose-ranging study. *Inflamm Bowel Dis* 18, 1470-1479.

Park, M.J., Moon, S.J., Lee, S.H., Kim, E.K., Yang, E.J., Min, J.K., Park, S.H., Kim, H.Y., Yang, C.W., and Cho, M.L. (2014). Blocking activator protein 1 activity in donor cells reduces severity of acute graft-versus-host disease through reciprocal regulation of

- IL-17-producing T cells/regulatory T cells. *Biol Blood Marrow Transplant* 20, 1112-1120.
- Parkes, M., Barrett, J.C., Prescott, N.J., Tremelling, M., Anderson, C.A., Fisher, S.A., Roberts, R.G., Nimmo, E.R., Cummings, F.R., Soars, D., *et al.* (2007). Sequence variants in the autophagy gene IRGM and multiple other replicating loci contribute to Crohn's disease susceptibility. *Nat Genet* 39, 830-832.
- Parkin, J., and Cohen, B. (2001). An overview of the immune system. *Lancet* 357, 1777-1789.
- Parronchi, P., De Carli, M., Manetti, R., Simonelli, C., Sampognaro, S., Piccinni, M.P., Macchia, D., Maggi, E., Del Prete, G., and Romagnani, S. (1992). IL-4 and IFN (alpha and gamma) exert opposite regulatory effects on the development of cytolytic potential by Th1 or Th2 human T cell clones. *J Immunol* 149, 2977-2983.
- Paul, G., Khare, V., and Gasche, C. (2012). Inflamed gut mucosa: downstream of interleukin-10. *Eur J Clin Invest* 42, 95-109.
- Peine, M., Rausch, S., Helmstetter, C., Frohlich, A., Hegazy, A.N., Kuhl, A.A., Grevelding, C.G., Hofer, T., Hartmann, S., and Lohning, M. (2013). Stable Tbet(+)GATA-3(+) Th1/Th2 hybrid cells arise in vivo, can develop directly from naive precursors, and limit immunopathologic inflammation. *PLoS Biol* 11, e1001633.
- Pham, D., Vincentz, J.W., Firulli, A.B., and Kaplan, M.H. (2012). Twist1 regulates Ifng expression in Th1 cells by interfering with Runx3 function. *J Immunol* 189, 832-840.
- Pham, D., Walline, C.C., Hollister, K., Dent, A.L., Blum, J.S., Firulli, A.B., and Kaplan, M.H. (2013). The transcription factor Twist1 limits T helper 17 and T follicular helper cell development by repressing the gene encoding the interleukin-6 receptor alpha chain. *J Biol Chem* 288, 27423-27433.
- Picca, C.C., Larkin, J., 3rd, Boesteanu, A., Lerman, M.A., Rankin, A.L., and Caton, A.J. (2006). Role of TCR specificity in CD4+ CD25+ regulatory T-cell selection. *Immunol Rev* 212, 74-85.
- Pieters, J., Muller, P., and Jayachandran, R. (2013). On guard: coronin proteins in innate and adaptive immunity. *Nat Rev Immunol* 13, 510-518.
- Porrello, E.R., Johnson, B.A., Aurora, A.B., Simpson, E., Nam, Y.J., Matkovich, S.J., Dorn, G.W., 2nd, van Rooij, E., and Olson, E.N. (2011). MiR-15 family regulates postnatal mitotic arrest of cardiomyocytes. *Circ Res* 109, 670-679.
- Porrello, E.R., Mahmoud, A.I., Simpson, E., Johnson, B.A., Grinsfelder, D., Canseco, D., Mammen, P.P., Rothenmel, B.A., Olson, E.N., and Sadek, H.A. (2013). Regulation of neonatal and adult mammalian heart regeneration by the miR-15 family. *Proc Natl Acad Sci U S A* 110, 187-192.
- Powrie, F., Carlino, J., Leach, M.W., Mauze, S., and Coffman, R.L. (1996). A critical role for transforming growth factor-beta but not interleukin 4 in the suppression of T helper type 1-mediated colitis by CD45RB(low) CD4+ T cells. *J Exp Med* 183, 2669-2674.

Powrie, F., Leach, M.W., Mauze, S., Caddle, L.B., and Coffman, R.L. (1993). Phenotypically distinct subsets of CD4<sup>+</sup> T cells induce or protect from chronic intestinal inflammation in C. B-17 scid mice. *Int Immunol* 5, 1461-1471.

Pritchard, C.C., Cheng, H.H., and Tewari, M. (2012). MicroRNA profiling: approaches and considerations. *Nat Rev Genet* 13, 358-369.

Pulendran, B., and Artis, D. (2012). New paradigms in type 2 immunity. *Science* 337, 431-435.

Qi, J., Qiao, Y., Wang, P., Li, S., Zhao, W., and Gao, C. (2012). microRNA-210 negatively regulates LPS-induced production of proinflammatory cytokines by targeting NF-kappaB1 in murine macrophages. *FEBS Lett* 586, 1201-1207.

Qureshi, O.S., Zheng, Y., Nakamura, K., Attridge, K., Manzotti, C., Schmidt, E.M., Baker, J., Jeffery, L.E., Kaur, S., Briggs, Z., *et al.* (2011). Trans-endocytosis of CD80 and CD86: a molecular basis for the cell-extrinsic function of CTLA-4. *Science* 332, 600-603.

Raphael, I., and Forsthuber, T.G. (2012). Stability of T-cell lineages in autoimmune diseases. *Expert Rev Clin Immunol* 8, 299-301.

Rath, H.C., Herfarth, H.H., Ikeda, J.S., Grenther, W.B., Hamm, T.E., Jr., Balish, E., Taurog, J.D., Hammer, R.E., Wilson, K.H., and Sartor, R.B. (1996). Normal luminal bacteria, especially *Bacteroides* species, mediate chronic colitis, gastritis, and arthritis in HLA-B27/human beta2 microglobulin transgenic rats. *J Clin Invest* 98, 945-953.

Rio, A., Hannon and Nilsen (2011). *RNA a laboratory manual* (New York: John Inglis).

Rizzo, A., De Mare, V., Rocchi, C., Stolfi, C., Colantoni, A., Neurath, M.F., Macdonald, T.T., Pallone, F., Monteleone, G., and Fantini, M.C. (2014). Smad7 induces plasticity in tumor-infiltrating Th17 cells and enables TNF-alpha-mediated killing of colorectal cancer cells. *Carcinogenesis* 35, 1536-1546.

Rodriguez-Diez, R.R., Garcia-Redondo, A.B., Orejudo, M., Rodriguez-Diez, R., Briones, A.M., Bosch-Panadero, E., Kery, G., Pato, J., Ortiz, A., Salaices, M., *et al.* (2015). The C-terminal module IV of connective tissue growth factor, through EGFR/Nox1 signaling, activates the NF-kappaB pathway and proinflammatory factors in vascular smooth muscle cells. *Antioxid Redox Signal* 22, 29-47.

Rodriguez, A., Vigorito, E., Clare, S., Warren, M.V., Couttet, P., Soond, D.R., van Dongen, S., Grocock, R.J., Das, P.P., Miska, E.A., *et al.* (2007). Requirement of bic/microRNA-155 for normal immune function. *Science* 316, 608-611.

Roers, A., Siewe, L., Strittmatter, E., Deckert, M., Schluter, D., Stenzel, W., Gruber, A.D., Krieg, T., Rajewsky, K., and Muller, W. (2004). T cell-specific inactivation of the interleukin 10 gene in mice results in enhanced T cell responses but normal innate responses to lipopolysaccharide or skin irritation. *J Exp Med* 200, 1289-1297.

Roncarolo, M.G., Gregori, S., Battaglia, M., Bacchetta, R., Fleischhauer, K., and Levings, M.K. (2006). Interleukin-10-secreting type 1 regulatory T cells in rodents and humans. *Immunol Rev* 212, 28-50.

- Roncarolo, M.G., Gregori, S., Lucarelli, B., Ciceri, F., and Bacchetta, R. (2011). Clinical tolerance in allogeneic hematopoietic stem cell transplantation. *Immunol Rev* 241, 145-163.
- Rouas, R., Fayyad-Kazan, H., El Zein, N., Lewalle, P., Rothe, F., Simion, A., Akl, H., Mourtada, M., El Rifai, M., Burny, A., *et al.* (2009). Human natural Treg microRNA signature: role of microRNA-31 and microRNA-21 in FOXP3 expression. *Eur J Immunol* 39, 1608-1618.
- Round, J.L., and Mazmanian, S.K. (2010). Inducible Foxp3<sup>+</sup> regulatory T-cell development by a commensal bacterium of the intestinal microbiota. *Proc Natl Acad Sci U S A* 107, 12204-12209.
- Ruan, Q., Wang, T., Kameswaran, V., Wei, Q., Johnson, D.S., Matschinsky, F., Shi, W., and Chen, Y.H. (2011). The microRNA-21-PDCD4 axis prevents type 1 diabetes by blocking pancreatic beta cell death. *Proc Natl Acad Sci U S A* 108, 12030-12035.
- Rubtsov, Y.P., Rasmussen, J.P., Chi, E.Y., Fontenot, J., Castelli, L., Ye, X., Treuting, P., Siewe, L., Roers, A., Henderson, W.R., Jr., *et al.* (2008). Regulatory T cell-derived interleukin-10 limits inflammation at environmental interfaces. *Immunity* 28, 546-558.
- Ruvkun, G., and Giusto, J. (1989). The *Caenorhabditis elegans* heterochronic gene *lin-14* encodes a nuclear protein that forms a temporal developmental switch. *Nature* 338, 313-319.
- Sadlack, B., Merz, H., Schorle, H., Schimpl, A., Feller, A.C., and Horak, I. (1993). Ulcerative colitis-like disease in mice with a disrupted interleukin-2 gene. *Cell* 75, 253-261.
- Sagoo, P., Ali, N., Garg, G., Nestle, F.O., Lechler, R.I., and Lombardi, G. (2011). Human regulatory T cells with alloantigen specificity are more potent inhibitors of alloimmune skin graft damage than polyclonal regulatory T cells. *Sci Transl Med* 3, 83ra42.
- Sakaguchi, S., Sakaguchi, N., Asano, M., Itoh, M., and Toda, M. (1995). Immunologic self-tolerance maintained by activated T cells expressing IL-2 receptor alpha-chains (CD25). Breakdown of a single mechanism of self-tolerance causes various autoimmune diseases. *J Immunol* 155, 1151-1164.
- Sakaguchi, S., Takahashi, T., and Nishizuka, Y. (1982). Study on cellular events in post-thymectomy autoimmune oophoritis in mice. II. Requirement of Lyt-1 cells in normal female mice for the prevention of oophoritis. *J Exp Med* 156, 1577-1586.
- Sakaguchi, S., Toda, M., Asano, M., Itoh, M., Morse, S.S., and Sakaguchi, N. (1996). T cell-mediated maintenance of natural self-tolerance: its breakdown as a possible cause of various autoimmune diseases. *J Autoimmun* 9, 211-220.
- Sakata, D., Yao, C., and Narumiya, S. (2010). Emerging roles of prostanoids in T cell-mediated immunity. *IUBMB Life* 62, 591-596.
- Sandborn, W.J., Colombel, J.F., Enns, R., Feagan, B.G., Hanauer, S.B., Lawrance, I.C., Panaccione, R., Sanders, M., Schreiber, S., Targan, S., *et al.* (2005). Natalizumab induction and maintenance therapy for Crohn's disease. *N Engl J Med* 353, 1912-1925.

- Sandborn, W.J., Feagan, B.G., Rutgeerts, P., Hanauer, S., Colombel, J.F., Sands, B.E., Lukas, M., Fedorak, R.N., Lee, S., Bressler, B., *et al.* (2013). Vedolizumab as induction and maintenance therapy for Crohn's disease. *N Engl J Med* 369, 711-721.
- Sanin, D.E., Prendergast, C.T., Bourke, C.D., and Mountford, A.P. (2015). Helminth Infection and Commensal Microbiota Drive Early IL-10 Production in the Skin by CD4+ T Cells That Are Functionally Suppressive. *PLoS Pathog* 11, e1004841.
- Saraiva, M., Christensen, J.R., Veldhoen, M., Murphy, T.L., Murphy, K.M., and O'Garra, A. (2009). Interleukin-10 production by Th1 cells requires interleukin-12-induced STAT4 transcription factor and ERK MAP kinase activation by high antigen dose. *Immunity* 31, 209-219.
- Sasaki, M., Mathis, J.M., Jennings, M.H., Jordan, P., Wang, Y., Ando, T., Joh, T., and Alexander, J.S. (2005). Reversal of experimental colitis disease activity in mice following administration of an adenoviral IL-10 vector. *J Inflamm (Lond)* 2, 13.
- Sawant, D.V., Yao, W., Wright, Z., Sawyers, C., Tepper, R.S., Gupta, S.K., Kaplan, M.H., and Dent, A.L. (2015). Serum MicroRNA-21 as a Biomarker for Allergic Inflammatory Disease in Children. *Microna*.
- Schaefer, J.S., Montufar-Solis, D., Vigneswaran, N., and Klein, J.R. (2011). Selective upregulation of microRNA expression in peripheral blood leukocytes in IL-10<sup>-/-</sup> mice precedes expression in the colon. *J Immunol* 187, 5834-5841.
- Schraml, B.U., Hildner, K., Ise, W., Lee, W.L., Smith, W.A., Solomon, B., Sahota, G., Sim, J., Mukasa, R., Cemurski, S., *et al.* (2009). The AP-1 transcription factor Batf controls T(H)17 differentiation. *Nature* 460, 405-409.
- Schreiber, S., Fedorak, R.N., Nielsen, O.H., Wild, G., Williams, C.N., Nikolaus, S., Jacyna, M., Lashner, B.A., Gangl, A., Rutgeerts, P., *et al.* (2000). Safety and efficacy of recombinant human interleukin 10 in chronic active Crohn's disease. Crohn's Disease IL-10 Cooperative Study Group. *Gastroenterology* 119, 1461-1472.
- Scotta, C., Esposito, M., Fazekasova, H., Fanelli, G., Edozie, F.C., Ali, N., Xiao, F., Peakman, M., Afzali, B., Sagoo, P., *et al.* (2013). Differential effects of rapamycin and retinoic acid on expansion, stability and suppressive qualities of human CD4(+)CD25(+)FOXP3(+) T regulatory cell subpopulations. *Haematologica* 98, 1291-1299.
- Sebastiani, G., Grieco, F.A., Spagnuolo, I., Galleri, L., Cataldo, D., and Dotta, F. (2011). Increased expression of microRNA miR-326 in type 1 diabetic patients with ongoing islet autoimmunity. *Diabetes Metab Res Rev* 27, 862-866.
- Sellon, R.K., Tonkonogy, S., Schultz, M., Dieleman, L.A., Grenther, W., Balish, E., Rennick, D.M., and Sartor, R.B. (1998). Resident enteric bacteria are necessary for development of spontaneous colitis and immune system activation in interleukin-10-deficient mice. *Infect Immun* 66, 5224-5231.
- Shaker, O., Maher, M., Nassar, Y., Morcos, G., and Gad, Z. (2015). Role of microRNAs -29b-2, -155, -197 and -205 as diagnostic biomarkers in serum of breast cancer females. *Gene* 560, 77-82.

Shang, C., Hong, Y., Guo, Y., Liu, Y.H., and Xue, Y.X. (2014). MiR-210 up-regulation inhibits proliferation and induces apoptosis in glioma cells by targeting SIN3A. *Med Sci Monit* 20, 2571-2577.

Shevach, E.M., and Thornton, A.M. (2014). tTregs, pTregs, and iTregs: similarities and differences. *Immunol Rev* 259, 88-102.

Shi, C., Liang, Y., Yang, J., Xia, Y., Chen, H., Han, H., Yang, Y., Wu, W., Gao, R., and Qin, H. (2013). MicroRNA-21 knockout improve the survival rate in DSS induced fatal colitis through protecting against inflammation and tissue injury. *PLoS One* 8, e66814.

Shi, M., Zhu, J., Wang, R., Chen, X., Mi, L., Walz, T., and Springer, T.A. (2011). Latent TGF-beta structure and activation. *Nature* 474, 343-349.

Shim, J.O., and Seo, J.K. (2014). Very early-onset inflammatory bowel disease (IBD) in infancy is a different disease entity from adult-onset IBD; one form of interleukin-10 receptor mutations. *J Hum Genet* 59, 337-341.

Singh, B., Schwartz, J.A., Sandrock, C., Bellemore, S.M., and Nikoopour, E. (2013). Modulation of autoimmune diseases by interleukin (IL)-17 producing regulatory T helper (Th17) cells. *Indian J Med Res* 138, 591-594.

Singh, K., Hjort, M., Thorvaldson, L., and Sandler, S. (2015). Concomitant analysis of Helios and Neuropilin-1 as a marker to detect thymic derived regulatory T cells in naive mice. *Sci Rep* 5, 7767.

Singh, N., Gurav, A., Sivaprakasam, S., Brady, E., Padia, R., Shi, H., Thangaraju, M., Prasad, P.D., Manicassamy, S., Munn, D.H., *et al.* (2014a). Activation of Gpr109a, receptor for niacin and the commensal metabolite butyrate, suppresses colonic inflammation and carcinogenesis. *Immunity* 40, 128-139.

Singh, U.P., Murphy, A.E., Enos, R.T., Shamran, H.A., Singh, N.P., Guan, H., Hegde, V.L., Fan, D., Price, R.L., Taub, D.D., *et al.* (2014b). miR-155 deficiency protects mice from experimental colitis by reducing T helper type 1/type 17 responses. *Immunology* 143, 478-489.

Skurkovich, S., and Skurkovich, B. (2005). Anticytokine therapy, especially anti-interferon-gamma, as a pathogenetic treatment in TH-1 autoimmune diseases. *Ann N Y Acad Sci* 1051, 684-700.

Smigielska-Czepiel, K., van den Berg, A., Jellema, P., Slezak-Prochazka, I., Maat, H., van den Bos, H., van der Lei, R.J., Kluiver, J., Brouwer, E., Boots, A.M., and Kroesen, B.J. (2013). Dual role of miR-21 in CD4+ T-cells: activation-induced miR-21 supports survival of memory T-cells and regulates CCR7 expression in naive T-cells. *PLoS One* 8, e76217.

Smith, K.A., Filbey, K.J., Reynolds, L.A., Hewitson, J.P., Harcus, Y., Boon, L., Sparwasser, T., Hammerling, G., and Maizels, R.M. (2015). Low-level regulatory T-cell activity is essential for functional type-2 effector immunity to expel gastrointestinal helminths. *Mucosal Immunol*.

Smith, K.M., Guerau-de-Arellano, M., Costinean, S., Williams, J.L., Bottoni, A., Mavrikis Cox, G., Satoskar, A.R., Croce, C.M., Racke, M.K., Lovett-Racke, A.E., and Whitacre, C.C. (2012). miR-29ab1 deficiency identifies a negative feedback loop

- controlling Th1 bias that is dysregulated in multiple sclerosis. *J Immunol* *189*, 1567-1576.
- Snapper, C.M., and Paul, W.E. (1987). Interferon-gamma and B cell stimulatory factor-1 reciprocally regulate Ig isotype production. *Science* *236*, 944-947.
- Solnick, J.V., and Schauer, D.B. (2001). Emergence of diverse *Helicobacter* species in the pathogenesis of gastric and enterohepatic diseases. *Clin Microbiol Rev* *14*, 59-97.
- Soroosh, P., and Doherty, T.A. (2009). Th9 and allergic disease. *Immunology* *127*, 450-458.
- Spencer, S.D., Di Marco, F., Hooley, J., Pitts-Meek, S., Bauer, M., Ryan, A.M., Sordat, B., Gibbs, V.C., and Aguet, M. (1998). The orphan receptor CRF2-4 is an essential subunit of the interleukin 10 receptor. *J Exp Med* *187*, 571-578.
- Stagakis, E., Bertsiadis, G., Verginis, P., Nakou, M., Hatziapostolou, M., Kritikos, H., Iliopoulos, D., and Boumpas, D.T. (2011). Identification of novel microRNA signatures linked to human lupus disease activity and pathogenesis: miR-21 regulates aberrant T cell responses through regulation of PDCD4 expression. *Ann Rheum Dis* *70*, 1496-1506.
- Stanczyk, J., Pedrioli, D.M., Brentano, F., Sanchez-Pernaute, O., Kolling, C., Gay, R.E., Detmar, M., Gay, S., and Kyburz, D. (2008). Altered expression of MicroRNA in synovial fibroblasts and synovial tissue in rheumatoid arthritis. *Arthritis Rheum* *58*, 1001-1009.
- Staudt, V., Bothur, E., Klein, M., Lingnau, K., Reuter, S., Grebe, N., Gerlitzki, B., Hoffmann, M., Ulges, A., Taube, C., *et al.* (2010). Interferon-regulatory factor 4 is essential for the developmental program of T helper 9 cells. *Immunity* *33*, 192-202.
- Stenvang, J., Petri, A., Lindow, M., Obad, S., and Kauppinen, S. (2012). Inhibition of microRNA function by antimiR oligonucleotides. *Silence* *3*, 1.
- Stepankova, R., Powrie, F., Kofronova, O., Kozakova, H., Hudcovic, T., Hrnecir, T., Uhlig, H., Read, S., Rehakova, Z., Benada, O., *et al.* (2007). Segmented filamentous bacteria in a defined bacterial cocktail induce intestinal inflammation in SCID mice reconstituted with CD45RB<sup>high</sup> CD4<sup>+</sup> T cells. *Inflamm Bowel Dis* *13*, 1202-1211.
- Stritesky, G.L., Yeh, N., and Kaplan, M.H. (2008). IL-23 promotes maintenance but not commitment to the Th17 lineage. *J Immunol* *181*, 5948-5955.
- Sun, C.M., Hall, J.A., Blank, R.B., Bouladoux, N., Oukka, M., Mora, J.R., and Belkaid, Y. (2007). Small intestine lamina propria dendritic cells promote de novo generation of Foxp3 T reg cells via retinoic acid. *J Exp Med* *204*, 1775-1785.
- Sun, Y., Sun, J., Tomomi, T., Nieves, E., Mathewson, N., Tamaki, H., Evers, R., and Reddy, P. (2013). PU.1-dependent transcriptional regulation of miR-142 contributes to its hematopoietic cell-specific expression and modulation of IL-6. *J Immunol* *190*, 4005-4013.
- Sundrud, M.S., Koralov, S.B., Feuerer, M., Calado, D.P., Kozhaya, A.E., Rhule-Smith, A., Lefebvre, R.E., Unutmaz, D., Mazitschek, R., Waldner, H., *et al.* (2009).

Halofuginone inhibits TH17 cell differentiation by activating the amino acid starvation response. *Science* *324*, 1334-1338.

Suri-Payer, E., Amar, A.Z., Thornton, A.M., and Shevach, E.M. (1998). CD4<sup>+</sup>CD25<sup>+</sup> T cells inhibit both the induction and effector function of autoreactive T cells and represent a unique lineage of immunoregulatory cells. *J Immunol* *160*, 1212-1218.

Svensson, M., Marsal, J., Ericsson, A., Carramolino, L., Broden, T., Marquez, G., and Agace, W.W. (2002). CCL25 mediates the localization of recently activated CD8 $\alpha$ beta(+) lymphocytes to the small-intestinal mucosa. *J Clin Invest* *110*, 1113-1121.

Szabo, S.J., Kim, S.T., Costa, G.L., Zhang, X., Fathman, C.G., and Glimcher, L.H. (2000). A novel transcription factor, T-bet, directs Th1 lineage commitment. *Cell* *100*, 655-669.

Taganov, K.D., Boldin, M.P., Chang, K.J., and Baltimore, D. (2006). NF-kappaB-dependent induction of microRNA miR-146, an inhibitor targeted to signaling proteins of innate immune responses. *Proc Natl Acad Sci U S A* *103*, 12481-12486.

Taguchi, O., and Nishizuka, Y. (1981). Experimental autoimmune orchitis after neonatal thymectomy in the mouse. *Clin Exp Immunol* *46*, 425-434.

Tai, X., Cowan, M., Feigenbaum, L., and Singer, A. (2005). CD28 costimulation of developing thymocytes induces Foxp3 expression and regulatory T cell differentiation independently of interleukin 2. *Nat Immunol* *6*, 152-162.

Takahashi, T., Kuniyasu, Y., Toda, M., Sakaguchi, N., Itoh, M., Iwata, M., Shimizu, J., and Sakaguchi, S. (1998). Immunologic self-tolerance maintained by CD25<sup>+</sup>CD4<sup>+</sup> naturally anergic and suppressive T cells: induction of autoimmune disease by breaking their anergic/suppressive state. *Int Immunol* *10*, 1969-1980.

Takamori, M., Hatano, M., Arima, M., Sakamoto, A., Fujimura, L., Hartatik, T., Kuriyama, T., and Tokuhisa, T. (2004). BAZF is required for activation of naive CD4 T cells by TCR triggering. *Int Immunol* *16*, 1439-1449.

Tang, Y.F., Zhang, Y., Li, X.Y., Li, C., Tian, W., and Liu, L. (2009). Expression of miR-31, miR-125b-5p, and miR-326 in the adipogenic differentiation process of adipose-derived stem cells. *OMICS* *13*, 331-336.

Tao, X., Constant, S., Jorritsma, P., and Bottomly, K. (1997). Strength of TCR signal determines the costimulatory requirements for Th1 and Th2 CD4<sup>+</sup> T cell differentiation. *J Immunol* *159*, 5956-5963.

Targan, S.R., Feagan, B.G., Fedorak, R.N., Lashner, B.A., Panaccione, R., Present, D.H., Spehlmann, M.E., Rutgeerts, P.J., Tulassay, Z., Volfova, M., *et al.* (2007). Natalizumab for the treatment of active Crohn's disease: results of the ENCORE Trial. *Gastroenterology* *132*, 1672-1683.

Taurog, J.D., Richardson, J.A., Croft, J.T., Simmons, W.A., Zhou, M., Fernandez-Sueiro, J.L., Balish, E., and Hammer, R.E. (1994). The germfree state prevents development of gut and joint inflammatory disease in HLA-B27 transgenic rats. *J Exp Med* *180*, 2359-2364.

Thai, T.H., Calado, D.P., Casola, S., Ansel, K.M., Xiao, C., Xue, Y., Murphy, A., Friendewey, D., Valenzuela, D., Kutok, J.L., *et al.* (2007). Regulation of the germinal center response by microRNA-155. *Science* 316, 604-608.

Thermann, R., and Hentze, M.W. (2007). *Drosophila* miR2 induces pseudo-polysomes and inhibits translation initiation. *Nature* 447, 875-878.

Thierfelder, W.E., van Deursen, J.M., Yamamoto, K., Tripp, R.A., Sarawar, S.R., Carson, R.T., Sangster, M.Y., Vignali, D.A., Doherty, P.C., Grosveld, G.C., and Ihle, J.N. (1996). Requirement for Stat4 in interleukin-12-mediated responses of natural killer and T cells. *Nature* 382, 171-174.

Thompson, A.I., and Lees, C.W. (2011). Genetics of ulcerative colitis. *Inflamm Bowel Dis* 17, 831-848.

Thornton, A.M., Korty, P.E., Tran, D.Q., Wohlfert, E.A., Murray, P.E., Belkaid, Y., and Shevach, E.M. (2010). Expression of Helios, an Ikaros transcription factor family member, differentiates thymic-derived from peripherally induced Foxp3<sup>+</sup> T regulatory cells. *J Immunol* 184, 3433-3441.

Thornton, A.M., and Shevach, E.M. (1998). CD4<sup>+</sup>CD25<sup>+</sup> immunoregulatory T cells suppress polyclonal T cell activation *in vitro* by inhibiting interleukin 2 production. *J Exp Med* 188, 287-296.

Thum, T., Gross, C., Fiedler, J., Fischer, T., Kissler, S., Bussen, M., Galuppo, P., Just, S., Rottbauer, W., Frantz, S., *et al.* (2008). MicroRNA-21 contributes to myocardial disease by stimulating MAP kinase signalling in fibroblasts. *Nature* 456, 980-U983.

Toms, C., and Powrie, F. (2001). Control of intestinal inflammation by regulatory T cells. *Microbes Infect* 3, 929-935.

Tong, Y., Aune, T., and Boothby, M. (2005). T-bet antagonizes mSin3a recruitment and transactivates a fully methylated IFN-gamma promoter via a conserved T-box half-site. *Proc Natl Acad Sci U S A* 102, 2034-2039.

Trajkovski, M., Hausser, J., Soutschek, J., Bhat, B., Akin, A., Zavolan, M., Heim, M.H., and Stoffel, M. (2011). MicroRNAs 103 and 107 regulate insulin sensitivity. *Nature* 474, 649-U127.

Trang, P., Medina, P.P., Wiggins, J.F., Ruffino, L., Kelnar, K., Omotola, M., Homer, R., Brown, D., Bader, A.G., Weidhaas, J.B., and Slack, F.J. (2010). Regression of murine lung tumors by the let-7 microRNA. *Oncogene* 29, 1580-1587.

Travis, M.A., Reizis, B., Melton, A.C., Masteller, E., Tang, Q., Proctor, J.M., Wang, Y., Bernstein, X., Huang, X., Reichardt, L.F., *et al.* (2007). Loss of integrin alpha(v)beta8 on dendritic cells causes autoimmunity and colitis in mice. *Nature* 449, 361-365.

Trifari, S., Kaplan, C.D., Tran, E.H., Crellin, N.K., and Spits, H. (2009). Identification of a human helper T cell population that has abundant production of interleukin 22 and is distinct from T(H)-17, T(H)1 and T(H)2 cells. *Nat Immunol* 10, 864-871.

Trzonkowski, P., Bieniaszewska, M., Juscinska, J., Dobyszyk, A., Krzystyniak, A., Marek, N., Mysliwska, J., and Hellmann, A. (2009). First-in-man clinical results of the

treatment of patients with graft versus host disease with human ex vivo expanded CD4+CD25+CD127- T regulatory cells. *Clin Immunol* 133, 22-26.

Ueda, A., Zhou, L., and Stein, P.L. (2012). Fyn promotes Th17 differentiation by regulating the kinetics of ROR $\gamma$  and Foxp3 expression. *J Immunol* 188, 5247-5256.

Uhlig, H.H., Coombes, J., Mottet, C., Izcue, A., Thompson, C., Fanger, A., Tannapfel, A., Fontenot, J.D., Ramsdell, F., and Powrie, F. (2006). Characterization of Foxp3+CD4+CD25+ and IL-10-secreting CD4+CD25+ T cells during cure of colitis. *J Immunol* 177, 5852-5860.

Valencia-Sanchez, M.A., Liu, J., Hannon, G.J., and Parker, R. (2006). Control of translation and mRNA degradation by miRNAs and siRNAs. *Genes Dev* 20, 515-524.

van Deventer, S.J., Elson, C.O., and Fedorak, R.N. (1997). Multiple doses of intravenous interleukin 10 in steroid-refractory Crohn's disease. Crohn's Disease Study Group. *Gastroenterology* 113, 383-389.

van Rooij, E., Purcell, A.L., and Levin, A.A. (2012). Developing microRNA therapeutics. *Circ Res* 110, 496-507.

van Rooij, E., Sutherland, L.B., Qi, X., Richardson, J.A., Hill, J., and Olson, E.N. (2007). Control of stress-dependent cardiac growth and gene expression by a microRNA. *Science* 316, 575-579.

Veldhoen, M., Hocking, R.J., Atkins, C.J., Locksley, R.M., and Stockinger, B. (2006). TGF $\beta$  in the context of an inflammatory cytokine milieu supports de novo differentiation of IL-17-producing T cells. *Immunity* 24, 179-189.

Veldhoen, M., Uyttenhove, C., van Snick, J., Helmby, H., Westendorf, A., Buer, J., Martin, B., Wilhelm, C., and Stockinger, B. (2008). Transforming growth factor- $\beta$  'reprograms' the differentiation of T helper 2 cells and promotes an interleukin 9-producing subset. *Nat Immunol* 9, 1341-1346.

Ventura, A., Young, A.G., Winslow, M.M., Lintault, L., Meissner, A., Erkeland, S.J., Newman, J., Bronson, R.T., Crowley, D., Stone, J.R., *et al.* (2008). Targeted deletion reveals essential and overlapping functions of the miR-17 through 92 family of miRNA clusters. *Cell* 132, 875-886.

Verhagen, J., and Wraith, D.C. (2010). Comment on "Expression of Helios, an Ikaros transcription factor family member, differentiates thymic-derived from peripherally induced Foxp3+ T regulatory cells". *J Immunol* 185, 7129; author reply 7130.

Vieira, P.L., Christensen, J.R., Minaee, S., O'Neill, E.J., Barrat, F.J., Boonstra, A., Barthlott, T., Stockinger, B., Wraith, D.C., and O'Garra, A. (2004). IL-10-secreting regulatory T cells do not express Foxp3 but have comparable regulatory function to naturally occurring CD4+CD25+ regulatory T cells. *J Immunol* 172, 5986-5993.

Vigorito, E., Perks, K.L., Abreu-Goodger, C., Bunting, S., Xiang, Z., Kohlhaas, S., Das, P.P., Miska, E.A., Rodriguez, A., Bradley, A., *et al.* (2007). microRNA-155 regulates the generation of immunoglobulin class-switched plasma cells. *Immunity* 27, 847-859.

- Voo, K.S., Wang, Y.H., Santori, F.R., Boggiano, C., Wang, Y.H., Arima, K., Bover, L., Hanabuchi, S., Khalili, J., Marinova, E., *et al.* (2009). Identification of IL-17-producing FOXP3<sup>+</sup> regulatory T cells in humans. *Proc Natl Acad Sci U S A* *106*, 4793-4798.
- Wahid, F., Shehzad, A., Khan, T., and Kim, Y.Y. (2010). MicroRNAs: synthesis, mechanism, function, and recent clinical trials. *Biochim Biophys Acta* *1803*, 1231-1243.
- Wakiyama, M., Takimoto, K., Ohara, O., and Yokoyama, S. (2007). Let-7 microRNA-mediated mRNA deadenylation and translational repression in a mammalian cell-free system. *Genes Dev* *21*, 1857-1862.
- Wan, Y.Y., and Flavell, R.A. (2005). Identifying Foxp3-expressing suppressor T cells with a bicistronic reporter. *Proc Natl Acad Sci U S A* *102*, 5126-5131.
- Wang, H., Flach, H., Onizawa, M., Wei, L., McManus, M.T., and Weiss, A. (2014a). Negative regulation of Hif1 $\alpha$  expression and TH17 differentiation by the hypoxia-regulated microRNA miR-210. *Nat Immunol* *15*, 393-401.
- Wang, H., Pan, K., and Xia, J.C. (2009a). Interaction of indoleamine-2,3-dioxygenase and CD4<sup>+</sup>CD25<sup>+</sup> regulatory T cells in tumor immune escape. *Ai Zheng* *28*, 184-187.
- Wang, J., Lee, S., Teh, C.E., Bunting, K., Ma, L., and Shannon, M.F. (2009b). The transcription repressor, ZEB1, cooperates with CtBP2 and HDAC1 to suppress IL-2 gene activation in T cells. *Int Immunol* *21*, 227-235.
- Wang, L., He, L., Zhang, R., Liu, X., Ren, Y., Liu, Z., Zhang, X., Cheng, W., and Hua, Z.C. (2014b). Regulation of T lymphocyte activation by microRNA-21. *Mol Immunol* *59*, 163-171.
- Wang, P., Yang, D., Zhang, H., Wei, X., Ma, T., Cheng, Z., Hong, Q., Hu, J., Zhuo, H., Song, Y., *et al.* (2014c). Early Detection of Lung Cancer in Serum by a Panel of MicroRNA Biomarkers. *Clin Lung Cancer*.
- Wang, S., Lu, S., Geng, S., Ma, S., Liang, Z., and Jiao, B. (2013). Expression and clinical significance of microRNA-326 in human glioma miR-326 expression in glioma. *Med Oncol* *30*, 373.
- Wang, Y., Godec, J., Ben-Aissa, K., Cui, K., Zhao, K., Pucsek, A.B., Lee, Y.K., Weaver, C.T., Yagi, R., and Lazarevic, V. (2014d). The transcription factors T-bet and Runx are required for the ontogeny of pathogenic interferon-gamma-producing T helper 17 cells. *Immunity* *40*, 355-366.
- Wang, Y., Juranek, S., Li, H., Sheng, G., Tuschl, T., and Patel, D.J. (2008). Structure of an argonaute silencing complex with a seed-containing guide DNA and target RNA duplex. *Nature* *456*, 921-926.
- Wang, Y.H., Voo, K.S., Liu, B., Chen, C.Y., Uygungil, B., Spoede, W., Bernstein, J.A., Huston, D.P., and Liu, Y.J. (2010). A novel subset of CD4(+) T(H)2 memory/effector cells that produce inflammatory IL-17 cytokine and promote the exacerbation of chronic allergic asthma. *J Exp Med* *207*, 2479-2491.
- Ward, J.M., Anver, M.R., Haines, D.C., and Benveniste, R.E. (1994a). Chronic active hepatitis in mice caused by *Helicobacter hepaticus*. *Am J Pathol* *145*, 959-968.

- Ward, J.M., Fox, J.G., Anver, M.R., Haines, D.C., George, C.V., Collins, M.J., Jr., Gorelick, P.L., Nagashima, K., Gonda, M.A., Gilden, R.V., and et al. (1994b). Chronic active hepatitis and associated liver tumors in mice caused by a persistent bacterial infection with a novel *Helicobacter* species. *J Natl Cancer Inst* *86*, 1222-1227.
- Weber, J.A., Baxter, D.H., Zhang, S., Huang, D.Y., Huang, K.H., Lee, M.J., Galas, D.J., and Wang, K. (2010). The microRNA spectrum in 12 body fluids. *Clin Chem* *56*, 1733-1741.
- Weiner, H.L. (2001a). Induction and mechanism of action of transforming growth factor-beta-secreting Th3 regulatory cells. *Immunol Rev* *182*, 207-214.
- Weiner, H.L. (2001b). Oral tolerance: immune mechanisms and the generation of Th3-type TGF-beta-secreting regulatory cells. *Microbes Infect* *3*, 947-954.
- Weiss, J.M., Bilate, A.M., Gobert, M., Ding, Y., Curotto de Lafaille, M.A., Parkhurst, C.N., Xiong, H., Dolpady, J., Frey, A.B., Ruocco, M.G., *et al.* (2012). Neuropilin 1 is expressed on thymus-derived natural regulatory T cells, but not mucosa-generated induced Foxp3+ T reg cells. *J Exp Med* *209*, 1723-1742, S1721.
- Wherry, E.J. (2011). T cell exhaustion. *Nat Immunol* *12*, 492-499.
- Wiggins, J.F., Ruffino, L., Kelnar, K., Omotola, M., Patrawala, L., Brown, D., and Bader, A.G. (2010). Development of a lung cancer therapeutic based on the tumor suppressor microRNA-34. *Cancer Res* *70*, 5923-5930.
- Wildin, R.S., Ramsdell, F., Peake, J., Faravelli, F., Casanova, J.L., Buist, N., Levy-Lahad, E., Mazzella, M., Goulet, O., Perroni, L., *et al.* (2001). X-linked neonatal diabetes mellitus, enteropathy and endocrinopathy syndrome is the human equivalent of mouse scurfy. *Nat Genet* *27*, 18-20.
- Wing, K., Onishi, Y., Prieto-Martin, P., Yamaguchi, T., Miyara, M., Fehervari, Z., Nomura, T., and Sakaguchi, S. (2008). CTLA-4 control over Foxp3+ regulatory T cell function. *Science* *322*, 271-275.
- Wirtz, S., Finotto, S., Kanzler, S., Lohse, A.W., Blessing, M., Lehr, H.A., Galle, P.R., and Neurath, M.F. (1999). Cutting edge: chronic intestinal inflammation in STAT-4 transgenic mice: characterization of disease and adoptive transfer by TNF- plus IFN-gamma-producing CD4+ T cells that respond to bacterial antigens. *J Immunol* *162*, 1884-1888.
- Wolff, M.J., Leung, J.M., Davenport, M., Poles, M.A., Cho, I., and Loke, P. (2012). TH17, TH22 and Treg cells are enriched in the healthy human cecum. *PLoS One* *7*, e41373.
- Workman, C.J., Rice, D.S., Dugger, K.J., Kurschner, C., and Vignali, D.A. (2002). Phenotypic analysis of the murine CD4-related glycoprotein, CD223 (LAG-3). *Eur J Immunol* *32*, 2255-2263.
- Worthington, J.J., Czajkowska, B.I., Melton, A.C., and Travis, M.A. (2011). Intestinal dendritic cells specialize to activate transforming growth factor-beta and induce Foxp3+ regulatory T cells via integrin alphavbeta8. *Gastroenterology* *141*, 1802-1812.

- Wu, F., Dong, F., Arendovich, N., Zhang, J., Huang, Y., and Kwon, J.H. (2014). Divergent influence of microRNA-21 deletion on murine colitis phenotypes. *Inflamm Bowel Dis* 20, 1972-1985.
- Wu, F., Guo, N.J., Tian, H., Marohn, M., Gearhart, S., Bayless, T.M., Brant, S.R., and Kwon, J.H. (2011). Peripheral blood microRNAs distinguish active ulcerative colitis and Crohn's disease. *Inflamm Bowel Dis* 17, 241-250.
- Wu, F., Zhang, S., Dassopoulos, T., Harris, M.L., Bayless, T.M., Meltzer, S.J., Brant, S.R., and Kwon, J.H. (2010). Identification of microRNAs associated with ileal and colonic Crohn's disease. *Inflamm Bowel Dis* 16, 1729-1738.
- Wu, F., Zikusoka, M., Trindade, A., Dassopoulos, T., Harris, M.L., Bayless, T.M., Brant, S.R., Chakravarti, S., and Kwon, J.H. (2008). MicroRNAs are differentially expressed in ulcerative colitis and alter expression of macrophage inflammatory peptide-2 alpha. *Gastroenterology* 135, 1624-1635 e1624.
- Wu, L., Fan, J., and Belasco, J.G. (2006). MicroRNAs direct rapid deadenylation of mRNA. *Proc Natl Acad Sci U S A* 103, 4034-4039.
- Wu, L., Hui, H., Wang, L.J., Wang, H., Liu, Q.F., and Han, S.X. (2015). MicroRNA-326 functions as a tumor suppressor in colorectal cancer by targeting the nin one binding protein. *Oncol Rep* 33, 2309-2318.
- Xavier, R.J., and Podolsky, D.K. (2007). Unravelling the pathogenesis of inflammatory bowel disease. *Nature* 448, 427-434.
- Xiao, X., Balasubramanian, S., Liu, W., Chu, X., Wang, H., Taparowsky, E.J., Fu, Y.X., Choi, Y., Walsh, M.C., and Li, X.C. (2012). OX40 signaling favors the induction of T(H)9 cells and airway inflammation. *Nat Immunol* 13, 981-990.
- Xie, J.H., Nomura, N., Lu, M., Chen, S.L., Koch, G.E., Weng, Y., Rosa, R., Di Salvo, J., Mudgett, J., Peterson, L.B., *et al.* (2003). Antibody-mediated blockade of the CXCR3 chemokine receptor results in diminished recruitment of T helper 1 cells into sites of inflammation. *J Leukoc Biol* 73, 771-780.
- Xue, F., Li, H., Zhang, J., Lu, J., Xia, Y., and Xia, Q. (2013). miR-31 regulates interleukin 2 and kinase suppressor of ras 2 during T cell activation. *Genes Immun* 14, 127-131.
- Xue, X., Feng, T., Yao, S., Wolf, K.J., Liu, C.G., Liu, X., Elson, C.O., and Cong, Y. (2011). Microbiota downregulates dendritic cell expression of miR-10a, which targets IL-12/IL-23p40. *J Immunol* 187, 5879-5886.
- Yadav, M., Louvet, C., Davini, D., Gardner, J.M., Martinez-Llordella, M., Bailey-Bucktrout, S., Anthony, B.A., Sverdrup, F.M., Head, R., Kuster, D.J., *et al.* (2012). Neuropilin-1 distinguishes natural and inducible regulatory T cells among regulatory T cell subsets in vivo. *J Exp Med* 209, 1713-1722, S1711-1719.
- Yang, X.O., Panopoulos, A.D., Nurieva, R., Chang, S.H., Wang, D., Watowich, S.S., and Dong, C. (2007). STAT3 regulates cytokine-mediated generation of inflammatory helper T cells. *J Biol Chem* 282, 9358-9363.

- Yang, Y., Ma, Y., Shi, C., Chen, H., Zhang, H., Chen, N., Zhang, P., Wang, F., Yang, J., Yang, J., *et al.* (2013). Overexpression of miR-21 in patients with ulcerative colitis impairs intestinal epithelial barrier function through targeting the Rho GTPase RhoB. *Biochem Biophys Res Commun* 434, 746-752.
- Yao, R., Ma, Y.L., Liang, W., Li, H.H., Ma, Z.J., Yu, X., and Liao, Y.H. (2012). MicroRNA-155 modulates Treg and Th17 cells differentiation and Th17 cell function by targeting SOCS1. *PLoS One* 7, e46082.
- Yao, Z., Kanno, Y., Kerenyi, M., Stephens, G., Durant, L., Watford, W.T., Laurence, A., Robinson, G.W., Shevach, E.M., Moriggl, R., *et al.* (2007). Nonredundant roles for Stat5a/b in directly regulating Foxp3. *Blood* 109, 4368-4375.
- Yi, R., Qin, Y., Macara, I.G., and Cullen, B.R. (2003). Exportin-5 mediates the nuclear export of pre-microRNAs and short hairpin RNAs. *Genes Dev* 17, 3011-3016.
- Yu, X., Guo, C., Yi, H., Qian, J., Fisher, P.B., Subjeck, J.R., and Wang, X.Y. (2013). A multifunctional chimeric chaperone serves as a novel immune modulator inducing therapeutic antitumor immunity. *Cancer Res* 73, 2093-2103.
- Yu, X., Harden, K., Gonzalez, L.C., Francesco, M., Chiang, E., Irving, B., Tom, I., Ivelja, S., Refino, C.J., Clark, H., *et al.* (2009). The surface protein TIGIT suppresses T cell activation by promoting the generation of mature immunoregulatory dendritic cells. *Nat Immunol* 10, 48-57.
- Yue, D., Liu, H., and Huang, Y. (2009). Survey of Computational Algorithms for MicroRNA Target Prediction. *Curr Genomics* 10, 478-492.
- Zambrano-Zaragoza, J.F., Romo-Martinez, E.J., Duran-Avelar Mde, J., Garcia-Magallanes, N., and Vibanco-Perez, N. (2014). Th17 cells in autoimmune and infectious diseases. *Int J Inflam* 2014, 651503.
- Zarek, P.E., Huang, C.T., Lutz, E.R., Kowalski, J., Horton, M.R., Linden, J., Drake, C.G., and Powell, J.D. (2008). A2A receptor signaling promotes peripheral tolerance by inducing T-cell anergy and the generation of adaptive regulatory T cells. *Blood* 111, 251-259.
- Zhai, Z., Wu, F., Dong, F., Chuang, A.Y., Messer, J.S., Boone, D.L., and Kwon, J.H. (2014). Human autophagy gene ATG16L1 is post-transcriptionally regulated by MIR142-3p. *Autophagy* 10, 468-479.
- Zhang, D.G., Zheng, J.N., and Pei, D.S. (2014a). P53/microRNA-34-induced metabolic regulation: new opportunities in anticancer therapy. *Mol Cancer* 13, 115.
- Zhang, J., Cheng, Y., Cui, W., Li, M., Li, B., and Guo, L. (2014b). MicroRNA-155 modulates Th1 and Th17 cell differentiation and is associated with multiple sclerosis and experimental autoimmune encephalomyelitis. *J Neuroimmunol* 266, 56-63.
- Zhang, L., Ke, F., Liu, Z., Bai, J., Liu, J., Yan, S., Xu, Z., Lou, F., Wang, H., Zhu, H., *et al.* (2015a). MicroRNA-31 negatively regulates peripherally derived regulatory T-cell generation by repressing retinoic acid-inducible protein 3. *Nat Commun* 6, 7639.

- Zhang, R., Tian, A., Wang, J., Shen, X., Qi, G., and Tang, Y. (2015b). miR26a modulates Th17/T reg balance in the EAE model of multiple sclerosis by targeting IL6. *Neuromolecular Med* 17, 24-34.
- Zhang, Y., Liu, D., Chen, X., Li, J., Li, L., Bian, Z., Sun, F., Lu, J., Yin, Y., Cai, X., *et al.* (2010). Secreted monocytic miR-150 enhances targeted endothelial cell migration. *Mol Cell* 39, 133-144.
- Zhang, Y., Lv, K., Zhang, C.M., Jin, B.Q., Zhuang, R., and Ding, Y. (2014c). The role of LAIR-1 (CD305) in T cells and monocytes/macrophages in patients with rheumatoid arthritis. *Cell Immunol* 287, 46-52.
- Zhang, Y., Yang, Z., Cao, Y., Zhang, S., Li, H., Huang, Y., Ding, Y.Q., and Liu, X. (2008). The Hsp40 family chaperone protein DnaJB6 enhances Schlafen1 nuclear localization which is critical for promotion of cell-cycle arrest in T-cells. *Biochem J* 413, 239-250.
- Zhao, M., Wang, L.T., Liang, G.P., Zhang, P., Deng, X.J., Tang, Q., Zhai, H.Y., Chang, C.C., Su, Y.W., and Lu, Q.J. (2014). Up-regulation of microRNA-210 induces immune dysfunction via targeting FOXP3 in CD4(+) T cells of psoriasis vulgaris. *Clin Immunol* 150, 22-30.
- Zhao, X., Tang, Y., Qu, B., Cui, H., Wang, S., Wang, L., Luo, X., Huang, X., Li, J., Chen, S., and Shen, N. (2010). MicroRNA-125a contributes to elevated inflammatory chemokine RANTES levels via targeting KLF13 in systemic lupus erythematosus. *Arthritis Rheum* 62, 3425-3435.
- Zheng, S.G., Wang, J., and Horwitz, D.A. (2008a). Cutting edge: Foxp3+CD4+CD25+ regulatory T cells induced by IL-2 and TGF-beta are resistant to Th17 conversion by IL-6. *J Immunol* 180, 7112-7116.
- Zheng, W., and Flavell, R.A. (1997). The transcription factor GATA-3 is necessary and sufficient for Th2 cytokine gene expression in CD4 T cells. *Cell* 89, 587-596.
- Zheng, Y., Josefowicz, S., Chaudhry, A., Peng, X.P., Forbush, K., and Rudensky, A.Y. (2010). Role of conserved non-coding DNA elements in the Foxp3 gene in regulatory T-cell fate. *Nature* 463, 808-812.
- Zheng, Y., Valdez, P.A., Danilenko, D.M., Hu, Y., Sa, S.M., Gong, Q., Abbas, A.R., Modrusan, Z., Ghilardi, N., de Sauvage, F.J., and Ouyang, W. (2008b). Interleukin-22 mediates early host defense against attaching and effacing bacterial pathogens. *Nat Med* 14, 282-289.
- Zhou, Q., Haupt, S., Kreuzer, J.T., Hammitzsch, A., Proft, F., Neumann, C., Leipe, J., Witt, M., Schulze-Koops, H., and Skapenko, A. (2014). Decreased expression of miR-146a and miR-155 contributes to an abnormal Treg phenotype in patients with rheumatoid arthritis. *Ann Rheum Dis*.
- Zhu, E., Wang, X., Zheng, B., Wang, Q., Hao, J., Chen, S., Zhao, Q., Zhao, L., Wu, Z., and Yin, Z. (2014a). miR-20b suppresses Th17 differentiation and the pathogenesis of experimental autoimmune encephalomyelitis by targeting RORgammat and STAT3. *J Immunol* 192, 5599-5609.

Zhu, J., Chen, L., Zou, L., Yang, P., Wu, R., Mao, Y., Zhou, H., Li, R., Wang, K., Wang, W., *et al.* (2014b). MiR-20b, -21, and -130b inhibit PTEN expression resulting in B7-H1 over-expression in advanced colorectal cancer. *Hum Immunol* 75, 348-353.

Zhu, S., Si, M.L., Wu, H., and Mo, Y.Y. (2007). MicroRNA-21 targets the tumor suppressor gene tropomyosin 1 (TPM1). *J Biol Chem* 282, 14328-14336.

Zielinski, C.E., Mele, F., Aschenbrenner, D., Jarrossay, D., Ronchi, F., Gattorno, M., Monticelli, S., Lanzavecchia, A., and Sallusto, F. (2012). Pathogen-induced human TH17 cells produce IFN-gamma or IL-10 and are regulated by IL-1beta. *Nature* 484, 514-518.

Zigmond, E., Bernshtein, B., Friedlander, G., Walker, C.R., Yona, S., Kim, K.W., Brenner, O., Krauthgamer, R., Varol, C., Muller, W., and Jung, S. (2014). Macrophage-restricted interleukin-10 receptor deficiency, but not IL-10 deficiency, causes severe spontaneous colitis. *Immunity* 40, 720-733.

Zorzi, F., Angelucci, E., Sedda, S., Pallone, F., and Monteleone, G. (2013). Smad7 antisense oligonucleotide-based therapy for inflammatory bowel diseases. *Dig Liver Dis* 45, 552-555.

Zou, C., Li, Y., Cao, Y., Zhang, J., Jiang, J., Sheng, Y., Wang, S., Huang, A., and Tang, H. (2014). Up-regulated MicroRNA-181a induces carcinogenesis in hepatitis B virus-related hepatocellular carcinoma by targeting E2F5. *BMC Cancer* 14, 97.